COMRISK

Flanders/Zeeuws-Vlaanderen Case Study

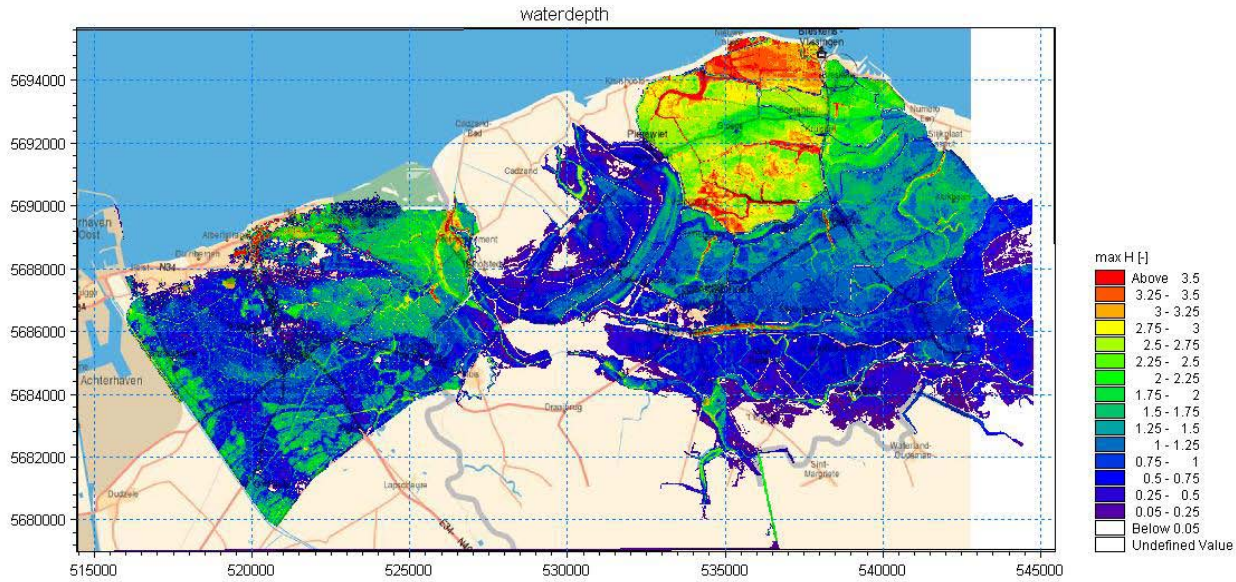

February 2005

DRAFT

I/RA/11226/04.059/KTR

Document Control Sheet

Document Identification

Title:	Flood Risk Flanders/Zeeuws-Vlaanderen
Project:	COMRISK
Principal:	Coastal Waterways Department
Reference number:	I/RA/11226/04.059/KTR

Revisions

Version	Date	Author	Description
2.0	21/02/2005	IMDC	
2.0	28/01/2005	CKE/PWA/EST	

Distribution list

Name	# copies	Company/authorities	Function in the project

Approval

Version	Date	Author	Project leader	Department head
2.0	21/02/2005	KTR/BVW/KSU	KTR	BND
2.0	31/01/2005	PWA/CKE/EST	KTR	BND

TABLE OF CONTENTS

1. INTRODUCTION 1

2. DESCRIPTION OF THE PROJECT AREA 3

2.1. INTRODUCTION 3
2.2. DIKE STRUCTURE 4
2.2.1. Flanders 4
2.2.2. Zwin 5
2.2.3. Zeeuws-Vlaanderen 5

3. HYDRODYNAMIC BOUNDARY CONDITIONS 8

3.1. FORMULATION OF THE HYDRODYNAMIC BOUNDARY CONDITIONS IN DEEP WATER 8
3.1.1. Water level 8
3.1.2. Waves and wind 9
3.1.3. Statistische verdeling 10
3.2. VERLOOP VAN DE STORM 10
3.2.1. Verloop van de waterstand tijdens een storm 10
3.2.2. Some examples for Ostend 11
3.2.3. Conclusions 14
3.2.4. Conclusions 20
3.3. BEACH EROSION DURING THE STORM 21
3.4. DETERMINATION OF THE WAVE HEIGHT AND WATER LEVEL AT THE TOE OF THE DIKE 21
3.5. COMPARISON OF THE RESULTS WITH THE EXISTING DUTCH RESULTS 22
3.5.1. Peak wave period for dune erosion 22
3.5.2. Wave period for dikes (overtopping) 22
3.5.3. Water level 24
3.5.4. Wave height for assessment of dunes 24

4. DUNE EROSION 26

4.1. GUIDELINE TO ASSESS THE SAFETY OF DUNES AS SEA DEFENCE 26
4.2. METHODOLOGY 27
4.2.1. General 27
4.3. BOUNDARY CONDITIONS 31
4.3.1. Water level 31
4.3.2. Wave height and peak period 31
4.3.3. Superdune corrections 31

5. STABILITY OF DIKES 33

5.1. INTRODUCTION 33
5.2. DESCRIPTION OF THE METHOD 33
5.3. ASSUMPTIONS 33
5.4. CALCULATION PROGRAMMES USED 33
5.5. PIPING EN HEAVE 33
5.6. OUTWARD MACROSTABILITY 34
5.6.1. Sliding and liquefaction 34
5.6.2. Sliding equilibrium with low outer water 41
5.6.2.1. Loads 41
5.6.2.2. Water pressures 42
5.6.2.3. Soil resistance characteristics 43
5.7. INWARD MACROSTABILITY 44
5.8. MICROSTABILITY 44
5.9. CONDITION OF THE REVETMENT 45
5.9.1. Residual strength of the grass cover and clay layer 46
5.9.2. Stone pitching 49

5.9.3. Asphalt revetments ... 56
5.10. CREST HEIGHT ASSESSMENT ... 57
5.10.1. Erosion of inner slope by overtopping water ... 58
5.10.2. Sliding of the inner slope due to liquefaction ... 60

6. FAILURE OF SEA DEFENCE: RESULTS FOR FLANDERS ... 62

6.1. INTRODUCTION ... 62
6.2. DUNE EROSION ... 62
6.3. BEACH EROSION ... 62
6.4. PIPING EN HEAVE ... 64
6.5. INWARD MACROSTABILITY ... 65
6.6. OUTWARD MACROSTABILITY ... 65
6.6.1. Sliding and liquefaction of the foreshore ... 65
6.6.2. Sliding of outer slope ... 66
6.7. OUTWARD MICROSTABILITY OF THE SLOPE ... 70
6.8. REVETMENT ... 70
6.8.1. Material transport ... 71
6.8.2. Stability of outer slope element ... 71
6.8.2.1. Concrete slabs ... 71
6.8.3. Crest element stability ... 73
6.9. EROSION OF THE DIKE CORE BY OVERTOPPING DISCHARGES (=ASSESSMENT OF CREST HEIGHT) ... 74
6.9.1. Results for 1000-year return period ... 75
6.9.2. Results for 4000-year return period ... 76
6.9.3. Results for 40000-year return period ... 77
6.10. SUMMARY OF THE RESULTS – CONCLUSIONS ... 78

7. FAILURE OF SEA DEFENCE: RESULTS FOR THE ZWIN ... 80

7.1. DIKE STRUCTURE ... 81
7.2. WAVE MODEL ... 82
7.2.1. Boundary Conditions ... 82
7.2.2. Results for the 1000-year return period ... 83
7.2.3. Results for a return period of 4000 year ... 85
7.2.4. Results for a return period of 40000 years ... 88
7.3. PIPING EN HEAVE ... 89
7.4. OUTWARD SLOPE MACROSTABILITY ... 89
7.4.1. Liquefaction and sliding ... 89
7.4.2. Sliding equilibrium at low outer water ... 89
7.5. INWARD SLOPE STABILITY ... 90
7.6. MICROSTABILITY ... 91
7.7. REVETMENT ... 93
7.8. ASSESSMENT OF CREST LEVEL ... 94
7.8.1. Return period of 1000 years ... 94
7.8.2. Return period of 4000 year ... 95
7.8.3. Return period of 40000 years ... 96
7.9. SUMMARY OF THE ZWIN RESULTS ... 96

8. FAILURE OF THE SEA DEFENCE: RESULTS FOR ZEEUWS-VLAANDEREN ... 97

8.1. INTRODUCTION ... 97
8.2. DUNE EROSION ... 99
8.3. BEACH EROSION IN FRONT OF DIKES ... 99
8.4. PIPING EN HEAVE ... 110
8.5. OUTWARD MACROSTABILITY ... 112
8.5.1. Sliding and liquefaction ... 112
8.5.2. Sliding of outer slope ... 124
8.6. INWARD MACROSTABILITY (LANDWARD SLOPE) ... 133
8.7. MICROSTABILITY ... 136

8.8. CONDITION OF THE REVETMENT 136
8.8.1. Stone pitching 136
8.8.2. Asphalt revetment 140
8.8.3. Erosion of dike body 141
8.8.4. Grass cover 144
8.9. CONCLUSIONS 144

9. FLOOD MODELLING 146

9.1. INTRODUCTION 146
9.2. OBJECTIVE AND STUDY AREA 146
9.2.1. Study area 146
9.3. DEVELOPMENT OF THE FLOOD MODEL 147
9.3.1. The 2D-model 147
9.3.1.1. The model grid 147
9.3.1.2. Topography 147
9.3.1.3. Roughness and viscosity: 149
9.3.1.4. The model borders 149
9.3.2. The 1D-model 149
9.3.3. Link between 1D and 2D-model 150
9.3.4. Calculation time and calculation transient of the model 150
9.4. SCENARIOS: DIKE BREACH 151
9.4.1. Boundary conditions 153
9.4.1.1. Water levels 153
9.4.1.2. Wind 153
9.4.2. Dike breach: breach evolution 153
9.4.3. Wave overtopping 164
9.5. DIKE BREACH RESULTS 164
9.5.1. Scenario 1: Dike breach for a return period of 1000 years 167
9.5.2. Scenario 2: Dike breach for a 4000-year return period 169
9.5.3. Scenario 3: Dike breach with a 10000-year return period 171
9.5.4. Scenario 4: Dike breach with a 40000-year return period 173

10. DAMAGE AND CASUALTIES 177

10.1. METHODOLOGY 177
10.1.1. Damage definition 177
10.1.2. Procedure 177
10.1.3. Damage functions and maximum damage 178
10.1.3.1. Damage to houses 179
10.1.3.2. Damage to industry 180
10.1.3.3. Infrastructure and airport 180
10.1.3.4. Recreation 180
10.1.3.5. Orchards, arable farming and meadow 180
10.1.3.6. Vehicles 181
10.1.3.7. Water, nature and forests 181
10.1.3.8. Roads and railways 181
10.1.4. Land use 184
10.1.4.1. Flanders 184
10.1.4.2. The Netherlands 186
10.1.5. Casualties 186
10.2. RESULTS 189
10.2.1. T=1000jaar 192
10.2.2. T=4000 jaar 193
10.2.3. T=10000 jaar 194
10.2.4. T=40000 jaar 195

11. SENSITIVITY ANALYSIS 197

11.1. DIKE FAILURE FLANDERS 197
11.1.1. Sensitivity analysis of Durosta calculations 197

11.2. DIKE FAILURE THE ZWIN 198
11.2.1. Wave period 198
11.2.2. Roughness factor of grass cover 199
11.2.3. Clay and grass quality 200
11.2.4. Crest height 201
11.3. DIKE FAILURE ZEEUWS-VLAANDEREN 202
11.3.1. Macrostability of seaward slope 202
11.3.2. Stability of landward slope 207
11.3.3. Erosion of dike body – residual strength 208
11.4. SENSITIVITY ANALYSIS OF THE FLOOD MODEL AND ASSOCIATED DAMAGE 210
11.4.1. Influence of the roughness 210
11.4.2. Influence of breach width 213
11.4.3. Influence of the moment of dike breach 219
11.4.4. Influence of additional dike breaches 223
11.4.5. Other uncertainties for damage calculations 227

12. CONCLUSIONS 228

12.1. GOAL 228
12.2. HYDRODYNAMIC BOUNDARY CONDITIONS 228
12.3. FAILURE OF DUNES AND DIKES 228
12.4. FLOOD MODELLING 230
12.5. DAMAGE CALCULATIONS 230
12.6. RISK 230

13. REFERENTIES 232

LIST OF TABLES

TABLE 1 REPRESENTATIVE APPARENT DENSITIES USED FOR VARIOUS TYPES OF SOIL ACCORDING TO NEN 6740. 42
TABLE 2 REPRESENTATIVE SOIL CHARACTERISTICS USED IN ACCORDANCE WITH NEN 6740. 43
TABLE 3 OVERALL CLASSIFICATION OF DIKE AND SUBSOIL. 64
TABLE 4 RESULTS FOR THE ASSESSMENT OF COVERING, SLIDING AND LIQUEFACTION CRITERIA. 65
TABLE 5: OVERWIDTH OF PROFILES. 66
TABLE 6 IRIBARREN NUMBERS FOR THE VARIOUS PROFILES. 72
TABLE 7 WAVE RUN-UP AND OVERTOPPING DISCHARGES FOR A STORM WITH A 1000-YEAR RETURN PERIOD. 75
TABLE 8 WAVE RUN-UP AND OVERTOPPING DISCHARGES FOR A STORM WITH A 4000-YEAR RETURN PERIOD. 76
TABLE 9 DAMAGE OF CREST AND EROSION OF DIKE CORE BY OVERTOPPING VOLUMES FOR A RETURN PERIOD OF 4000 YEARS. 76
TABLE 10 WAVE RUN-UP AND OVERTOPPING DISCHARGES FOR A STORM WTH A 40000-YEAR RETURN PERIOD. 77
TABLE 11 DAMAGE TO CREST AND EROSION OF DIKE CORE BY OVERTOPPING VOLUMES FOR A RETURN PERIOD OF 40000 YEARS. 77
TABLE 12 BOUNDARY CONDITIONS OF THE SWAN MODEL FOR THE ZWIN BASIN 83
TABLE 13 SWAN OUTPUT FOR A RETURN PERIOD OF 1000 YEARS. 85
TABLE 14 SWAN OUTPUT FOR A RETURN PERIOD OF 4000 YEARS 87
TABLE 15 SWAN OUTPUT FOR A RETURN PERIOD OF 40000 YEARS 89
TABLE 16 WAVE RUN-UP AND OVERTOPPING DISCHARGES OF ZWIN DIKES FOR A RETURN PERIOD OF 1000 YEARS. 94
TABLE 17 WAVE RUN-UP AND OVERTOPPING DISCHARGES OF ZWIN DIKES FOR A RETURN PERIOD OF 4000 YEARS. 95
TABLE 18 WAVE RUN-UP AND OVERTOPPING DISCHARGES OF ZWIN DIKES FOR A RETURN PERIOD OF 40000 YEARS. 96
TABLE 19 : OVERVIEW OF ZEEUWS-VLAANDEREN PROFILES 98
TABLE 20 SIGNIFICANT WAVE HEIGHTS, OVERTOPPING DISCHARGES, WAVE RUN-UP HEIGHTS. 110
TABLE 21 BASIC GEOMETRIC ASSESSMENT FOR A 1000-YEAR RETURN PERIOD. 111
TABLE 22 : BASIC GEOMETRIC ASSESSMENT FOR A 4000-YEAR RETURN PERIOD. 111
TABLE 23 BASIC GEOMETRIC ASSESSMENT FOR A 4000-YEAR RETURN PERIOD. 112
TABLE 24 OVERVIEW OF LOCAL/TOTAL TROUGH DEPTHS. 124
TABLE 25 GEOMETRIC ASSESSMENT OF SLIDING/LIQUEFACTION OF THE FORESHORE 124
TABLE 26 PHREATIC LEVEL IN DIKE. 126
TABLE 27 SAFETY COEFFICIENTS (40000 Y) FOR D_20, D_21, D_29. 126
TABLE 28 SAFETY COEFFICIENTS FOR PROFILE 496 (D_17). 126
TABLE 29 SAFETY COEFFICIENTS FOR PROFILE 512 (D_17). 127
TABLE 30 BASIC ASSESSMENT OF MACROSTABILITY OF LANDWARD SLOPE. 135
TABLE 31 PEAK WAVE PERIODS FOR THE CONSIDERED RETURN PERIODS. 136
TABLE 32 RESULT OF THE BASIC ASSESSMENT OF THE TOP LAYER INSTABILITY UNDER WAVE IMPACT. 137
TABLE 33 RESULT OF THE BASIC ASSESSMENT OF THE TOP LAYER INSTABILITY UNDER CURRENT ATTACK. 138
TABLE 34 FAILURE OF STONE PITCHING FOR THE DIFFERENT RETURN PERIODS. 139
TABLE 35 LOCATION OF ASPHALT REVETMENT. 140
TABLE 36: NECESSARY ASPHALT LAYER THICKNESS FOR LARGEST WAVE HEIGHTS. 141
TABLE 37 RESIDUAL STRENGTH CALCULATION OF DIKE CORE FOR 40000-YEAR RETURN PERIOD. 143
TABLE 38 RESIDUAL STRENGTH CALCULATION OF DIKE CORE FOR 4000-YEAR RETURN PERIOD. 143
TABLE 39 RESIDUAL STRENGTH CALCULATION OF DIKE CORE FOR 1000-YEAR RETURN PERIOD. 143
TABLE 40 BREACHES AND TIMES OF FAILURE. 145
TABLE 41: SCENARIOS FOR DIKE BREACHES 151
TABLE 42: OVERVIEW OF RESULT OF SHORT INVENTORY. 155
TABLE 43: PARAMETERS FOR BREACH DEVELOPMENT WITH SEAWALL FAILURE DURING A STORM TIDE WITH A 1000-YEAR RETURN PERIOD: SCENARIO 1 156
TABLE 44: PARAMETERS FOR BREACH EVOLUTION WITH SEAWALL FAILURE DURING A STORM TIDE WITH A 4000-YEAR RETURN PERIOD: SCENARIO 2 158
TABLE 45: PARAMETERS FOR BREACH EVOLUTION WITH SEAWALL FAILURE DURING A STORM TIDE WITH A 10000-YEAR RETURN PERIOD IN ZEELAND FLANDERS : SCENARIO 3 159
TABLE 46: PARAMETERS FOR BREACH EVOLUTION WITH SEAWALL FAILURE DURING A STORM TIDE WITH A 10000-YEAR RETURN PERIOD IN FLANDERS: SCENARIO 3 160
TABLE 47: PARAMETERS FOR BREACH EVOLUTION WITH SEAWALL FAILURE DURING A STORM TIDE WITH A 40000-YEAR RETURN PERIOD IN ZEELAND FLANDERS: SCENARIO 4 161

TABLE 48: PARAMETERS FOR BREACH EVOLUTION WITH SEAWALL FAILURE DURING A STORM TIDE WITH A 40000-YEAR REUTURN PERIOD IN FLANDERS: SCENARIO 4 162
TABLE 49: ALTITUDES OF THE LOCATIONS FOR THE RESULTS OF FLOOD DEPTHS IN ZEELAND FLANDERS 165
TABLE 50: ALTITUDE OF THE LOCATIONS FOR THE RESULTS OF FLOOD DEPTHS IN FLANDERS 166
TABLE 51CONTINGENCY TABLE FOR LAND USE 185
TABLE 52 DAMAGE IN FLANDERS (X1000 EURO)(EVACUATIE FACTOR: 50%) 189
TABLE 53SCHADE IN NEDERLAND (X1000 EURO)(EVACUATIEFACTOR: 50%) 191
TABLE 54TOTAL DAMAGE (X1000EURO) 191
TABLE 55 TOTAL NUMBER OF CASUALTIES 191
TABLE 56: SENSITIVITY ANALYSIS OF MACROSTABILITY OF SEAWARD SLOPE 202
TABLE 57: STABILITY OF LANDWARD SLOPE OF PROFILE 308 (D_25) 207
TABLE 58 RESIDUAL STRENGTH OF THE DIKE CORE FOR DIFFERENT EROSION RESISTANCES (40000-YEAR RETURN PERIOD). 209
TABLE 59 REMAINING RESIDUAL STRENGTH OF THE DIKE CORE FOR VARIOUS EROSION RESISTANCES (40000-YEAR RETURN PERIOD) 210
TABLE 60: PARAMETERS FOR BREACH DEVELOPMENT WITH SEAWALL FAILURE: SENSITIVITY ANALYSIS OF BREACH WIDTH 213
TABLE 61DAMAGE DEPENDING ON BREACH WIDTH (X1000 EURO) 216
TABLE 62DAMAGE DEPENDING ON TIMING OF BREACHING 221
TABLE 63DAMAGE (X1000 EURO) 221
TABLE 64 DAMAGE FOR EXTRA FAILURES (X1000 EURO) 225

LIST OF FIGURES

FIGURE 1 PROJECT AREA OVERVIEW. 3
FIGURE 2 EVOLUTION OF EXTREME HIGH WATER LEVELS, FOR THE 100-YEAR STORM ALONG THE COAST. 9
FIGURE 3 EVOLUTION OF THE ASTRONOMICAL TIDE, STORM SURGE AND WATER LEVEL. 11
FIGURE 4 EVOLUTION OF THE STORM SURGE DURING THE STORM OF 1953. 11
FIGURE 5 EVOLUTION OF THE STORM SURGE DURING THE STORM OF 1930. 12
FIGURE 6 EVOLUTION OF THE STORM SURGE OF 1965. 12
FIGURE 7 EVOLUTION OF THE STORM SURGE DURING THE STORM OF 1990. 13
FIGURE 8 STORM OF JANUARY 1995. 13
FIGURE 9 WAVES AND WIND DIRECTIONS DURING THE STORM OF JANUARY 1995. 14
FIGURE 10 STORM DURATION DEPENDING ON THE MAXIMUM STORM SURGE. 15
FIGURE 11 SURGE WITH HW RIGHT BEFORE AND AFTER POT-HW. 15
FIGURE 12 RELATIONS FOR VLISSINGEN (WITH WATER LEVELS INSTEAD OF SURGE) (IMDC, 2003, WITHIN THE SCOPE OF THE SIGMA PLAN). 16
FIGURE 13 EVOLUTION OF A NUMBER OF STORM PROFILES DURING 45 HOURS. 16
FIGURE 14 EROSION PROFILES AFTER STORM (INITIAL PROFILE FOR KNOKKE, PROFILE 239)FOR THE STORM PROFILES OF FIGURE 13) 17
FIGURE 15 COMPARISON OF THE MEASURED AND THEORETICAL SURGE (AVERAGE OF RIGHT BEFORE AND RIGHT AFTER POT). 18
FIGURE 16 2ND HW BEFORE AND AFTER POT 19
FIGURE 17 EROSION PROFILE FOR TWO STORMS WITH DIFFERENT RETURN PERIODS (1000 Y AND 100 Y, WITH CORRESPONDING SURGES OF 2.2 AND 1.6M, RESPECTIVELY) AND DURATIONS (45 AND 90H, RESPECTIVELY).20
FIGURE 18 EVOLUTION OF THE BEACH DURING A STORM AND CONSEQUENCES FOR THE WAVE HEIGHT AT THE TOE OF THE DIKE. 22
FIGURE 19 SPECTRUMS TO THE EAST OF ZEEBRUGGE. 23
FIGURE 20 EVOLUTION OF THE WAVE HEIGHT AND PERIOD ($T_{M-1,0}$) FOR A TYPICAL BOTTOM PROFILE. 24
FIGURE 21 OVERVIEW OF THE METHOD APPLIED WHEN TESTING DUNE FOOT EROSION (V= VEILIG (SAFE), G=GEAVANCEERD ONDERZOEK NODIG (ADVANCED INVESTIGATION NEEDED), O=ONVEILIG (UNSAFE); EO=EXPERT OPINIE NODIG (EXPERT OPINION NEEDED)) 29
FIGURE 22 DEFINITION SKETCH 29
FIGURE 23 STANDARD LIMIT PROFILE. 30

FIGURE 24 ASSESSMENT SCHEME FOR SLIDING AND LIQUEFACTION. 35
FIGURE 25 DEFINITION OF COVERING CRITERION. 36
FIGURE 26 DEFINITION OF 'MARGIN'. 37
FIGURE 27 ASSESSMENT OF THE MACROSTABILITY OF THE OUTER SLOPE 38
FIGURE 28 DETERMINATION OF SIGNALLING POINT, SLIDING POINT FOR (A) A COVER-FREE FORESHORE, (B) A COVERED FORESHORE. 40
FIGURE 29 DETERMINATION OF SIGNALLING POINT, LIQUEFACTION POINT FOR A COVER-FREE FORESHORE. 41
FIGURE 30 WATER LEVEL IN DIKE. 42
FIGURE 31 MICROSTABILITY ASSESSMENT. 44
FIGURE 32 ASSESSMENT DIAGRAM FOR CONCRETE SLABS. 48
FIGURE 33 STONE PITCHING ASSESSMENT DIAGRAM. 49
FIGURE 34 ASSESSMENT DIAGRAM FOR TOP LAYER STABILITY UNDER WAVE ATTACK. 50
FIGURE 35 BASIC ASSESSMENT FOR STONE PITCHING UNDER WAVE ATTACK. 53
FIGURE 36 ASSESSMENT OF TOP LAYER STABILITY UNDER CURRENT ATTACK 53
FIGURE 37 BASIC ASSESSMENT OF STONE PITCHING UNDER CURRENT ATTACK. 54
FIGURE 38 SLIDING ASSESSMENT. 55
FIGURE 39 ASSESSMENT DIAGRAM FOR ASPHALT REVETMENT. 56
FIGURE 40 WAVE IMPACT ASSESSMENT 57
FIGURE 41 EROSION RESISTANCE OF SLOPES COVERED WITH GRASS (IN CASE OF OVERFLOW). 59
FIGURE 42 ACCEPTABLE OVERTOPPING DISCHARGES (FROM CIRIA/CUR MANUAL, 1991). 61
FIGURE 43 BEACH PROFILE OF PROFILE 236 AFTER A STORM WITH A 1000-YEAR RETURN PERIOD. 63
FIGURE 44 BEACH PROFILE OF PROFILE 236 AFTER A STORM WITH A 4000-YEAR RETURN PERIOD. 63
FIGURE 45 BEACH PROFILE OF PROFILE 236 AFTER A STORM WITH A 40000-YEAR RETURN PERIOD. 64
FIGURE 46 ASSESSMENT OF SLIDING AND LIQUEFACTION OF THE FORESHORE FOR PROFILE 234. 65
FIGURE 47 ASSESSMENT OF SLIDING AND LIQUEFACTION OF THE FORESHORE FOR PROFILE 238. 66
FIGURE 48 ASSESSMENT OF SLIDING AND LIQUEFACTION OF THE FORESHORE FOR PROFILE 239. 66
FIGURE 49: SUMMARY OF THE RESULTS OF THE OUTWARD MACROSTABILITY ASSESSMENT. 67
FIGURE 50 MOST CRITICAL SLIP SURFACE FOR PROFILE 234 FOR A 40000-YEAR RETURN PERIOD. 67
FIGURE 51 MOST CRITICAL SLIP SURFACE FOR PROFILE 235 FOR A 40000-YEAR RETURN PERIOD. 68
FIGURE 52 MOST CRITICAL SLIP SURFACE FOR PROFILE 243 FOR A 40000-YEAR RETURN PERIOD. 69
FIGURE 53 MOST CRITICAL SLIP SURFACE FOR PROFILE 246 FOR A 40000-YEAR RETURN PERIOD. 69
FIGURE 54: EROSION RESISTANCE OF GRASS-COVERED SLOPES. 73
FIGURE 55: KRITIEKE STROOMSNELHEID U_{CR} [M/S] I.F.V. DE DIKTE VAN DE BEKLEDING 74
FIGURE 56 BREACH FORMATION OF DIKES IN FLANDERS (RETURN PERIOD OF 4000 YEARS). 78
FIGURE 57 BREACH FORMATION OF DIKES IN FLANDERS (RETURN PERIOD OF 40000 YEARS) 79
FIGURE 58 RESULTS OF THE BOUSSINESQ WAVE MODEL MIKE 21 (SIGNIFICANT WAVE HEIGHT ZWIN) 80
FIGURE 59 RESULTS OF THE SWAN MODEL (SIGNIFICANT WAVE HEIGHT ZWIN, RETURN PERIOD OF 1000 YEARS). 81
FIGURE 60 DIKE PROFILE AT 11.10M TAW (ZWIN DIKE) 82
FIGURE 61 DIKE PROFILE AT 9.55M TAW (ZWIN DIKE) 82
FIGURE 62 BATHYMETRY AND OUTPUT POINTS ZWIN 83
FIGURE 63 SIGNIFICANT WAVE HEIGHT OF THE ZWIN FOR A RETURN PERIOD OF 1000 YEARS (NNE WIND DIRECTION)) 84
FIGURE 64 SIGNIFICANT WAVE HEIGHT IN THE ZWIN FOR A RETURN PERIOD OF 4000 YEARS (NNE WIND DIRECTION). 86
FIGURE 65 SIGNIFICANT WAVE HEIGHT FOR THE ZWIN FOR A 40000-YEAR RETURN PERIOD (WIND DIRECTION NNE) 88
FIGURE 66 VOORWAARDEN AAN DE PROFIELOPBOUW VOOR ZEEDIJKEN (FIGUUR 4.3.3.2 UIT LTV) 90
FIGURE 67 RESIDUAL STRENGTH OF THE GRASS COVER (FROM CIRIA). 93
FIGURE 68 BEACH PROFILE OF PROFILE 373 AFTER STORM WITH RETURN PERIOD 1000 YEAR 99
FIGURE 69 BEACH PROFILE OF PROFILE 373 AFTER STORM WITH RETURN PERIOD 4000 YEAR 100
FIGURE 70 BEACH PROFILE OF PROFILE 373 AFTER STORM WITH RETURN PERIOD 40000 YEAR 100
FIGURE 71 BEACH PROFILE OF PROFILE 396 AFTER STORM WITH RETURN PERIOD 1000 YEAR 101
FIGURE 72 BEACH PROFILE OF PROFILE 396 AFTER STORM WITH RETURN PERIOD 4000 YEAR 101
FIGURE 73 BEACH PROFILE OF PROFILE 396 AFTER STORM WITH RETURN PERIOD 40000 YEAR 102
FIGURE 74 BEACH PROFILE OF PROFILE 413 AFTER STORM WITH RETURN PERIOD 1000 YEAR 102
FIGURE 75 BEACH PROFILE OF PROFILE 413 AFTER STORM WITH RETURN PERIOD 1000 YEAR 103
FIGURE 76 BEACH PROFILE OF PROFILE 413 AFTER STORM WITH RETURN PERIOD 4000 YEAR 103

FIGURE 77 BEACH PROFILE OF PROFILE 413 AFTER STORM WITH RETURN PERIOD 40000 YEAR..... 104
FIGURE 78 BEACH PROFILE OF PROFILE 496 AFTER STORM WITH RETURN PERIOD 40000 YEAR..... 104
FIGURE 79 BEACH PROFILE OF PROFILE 512 AFTER STORM WITH RETURN PERIOD 4000 YEAR..... 105
FIGURE 80 BEACH PROFILE OF PROFILE 512 AFTER STORM WITH RETURN PERIOD 40000 YEAR..... 105
FIGURE 81 BEACH PROFILE OF PROFILE 530 AFTER STORM WITH RETURN PERIOD 4000 YEAR..... 106
FIGURE 82 BEACH PROFILE OF PROFILE 530 AFTER STORM WITH RETURN PERIOD 40000 YEAR..... 106
FIGURE 83 BEACH PROFILE OF PROFILE 558 AFTER STORM WITH RETURN PERIOD 40000 YEAR..... 107
FIGURE 84 BEACH PROFILE OF PROFILE 584 AFTER STORM WITH RETURN PERIOD 40000 YEAR..... 107
FIGURE 85 BEACH PROFILE OF PROFILE 663 AFTER STORM WITH RETURN PERIOD 40000 YEAR..... 108
FIGURE 86 BEACH PROFILE OF PROFILE 684 AFTER STORM WITH RETURN PERIOD 40000 YEAR..... 108
FIGURE 87 COVERING, LIQUEFACTION AND SLIDING CRITERIA FOR DIKE SECTION D_8. 113
FIGURE 88 COVERING, LIQUEFACTION AND SLIDING CRITERIA FOR DIKE SECTION D_9. 113
FIGURE 89 COVERING, LIQUEFACTION AND SLIDING CRITERIA FOR DIKE SECTION D_12. 114
FIGURE 90 COVERING, LIQUEFACTION AND SLIDING CRITERIA FOR DIKE SECTION D_17. 114
FIGURE 91 COVERING, LIQUEFACTION AND SLIDING CRITERIA FOR DIKE SECTION D_20: (A) LOCAL TROUGH DEPTH, (B) TOTAL TROUGH DEPTH. 115
FIGURE 92 COVERING, LIQUEFACTION AND SLIDING CRITERIA FOR DIKE SECTION D_21: (A) LOCAL TROUGH DEPTH, (B) TOTAL TROUGH DEPTH. 116
FIGURE 93 COVERING, LIQUEFACTION AND SLIDING CRITERIA FOR DIKE SECTION D_22: (A) LOCAL TROUGH DEPTH H_{LOC}, (B) TOTAL TROUGH DEPTH H_{TOT}..... 117
FIGURE 94 COVERING, LIQUEFACTION AND SLIDING CRITERIA FOR DIKE SECTION D_23: (A) LOCAL TROUGHT DEPTH H_{LOC}, (B) TOTAL TROUGH DEPTH H_{TOT}..... 118
FIGURE 95 COVERING, LIQUEFACTION AND SLIDING CRITERIA FOR DIKE SECTION D_24: (A) LOCAL TROUGH DEPTH H_{LOC}, (B) TOTAL TROUGH DEPTH H_{TOT}..... 119
FIGURE 96 COVERING, LIQUEFACTION AND SLIDING CRITERIA OF DIKE SECTION D_25: (A) LOCAL TROUGH DEPTH H_{LOC}, (B) TOTAL TROUGH DEPTH H_{TOT}..... 120
FIGURE 97 COVERING, LIQUEFACTION AND SLIDING CRITERIA OF DIKE SECTION D_26: (A) LOCAL TROUGH DEPTH H_{LOC}, (B) TOTAL TROUGH DEPTH H_{TOT}..... 121
FIGURE 98 COVERING, LIQUEFACTION AND SLIDING CRITERIA OF DIKE SECTION D_28: (A) LOCAL TROUGH DEPTH H_{LOC}, (B) TOTAL TROUGH DEPTH H_{TOT}..... 122
FIGURE 99 COVERING, LIQUEFACTION AND SLIDING CRITERIA OF DIKE SECTION D_29: (A) LOCAL TROUGH DEPTH H_{LOC}, (B) TOTAL TROUGH DEPTH H_{TOT}..... 123
FIGURE 100 DIAGRAM OF NON-ERODABLE PROFILE..... 125
FIGURE 101 OUTWARD MACROSTABILITY D_17 (496) **FS= 0.87**..... 127
FIGURE 102 OUTWARD MACROSTABILITY D_17 (496) **FS= 1.00**..... 128
FIGURE 103 OUTWARD MACROSTABILITY D_17 (496) 4.000J **FS= 1.11**..... 128
FIGURE 104 OUTWARD MACROSTABILITY D_17 (512) **FS= 0.66**..... 129
FIGURE 105 OUTWARD MACROSTABILITY D_17 (512) **FS= 1.00**..... 129
FIGURE 106 OUTWARD MACROSTABILITY D_17 (512) 1000J **FS= 1.09**..... 130
FIGURE 107 OUTWARD MACROSTABILITY D_24 (324) **FS= 1.00**..... 130
FIGURE 108 OUTWARD MACROSTABILITY D_25 (308) **FS= 1.00**..... 131
FIGURE 109 OUTWARD MACROSTABILITY D_25 (308) **FS= 1.30**..... 131
FIGURE 110 OUTWARD MACROSTABILITY D_22 (373) **FS= 1.00**..... 132
FIGURE 111 OUTWARD MACROSTABILITY D_22 (396) **FS=1.00**..... 132
FIGURE 112 VNK DIKE SECTIONS (DIJKVAKKEN)..... 134
FIGURE 113 INWARD MACROSTABILITY D_25 (PROFILE 308) **SF= 1.43**..... 135
FIGURE 114 BASIC WAVE IMPACT ASSESSMENT..... 141
FIGURE 115: SITUATION OF THE STUDY AREA 146
FIGURE 116: TOPOGRAPHY MODEL FOR ZEEBRUGGE-BRESKENS 148
FIGURE 117: INNER DIKE OF DAMME WATERWAY AND LEOPOLD CANAL. 149
FIGURE 118: SCHEMATIC REPRESENTATION OF THE LINK BETWEEN THE 1D-MODEL AND THE 2D-MODEL..... 150
FIGURE 119: SITUATION OF THE ZEEBRUGGE- BRESKENS STUDY AREA, INCLUDING AN INDICATION OF THE PLACES WHERE BREACHES OCCUR..... 152
FIGURE 120: WATER LEVEL EVOLUTION OF STORM TIDES WITH A RETURN PERIOD OF 1000, 4000, 10000 AND 40000 YEARS..... 153
FIGURE 121: SCHEMATIC REPRESENTATION OF THE WIDTH EVOLUTION..... 154
FIGURE 122: LOCATIONS OF BREACHES (RED ARROWS)(SITUATION IN FLANDERS) 155

FIGURE 123: LOCATIONS OF FLOOD DEPTHS IN ZEELAND FLANDERS 165
FIGURE 124: LOCATIONS FOR THE RESULTS OF FLOOD DEPTHS IN FLANDERS 166
FIGURE 125: FLOOD DEPTH DURING A STORM FLOOD WITH A 1000-YEAR RETURN PERIOD AT DIKE PROFILES 373, 396 AND 413 NEAR NIEUWE SLUIS. 167
FIGURE 126: MAXIMUM WATER DEPTH (M) FOR SCENARIO 1 DURING A STORM TIDE WITH A 1000-YEAR RETURN PERIOD. 168
FIGURE 127: MAXIMUM VELOCITIES (M/S) FOR SCENARIO 1 DURING A STORM TIDE WITH A 1000-YEAR RETURN PERIOD. 168
FIGURE 128: FLOOD DEPTH DURING A STORM FLOOD WITH A 4000-YEAR RETURN PERIOD WITH A DIKE BREACH AT DIKE PROFILES 373, 396 AND 413 NEAR NIEUWE SLUIS AND PROFILE 512 AND 530 NEAR WALEN DIKE..... 169
FIGURE 129: FLOOD DEPTH DURING A STORM FLOOD WITH A 4000-YEAR RETURN PERIOD WITH A DIKE BREACH AT DIKE PROFILES 242 AND 243 NEAR HET ZOUTE AND PROFILE 233 IN KNOKKE. 170
FIGURE 130: MAXIMUM WATER DEPTH (M) FOR SCENARIO 2 DURING A STORM TIDE WITH A 4000-YEAR RETURN PERIOD. 170
FIGURE 131: MAXIMUM VELOCITIES (M/S) FOR SCENARIO 2 DURING A STORM TIDE WITH A 4000-YEAR RETURN PERIOD. 171
FIGURE 132: FLOOD DEPTH DURING A STORM FLOOD WITH A 10000-YEAR RETURN PERIOD WITH A DIKE BREACH AT DIKE PROFILES 373, 396 AND 413 NEAR NIEUWE SLUIS AND PROFILES 512, 530 AND 496 NEAR WALEN DIKE.172
FIGURE 133: FLOOD DEPTH DURING A STORM FLOOD WITH A 10000-YEAR RETURN PERIOD WITH A DIKE BREACH AT DIKE PROFILES 241, 242 AND 243 NEAR HET ZOUTE AND PROFILES 233, 234, 235 AND 236 IN KNOKKE.... 172
FIGURE 134: MAXIMUM WATER DEPTH (M) FOR SCENARIO 3 DURING A STORM TIDE WITH A 10000-YEAR RETURN PERIOD. 173
FIGURE 135: MAXIMUM VELOCITIES (M/S) FOR SCENARIO 3 DURING A STORM TIDE WITH A 10000-YEAR RETURN PERIOD. 173
FIGURE 136: FLOOD DEPTH DURING A STORM FLOOD WITH A 40000-YEAR RETURN PERIOD WITH A DIKE BREACH AT DIKE PROFILES 373, 396 AND 413 NEAR NIEUWE SLUIS, PROFILES 512, 530 AND 496 NEAR WALEN DIKE AND PROFILES 558, 584, 663 AND 684 NEAR ZEEWEG (ZWARTE GAT). 174
FIGURE 137: FLOOD DEPTH DURING A STORM FLOOD WITH A 10000-YEAR RETURN PERIOD WITH A DIKE BREACH AT DIKE PROFILES 241, 242 AND 243 NEAR HET ZOUTE, PROFILES 233, 234, 235 AND 236 IN KNOKKE AND THE INNER ZWIN DIKE (INTERNATIONAL DIKE). 175
FIGURE 138: MAXIMUM WATER DEPTH FOR SCENARIO 4 DURING A STORM TIDE WITH A 40000-YEAR RETURN PERIOD. 175
FIGURE 139: MAXIMUM VELOCITIES FOR SCENARIO 4 DURING A STORM TIDE WITH A 40000-YEAR RETURN PERIOD.176
FIGURE 140: DAMAGE FUNCTION, DAMAGE FACTOR ALPHA DEPENDING ON THE WATER DEPTH FOR ROADS AND RAILWAYS (SOURCE: TECHNICAL ADVISORY COMMITTEE FOR WATER-RETAINING STRUCTURES (TAW), VRISOU VAN ECK ET.AL., 1999, P. A-6). 182
FIGURE 141LAND USE MAP FOR FLANDERS (BACKGROUND: TOPOGRAPHIC MAP 1:10000 C NGI BELGIUM) 184
FIGURE 142 DROWNING FACTOR, NUMBERING NOT YET UNIFORM 188
FIGURE 143THE FACTOR FNG 189
FIGURE 144 SENSITIVITY ANALYSIS FOR DUROSTA CALCULATIONS P_235 (4000 YEARS). 197
FIGURE 145 SENSITIVITY ANALYSIS OF DUROSTA INPUT PARAMETERS FOR OVERTOPPING DISCHARGES. 198
FIGURE 146 PEAK PERIOD IN THE ZWIN BASIN (WIND DIRECTION NNE FOR 40000-YEAR RETURN PERIOD) 198
FIGURE 147 SENSITIVITY ANALYSIS OF WAVE PERIOD FOR OVERTOPPING DISCHARGE Q AND WAVE RUN-UP HEIGHT Z2% (ZWIN OUTPUT POINT 16 FOR A 40000-YEAR RETURN PERIOD). 199
FIGURE 148 SENSITIVITY OF WAVE RUN-UP HEIGHT WITH VARIATION OF ROUGHNESS FACTOR OF THE OUTER SLOPE GRASS COVER. 200
FIGURE 149 SENSITIVITY OF OVERTOPPING DISCHARGE WITH VARIATION OF ROUGHNESS FACTOR OF THE OUTER SLOPE GRASS COVER. 200
FIGURE 150 SENSITIVITY OF CRITICAL VELOCITY OF THE INNER SLOPE WITH VARYING CLAY AND GRASS QUALITY.201
FIGURE 151 SENSITIVITY ANALYSIS: EFFECT OF CREST HEIGHT ON OVERTOPPING DISCHARGES. 202
FIGURE 152 BASIC CASE **FS=0.66** 203
FIGURE 153 BASIC CASE **FS=1.00** (ALREADY SLIP CIRCLE WITH FS=0.66) 203
FIGURE 154 VARIANT 1 (PHREATIC LEVEL AT +3) **FS=1.03** (COMPARED TO 0.66 IN BASIC CASE). 204
FIGURE 155 VARIANT 2 ($\Phi_{DIKE\ SAND}$ 32.5°) **FS=0.71** (COMPARED TO 0.66 IN BASIC CASE). 204
FIGURE 156 VARIANT 2 ($\Phi_{DIKE\ SAND}$ 32.5°) **FS=1.00** (ALREADY SLIP CIRCLE WITH FS=0.71). 205
FIGURE 157 VARIANT 3 ($\Phi_{DIKE\ SAND}$ 32.5°, PHREATIC LEVEL +3) **FS=1.10** 205
FIGURE 158 VARIANT 4 ($\Phi_{CLAY\ DIKE}$ 17.5°, PHREATIC LEVEL +5.4) **FS=0.50** (COMPARED TO 0.66 IN BASIC CASE). 206

FIGURE 159 VARIANT 4 ($\Phi_{CLAY\ DIKE}$ 17.5°, PHREATIC LEVEL +5.4) **FS=1.00** (ALREADY SLIP CIRCLE WITH FS=0.50).206
FIGURE 160 INWARD MACROSTABILITY D_25 (308) **FS=1.43** 207
FIGURE 161 INWARD MACROSTABILITY D_25 (308) FICTITIOUS SLOPE 1:3 **FS=1.28** 208
FIGURE 162 INWARD MACROSTABILITY D_25 (308) FICTITIOUS SLOPE 1:2.5 **FS=1.18**..... 208
FIGURE 163: LOCATIONS FOR ANALYSIS OF THE INFLUENCE OF FLOOD DEPTH RESISTANCE..... 211
FIGURE 164: FLOOD DEPTH AT LOCATION A. 211
FIGURE 165: FLOOD DEPTH AT LOCATION B..... 212
FIGURE 166: FLOOD DEPTH AT LOCATION C..... 212
FIGURE 167: FLOOD DEPTH AT LOCATION D. 212
FIGURE 168: MAXIMUM WATER DEPTH (M) FOR A DIKE BREACH WITH A MAXIMUM BREACH WIDTH OF 100M..... 214
FIGURE 169: MAXIMUM WATER DEPTH (M) FOR A DIKE BREACH WITH A MAXIMUM BREACH WIDTH OF 200M..... 214
FIGURE 170: MAXIMUM VELOCITY (M/S) FOR A DIKE BREACH WITH A MAXIMUM BREACH WIDTH OF 100M 215
FIGURE 171: MAXIMUM VELOCITY (M/S) FOR A DIKE BREACH WITH A MAXIMUM BREACH WIDTH OF 200M 215
FIGURE 172DAMAGE DUE TO A BREACH OF RESP 100 AND 200 M IN ZEEUWS VLAANDEREN 217
FIGURE 173DAMAGE DUE TO A BREACH OF A) 100 AND B) 200 M IN FLANDERS 218
FIGURE 174: PARAMETERS FOR SEAWALL FAILURE: SENSITIVITY ANALYSIS OF STARTING MOMENT OF DIKE BREACH 219
FIGURE 175: MAXIMUM WATER DEPTH DURING A STORM TIDE WITH A 40000-YEAR RETURN PERIOD WHEREBY A DIKE BREACH OCCURS BEFOR HW.(TO BE COMPARED WITH FIGURE 138)..... 220
FIGURE 176: MAXIMUM VELOCITY DURING A STORM TIDE WITH A 40000-YEAR RETURN PERIOD WHEREBY A DIKE BREACH OCCURS BEFOR HW (FIGURE IS TO COMPARE WITH.FIGURE 139)..... 221
FIGURE 177DAMAGE MAPS FOR ZEEUWS-VLAANDEREN EN FLANDERS –EARLIER FAILURE..... 222
FIGURE 178: PARAMETERS FOR BREACH DEVELOPMENT FOLLOWING SEAWALL FAILURE DURING A STORM TIDE WITH A 40000-YEAR RETURN PERIOD: ADDITIONAL DIKE BREACH NEAR CADZAND 223
FIGURE 179: LOCATIONS OF ADDITIONAL DIKE BREACHES AT CADZAND..... 224
FIGURE 180: MAXIMUM WATER DEPTH DURING A STORM TIDE WITH A 40000-YEAR RETURN PERIOD WHEREBY 3 ADDITIONAL DIKE BREACHES OCCUR IN THE VICINITY OF CADZAND. 224
FIGURE 181: MAXIMUM SPEEDS DURING A STORM TIDE WITH A 40000-YEAR RETURN PERIOD WHEREBY 3 ADDITIONAL DIKE BREACHES OCCUR IN THE VICINITY OF CADZAND..... 225
FIGURE 182 DAMAGE MAPS FOR ZEEUWS-VLAANDEREN EN FLANDERS – EXTRA FAILURE..... 226

1. INTRODUCTION

The responsibilities of Dutch and Belgian coastal defence administrations end at the respective national borders. In order to achieve common approaches, a cross-border project, including some form of transnational co-operation with the responsible local authorities like the ”Zeeuws-Vlaanderen Water Board”, became necessary. Within the INTERREG IIIB project COMRISK (EU-project – www.comrisk.org) and under the auspices of the North Sea Coastal Management Group, an international platform to implement such a cross-border pilot study is founded. The Coastal Division of the Flemish Community leads the subproject about the Flood Risk in the cross boundary area Flanders-Zeeuws-Vlaanderen. The study is carried out by the consultant IMDC and advisers. The calculation of damage in the Netherlands was carried out by “Rijkswaterstaat” (DWW). A steering committee was established to guide and discuss the results. The committee consists of governmental organizations of Flanders (Coastal Division and Flanders Hydraulic Research) and the Netherlands (Rijkswaterstaat, the province and the polder board). The contribution of the Dutch and Flemish authorities was essential for their data and knowledge of the coastal defence structures.

The present report concerns the study of flood risks in Flanders and Zeeuws-Vlaanderen (Dutch name) resulting from possible failures in the sea defence structures between Zeebrugge and Breskens. The study was made within the scope of the COMRISK InterregIIIB project.

Risk is defined as the product of the probability of occurrence of events and the consequences (damage, casualties). Knowing the risk is interesting because of various reasons: the comparison of risks in order to set priorities, the determination of the expected damage for insurance purposes, the implementation of a cost-benefit analysis to assess investments in engineering works/dikes/beach supplementations.

Two methods exists to determine the risk: a probabilistic and a deterministic method. The probabilistic method uses the probability distribution of all relevant parameters, including the uncertainty about these parameters. All parameter combinations are checked to see whether or not they result in failure (resisting forces smaller than ‘driving’ forces) and the probability of occurrence is determined for every combination; integration results in the total probability of failure.

In the deterministic method for a number of return periods a determination is made where failure occurs. By doing so for a large number of return periods, the risk can be determined by means of integration.

In this study the deterministic method was opted for, for various reasons:

a) the method gives additional information about flood frequency: the same risk may be caused by relatively common floods involving minor damage or by very high return periods involving major damage.

b) in order to determine the housing policy in flood plains/insurance of damage during floods, the government wants to have damage maps for various return periods.

c) with the probabilistic method it is very computation-intensive if flood calculations/damage assessment must also be linked to the probability of failure. After all, a computation-intensive flood calculation must be made for all possible combinations. Thus failure may occur at a low water level and low resistance (e.g. resistance characteristics of the dike material) or at a high water level and a high resistance. In the first case, however, the damage will be a lot less than in the second case. In practice, one water level is determined (the water level contributing most to the probability of occurrence) for which the flood calculations are then made.

The drawback of the deterministic method is that it is more difficult to take the uncertainty of parameters into account. This can be overcome by calculating the 'expected' risk and the spread thereof. The added benefit is that it gives an overview of the sensitivities and the uncertainty of the end result (in other words, it is avoided that a very high risk is found due to a very high uncertainty of 1 parameter).

In this study the damage is calculated for a number of return periods. For this purpose, the external forces and characteristics of the sea defences were determined first. The extreme value distributions of the wave height and water levels in deep water were transformed, by means of a wave model, to a location just off the coast where the waves do not yet affect the morphology. To know the wave height at the toe of the dike, the variation of the bathymetry during the storm must be taken into account: after all, the beach in front of the dike will erode, resulting in a lower wave resistance and a greater wave height at the toe of the dike.

For the characteristics of the dikes and dunes, existing data were used (grain size diameters, a digital terrain model (DTM) to determine the height and geometry, building plans, …) and additional measurements were carried out (soundings, borings, groundwater level measurements).

It was then checked whether the dune or dike holds out. The existing (Dutch) method was used in part to check the sea defence, but it was adapted where necessary.

Once the locations are known where the dune or dike bursts and the necessary assumptions are made with regard to the dimensions of the dike breach, flood modelling can be carried out.

Based on a high-resolution DTM of Flanders and Zeeuws-Vlaanderen, a 2-dimensional hydrodynamic model of the hinterland was made. The boundary conditions are determined by the water level at sea, incorporating the dike breaches.

Both in Flanders and in the Netherlands, models exist to assess the damage and casualties by means of the maximum water level and the maximum horizontal flow velocity or the maximum rate of water level rise. Land use maps (GIS) are used, as well as functions that determine the relative damage compared to the maximum damage (the value of a house, for instance) depending on the water level.

The report first gives a short description of the hydrodynamic boundary conditions, the methodology used, the available data, the possible breaches for various return periods, the floods that may ensue and finally the corresponding damage and casualties.

2. DESCRIPTION OF THE PROJECT AREA

2.1. Introduction

The project area is located partly on Belgian (Flemish) and partly on Dutch soil. The project area can be divided into three zones:

- Flanders ('Vlaanderen' in Dutch language);
- Zwin (Flemish part, Dutch part);
- Zeeuws-Vlaanderen (Dutch name) (Netherlands).

Figure 1 shows these three zones.

Figure 1 Project area overview.

2.2. Dike structure

2.2.1. Flanders

An important part of the Flemish dikes were reinforced after 1953 (concrete slab revetment). A part of the dikes has a stone pitching revetment. The dikes have a broad width and always a beach in front of them, covering the dike. Below are some photos of Flemish dikes.

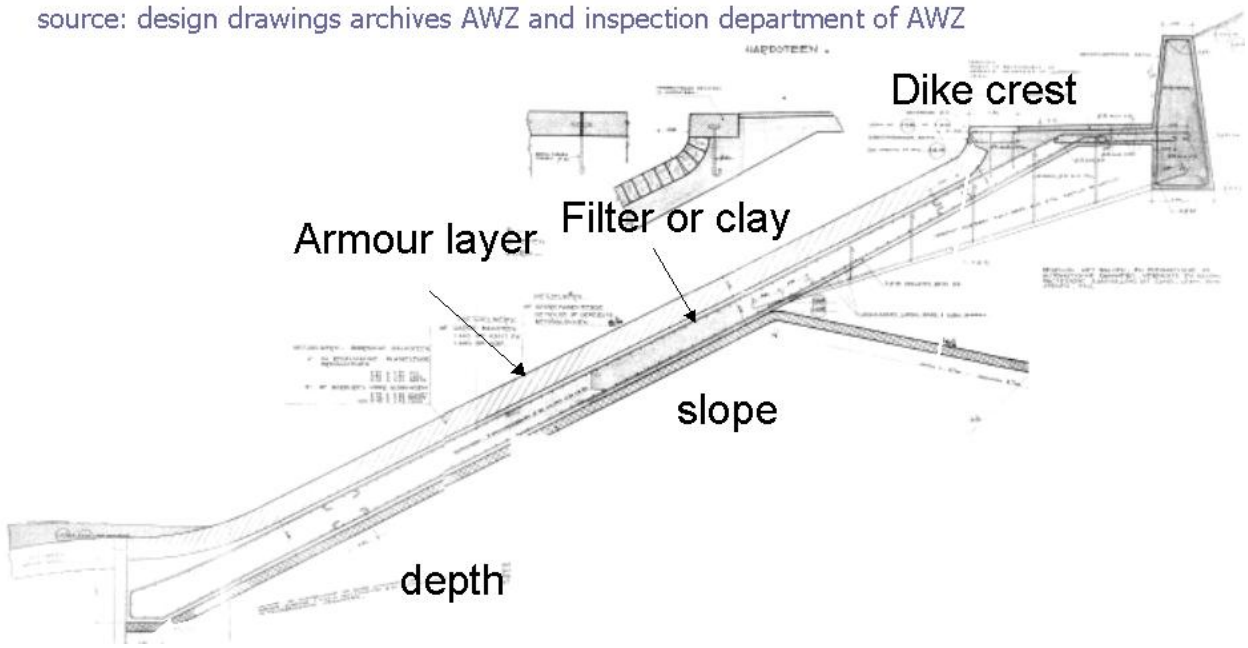

Concrete slab revetment drawing (source: drafts from the AWZ archives and AWZ inspection services).

Profile of the dike, with a sample each 0.5 m. Crest of the dike at the bottom right At the crest of the dike sand is found, going to clayed sand and at the deepest points (-15m) even organic material (wood) is found

Photo of Knokke sea defence.

2.2.2. Zwin

With regard to the Zwin inner dikes, the dike profile of Figure 60 and Figure 61 was assumed. The core material consists of sand, covered with a 0.5m-thick layer of clay, widened to 0.8m below +8m TAW. The landward slope consists of a berm with a somewhat gentler slope below it. The dikes are covered with grass.

2.2.3. Zeeuws-Vlaanderen

Zeeuws-Vlaanderen has both dikes and dunes. On the seaside the dikes typically have a revetment mainly consisting of stone pitching below a (flatter) berm and an asphalt revetment from just below the berm level to a few metres above this berm.

Stone pitching, asphalt revetment on the seaward side of the dike.

Asphalt revetment on the seaward side of the dike.

The landward side of the dike primarily has a grass cover.

3. HYDRODYNAMIC BOUNDARY CONDITIONS

To deduce the hydrodynamic boundary conditions the report on 'Hydrodynamic boundary condition book for the coast' ('Hydrodynamische randvoorwaardenboek kust', IMDC-report *I/RA/11226/03.041/KTR*) is referred to.

Below, a comparison is made between the hydrodynamic boundary conditions along the Dutch coast and the hydrodynamic boundary conditions deduced by DWW.

3.1. Formulation of the hydrodynamic boundary conditions in deep water

Three boundary conditions are important when designing structures and when predicting the morphological evolution: the water level, the waves and the wind. The **water level** has an influence on the wave height (due to depth limitations for the waves) on the one hand, and determines the (overtopping) discharge over the dike on the other hand.

The **waves** determine the action of forces on structures (pier, beach, …).

The **wind** determines the sand transport on the beach (aeolian transport) and provides energy to the waves.

For the extreme values, an extreme value analysis of deep water was made first (where most wave data are available). With regard to the water level, the time series of the Ostend observations (since 1925) were analysed.

The extreme values obtained were transformed towards Ostend by means of the numerical wave model developed.

As no measurement results but extrapolated extreme values are taken into account, certain assumptions need to be made with respect to the wave periods and the form of the spectrum. For the wave period a relation between wave height and wave period is assumed, for the spectrum a typical form during a storm (Jonswap) is assumed. A singular relation between water level and wave height is also assumed (1 relation per direction) (e.g. a 1000-year water level corresponds with a 1000-year wave height).

The extreme value analysis is made by selecting POT (Peak over Threshold) values per wind direction and design duration. POT values are selected per parameter, independent of each other.

3.1.1. Water level

The water level is the sum of the water height caused by the (astronomic) tide and by the (shifted) storm surge. It is important that this division is made, as only the storm surge is a stochastic parameter. In addition, no extreme values can be found for (wind) directions with relatively low extreme water levels if only the water level is considered, as the sum of surge and astronomic tide height is too small compared to the threshold value (e.g. a storm at neap tide results in a water level smaller than the water level at spring tide without a storm). It is necessary to know the extreme value distribution of the water level per direction. After all, the water level is important for the height of certain constructions on the one hand, but for constructions that can only be attacked from certain directions, the water level also determines the waves capable of reaching the construction (because they are limited by the water depth).

A statistical analysis of the storm surge per direction by means of the Peak Over Threshold method was made. The storm surge was obtained by deducting the astronomic tide (obtained with a tide analysis) from the measured tide.

For every water height the probability of occurrence must be determined, by means of integration: per (astronomic) high-water level (with known probability of occurrence), the necessary (shifted) surge is calculated (= difference between the astronomic and the considered water level), and the corresponding probability of occurrence of this surge. Integration of all possible astronomic high-water levels gives the total probability of occurrence.

The extreme value distributions of the water level above are deduced for the tide meter in Ostend. For other locations it is corrected by means of the high-water spring. It is assumed that the storm surge during the 1000-year storm is uniform over the entire coastline, and that only the tide causes variations. An analysis of the 100-year water levels (Verwaest, 2000), however, shows that the difference between the 100-year water level and the level of an average spring tide is higher in Vlissingen (1.88m) than in Zeebrugge/Ostend/Nieuwpoort (1.7m). This may be explained by the Scheldt mouth actually being formed by the Zeebrugge – Westkapelle line, as the water levels gradually increase from the estuary to the upstream river (e.g. Vlissingen-Terneuzen difference is 25 cm at spring tide, 45 cm during a storm). This extra increase will be taken into account linearly between Zeebrugge and Vlissingen.

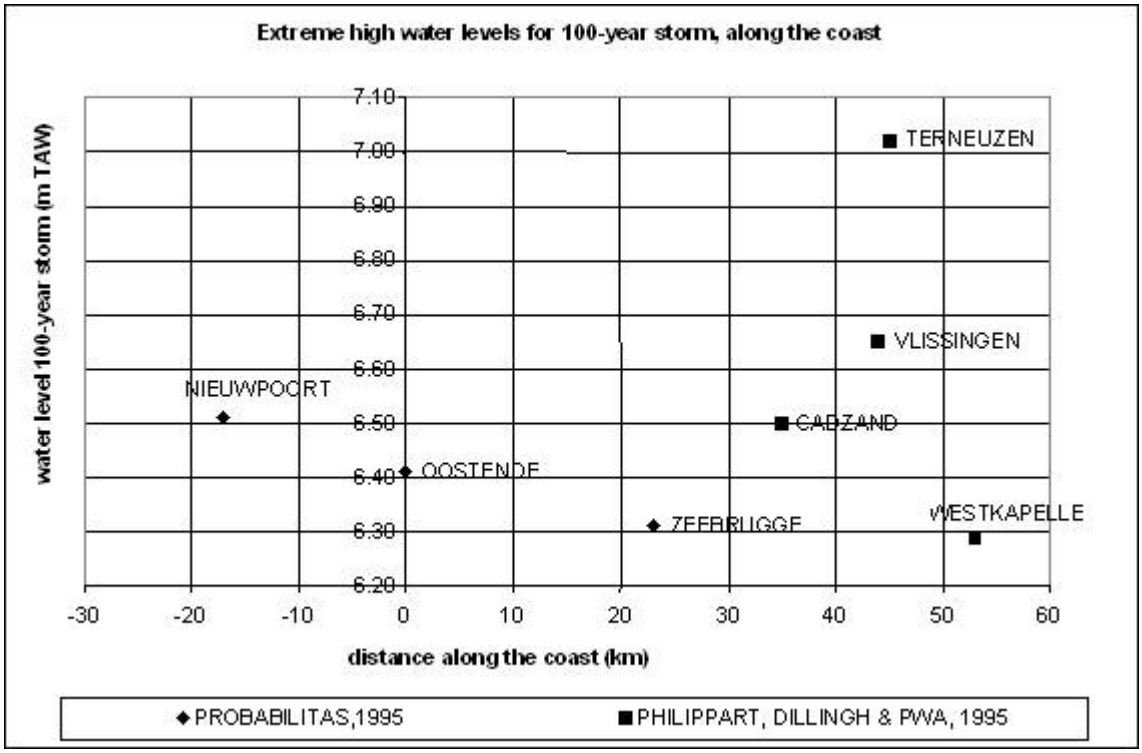

Figure 2 Evolution of extreme high water levels, for the 100-year storm along the coast.

3.1.2. Waves and wind

The results of various measurements were combined. First, relations were sought between the values measured in various different locations. Once these relations were known, the missing data in case of failure of the basic unit were complemented by adjusting the measurements of another unit using the relation obtained.

In addition, a relation was determined between the wave height and the wave period.

3.1.3. Statistische verdeling

No specific distribution function is assumed in the method used. While a specific distribution function is assumed in other methods and only the distribution-related parameters are unknowns (to be fitted), an unknown, being the type of distribution, is in fact added in the method used.

For this purpose, the various possible frequency distributions are categorised. These categories are then represented by a generalised extreme value distribution, describing the right-hand tail (the extreme values) of all probability density functions pertaining to that category. The other probability density functions in the category are called 'marginal probability density functions'.

The 3 categories or subsections can be categorised on the basis of the extreme value index γ, determining the shape of the tail of the generalised extreme value distribution and consequently all marginal probability distribution functions in that category. In case of an increasing γ the tail of the distribution becomes heavier, indicating a higher probability of occurrence of high values. The category of $\gamma = 0$ (called the 'exponential' category) includes, among other things, the following marginal distributions: the exponential, log normal, Weibull, gamma and Pearson type III distributions. The Pareto category ($\gamma > 0$) includes, among other things, the log hyperbolic and log Pearson type III distributions. The latter category concerns extreme value distributions with a heavy tail, meaning a large increase of the studied quantity with increasing return periods. As γ drops to 0, the tail of the distribution becomes lighter, and finally becomes a normal to light tail for $\gamma = 0$. The 'normal' tail is reached with the exponential distribution. In addition, the exponential category includes the Weibull distributions important for coastal engineering. The tail of these distributions can be described by means of the Weibull index τ. When $\tau = 1$, the Weibull distribution can be reduced to an ordinary exponential distribution. As τ becomes larger than 1, the tail will become lighter. This is called a super-exponential tail distribution. As τ becomes smaller than 1, the tail will become heavier (sub-exponential). In other words, there is an intermediate area where both the sub-exponential Weibull distribution and the Pareto distribution can be used to describe the extreme values.

Finally, there is the category whereby $\gamma < 0$ (Beta distributions), for which a maximum extreme value exists, meaning that the tail has an upper limit. Distributions of this category may be expected with depth limitation of waves, for instance, but are rather rare (and will probably not occur in deep water).

The probability distribution function and the corresponding parameters are determined in various phases:

- phase 1: deduction of POT values;
- phase 2: drafting of QQ plots;
- phase 3: deduction of the extreme value index γ and choice of optimum threshold;
- phase 4: deduction of the other parameters;
- phase 5: determination of the return periods.

3.2. Verloop van de storm

3.2.1. Verloop van de waterstand tijdens een storm

The theoretical storm can be described by means of the following equation:

$$S = S_{\max} \cos^2(\frac{\pi t}{T_s})$$

whereby S_{max} is the maximum storm surge at HW as deduced from a statistical analysis of storm surges and T_s is the duration of the storm. The evolution is shown graphically in Figure 3.

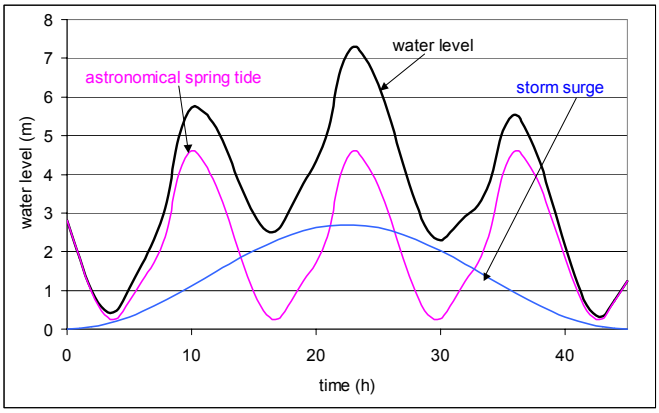

Figure 3 Evolution of the astronomical tide, storm surge and water level.

In the Netherlands a storm duration T_s of 35h was assumed for a long time, but in a recent study it is assumed that T_s=20 to 40 times S_{max}, which would result in a storm duration of 44 to 88 hours in a 1000-year storm (S_{max}=2.2 m).

3.2.2. Some examples for Ostend

The water levels measured are divided into a harmonic component and surge. The analysis is made based on the surge, as this parameter is more strongly related to the storm than the total water level (cf. storms occurring at neap tide give low water levels).

Storm of 1953 in Ostend: surge

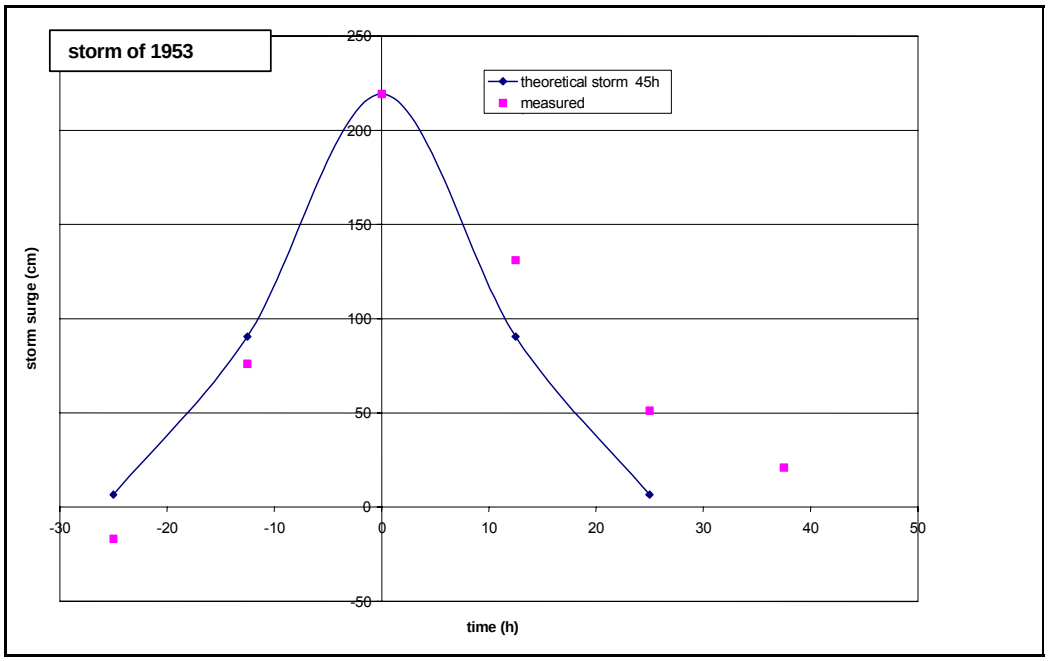

Figure 4 Evolution of the storm surge during the storm of 1953.

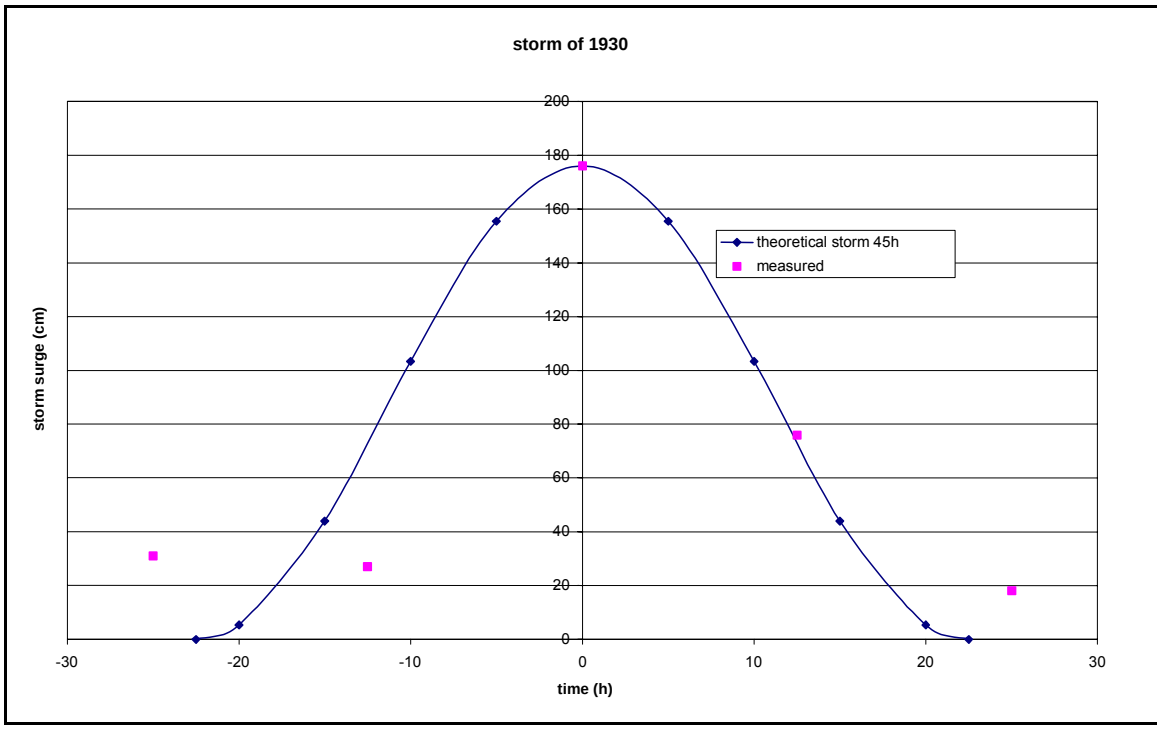

Figure 5 Evolution of the storm surge during the storm of 1930.

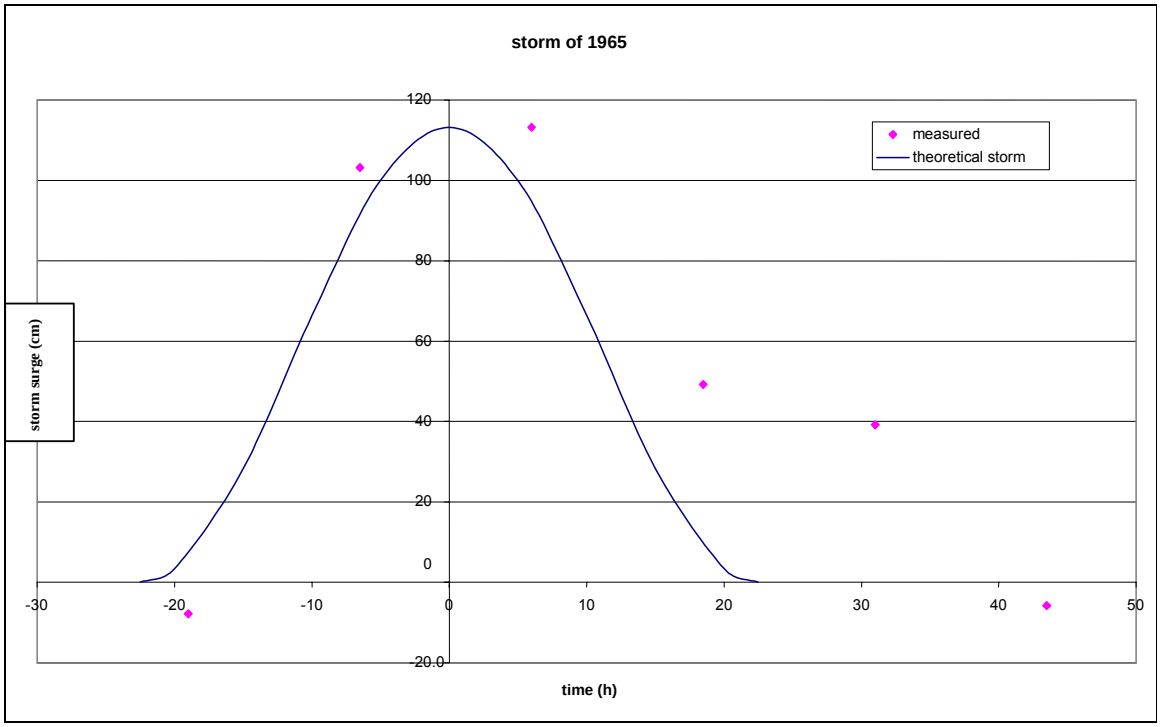

Figure 6 Evolution of the storm surge of 1965.

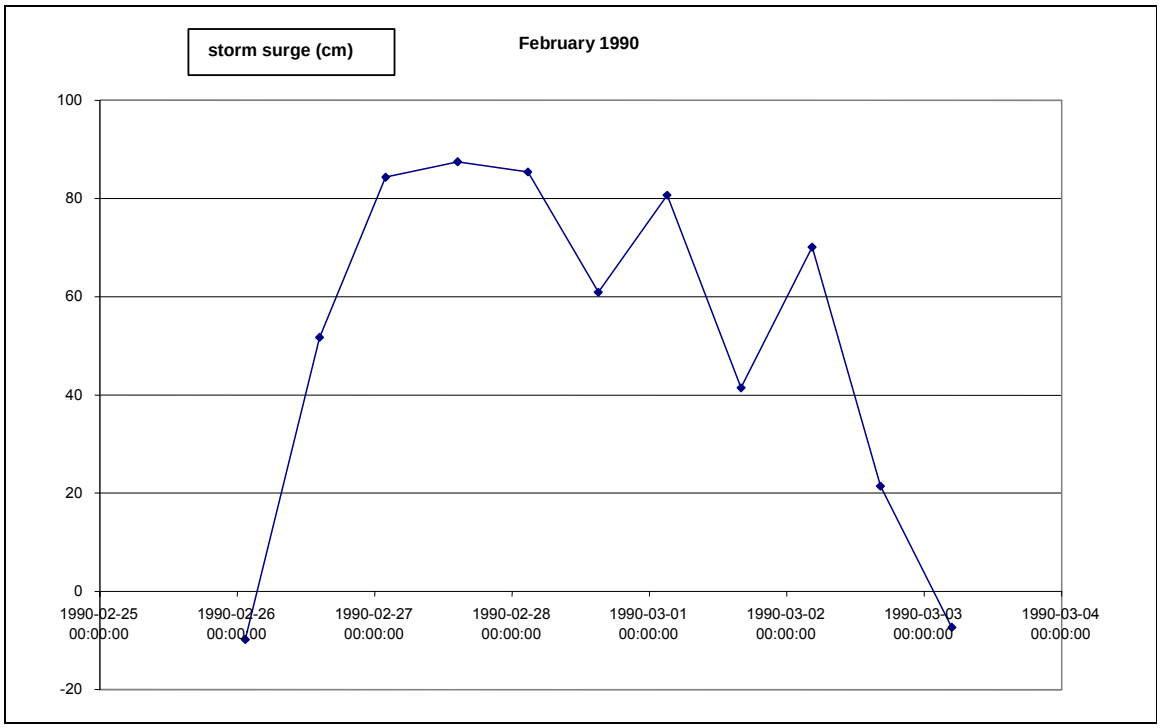

Figure 7 Evolution of the storm surge during the storm of 1990.

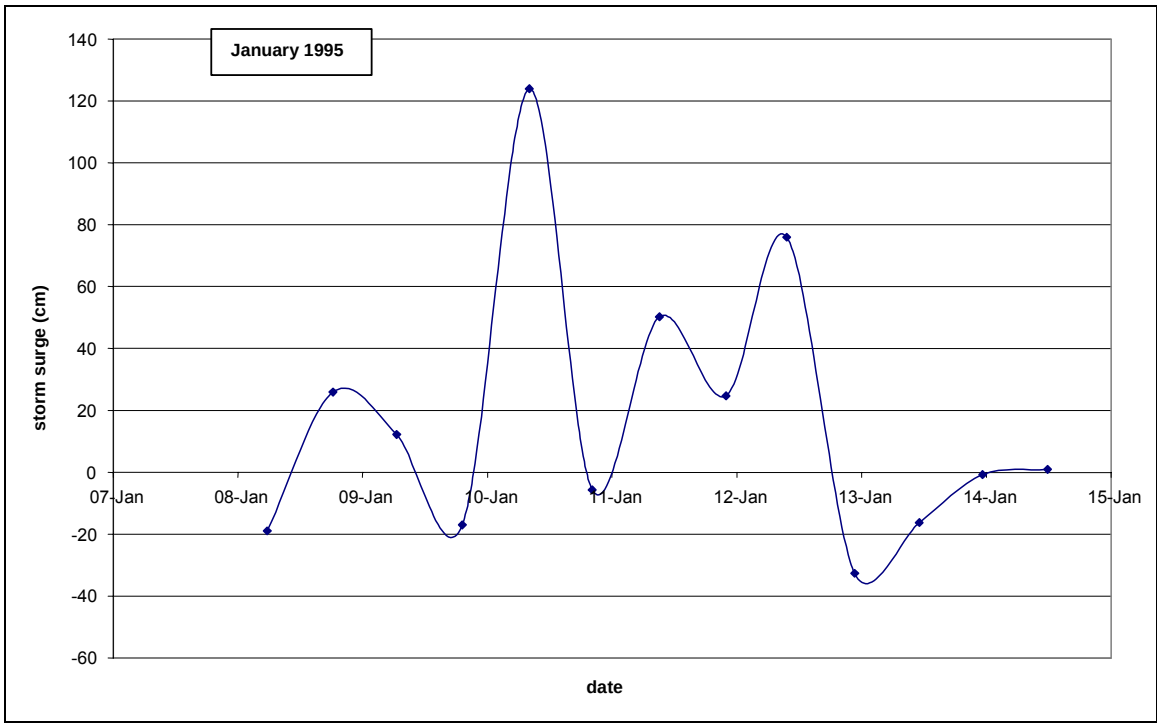

Figure 8 Storm of January 1995.

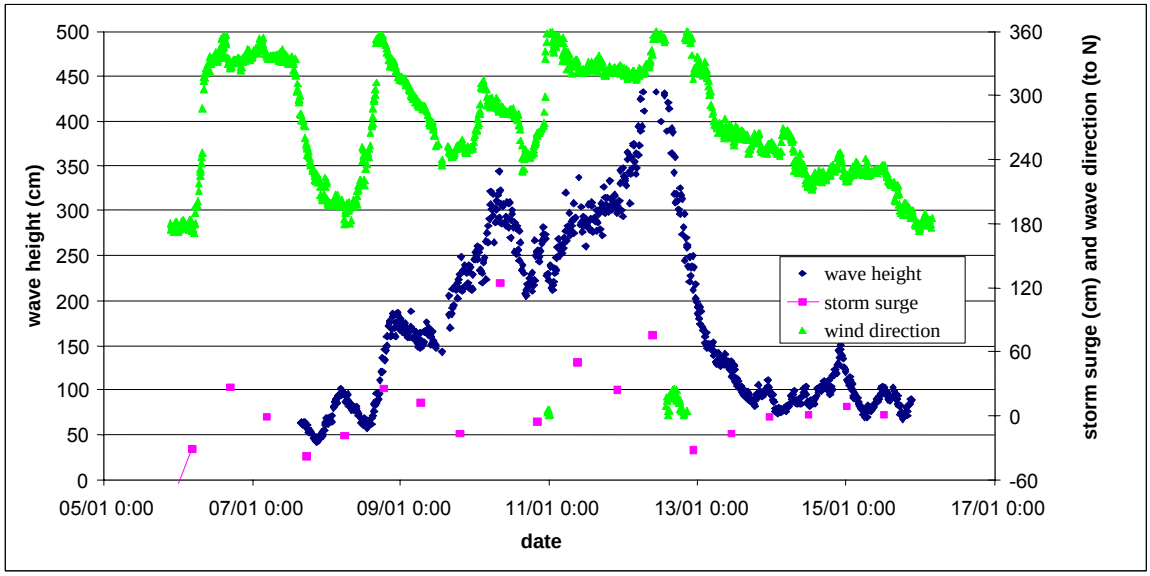

Figure 9 Waves and wind directions during the storm of January 1995.

3.2.3. Conclusions

The storm evolution is rather asymmetric, with a sudden rise of the surges and a slower drop of the surges after the peak.

Usually a storm duration of 45 hours seems realistic, but for instance in February 1990 the storm lasted 85 hours (with a limited surge though).

The figure below considers all the storms between 1929 and 2002. The storm duration is defined here as the duration with a storm surge in excess of 30cm. Only storms that have a surge in excess of 90cm at their peak, are considered.

Figure 9 shows that for short periods of time high surges may occur (in case of sudden wind turns).

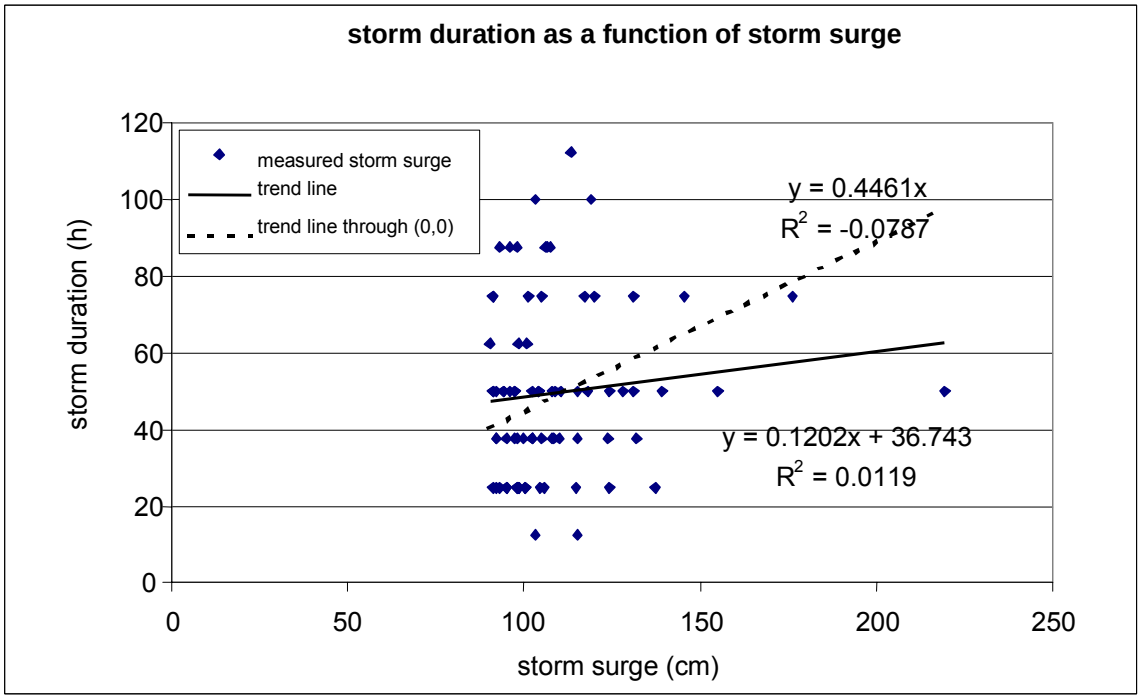

Figure 10 Storm duration depending on the maximum storm surge.

The spread of the results rather suggests that there is no or hardly any relation between the storm surge and storm duration. The high storm durations, however, appear to come from storms where the storm surge varies from 30 to 80cm during a number of tides (i.e., relatively small).

Therefore it was decided to make an analysis of the size of the storm surge.

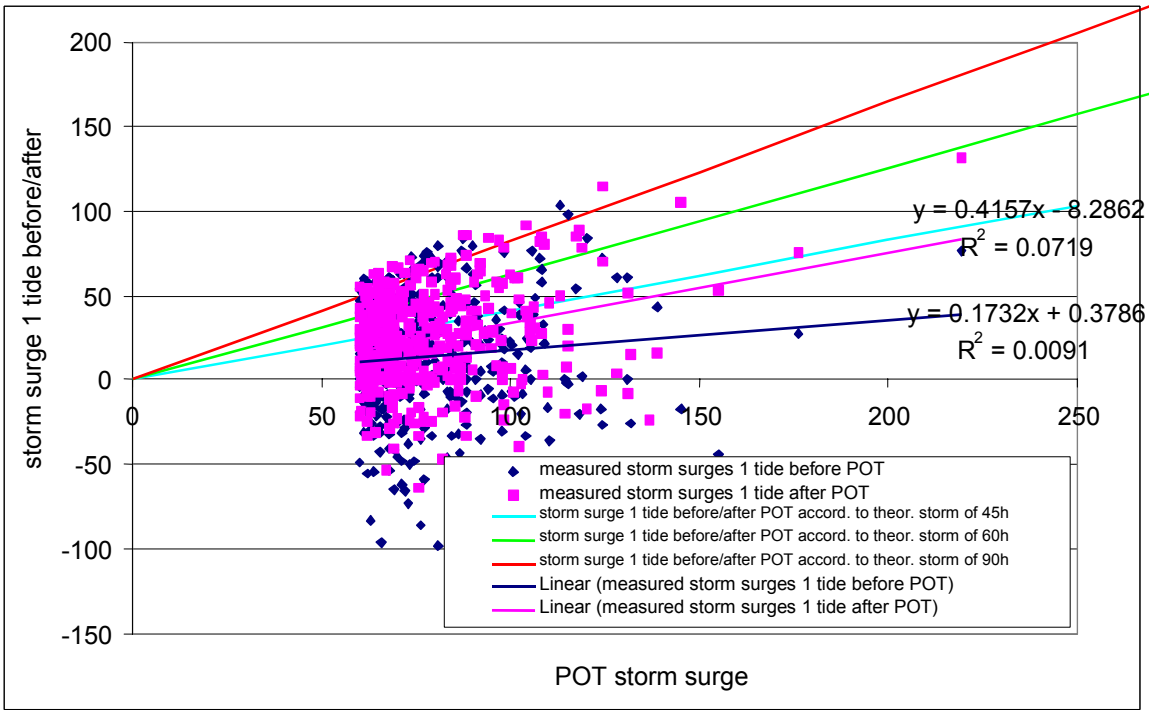

Figure 11 Surge with HW right before and after POT-HW.

Figure 11 confirms that the storm evolution is asymmetric (the surge with the previous peak is about half the next peak. The spread remains large. According to the trend analysis, a theoretical storm of 45h correctly predicts the next peak, while the previous one is overestimated.

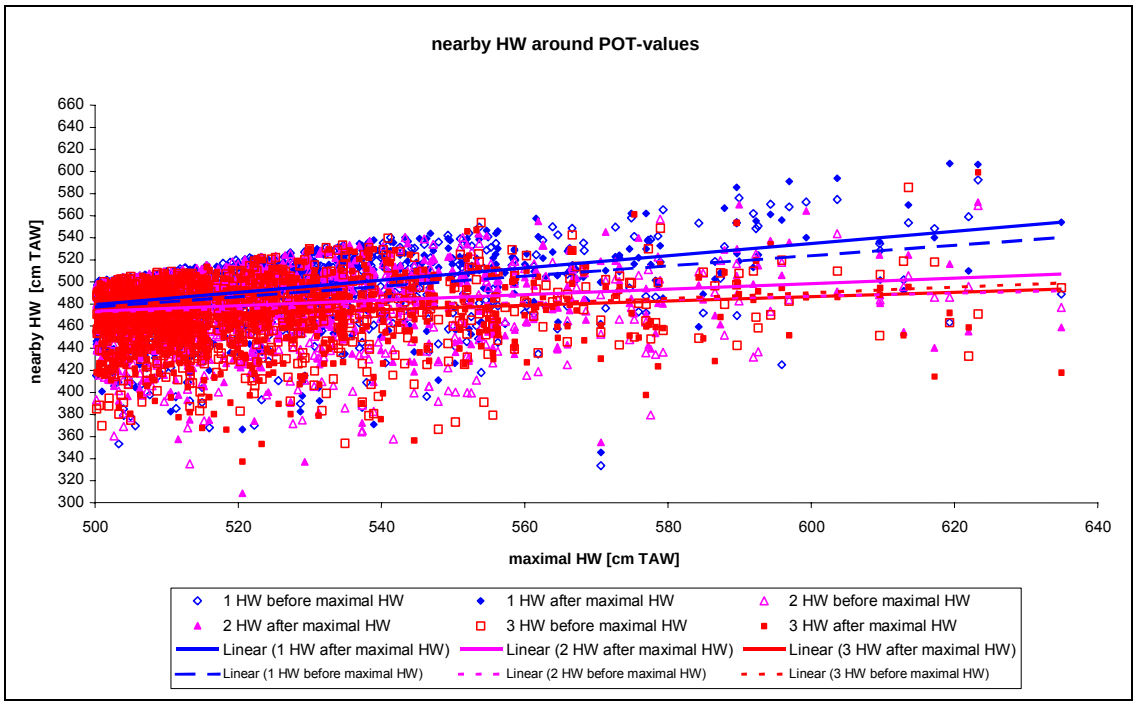

Figure 12 Relations for Vlissingen (with water levels instead of surge) (IMDC, 2003, within the scope of the Sigma plan).

However, Durosta calculations show that a slight asymmetry has no effect.

A comparison between the theoretical profile (graph0) and the asymmetric profile (graph1) shows that this has little to no effect.

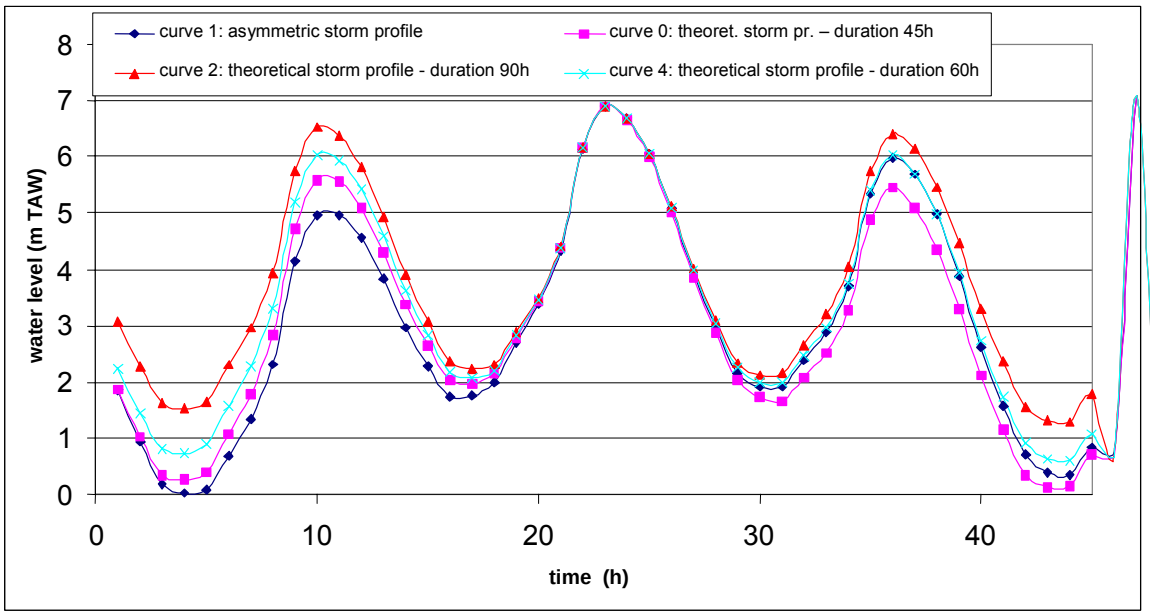

Figure 13 Evolution of a number of storm profiles during 45 hours.

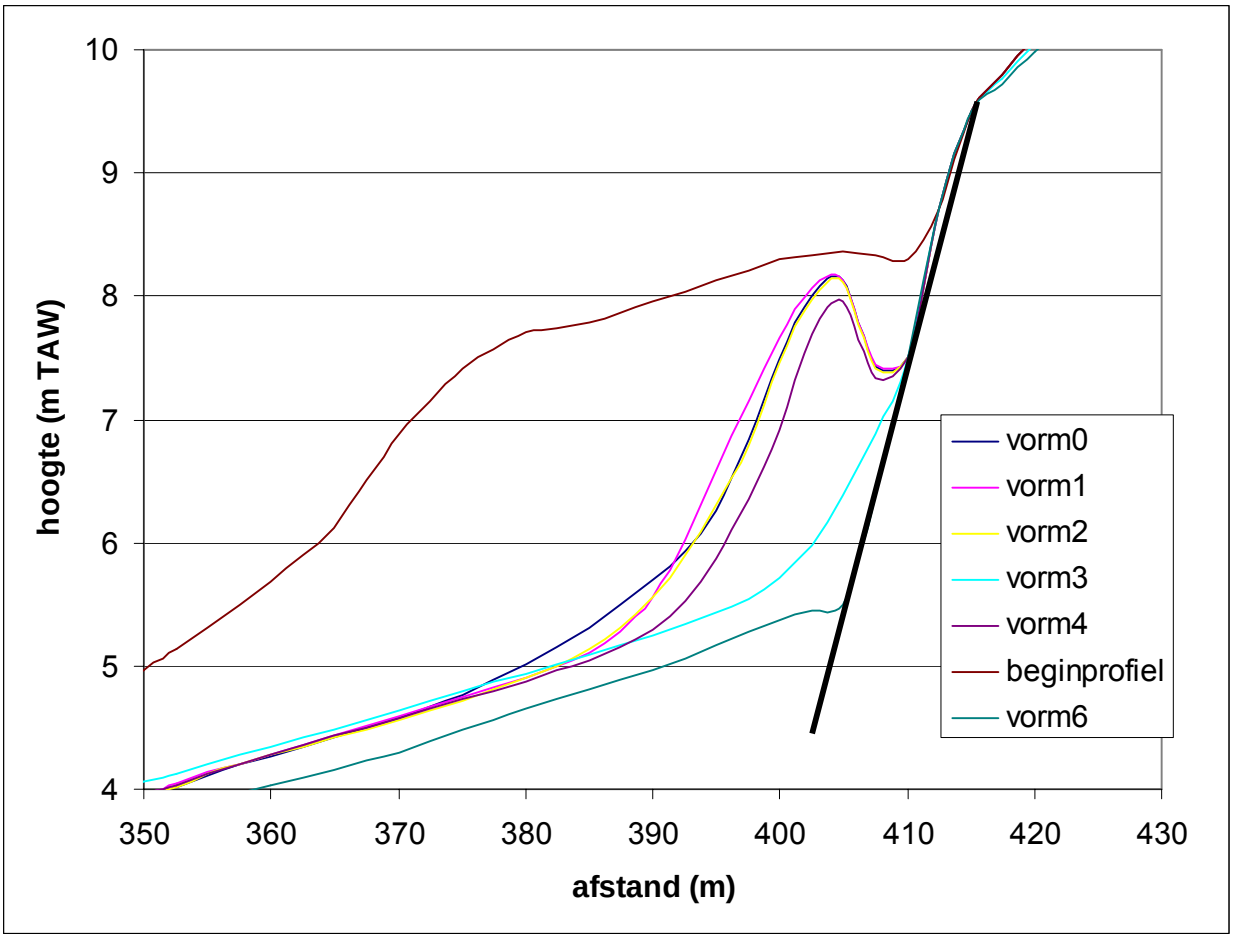

Figure 14 Erosion profiles after storm (initial profile for Knokke, profile 239)for the storm profiles of Figure 13)

If we take the average of the surge just before and just after the POT-HW, the assumption of a storm duration is a rather conservative estimate for the height of the surge during the first HW before and after the POT.

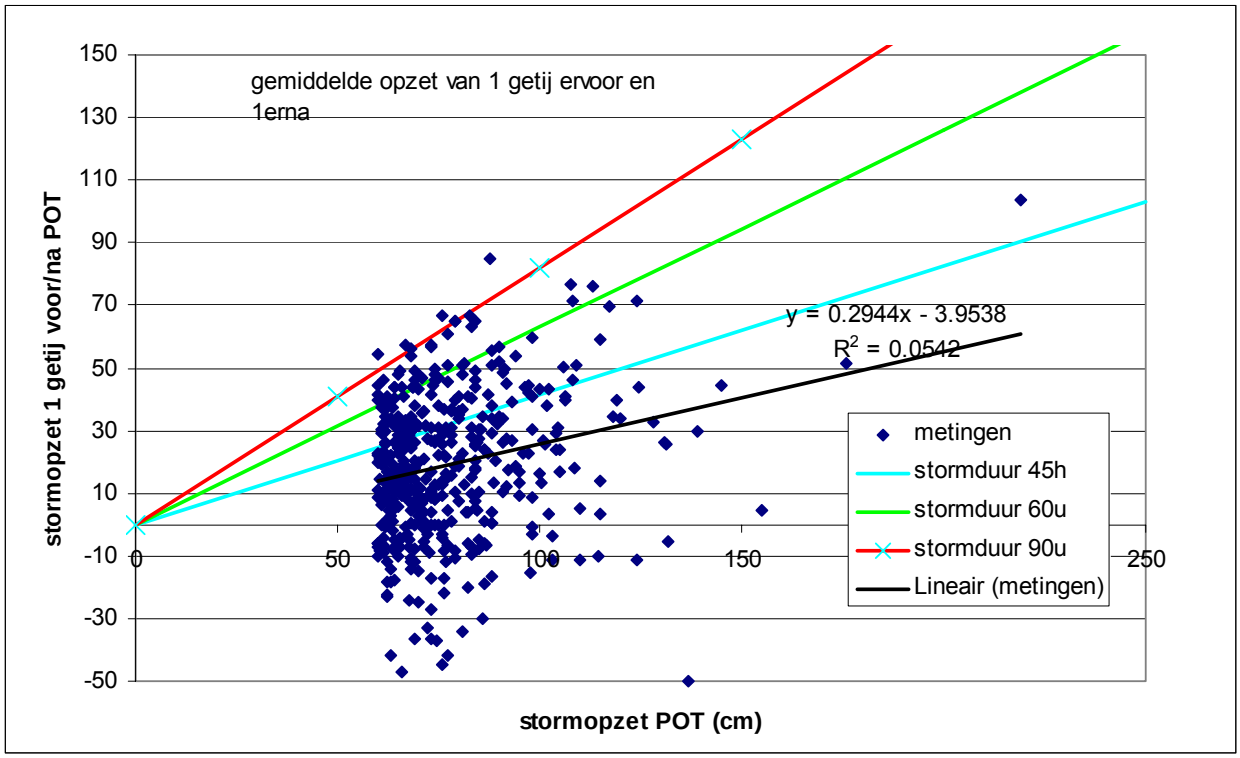

Dutch	English
stormopzet 1 getij voor/na POT	storm surge 1 tide before/after POT
gemiddelde opzet van 1 getij ervoor en 1 erna	average surge 1 tide before and 1 tide after
stormopzet POT (cm)	storm surge pot (cm)
metingen	measurements
stormduur	storm duration
lineair (metingen)	linear (measurements)

Figure 15 Comparison of the measured and theoretical surge (average of right before and right after POT).

Figure 15 shows that, according to the trend analysis, a storm duration of 45 hours is rather conservative. However, the spread is too extensive for the storm duration estimate of 45 hours to be called conservative. A storm duration of 90 hours does seem an upper limit. The influence of higher surges can also be seen in Figure 14: the actual storm duration was kept at 45 hours, but the evolution over these 45 hours is resp. according to the middle 45 hours of the theoretical storm of 90 hours (graph3) and 60 hours (graph4).

It was also examined what happens when the storm duration is a full 60 hours (no influence, not in the figure) and 90 hours (graph6, does have an influence).

Analysis of the second HW before and after the POT

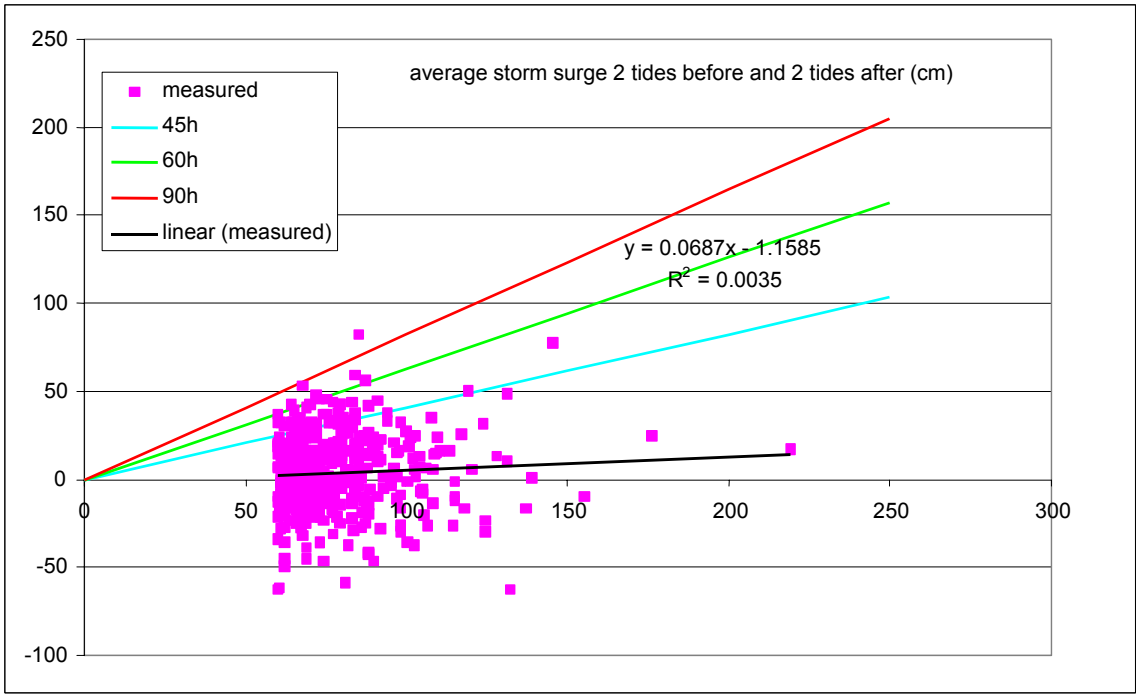

Figure 16 2nd HW before and after POT

Figure 16 shows that the second HW no longer has large surges. A storm duration of 45 hours also gives slightly conservative results.

Finally, it was examined whether a storm with a smaller return period, but with a longer duration, could cause more damage. Linking a lot less probable storm duration (90 hours) to a lot more probable storm peak (100-year storm instead of 1000-year storm) does not give a significantly higher erosion.

For information purposes it can be stated that 30% of the storms have a 'storm duration' in excess of 45 hours, 1.7% of the storms have a storm duration in excess of 90 hours (whereby the storm duration must be seen as a parameter giving the size of the nearby peak depending on the size of the peak). The 100-year storm with a duration of 90 hours is thus less probable than the 1000-year storm with a duration of 45 hours (even though it would be statistically inappropriate to put a figure on the probability of occurrence of the storm duration).

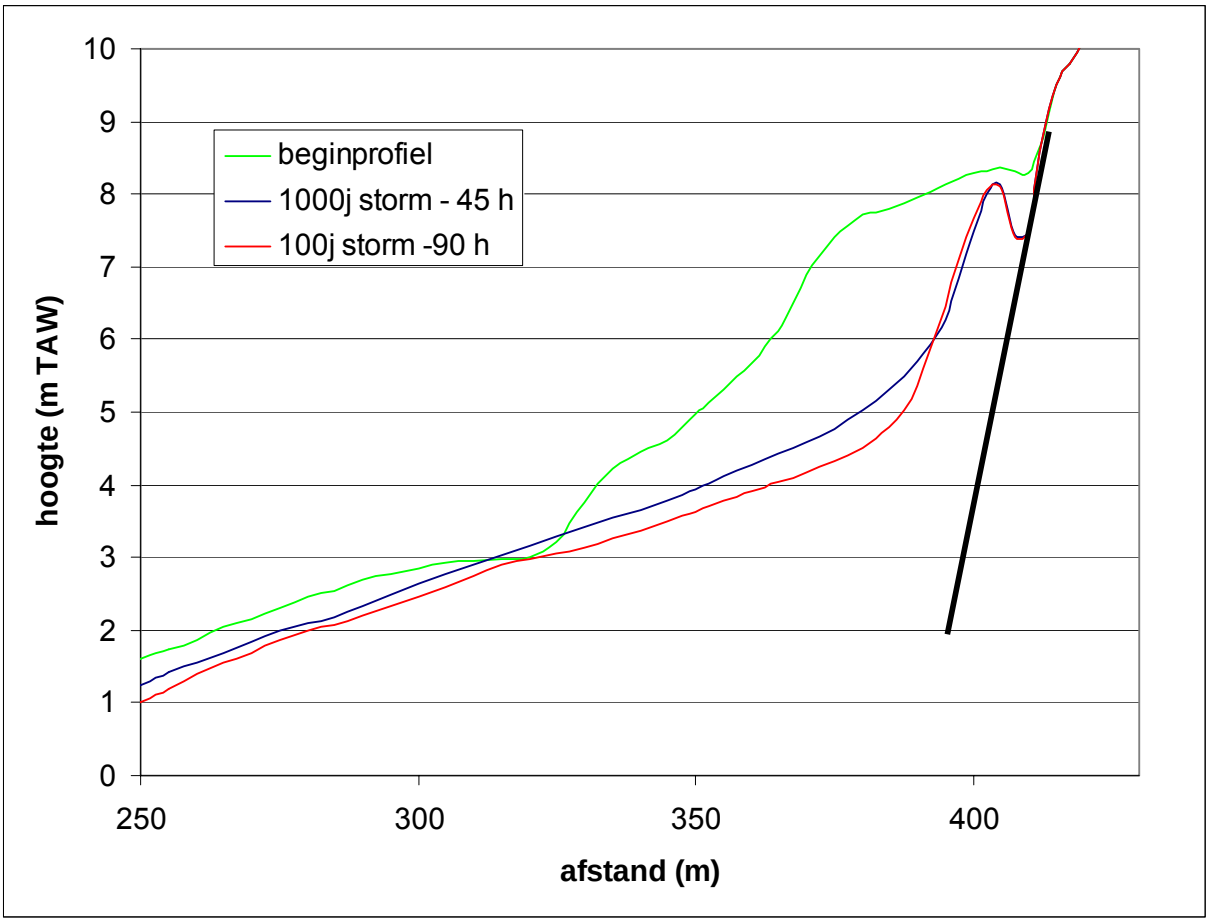

Dutch	English
beginprofile	original profile
afstand	distance
hoogte	level

Figure 17 Erosion profile for two storms with different return periods (1000 y and 100 y, with corresponding surges of 2.2 and 1.6m, respectively) and durations (45 and 90h, respectively).

3.2.4. Conclusions

- The storm duration and storm surge have a poor correlation.
- A better parameter would seem the size of the storm surge 1 tide before and after the HW with a maximum water level.
- If the commonly used evolution of the storm surge (in accordance with a cosine – square) is used, a storm duration of 45 hours gives good results, though with a great spread. A storm duration of 90 hours seems an upper limit.
- The storm surge 2 tides before and after the maximum tide has little relevance anymore.
- Linking a lot less probable storm duration (90 hours) to a lot more probable storm peak (100-year storm instead of a 1000-year storm) does not result in a significantly higher erosion (30% of the storms have a 'storm duration' in excess of 45 hours, 1.7% of the storms have a storm duration in excess of 90 hours (whereby storm duration must be seen as a parameter giving the size of the nearby peak depending on the size of the peak). The 100-year storm with a duration of 90 hours is thus less probable than the 1000-year storm with a duration of 45 hours (even though it would be statistically inappropriate to put a figure on the probability of occurrence of the storm duration)).

- It is proposed to continue working with a storm duration of 45 hours.

These conclusions cannot be simply extrapolated to other situations.

3.3. Beach erosion during the storm

During a storm the beach in front of the dike will erode. Because of this reduction in bottom level, the waves can penetrate further and the wave height at the toe of the dike will thus be larger than if there were no beach erosion. By means of Durosta (Steetzel, 1993) the beach erosion during the normative storm is determined. Durosta is a time-dependent, one-dimensional model that determines the evolution of the wave height in the cross-section considered, by means of an internal wave model. This wave climate causes sand displacement in the cross-section and possibly a loss of sand at the sea edge. The model takes into account the effect of hard structures such as sea dikes. The main parameters are the hydrodynamic parameters and grain size. The model takes the effect of hard structures (dikes) on the beach into account (the dike can be considered as not-erodable and will cause erosion holes, for instance).

3.4. Determination of the wave height and water level at the toe of the dike

A new profile is obtained after the storm. For this profile the wave height at the toe of the dike is then determined for hydrodynamic conditions occurring at the peak of the storm. This is slightly conservative, as the profile will have further evolved after the peak of the storm.

In principle, the wave height at the toe of the dike must be known. However, most wave models (e.g. Swan, Endec, …) give less reliable wave heights with very small water depths. A certain safety margin is applied to measure the wave height at half a wavelength off the toe of the dike. However, even without a wave model, it is clear that the wave height can never be larger than 0.9 times the water depth at the toe of the dike. This is thus used as a limiting value.

The period that must be used for overtopping calculations is Tm-1,0. In Durosta the period is assumed constant. Tm-1,0 is better predicted with Swan(1D). For Ostend, however, an underestimation of 11% is found in comparison with the measured value. It is unclear to what extent this underestimation depends on the water depth (this may be expected based on the fact that the shallower the water, the more the wave spectrum is flattened). It is proposed to work with the wave period obtained from Swan, plus 20% (additional safety margin compared to the 11%), with a minimum of 1.1 times the peak period in deep water (in deep water, because the spectrum may be double-peaked in shallow water, the peak with the largest period is best taken.)

Figure 18 shows an example of the beach evolution during a storm. Without erosion, the waves cannot reach the toe of the dike, but the berm before the dike erodes fully, resulting in waves of 1.2m at the toe of the dike.

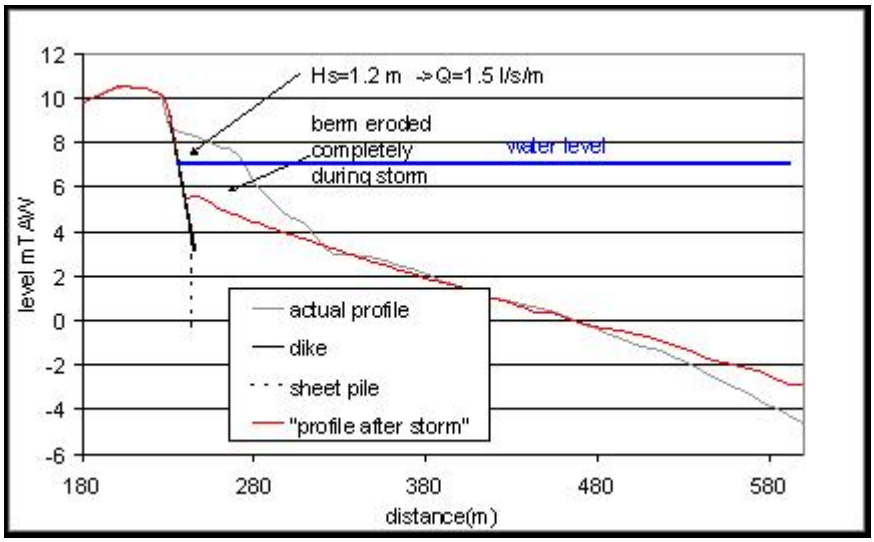

Figure 18 Evolution of the beach during a storm and consequences for the wave height at the toe of the dike.

3.5. Comparison of the results with the existing Dutch results

The results obtained were compared with the hydrodynamic boundary condition book issued by Rijkswaterstaat (the Dutch Department of Public Works).

3.5.1. Peak wave period for dune erosion

With regard to dune erosion, the decimation height is taken into account (see chapter on dune erosion).

The Netherlands (4000-y + decimation height) : 11.4s

Comrisk/Flanders (1000-y + decimation height = about the 4000-y) : 12.6s

3.5.2. Wave period for dikes (overtopping)

Spectrums for Zeeuws-Vlaanderen are double peaked (cf. Figure 19), with 1 peak of the wave energy in deep water and another peak because the waves break on the plains. This makes the wind input, which creates new waves, important. This input typically occurs with higher frequencies.

The Netherlands

2 peculiarities: 1) the low $T_{m-1,0}$ wave period (in the order of 9s and less (if T_p=12s /1.1 were used, $T_{m-1,0}$ would be 11s) – 2) a low wave height implies low periods, while one would expect the longest wave periods to lose the least energy.

Isn't the second peak of the spectrum overly taken into account, and is this safe when using overtopping discharges?

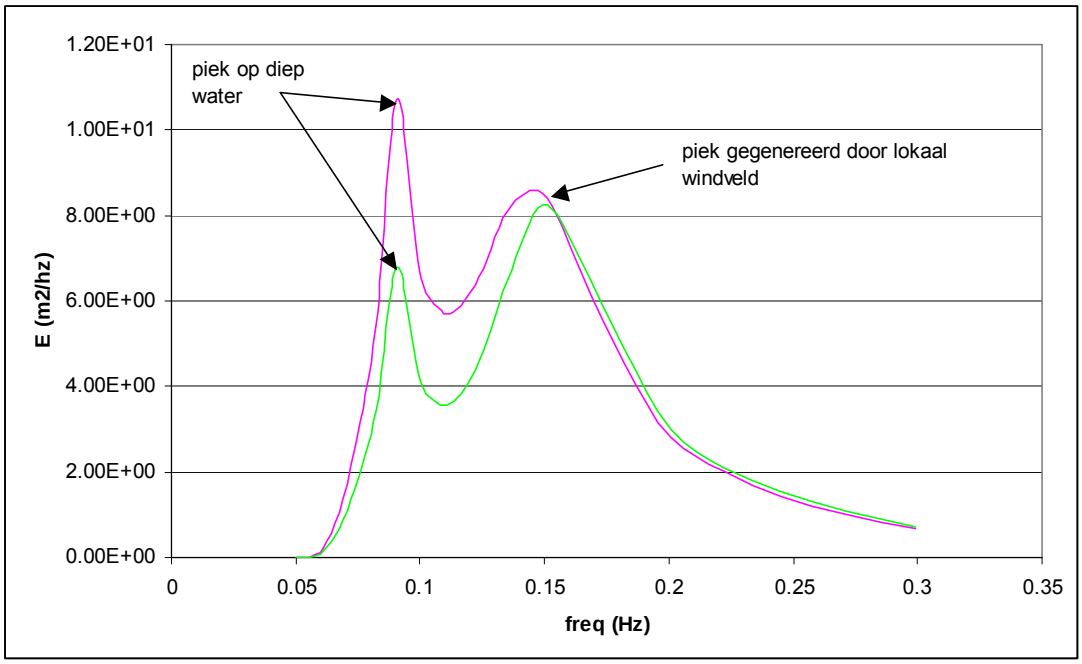

Figure 19 Spectrums to the east of Zeebrugge.

However, the new wave boundary conditions do not mention T_p but $T_{m-1,0}$ at the toe of the dike. This value is deduced from Swan calculations. This measure does take into account the double-peaked nature of the spectrum, making the period much lower than what can be expected on the basis of the proposed peak period used before.

An additional problem is that Swan appears unable to correctly predict the change of wave period from relatively deep water (foreshore) to right before the dike. In theory, this requires Boussinesq models. By means of the Groenendijk tests, however, it can be verified which mistake was made when using Swan.

Flanders

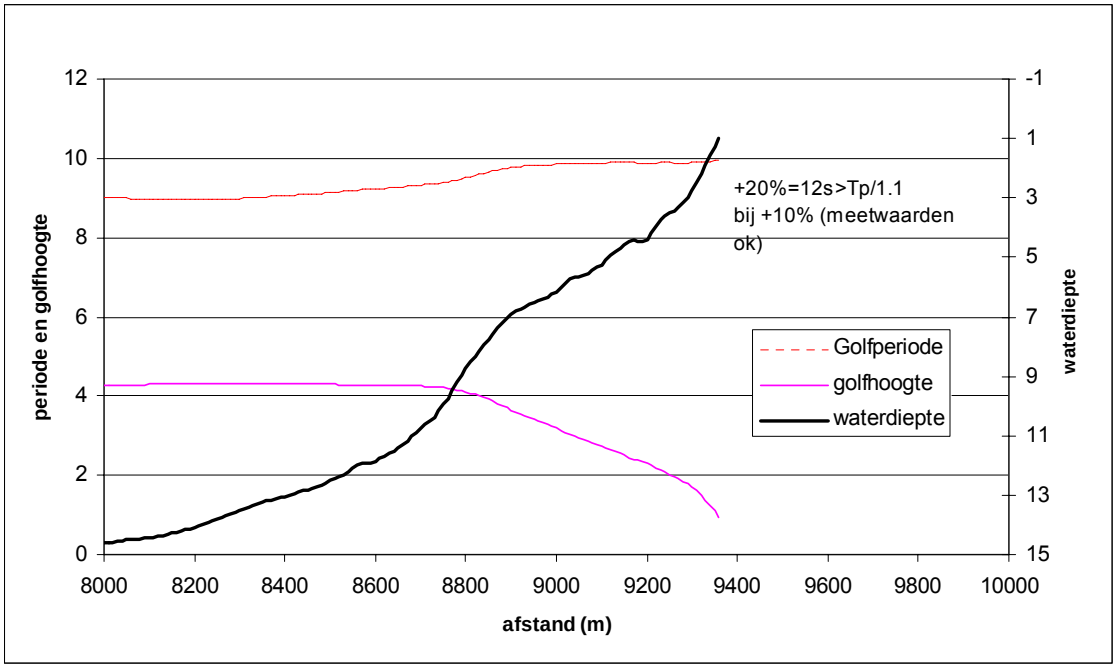

Dutch	English
periode en golfhoogte	periode and wave height
afstand	distance
golfperiode	wave period
golfhoogte	wave hight
waterdiepte	water level

Figure 20 Evolution of the wave height and period ($T_{m-1,0}$) for a typical bottom profile.

Figure 20 shows the evolution of the wave height and period for the Ostend beach according to a 1D Swan calculation. The proposed wave period is $T_{m-1,0}$. This appears to be fairly constant in the shallow part, contrary to what is expected: the breaking and friction in Swan do not have any effect on the form of the spectrum. The increase of $T_{m-1,0}$ by 20% (RIKZ advice + findings from comparison with wave measurements in Ostend) results in a value that is still comparable to $T_p/1.1$ (period measure to be used if $T_{m-1,0}$ is not known).

It is thus probably preferable, but perhaps too conservative, to take $T_p/1.1$ as period measure.

3.5.3. Water level

A comparison was made for the 4000-year water level.

Cadzand

Flanders : 7.40 m TAW= 5.1 m NAP

Netherlands: 7.35 m TAW= 5.05 m NAP (according to the latest boundary conditions)

Vlissingen

Flanders: 7.6 m TAW= 5.3 m NAP

Netherlands: 7.5 m TAW= 5.2 m NAP

Conclusion: the differences are negligible.

3.5.4. Wave height for assessment of dunes

(i.e., including decimation height) 4000-year conditions

Example for Tienhonderd polder

Comrisk/Flanders Hs=5.0 m

Netherlands Hs= 5.45 m

Probable cause: in the Netherlands the wave heights for dune erosion are determined in the middle of the channels above; this is difficult to do in Flanders, so the –5m TAW line was opted for, which is closer to the coast.

However, the wave height appears to have little relevance in dune erosion calculations, unless when determining the limit volume.

4. DUNE EROSION

4.1. Guideline to assess the safety of dunes as sea defence

As a basis for the investigation, the 'Safety assessment guideline' ('Leidraad toetsen op veiligheid') is used. The methodology of a Dutch report is applied, the 'Basic Report Sandy Coast' ('Basisrapport Zandige Kust'), drawn up by the Technical Advisory Committee for Water-retaining Structures (TAW) which also includes the Guideline to assess the safety of dunes as water-retaining structure (hereafter called the 'Guideline (dunes)').

The dune erosion during a storm flood is calculated by means of the principles of the Duros model. The principles forming the basis of Duros are:

- the model calculates the dune erosion of an undefended dune profile, assuming a closed sand balance in the transverse direction, i.e. in the cross-section considered;
- the calculation model is time independent: *in practice, this meant that the storm level lasted for 5 hours ('Basic report Sandy Coast', p. 296). However, this is very long for the Flemish coast, where 2.5 hours before and after the storm a reduction in water level of 1 m may be expected (due to the tide). Therefore this assumption is conservative. The influence could be verified with Durosta*;
- the form of the transverse section after the storm surge is considered known: the erosion profile. This erosion profile is an equilibrium profile (Vellinga, 1986), which can be described by means of a formula expressing the location in relation to the maximum storm surge level;
- The data required for the calculation are:
- the storm surge level;
- the significant wave height;
- the grain size of the dune sand;
- the beach profile just before the storm surge.

The necessary characteristics to calculate the limit profile are the peak period of the wave energy spectrum and the expected value of the significant wave height in deep water, corresponding with the calculated level. The calculated level is defined as the design level/water level + 2/3 of the decimation height. The decimation height is the height difference between the water level corresponding with a 10 times smaller exceedance frequency as that of the design level/water height and this design level/water height. The calculations always use the level calculated in this way. This takes into account the uncertainties with regard to the entry parameters (semi-probabilistic).

In case of a positive evaluation, the dune erosion will be reduced; in case of a negative evaluation the section will be characterised as 'insufficient'.

For the evaluation the dune data of 2000 (VITO, 2000) are used, as well as measurements of the foreshore (work boat Ter Streep, 2000 – 2002, AWK) and the measurements of 'Flemish Banks' ('Vlaamse Banken', AWK). The results thus apply to 2000, the evolution of the critical erosion point since then is not taken into account. However, the dune and beach trends will be given per profile. For the Netherlands the Jarkus profiles are used.

When assessing the safety of dunes as sea defence structures, a consideration of separate transverse profiles must suffise as yet. Each transverse profile of a stretch of coast must have a minimum safety to prevent failure from occurring during a design storm flood - barely. An assessment method is included in the 'Dune erosion' ('Duinafslag') guideline for the assessment thereof. This method is applicable to an undefended dune profile. For background information, Van de Graaff (1984) is referred to.

However, a probabilistic approach requires the determination of a (permissible) failure probability. A good dike design must not result in an immediate breach when the design level is ‘somewhat exceeded’. The exceedance frequency of the design level must not be interpreted as a failure frequency. This required safety margin in case of a water level equal to the design level is expressed as a factor with which the exceedance frequency of the design level must be multiplied to obtain an indicative breach probability per year for a dune profile. This factor is set at 0.1. Based on the permissible failure probability, the normative erosion can be calculated per profile: the design erosion.

In the current approach a deterministic calculation is opted for, without safety parameters but with a sensitivity analysis.

4.2. Methodology

4.2.1. General

Dune erosion is a process that, in its ultimate form, may result in the loss of the water-retaining function of the sea defence. Two stages can be distinguished in the failure behaviour of a dune profile:

1. reduction of the dune volume above the storm surge level because of dune erosion;
2. dune erosion has progressed to such an extent that wave overtopping over the residual profile becomes possible. The residual profile may fail as a result of erosion of the crest and of the inner slope.

A dune is considered to guarantee the safety of the hinterland if the second stage is not reached during design conditions. For the safety assessment of a transverse profile, it is therefore necessary that the extent of dune erosion under design storm conditions can be quantified.

The assessment method, used in the T.A.W. ‘Dune erosion’ ('Duinafslag') guideline, is such that the average annual exceedance probability of the erosion calculated with this method is equal to the permissible failure probability (see section 4.1). This normative erosion is calculated in a relatively simple manner, using specific calculation values for the erosion-determining quantities

('calculation recipe').

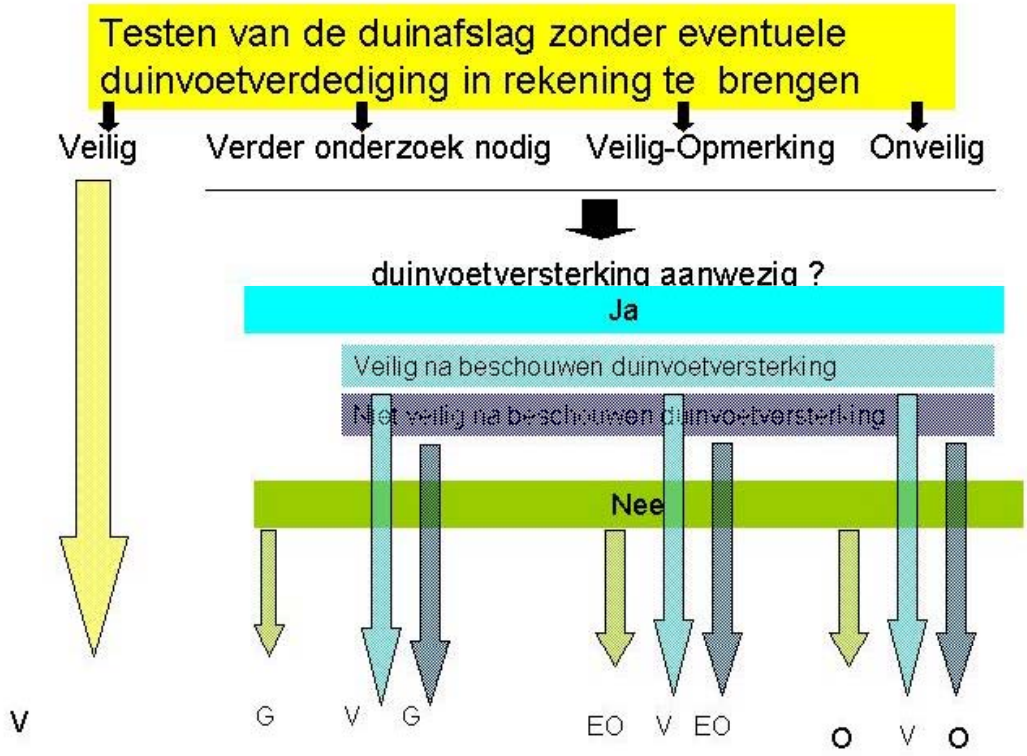

Figure 21 gives an overview of the steps to be taken.

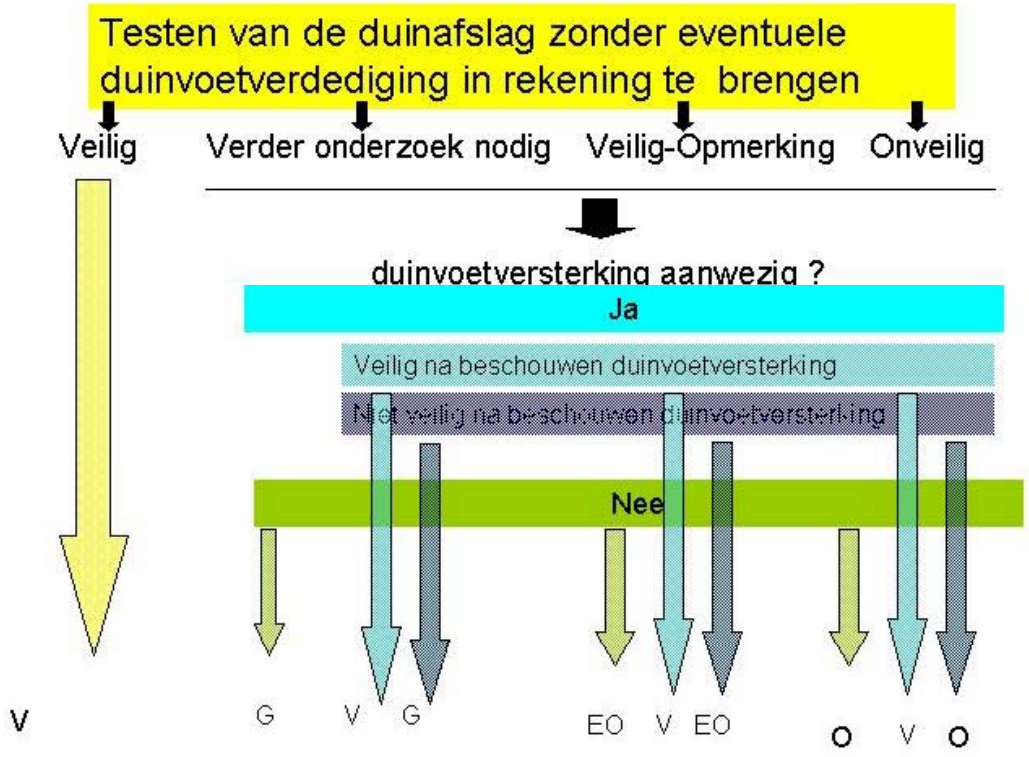

Figure 21 Overview of the method applied when testing dune foot erosion (V= Veilig (Safe), G=Geavanceerd onderzoek nodig (Advanced investigation needed), O=Onveilig (Unsafe); EO=Expert Opinie nodig (Expert Opinion needed))

Erosion calculation (see Figure 22)

In the assessment method the extent of dune erosion is calculated on the basis of a so-called basic erosion and an allowance which must be superimposed. The erosion value thus obtained can be used to calculate the location of the erosion point.

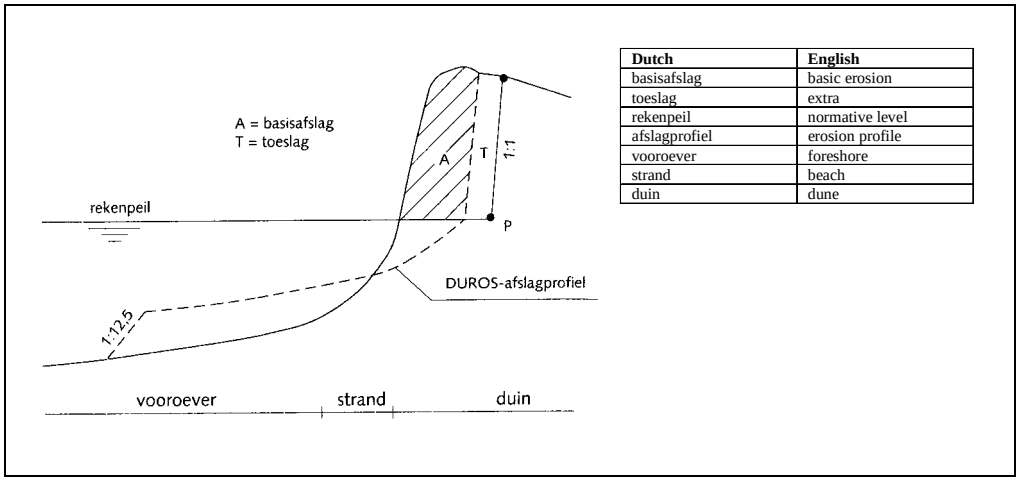

Dutch	English
basisafslag	basic erosion
toeslag	extra
rekenpeil	normative level
afslagprofiel	erosion profile
vooroever	foreshore
strand	beach
duin	dune

Figure 22 Definition sketch

Limit profile (see Figure 23)

At any given time a minimal but stable limit profile must be present inland of the design erosion line. The 'Dune ersion' ('Duinafslag') guideline gives the dimensions the limit profile must have. The crest height of the limit profile (in relation to the design level) follows from the wave run-up formula for dikes and is related to the peak period of the wave energy spectrum and the significant wave height in deep water.

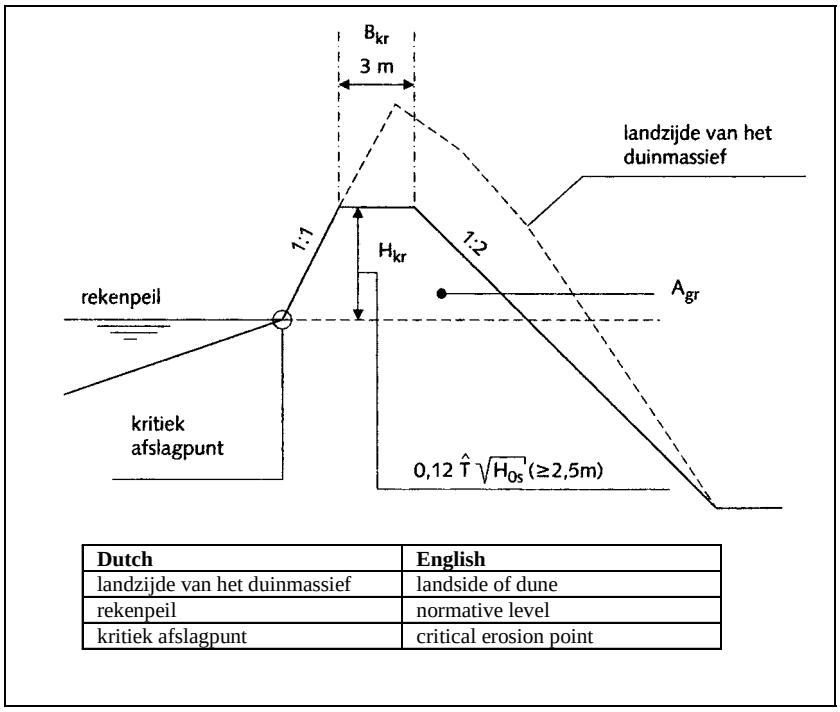

Dutch	English
landzijde van het duinmassief	landside of dune
rekenpeil	normative level
kritiek afslagpunt	critical erosion point

Figure 23 Standard limit profile.

Volumes

V_{limit} is the required volume of the limit profile under the prevailing conditions for wave height, wave period, design level, …m^3/m. $V_{residual}$ is the volume of the residual profile. Residual profile is understood to mean: the dune profile remaining after a superstorm in which the allowance and a possible additional shift as a result of the longitudinal material transport effect is included. It is a momentary consideration, it does not yet take into account an additional shift as a consequence of a regression calculation of the erosion point. The calculation of $V_{residual}$ takes into account the entire remaining profile, including any dune lines behind it.

Critical limit profile

A so-called critical limit profile is a limit profile that can be defined as far as possible on the landward side of the dune area. If the critical limit profile breaks, i.e. if the erosion progresses beyond the critical erosion point, the dune is considered totally succumbed and the hinterland is flooded or the infrastructure present in the dunes is damaged. Only in the case of barely safe cross-sections the probability that the critical limit profile is reached during a storm flood, is exactly equal to the safety standard agreed on. In relatively wide dune areas the probability that the critical limit profile is reached is a lot smaller than the safety standard.

Longitudinal transport gradient

When the longitudinal transport of sand, for instance caused by slanting waves, varies along the coast, the sand balance is not closed for a specific coastal area. From a safety viewpoint, those coastal areas are important where the sand balance is negative (total outgoing longitudinal transport is greater than the total incoming longitudinal transport). The consequence is an additional landward shift of the erosion profile over such a distance that the surface of the shift corresponds with the longitudinal transport difference.

Two cases can be distinguished whereby the longitudinal transport must be taken into account. The first applies to curved coastal areas where the longitudinal transport difference can be calculated by means of a formula.

A second case applies to those situations where a longitudinal transport gradient can be expected, as with the dune-engineering structure transitions (pier, dike, shore defence) and with the occurrence of strong wave height differences in the longitudinal direction. Further investigation is required in this case.

Land side limit profile

The landside limit profile is the point indicating where the landward side of the dune limit volume crosses the design level.

4.3. Boundary conditions

In order to assess the safety, allowances are calculated for the boundary conditions. However, for a risk assessment, calculations without allowances are opted for. However, the uncertainty of the parameters is examined by means of a sensitivity study.

4.3.1. Water level

The water level was deduced in §3.1.1. No allowances are adjusted.

4.3.2. Wave height and peak period

The Dutch standard stipulates that the wave height in deep water (-20m NAP, or –18m TAW) must be used. In the case of shallow banks off the coast, this is the middle of the main channel off the coast. So, only with very low broad banks a reduction can be applied. The basis of the dune erosion calculation consists of erosion profiles after a storm, as obtained in ‘Deltagoot’ (WL Delft). As for the Dutch coast, there is only a small distance between deep water and the dune. This distance is large on the Belgian Continental Shelf, with lots of banks in between. Therefore it is necessary to use a ‘deep-water’ wave height resulting in the same wave height at the toe of the dune/beach as in the Dutch situation. The toe of the dune/beach was taken (somewhat arbitrarily) here at the –5m line. As the distance to ‘deep water’ is short, only the shoaling process must be considered. For a peak period of 12s the shoaling coefficient on the –5m line (with a water level of approximately 12 m) is virtually equal to 1 (1.02). Furthermore it must be noted that the wave height has little influence. As the shallow parts are mainly important for dunes, the wave height at the toe of the dune is entirely determined by the water level.

4.3.3. Superdune corrections

The Deltagoot experiments assumed a peak period of about 8 to 9 s. The Superdune results thus apply to these profiles. The peak period with a 1000-year storm, however, is 12.6 s. In the Netherlands a method was developed to compensate for this. Durosta was used to check the

influence on the erosion volume. For a peak period of 12s this turned out to be 35% higher than for a peak period of 8s (Superdune). It was then verified how much finer the grain diameter should be to reach the same erosion. As a conclusion, the grain diameter should be reduced by 14%. This reduction is thus applied in this project.

5. STABILITY OF DIKES

5.1. Introduction

The first sea defence is defined as all the beaches, dunes, dikes and quay walls located on the seaward side of the residential areas, to protect the areas behind it against storms. Only the part of the first sea defence consisting of dikes is subjected to a stability assessment. The dikes that are a part of a (sufficiently wide) dune may not be assessed as a dike, but as a dune. After all, the downslide of a part of the dike does not imply any danger to the stability of the dune behind it, on condition that this dune is wide enough and dune erosion calculations show that the stability of the dune is indeed not jeopardised.

The stability is determined by the aspects

- piping and heave;
- inward macrostability;
- outward macrostability;
- microstability;
- condition of the revetment;
- condition of the non-water-retaining constructions.

5.2. Description of the method

The method from the 'Safety Assessment Guideline' ('Leidraad Toetsen op Veiligheid', 1999) was used. Where the applied method was unclear, the method from 'Safety of primary water-retaining structures in the Netherlands, Safety Assessment Regulation for the second assessment round 2001 – 2006 (VTV), January 2004' ('De veiligheid van de primaire waterkeringen in Nederland, Voorschrift Toetsen op Veiligheid voor de tweede toetsronde 2001 – 2006 (VTV), januari 2004') was applied. In addition, the method of Schüttrumpf (2001) and Schüttrumpf (2003) was applied for the calculation of the indicative layer thicknesses and overtopping velocities. The methods mentioned in the 'Theory Manual PC-Ring Version 4.0' ('Theoriehandleiding PC-Ring Versie 4.0') were used as a basis for the calculation of the residual strength of a grass cover, covering layer of clay and dike core.

5.3. Assumptions

The assumptions are mentioned in the text where relevant. Especially with regard to quantitative data of the subsoil, it was usually a case of groping in the dark. Average values, values used in the Dutch standards or values determined with common sense were used. Drillings and laboratory tests currently being conducted in Flanders will give a better idea about the correctness of the assumptions. The (possible) presence of the (new or old, wood or metal) sheet piles was not taken into account.

5.4. Calculation programmes used

The SLOPE/W stability programme (http://www.geo-slope.com) was used to examine the stability of the outer slope at low tide. An EXCEL spreadsheet suffised for other problems.

5.5. Piping en heave

Stability loss due to piping may be the result when too many soil particles from the underlying layers are carried off by seepage during (prolonged) high-water levels. The occurrence of this

internal erosion is visible on the landward side of the dike because sand is carried off with seepage water welling up in ditches or on ground level. The resistance to piping is determined by:

- the (seepage or) leak length;
- the thickness, composition and hydraulic conductivity of the water-bearing layer under and in the dike body;
- the thickness of a covering layer of clay;
- the width of a possible seepage ditch.

5.6. Outward macrostability

The stability of a water-retaining structure is largely determined by the macrostability of the dike body. When assessing the macrostability of the outer slope, the following mechanisms must be assessed:

- liquefaction of the foreshore (§5.6.1);
- sliding of the foreshore (§5.6.1);
- sliding of the outer slope due to low tide (§5.6.2).

5.6.1. Sliding and liquefaction

First, it must be examined whether the foreshore can threaten the dike stability due to sliding or liquefaction. The assessment scheme in Figure 24 was used. Based on the presence of liquefaction-sensitive areas, an assessment may or may not be made with regard to liquefaction or sliding. This requires knowledge of the liquefaction-sensitive areas in the foreshore. As it is unclear whether or not liquefaction-sensitive layers are present, both the sliding and liquefaction were checked. The soil profile resulting from the beach erosion (DUROSTA) calculations was taken into account.

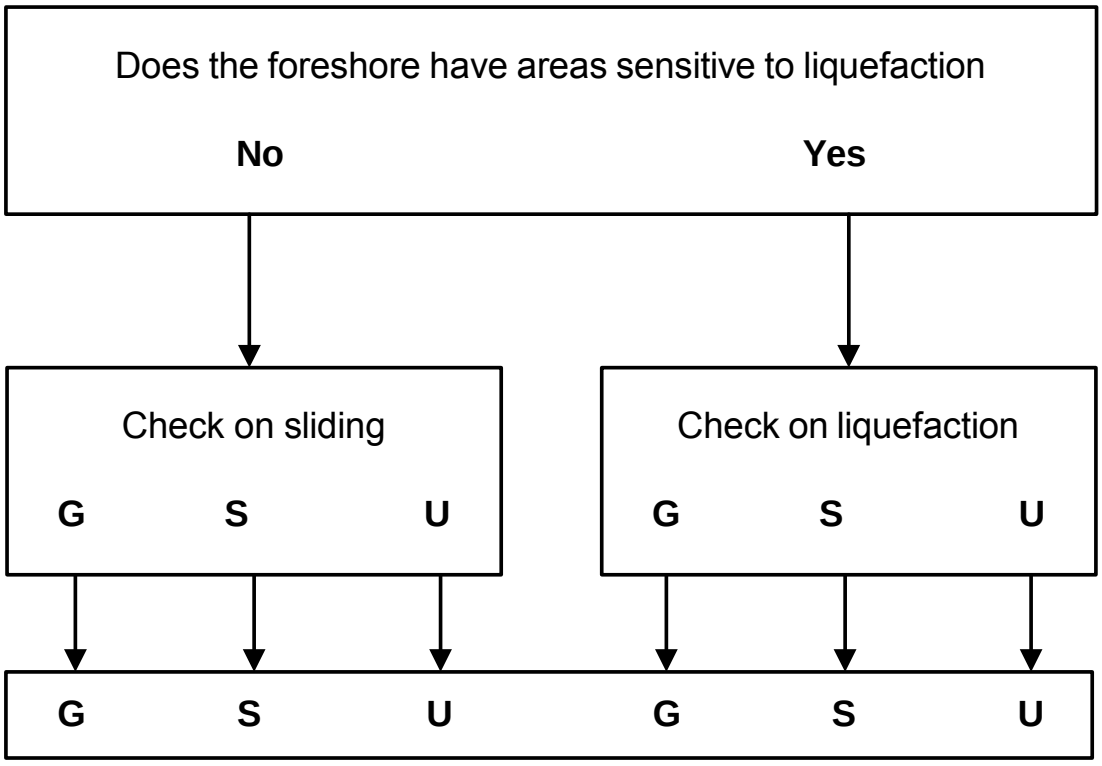

Figure 24 Assessment scheme for sliding and liquefaction.

Next, the assessment scheme in Figure 27 was used. Both assessments must first meet the covering criterion and a favourable development of the foreshore must be expected. The covering criterion implies that an imaginary slope of 1:2.5, starting from

(1) the toe of the dike or

(2) the outside limit of the berm or

(3) the seaward edge of a cover,

is not crossed by the soil profile (see Figure 25). This will help discover any undercutting of possible sheet piles.

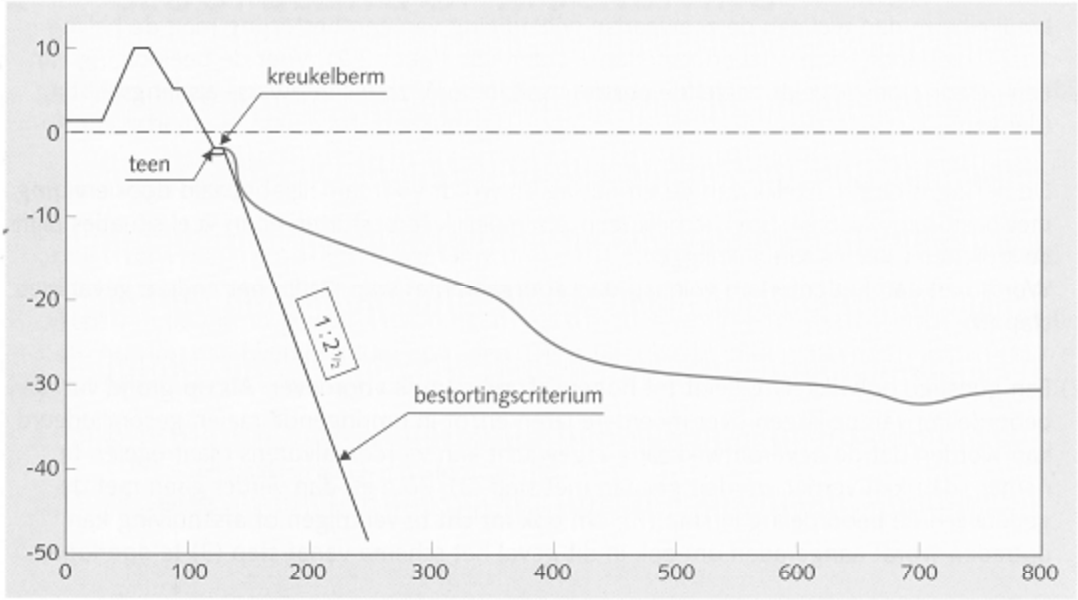

Dutch	English
kreukelberm	bench
teen	toe
bestortingscriterium	covering criterion

Figure 25 Definition of covering criterion.

It was assumed that a favourable development of the foreshore may be expected. A favourable development is understood to mean that based on the assessment of bathymetrical soundings over several years (possibly in nearby profiles) it can be concluded that the foreshore development can be awaited before taking measures. In case of a favourable development, the trough depth H is then determined. This is the height difference between the edge of the trough and the bottom of the trough. In case of a clear intermediate plateau in the bottom profile, a distinction must be made between the total trough depth H_{tot} and the local trough depth H_{lok}. Both must be taken into account. The assessment prescribes that in case of trough depths > 9m the signalling, liquefaction and sliding points must be determined. First, the so-called 'margin', calculated from the toe of the dike, must be determined (Figure 4):

$$\text{margin} = 2\,H_{zv} + 1.5\,(H - H_{zv})$$

with H_{zv} = thickness of the liquefaction-sensitive layer. If no liquefaction-sensitive layers are present, H_{zv} = 0 m and the margin is thus equal to 1.5H. With a covered foreshore the margin is at least equal to the horizontal distance between the seaward end of the cover and the toe of the dike.

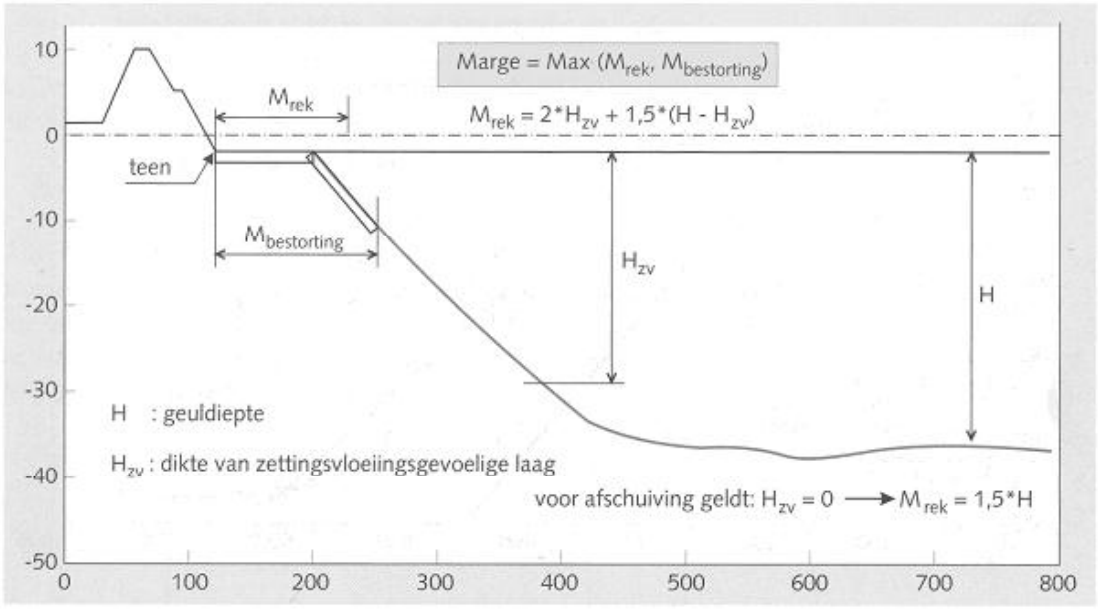

Dutch	English
marge	margin
teen	toe
geuldiepte	trough depth
dikte van zettingsvloeiingsgevoelige laag	thickness of layer sensitive to liquefaction
voor afschuiving geldt	for sliding

Figure 26 Definition of 'margin'.

The LTV (1999) reads: "For the determination and definition of the signalling point S_{ign} and the sliding point S_{af} Figure 5 is referred to. Both points are on the 'assessment level'. This level is located at a depth of 0.5H above the trough bottom in the case of a foreshore without cover (Figure 5(a)). The signalling profile goes downards from the toe of the dike, via the margin, at an angle of 1:6. The crossing of this profile with the assessment level gives the S_{ign} point. The red line shows the profile present before sliding. The average slope of this profile is schematically represented by a straight line, determined by eye. The crossing of this straight line with the assessment level gives the S_{af} point. The assessment level lies halfway the height of the cover-free part of the trough edge in the case of a covered foreshore (Figure 28(b)).

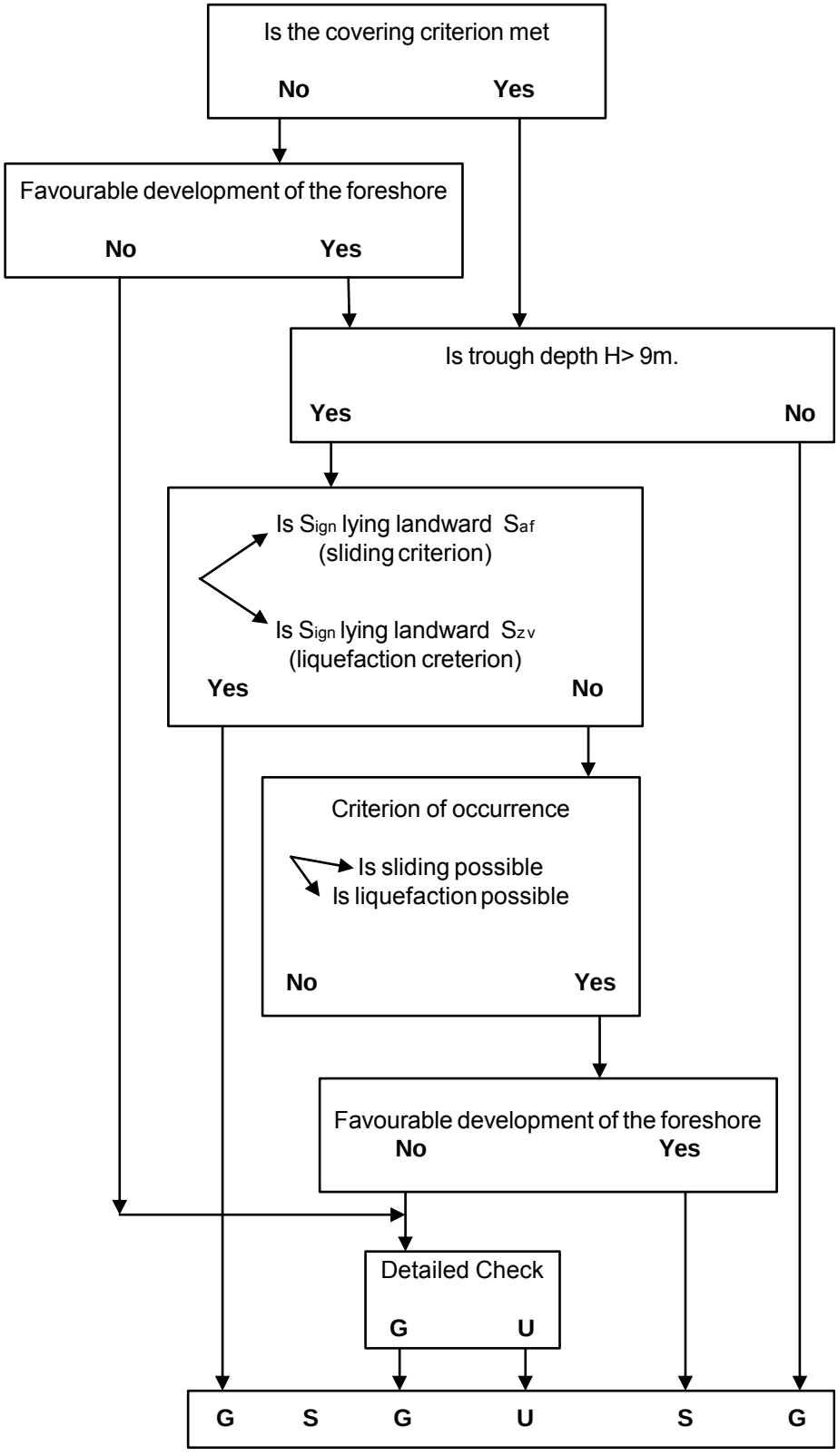

(*) the score is 'sufficient' if the covering criterion is met

Figure 27 Assessment of the macrostability of the outer slope.

If the signalling point S_{ign} is landwards of the sliding point S_{af}, a possible sliding will not have any consequences for the stability of the sea defence. This will then give the score 'good' if the covering criterion is also met. Otherwise the score is 'sufficient'. If the signalling point S_{ign} is located seawards of the sliding point S_{af}, the assessment must be continued.

To determine and define the signalling point S_{ign} and the liquefaction point S_{zv} for a cover-free foreshore, Figure 29 is referred to. Both points are on the assessment level. This level generally corresponds with the lower limit of the liquefaction-sensitive layer, but lies at a minimum depth of 1/3 H and a maximum depth of 0.5 H above the through bottom. The signalling profile reference is generally the toe of the dike with the corresponding margin. For a covered foreshore the signalling profile joins the toe of the dike as shown in Figure 28(b). 1/3 H_{best} and 0.5 H_{best} above the through bottom apply as minimum and maximum levels for the assessment level, respectively (H_{best} = height of the cover-free part of the foreshore (see Figure 28(b)).

The sliding criterion applies to the layer under the liquefaction-sensitive layer. Its influence is only important if $H_{zv} \leq 2/3$ H.

If the signalling point S_{ign} is landwards of the liquefaction point S_{zv}, a possible liquefaction will not have any consequences for the stability of the sea-defence structure. This will give the score 'good' if the covering-criterion is also met, otherwise the score is 'sufficient'. If the signalling point S_{ign} is located seawards of the liquefaction point S_{zv} the assessment must be continued.

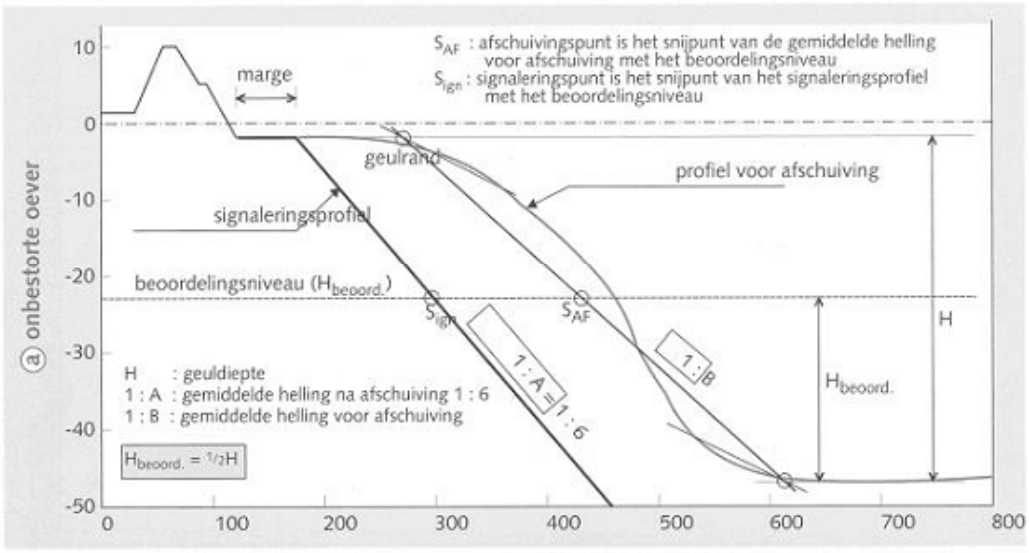

Dutch	English
marge	margin
geulrand	edge of trough
profiel voor afschuiving	profile before sliding
signaleringsprofiel	signalling profile
beoordelingsniveau	assessment level
geuldiepte	trough depth
gemiddelde helling na afschuiving 1 : 6	average slope after sliding 1 : 6
gemiddelde helling voor afschuiving	avergae slope before sliding
onbestorte oever	no cover

(a)

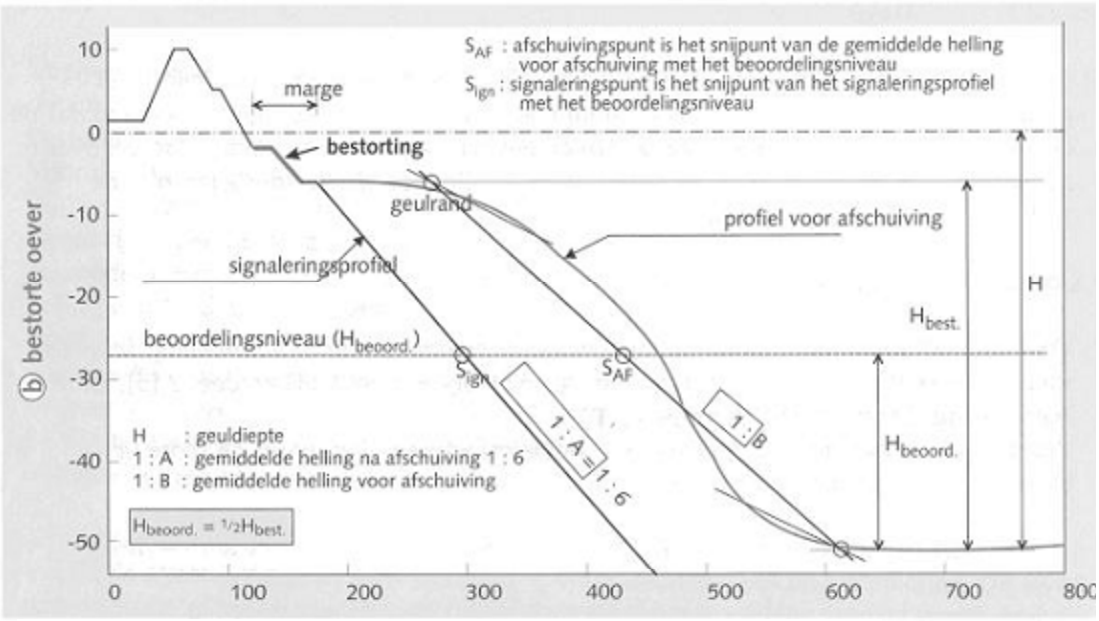

Dutch	English
marge	margin
bestorting	cover
geulrand	edge of trough
profiel voor afschuiving	profile before sliding
signaleringsprofiel	signalling profile
beoordelingsniveau	assessment level
geuldiepte	trough depth
gemiddelde helling na afschuiving 1 : 6	average slope after sliding 1 : 6
gemiddelde helling voor afschuiving	avergae slope before sliding
onbestorte oever	no cover

(b)

Figure 28 Determination of signalling point, sliding point for (a) a cover-free foreshore, (b) a covered foreshore.

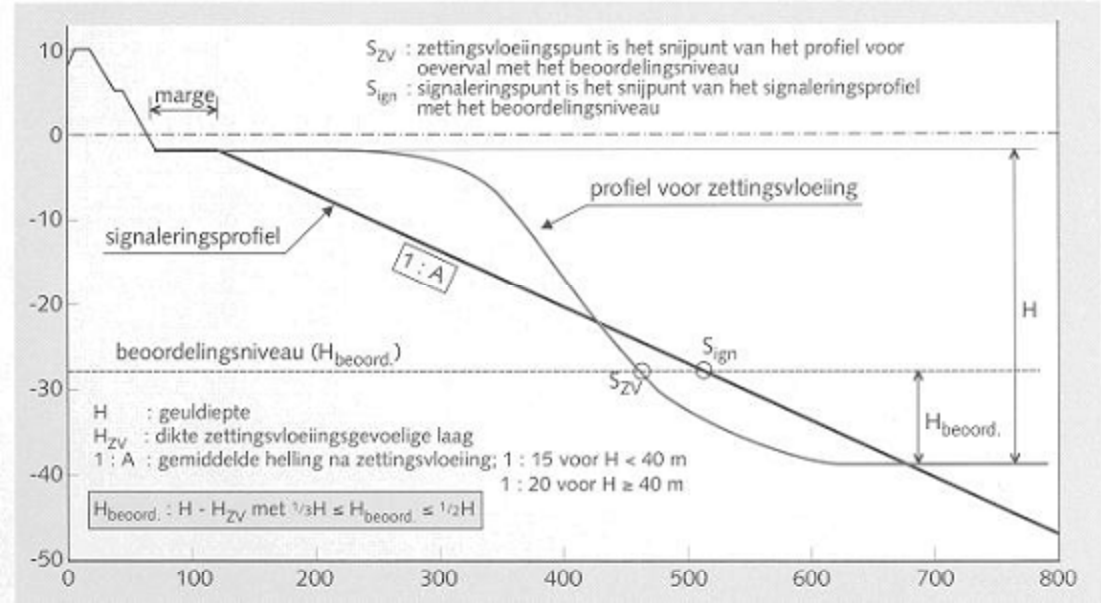

Dutch	English
marge	margin
profiel voor zettingsvloeiing	profile before liquefaction
signaleringsprofiel	signalling profile
beoordelingsniveau	assessment level
geuldiepte	trough depth
dikte zettingsvloeiingsgevoelige laag	thickness of layer sensitive to liqueficaction
gemiddelde helling na zettingsvloeiing	average slope after liquefaction
onbestorte oever	no cover

Figure 29 Determination of signalling point, liquefaction point for a cover-free foreshore.

5.6.2. Sliding equilibrium with low outer water

In addition, it must be examined whether the stability of the outer slope of the construction is jeopardised in case of low outer water. The score for this is 'good' if the dike has a berm or foreshore at least on the NAP level (NAP +0.00 = TAW +2.32m) and an outer slope gentler than or equal to 1:3. If these conditions are not met, a decision cannot be given and further investigation is necessary. The SLOPE/W computer programme is used. The Bishop method is applied.

5.6.2.1. Loads

The following loads are taken into account:

- soil (dike material) weight;
- water pressures.

The weight of the soil (and the dike revetment) may contribute to both a resisting and a driving moment, depending on the location of the slip circle's center point. A resisting moment results from the soil's own weight (if it acts favourably) and the friction along the slip surface. Any anchoring of the dike revetment in the solid ground behind it also contributes to the dike's overall stability.

Permanent loads (such as weight of the soil and the dike revetment) cannot be split up. Physically this would also be incorrect. The permanent loads can act either entirely favourable or unfavourable (for case C of Eurocode 7 the partial safety coefficient of a permanent load equals 1

for a favourable as well as an unfavourable action). The representative apparent densities are given in Table 1.

The 'Assessment Dike Ring 32' ('Toetsing Dijkring 32') in the Netherlands was made based on conservative boundary conditions and conservative representative soil characteristics. Figure 30 was taken from Stroo et al. (2003). Every type of soil was given a representative value for γ_{dry} and γ_{wet}. These values were determined by making an inventory of the properties of the types of soil, based on a large number of reports drawn up for previous dike reinforcement projects and the standards from NEN 6740.

type of soil	γ_{wet} [kN/m^3]	γ_{dry} [kN/m^3]
sand dike	20	17
clay dike	17	17
clay	16	16
weak clay	14	14
sandy clay	18	18
humous clay	13	13
peat	12	12
sand	20	17
clayey sand	18	18

Table 1 Representative apparent densities used for various types of soil according to NEN 6740.

Contrary to the assessment made in the Netherlands, the traffic load is not taken into account here. The traffic load during a storm with a large return period is very local and local loads have no influence.

The revetment was considered fully impermeable.

5.6.2.2. Water pressures

The water pressure distribution in the dike body during normative conditions is determining the stability. The failure mechanism 'Low Outer Water' has an outer water on the low-water level.

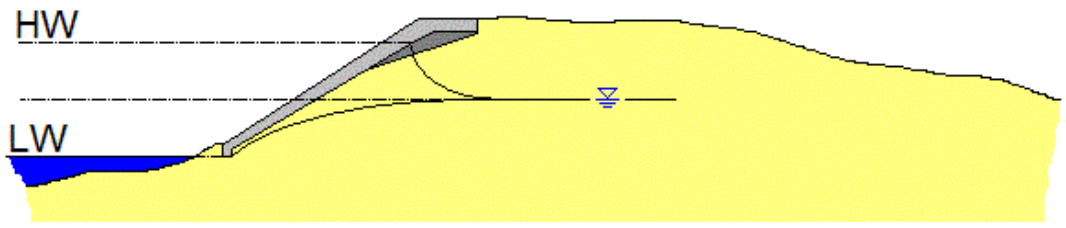

Figure 30 Water level in dike.

In case of low outer water, the beach in front of the dikes in question falls dry. As the subsoil mainly consists of sand, it was assumed that the phreatic water table in front of the dike immediately follows the decrease of the outer water and that from the rear of the toe of the dike revetment the phreatic water table will rise to an average water level. The average water level is the average of the high-water and low-water levels.

Two types of wave action must be considered: wave action (with peak wave period T_p as characterising period) on the one hand and tidal action (with 12h 24min as period) on the other hand. It is assumed that the wave action cannot be felt in the dike body. The tidal action, however, is felt in the dike body.

The phreatic line in the sea defence depends on the type of soil in the dike. Stability calculations assume a full saturation of the clay bodies in the dike at normative conditions. A well-permeable sandy material results in a phreatic line with a parabolic course; a straight line from the water level outside the dike to the inner toe of the dike appears to be a good approximation in practice. The method of Geuze et al. (1961) was used to determine the course of the phreatic water table under the dike revetment. The assumptions at the end of the paper were hereby taken into account and choices were made as to the hydraulic conductivity of the present sand. It was also assumed that the dike revetment is impermeable. The water pressure behind the revetment lags the water pressure on the revetment. The size of the water table fluctuations is not yet known.

On the seaward side of the dike the phreatic line follows the outer slope and the foreshore. If the foreland is on a lower level than the average low tide, the phreatic line can be assumed at the low-water level. With a dike consisting of sand, the phreatic line in the dike follows the outer water level. With a dike partly consisting of sand and partly clay, it must be examined whether sufficient drainage possibilities exist for the body of sand.

The inner water level depends on the ground level. If the ground level is below the assessment level of the outer water level, the course of the pore water pressures in the dike body is approximated by a straight line between the assessment level on the seaward side and the toe of the dike on the landward side (assume (conservatively) no drainage or a blocked drain) (Stroo et al. (2003)).

The density of the seawater is 1026 kg/m³ * 10 m/s² = 10.26 kN/m³.

5.6.2.3. Soil resistance characteristics

Based on borings and soundings available on http://dov.vlaanderen.be and the already available results of the soundings and borings conducted within the scope of this project, the geological profile was deduced. The additional soundings/borings will be more conclusive with regard to the stratification of the subsoil under the dike revetments, as well as the geotechnical information of the subsoil.

For the ‘Assessment Dike Ring 32’ the representative soil resistance characteristics given in Table 2 (Stroo et al., 2003) were used in the Netherlands. These representative soil characteristics were determined by means of the inventory of the characteristics of the types of soil present, drawn up by means of a large number of reports made for the previous dike reinforcement projects and the standards from NEN 6740.

type of soil	φ [°]	c [kPa]
sand dike	27.5	0
clay dike	17.5	10
clay	17.5	10
weak clay	17.5	0
sandy clay	22.5	10
humous clay	15	0
peat	15	2
sand	32.5	0
clayey sand	25	0

Table 2 Representative soil characteristics used in accordance with NEN 6740.

The representative soil characteristics used for the stability calculations of the outer slope with low outer water are based on this. For clay an internal friction angle of 22.5° is used and a lower cohesion than presented in Table 2 (5kPa).

5.7. Inward macrostability

The normative stability of the dike body on the landward side must be considered during the occurrence of the normative high-water level. Under these conditions the phreatic line of the dike body will rise due to infiltration of water into the outer slope. This possible failure mechanism is assessed in the LTV (1999).

5.8. Microstability

The wash-out phenomena and the uplifting of the top layer must be assessed with regard to microstability. A dike is given a score 'good' if one of the following conditions is met:

- the dike has been subjected to an (almost) normative load without loss of microstability. An almost normative load is understood to mean:
  - a water level that deviates less than half a metre from the normative high water level;
  - a comparable high water level duration (at least 90% of the duration);
- the inner toe of the dike has a properly functioning drainage construction: the phreatic line is drawn towards the drain, so that no water flows from the inner slope;
- the dike has an impermeable clay core. In this case too no water will flow from the inner slope, nor will uplifting of the top layer occur;
- the dike is sandy and has an inner slope with a slope of less than 1:5. The driving forces in such a case are smaller than the strength of the sand, preventing wash-out.

For most Flemish dikes the fourth point applies. A clear inner slope is not present. The slope is definitely less than 1:5 (see average slopes in Table 7).

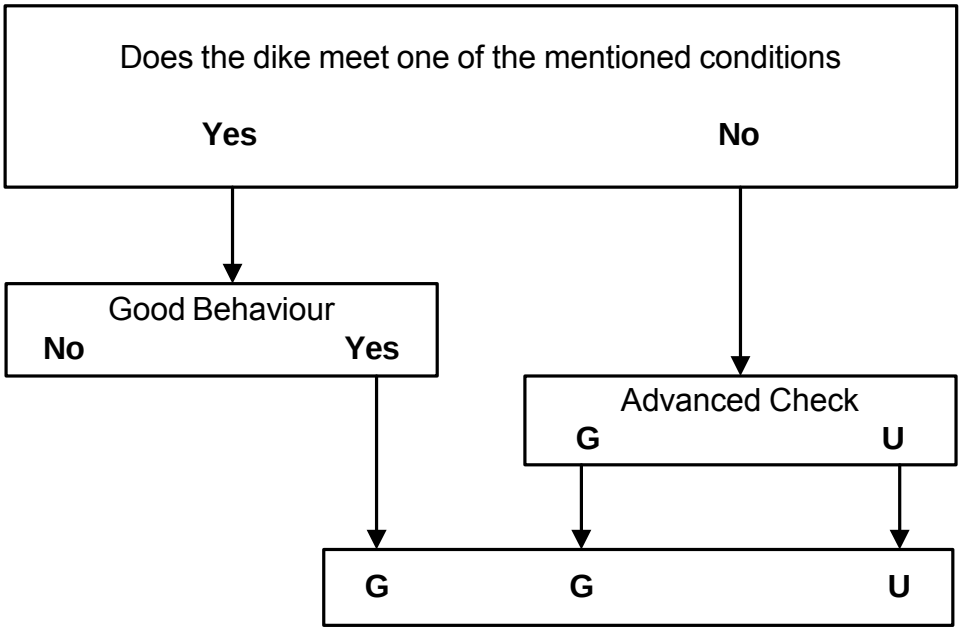

Figure 31 Microstability assessment.

Under the assumption that the dike does not meet the above-mentioned conditions, an advanced assessment is needed. The aspects to be considered are:

- perpendicular equilibrium;
- parallel equilibrium;
- uplifting.

Perpendicular equilibrium is assessed by means of the formula

$$\gamma_{\perp} = \frac{\gamma_g - \gamma_w}{\gamma_w}(\cot\alpha)^2 \qquad (2)$$

with · γ_g = soil density (wet);

· γ_w = water density;

· cot α = cotangent of the slope.

LTV (1999) mentions the formula to assess the uplifting of the top layer in case of a sandy core having a cover layer with a cover layer with a lower hydraulic conductivity (difference factor 30):

$$\gamma_{\perp} = \frac{\rho_g d \cos\alpha}{\rho_w (h_b - z)} \qquad (3)$$

The possibility of uplifting is examined by means of the formula

$$\Delta h \le d \frac{\rho_g}{\rho_w} \cos\alpha \left(1 - \frac{\tan\alpha}{\tan\varphi}\right) \qquad (4)$$

The above-mentioned assessment criteria are further elaborated in paragraphs 6.7, 7.6 and 8.4.

5.9. Condition of the revetment

For concrete slabs the assessment diagram of Figure 10 is applied. If the revetment is located above the assessment level + 0.5H_s, the sliding and material transport steps can be skipped. The revetment must at least ensure that any attack on the transverse profile during the normative conditions stays within the limits, thus avoiding the danger of breach formation.

If the dike body has no revetment, such as the Zwin dikes, only the residual strength of the grass cover and covering clay layer is calculated. If this residual strength is smaller than the storm duration, a failure can be expected.

For the dikes in Zeeuws-Vlaanderen the stone pitching and asphalt revetments are examined.

5.9.1. Residual strength of the grass cover and clay layer

To calculate the residual strength of the grass cover and clay layer, the method mentioned in the 2003 TNO report CI-R0020 is followed.

Residual strength of grass cover on the seaward side: $t_{RT,buiten}=d_w/E_g$

with $E_g = \frac{r^2 H_s^2}{c_g}$ = erosion speed of grass cover (based on large-scale model tests)

$c_g =$ erosion resistance of grass cover (3.3^E05ms for poor grass quality, 1^E6ms for a good grass quality)

$H_s =$ significant wave height

$r =$ correction factor for slanting waves

$d_w =$ rooting depth of the grass cover (0.05m – 0.07m)

Residual strength of clay: $t_{RK,buiten} = \frac{0.4 L_K c_{RK}}{r^2 H_s^2}$

with $L_K =$ width of the clay cover layer

$c_{RK} =$ erosion resistance of clay layer (7^E03ms for poor clay quality, 54^E03ms for good quality)

The above-mentioned formula for the residual strength of the clay layer can also be used to calculate the residual strength of a dike body assumed to be homogeneous ('erosion model without mixing') whereby the width L_k must be considered up to the inner crest.

To take into account the residual strength of the dike core itself as well, the so-called 'rudimentary erosion model' was developed. This rudimentary erosion model was developed for dikes with a sand core. The residual strength of the dike core is expressed as the time a storm takes to erode through the core. The residual strength is calculated as follows:

$$t_{RB} = \frac{0.4 L_K c_{RB}}{r^2 H_s^2}$$

In this comparison the width of the dike core is considered at a level $0.25H_s$ below the storm level and the coefficient c_{RB} is calculated, taking into account the relative quality of the material in the dike core in relation to the quality of the covering clay layer.

$$c_{RB} = \frac{c_{RK}}{v_{ZB}}$$

whereby $c_{RK} =$ erosion resistance of the clay

$v_{ZB} =$ acceleration factor for the erosion speed of the core in relation to the clay

$$v_{ZB} = (1 + \alpha_Z r_Z) h_Z$$

whereby $\alpha_z = 6$ for a sand core (=2 for a poorer clay quality in the core)

$r_Z =$ average share of sand in the dike profile

$h_z =$ deceleration factor which will account for a slower erosion process as the waves further penetrate the core

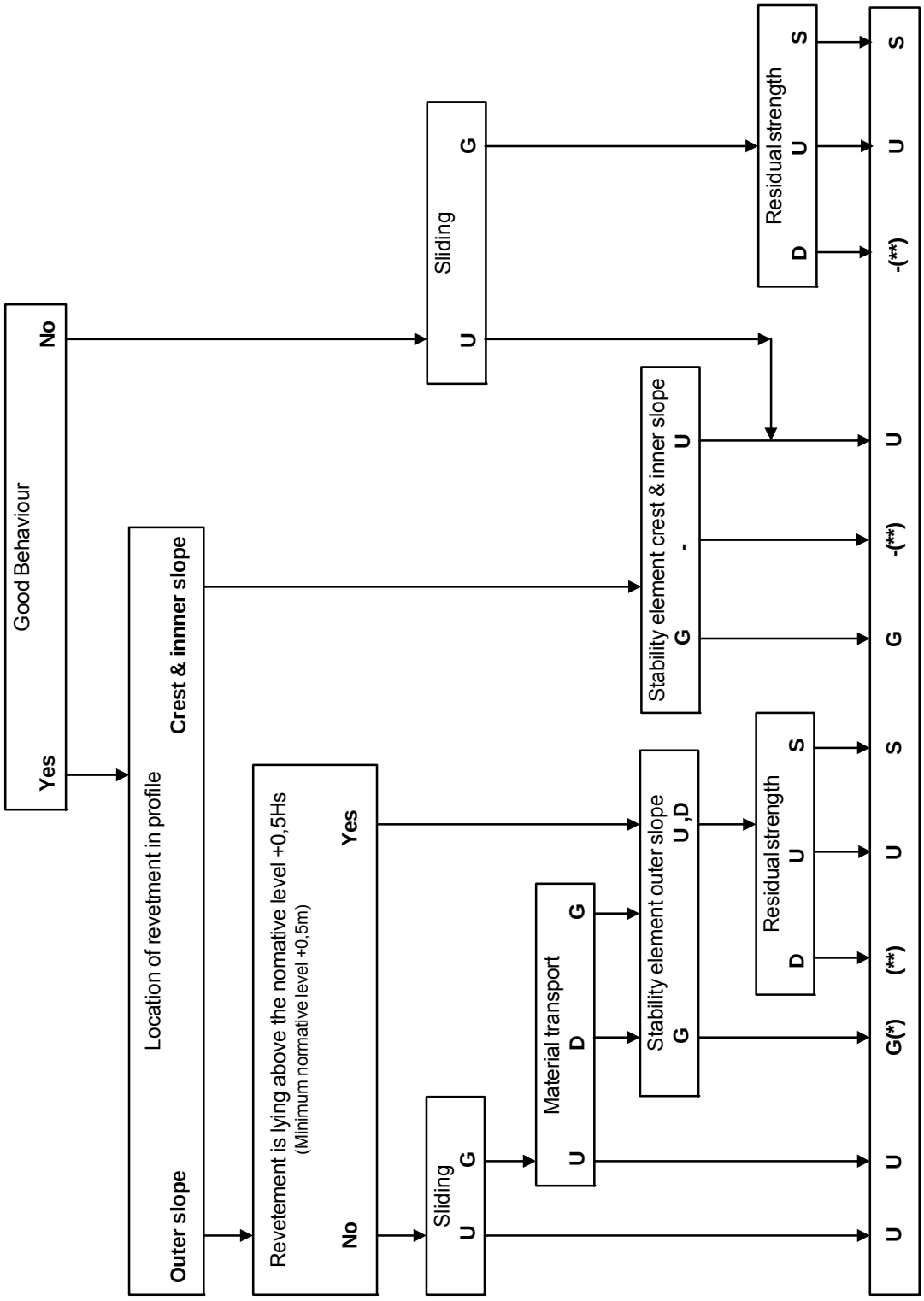

(*) score is 'sufficient' if material transport has a score 'doubtful'; (**) further examination is necessary.

Figure 32 Assessment diagram for concrete slabs.

5.9.2. Stone pitching

For the stone pitching the following assessment diagram must be followed (VTV, 2004):

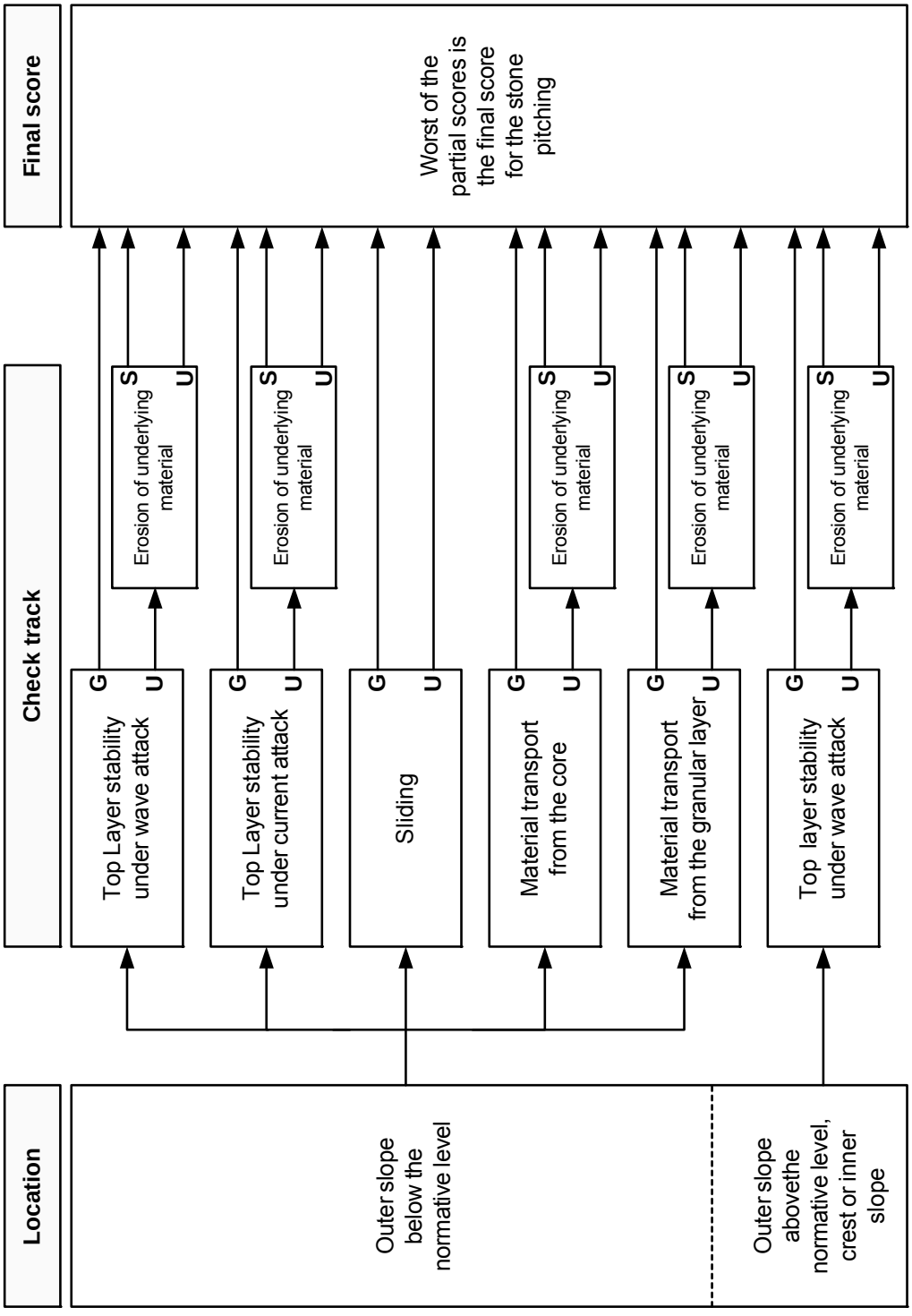

Figure 33 Stone pitching assessment diagram.

The top layer stability under wave attack is assessed by means of the diagram below (VTV, 2004):

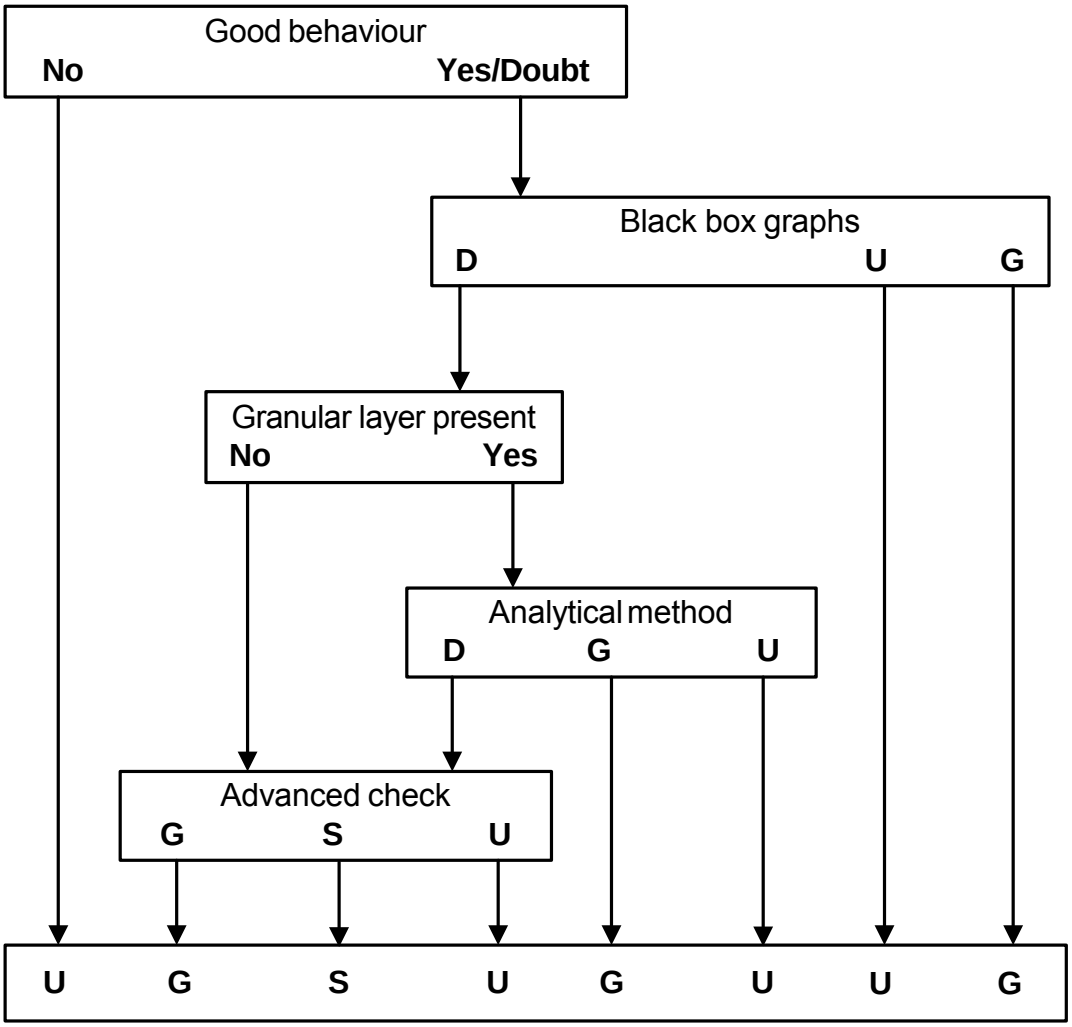

Figure 34 Assessment diagram for top layer stability under wave attack.

The so-called 'black-box graphs' for the basic assessment are as follows for the various types of constructions (VTV, 2004):

stone pitching on geotextile on sand or clay
(type 1)

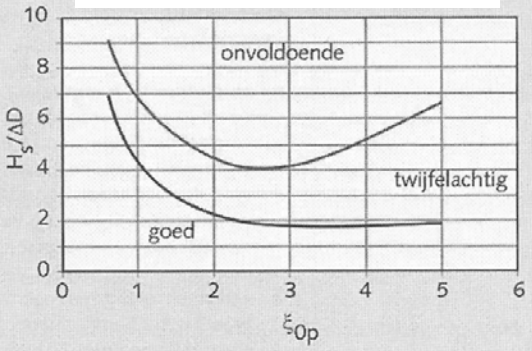

Voorwaarde voor score 'goed':
- als $0,6 < \xi_{0p} \leq 2,2$ dan $H_s/\Delta D < 4,31\ \xi_{0p}^{-0,926}$; of
- als $2,2 < \xi_{0p} \leq 5,0$ dan $H_s/\Delta D < 11,0\ \xi_{0p}^{-4} + 0,09\ \xi_{0p} + 1,38$.

Voorwaarde voor score 'onvoldoende':
- als $0,6 < \xi_{0p} \leq 2,2$ dan $H_s/\Delta D > 6,78\ \xi_{0p}^{-0,588}$; of
- als $2,2 < \xi_{0p} \leq 5,0$ dan $H_s/\Delta D > 17,0\ \xi_{0p}^{-2} + 1,84\ \xi_{0p} - 3,25$.

Dutch	English
goed	good
twijfelachtig	doubtful
onvoldoende	unsufficient
voorwaarde	condition
gunstige constructie	favourable construction
normale constructie	normal construction
ongunstige constructie	unfavourable construction

stone pitching on good clay
(type2)

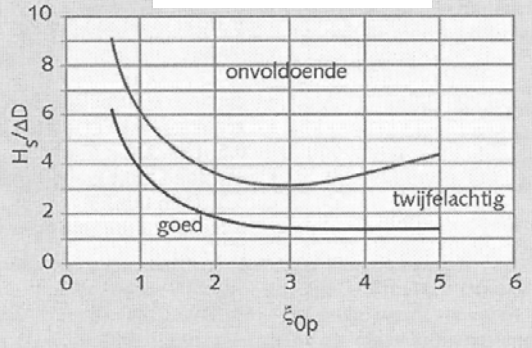

Voorwaarde voor score 'goed':
- als $0,6 < \xi_{0p} \leq 2,4$ dan $H_s/\Delta D < 3,75\ \xi_{0p}^{-1,001}$; of
- als $2,4 < \xi_{0p} \leq 5,0$ dan $H_s/\Delta D < 8,0\ \xi_{0p}^{-4} + 0,02\ \xi_{0p} + 1,25$.

Voorwaarde voor score 'onvoldoende':
- als $0,6 < \xi_{0p} \leq 2,1$ dan $H_s/\Delta D > 6,1\ \xi_{0p}^{-0,75}$; of
- als $2,1 < \xi_{0p} \leq 5,0$ dan $H_s/\Delta D > 11,0\ \xi_{0p}^{-2} + 0,98\ \xi_{0p} - 1,0$.

Dutch	English
goed	good
twijfelachtig	doubtful
onvoldoende	unsufficient
voorwaarde	condition
gunstige constructie	favourable construction
normale constructie	normal construction
ongunstige constructie	unfavourable construction

stone pitching on granular layer, favourable construction, met C_{slib}=1,0 (type 3a)

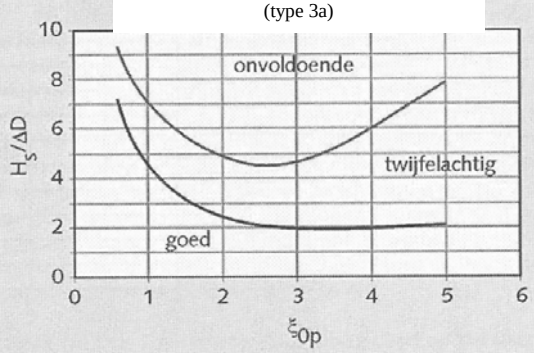

Voorwaarde voor score 'goed':
- als $0,6 < \xi_{0p} \leq 2,2$ dan $H_s/\Delta D < 4,58\ \xi_{0p}^{-0,903}$; of
- als $2,2 < \xi_{0p} \leq 5,0$ dan $H_s/\Delta D < 14,5\ \xi_{0p}^{-4} + 0,17\ \xi_{0p} + 1,27$.

Voorwaarde voor score 'onvoldoende':
- als $0,6 < \xi_{0p} \leq 2,2$ dan $H_s/\Delta D > 7,12\ C_{slib}\ \xi_{0p}^{-0,539}$; of
- als $2,2 < \xi_{0p} \leq 5,0$ dan $H_s/\Delta D > C_{slib}\ (17,8\ \xi_{0p}^{-1,5} + 2,54\ \xi_{0p} - 6,32)$.

Dutch	English
goed	good
twijfelachtig	doubtful
onvoldoende	unsufficient
voorwaarde	condition
gunstige constructie	favourable construction
normale constructie	normal construction
ongunstige constructie	unfavourable construction

stone pitching on granular layer, normal construction, C_{slib}=1,0 (type 3b)

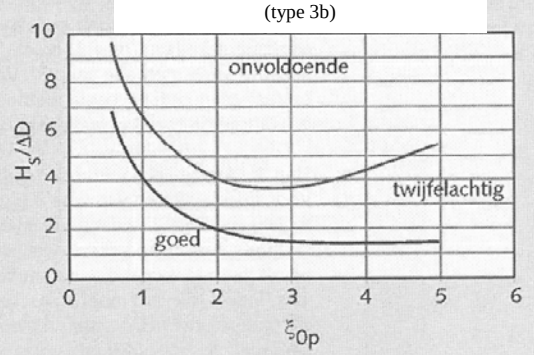

Voorwaarde voor score 'goed':
- als $0,6 < \xi_{0p} \leq 2,0$ dan $H_s/\Delta D < 4,08\ \xi_{0p}^{-1,014}$; of
- als $2,0 < \xi_{0p} \leq 5,0$ dan $H_s/\Delta D < 11,0\ \xi_{0p}^{-4} + 0,03\ \xi_{0p} + 1,25$.

Voorwaarde voor score 'onvoldoende':
- als $0,6 < \xi_{0p} \leq 2,1$ dan $H_s/\Delta D > 6,68\ C_{slib}\ \xi_{0p}^{-0,723}$; of
- als $2,1 < \xi_{0p} \leq 5,0$ dan $H_s/\Delta D > C_{slib}\ (12,0\ \xi_{0p}^{-1,5} + 1,5\ \xi_{0p} - 3,12)$.

Dutch	English
goed	good
twijfelachtig	doubtful
onvoldoende	unsufficient
voorwaarde	condition
gunstige constructie	favourable construction
normale constructie	normal construction
ongunstige constructie	unfavourable construction

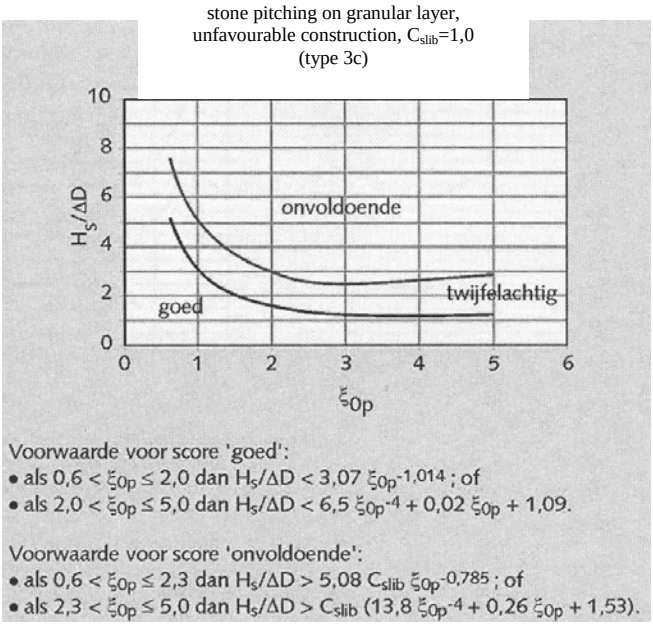

Dutch	English
goed	good
twijfelachtig	doubtful
onvoldoende	unsufficient
voorwaarde	condition
gunstige constructie	favourable construction
normale constructie	normal construction
ongunstige constructie	unfavourable construction

Figure 35 Basic assessment for stone pitching under wave attack.

The assessment diagram for the top layer stability under current attack (VTV, 2004):

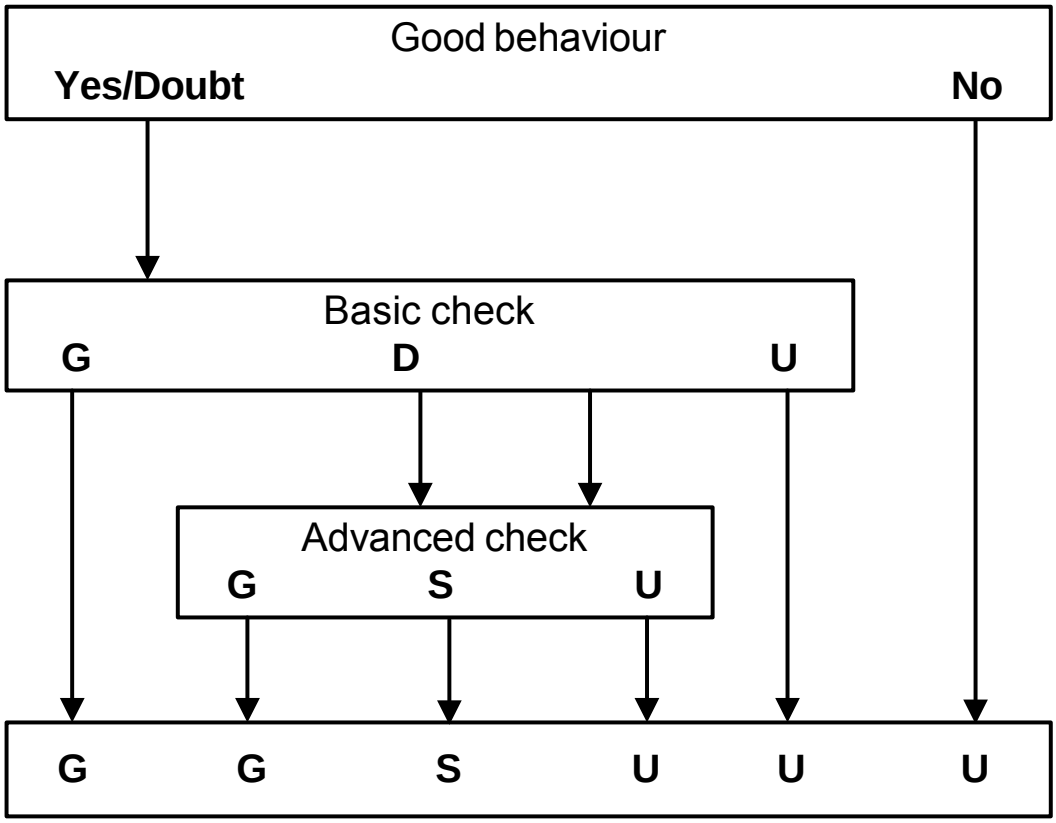

Figure 36 Assessment of top layer stability under current attack.

With regard to the top layer stability under current attack, the velocity is calculated by means of Schüttrumpf et al. (2000) whereby

$$u = 0.85\sqrt{2gRu}$$

with Ru = wave run-up height [m]

The basic assessment of the top layer stability under current attack is made in accordance with the following criterion (VTV, 2004):

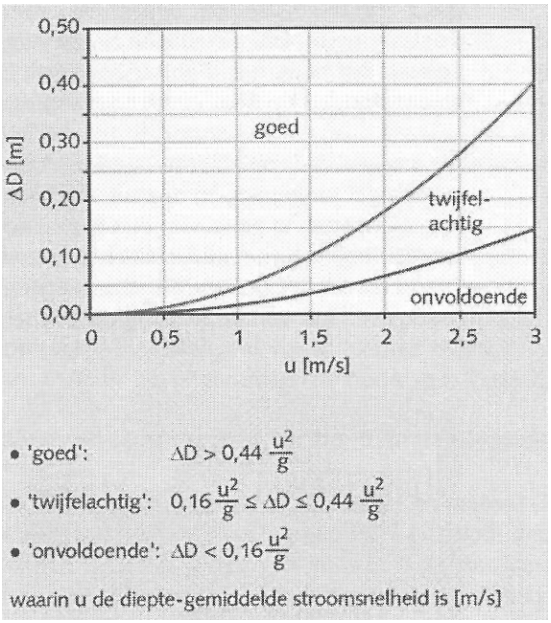

Dutch	English
goed	good
twijfelachtig	doubtful
onvoldoende	unsufficient
u	current velocity

Figure 37 Basic assessment of stone pitching under current attack.

With regard to sliding, the following assessment criterion must be followed (VTV, 2004):

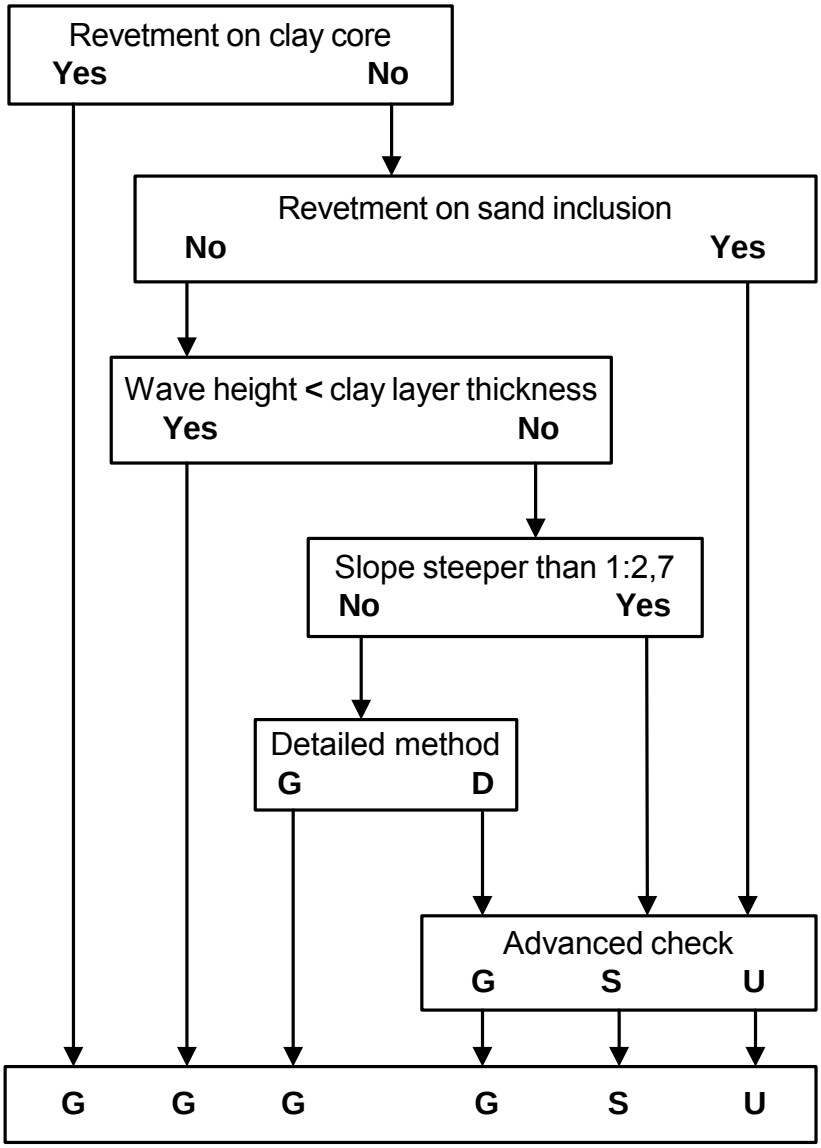

Figure 38 Sliding assessment.

5.9.3. Asphalt revetments

For asphalt revetments the following assessment diagram must be followed (VTV, 2004):

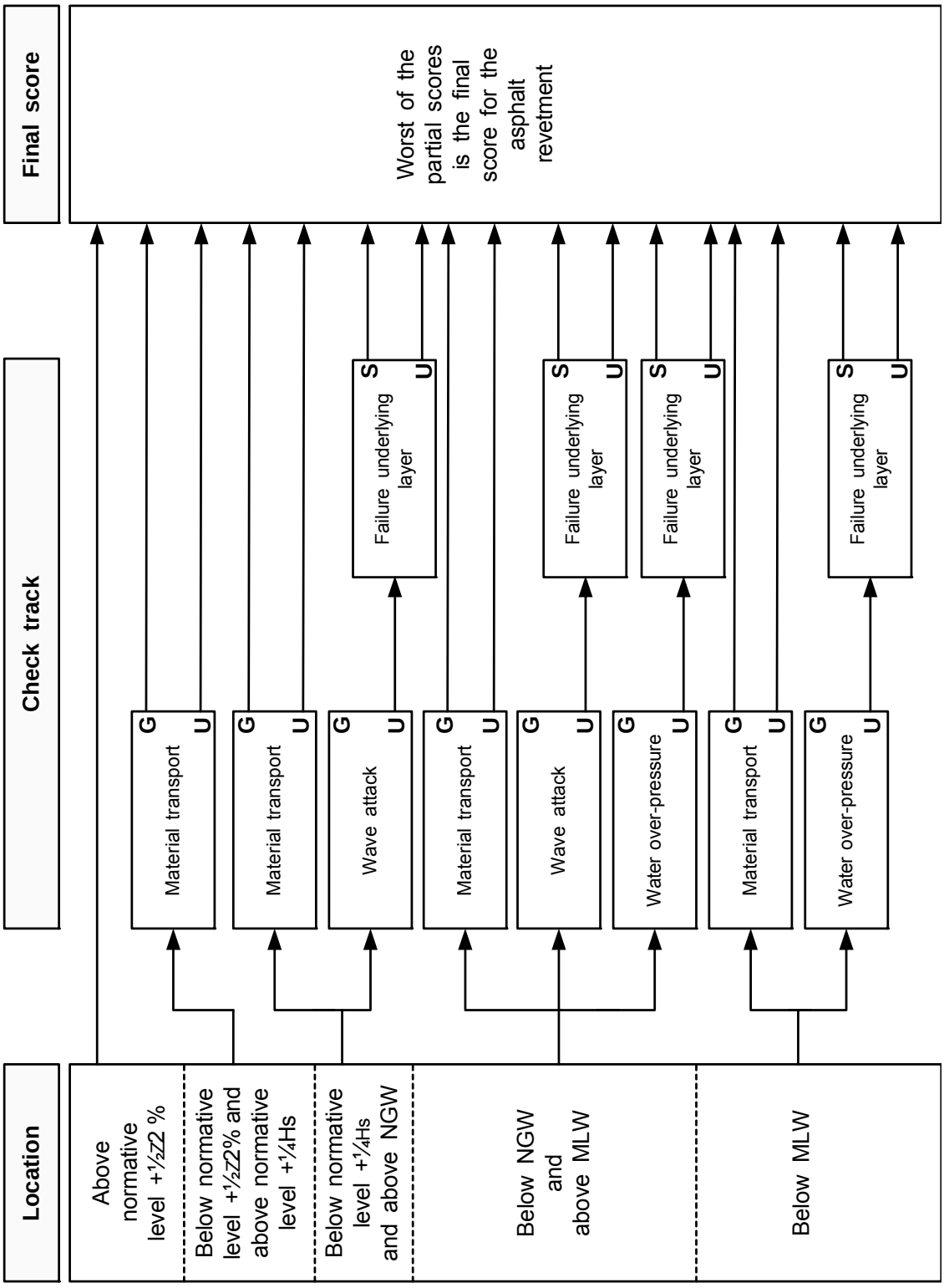

Figure 39 Assessment diagram for asphalt revetment.

For the 'wave impact' criterion the following assessment diagram must be followed (VTV, 2004):

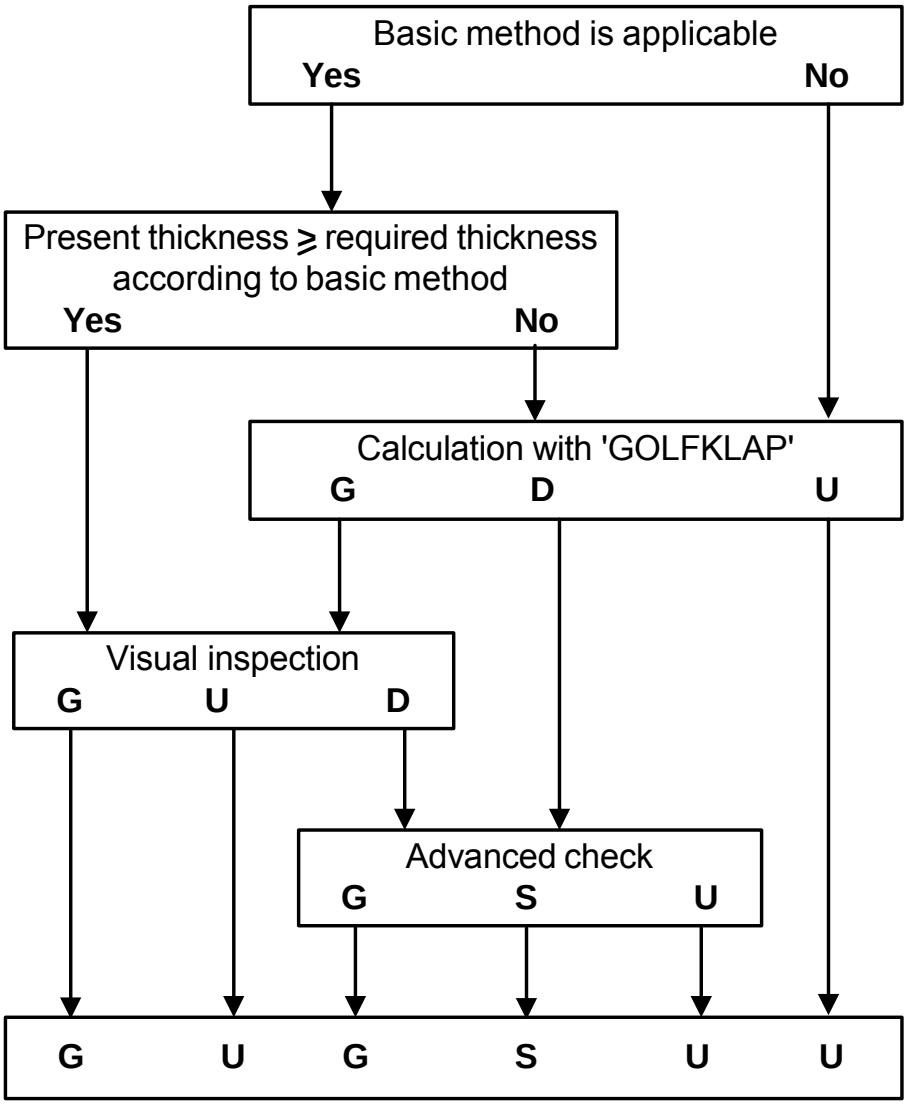

Figure 40 Wave impact assessment.

5.10. Crest height assessment

With regard to the failure mechanism for overflow and overtopping, the normative combination of water level and wave run-up exerts loads on dikes and dams.

The crest must be sufficiently high to avoid large overtopping or overflowing water volumes. Large overtopping volumes can cause critical current speeds over the crest and the inner slope.

Four strength characteristics exist for the 'height' assessment track, which together determine whether or not a dike can meet the requirements:

- the crest height (future settlements were not taken into account in this report);
- the resistance to erosion and local sliding of the crest and inner slope due to overtopping water. Insufficient resistance will lead to a loss of crest height, possibly followed by breach formation;
- the characteristics of the crest in relation to passableness/accessibility/rideability (the report did not take this into account);

- the possibilities for drainage and storage of overtopping water (only plays a role in the assessment insofar as the safety is jeopardised).

For all locations an average overtopping discharge is calculated for the dike construction and wave characteristics in question. By means of the Schüttrümpf method (Schüttrümpf, 2003) the corresponding speed of the overtopping water tongue can be calculated for this overtopping discharge at various locations of the dike profile: seaward side at water level, crest on seaward side, landward slope …

5.10.1. Erosion of inner slope by overtopping water

To determine the residual strength of the inner slope of a classic dike body, only the resistance of the grass cover and the underlying clay layer are taken into account. Thus it is assumed that if these layers do not hold out within the storm duration, the remaining sand package will be eroded in a short period of time by overtopping/overflowing water. To determine the residual strength of the inner slope, the method described in the TNO report 'Theory Manual PC Ring Version 4.0' under chapter *Mechanisme sterkte bekleiding binnentalud* (Mechanism of inner slope revetment strength, TNO report, 2003) is followed. It must be noted here that the dike bodies in Flanders definitely do not meet the definition of a *classic dike body.*

It is assumed here that the relation between the strength of the grass cover and the strength of the clay cover on the landward side is equal to the relation on the seaward side.

Residual strength of the grass cover on the seaward side: $t_{RT,buiten}=d_w/E_g$

with $E_g = \frac{r^2 H_s^2}{c_g}$ E_g = erosion speed of grass cover

c_g = erosion resistance of grass cover ($3.3^{E}05$ms for poor grass quality, $1^{E}6$ms for good grass quality)

H_s = significant wave height

r = correction factor for slanting waves

d_w = rooting depth of the grass cover (0.05m – 0.07m)

Residual strength of the clay top layer: $t_{RK,buiten} = \frac{0.4 L_K c_{RK}}{r^2 H_s^2}$

with L_K = width of clay top layer

c_{RK} = erosion resistance of clay layer ($7^{E}03$ms for poor clay quality, $54^{E}03$ms for good quality)

The relation of the grass cover quality to the clay cover on the inside is thus:

$$\frac{t_{RT,binnen}}{t_{RK,binnen}} = \frac{c_g d_w}{0.4 c_{RK} L_K}$$

To avoid dike failure due to erosion of the inner slope by overtopping water, the sum of the residual strength of the grass cover and the residual strength of the underlying clay layer must be smaller than the total storm duration t_s:

$$t_s \le t_{RT,binnen} + t_{RK,binnen} = t_{RT,binnen} + \frac{0.4 c_{RK} L_{K,binnen}}{c_g d_w} t_{RT,binnen} = \frac{c_g d_w + 0.4 c_{RK} L_{K,binnen}}{c_g d_w} t_{RT,binnen}$$

This means that the residual strength of the grass cover must equal at least

$$t_{RT,binnen} \ge \frac{c_g d_w}{c_g d_w + 0.4 c_{RK} L_{K,binnen}} t_s .$$

To take into account the fact that overtopping volumes have a pulsating nature (opposed to overflow water), this time must be multiplied with a factor P_t (part of the time the rear of the dike is attacked by wave overtopping water). The effective period of time the grass cover must resist the high speeds of overtopping water: $t_e = P_t t_{RT,binnen}$

Using the CIRIA formulas for the strength of a grass cover, the critical speed v_c can then be calculated in accordance with:

$v_c = f_g \frac{3.8}{1 + 0.8 \log t_e}$ with f_g= 0.7 for a poor grass cover and 1.4 for a good grass cover quality

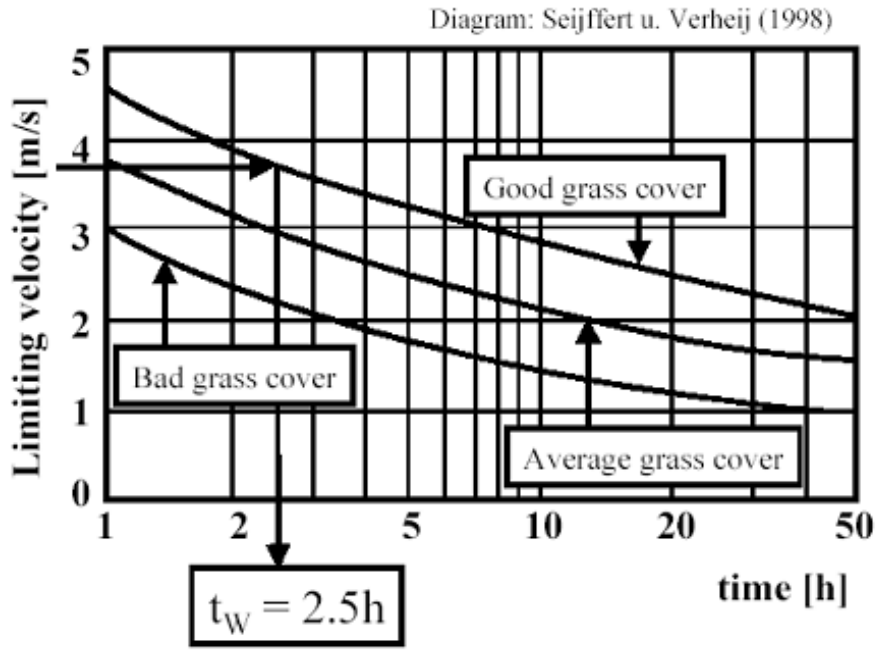

Figure 41 Erosion resistance of slopes covered with grass (in case of overflow).

This critical velocity v_c is then compared with the speeds actually occurring on the inner slope, calculated in accordance with the Schüttrümpf method (Schüttrümpf, 2003).

5.10.2. Sliding of the inner slope due to liquefaction

Due to large overtopping discharges, there is a possibility that the core of the dike body is saturated with water. As the soil gets more saturated with water the effective shear strength of the soil is reduced. If the slope of the dike is too steep, this will create the possibility that the inner slope will slide.

The 2003 TNO report CI-R0020 mentions a critical slope calculated in accordance with the method of Joustra and Edelman. This critical slope depends on the densities of soil and water, the internal friction angle and the soil cohesion. However, this method can lead to overly conservative requirements and – all the more so because few data are available about the clay characteristics – is not used further.

A more pragmatic evaluation will be made of the stability against sliding of the inner slope due to liquefaction. The description of the damage after the storm flood of February 1, 1953 showed that no damage had occurred for slopes gentler than 1:2.5. No examples are known of a dike breach due to erosion by overtopping water. During the 1953 flood, surface erosion was a rarity. Examples are known of dikes with steep inner slopes that collapsed due to overtopping in 1916 and 1953. Dikes with an inner slope gentler than 1:3 sustained significantly less damage. Large-scale tests showed that wave overtopping up to 10l/s/m puts a slight erosion load on the inner slope.

The figure below (cfr. Figure 42) gives 20 to 30l/m.s as a critical overtopping discharge for structural safety if the inner slope is unprotected.

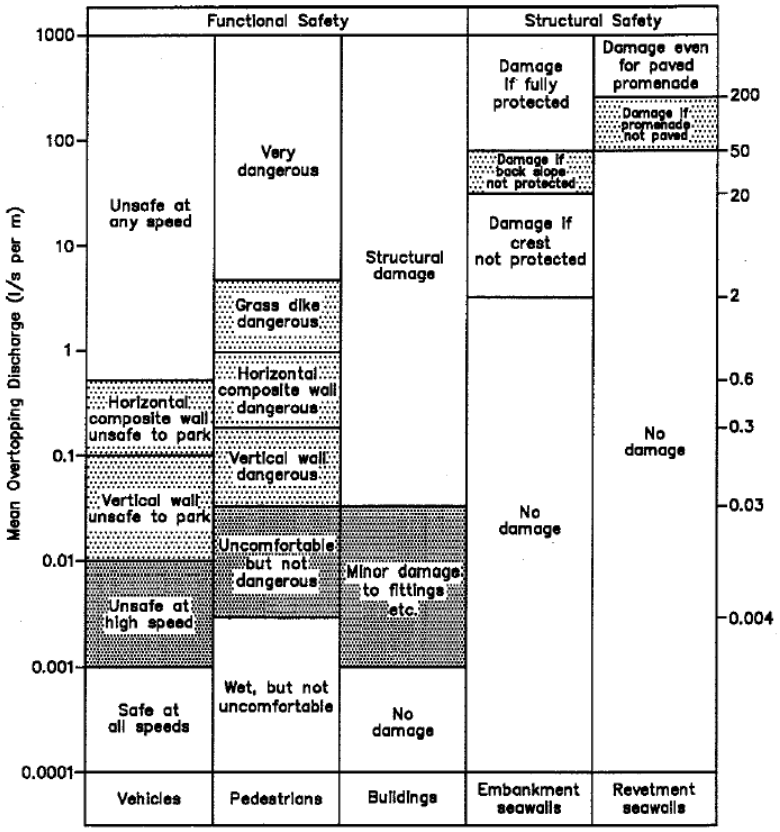

Figure 42 Acceptable overtopping discharges (from CIRIA/CUR Manual, 1991).

6. FAILURE OF SEA DEFENCE: RESULTS FOR FLANDERS

To assess the sea defence in Flanders, 3 return periods are considered: 1000, 4000 and 40000 years.

6.1. Introduction

The Flemish coast is divided into 259 profiles (1 at the French border, 259 at the Dutch border). For each dike section the most critical profile was selected.

With regard to Flanders, this project considers all the profiles to the east of the harbour of Zeebrugge profile (from profile 217) to the Zwin (profile 248).

6.2. Dune erosion

The only dunes occurring within the study area are those in the Zwin area. As these do not serve as primary sea defences, they are not subject to a test for the various return periods. In case of a possible breach it is also difficult to assess the effect on the Zwin basin, as the morphology within the basin probably changes greatly when such severe storms occur.

6.3. Beach erosion

Beach erosion in itself is not a failure, but strongly influences the results of other failure mechanisms. The wave height at the toe of the dike is strongly influenced by the beach in front of it and thus also by the wave impact on the dike and the overtopping discharges. The beach profile in front of the dike also determines the passive soil pressure and thus the stability of the dike body (sliding of the outer slope in case of low outer water).

In the figures below (Figure 43 through Figure 45) the erosion profile for profile 236 is given after a storm with 1000-, 4000- and 40000-year return periods. The *Hs 70* value mentioned above the figures is the minimum of the significant wave height at 70 m from the toe of the dike and the water depth at the toe of the dike.

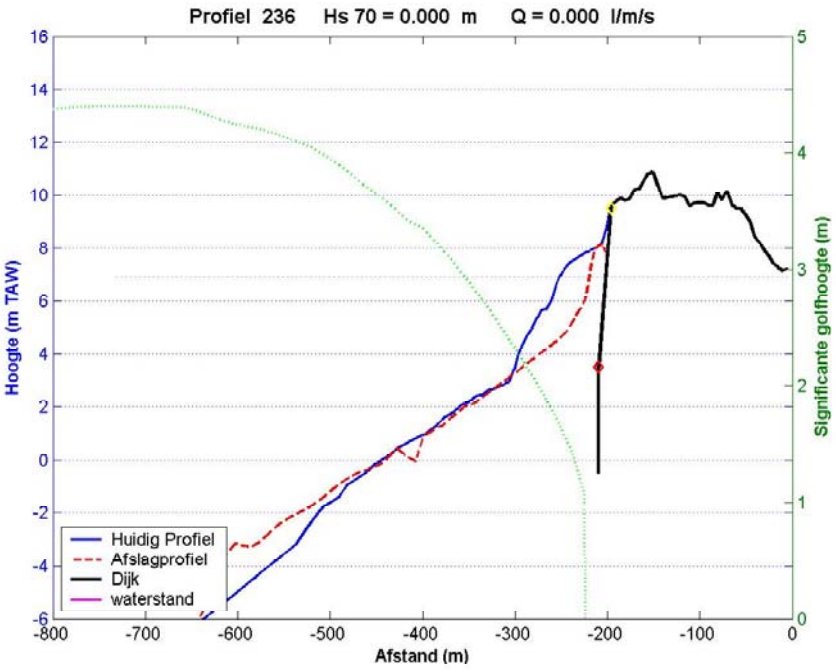

Dutch	English
hoogte	elevation
significante golfhoogte	significant wave height
afstand	distance
huidig profile	current profile
afslagprofiel	eroded profile
dijk	dike
waterstand	water level

Figure 43 Beach profile of profile 236 after a storm with a 1000-year return period.

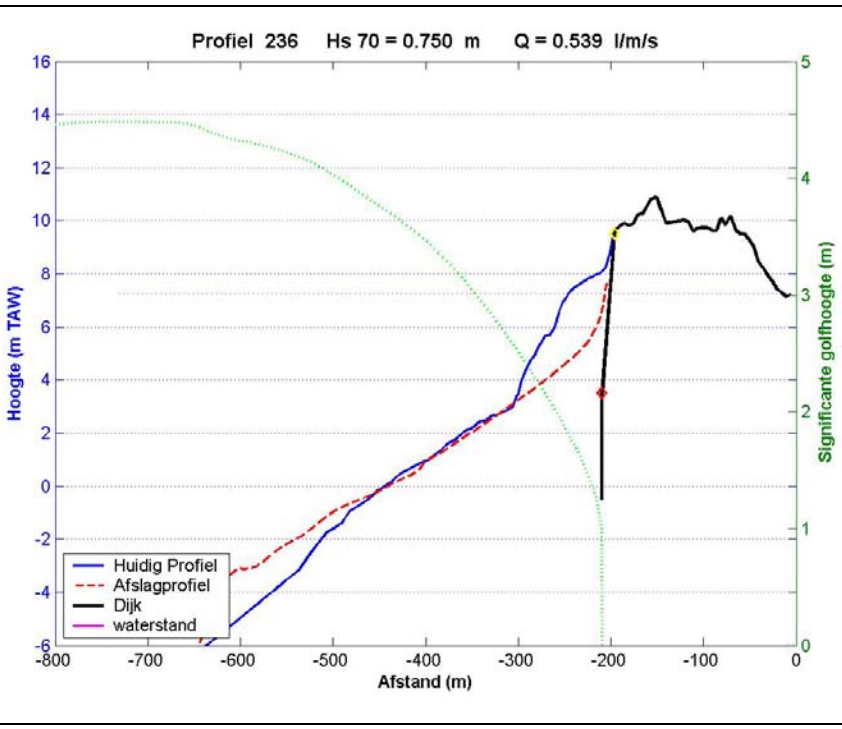

Figure 44 Beach profile of profile 236 after a storm with a 4000-year return period.

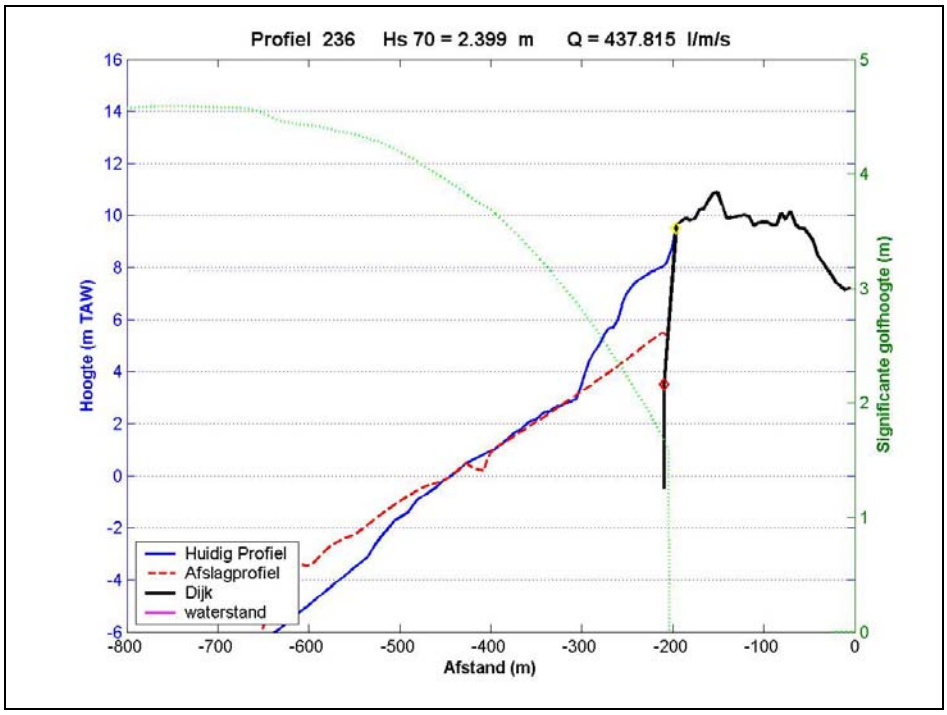

Figure 45 Beach profile of profile 236 after a storm with a 40000-year return period.

6.4. Piping en heave

Each dike profile was catalogued according to the overall dike structure (type 1 = clay core; type 2 = sand core) and according to the overall subsoil structure (type A = (relatively) impermeable with layer thickness D; type B = sand) in Table 3.

profile	dike(*)	subsoil(**)
p_225	2	B
p_233	2	B
p_234	2	B
p_235	2	B
p_238	2	B
p_239	2	B
p_242	2	B
p_243	2	B
p_246	2	B

(*) core: type 1 = clay core; type 2 = sand core
(**) subsoil: type A = (relatively) impermeable; type B = sand

Table 3 Overall classification of dike and subsoil.

All dikes are of type 2B (sand core on a sandy subsoil). Type 2B does not experience piping according to LTV, provided that no silt layer remained after construction. It is assumed that no silt layer remained after the construction of the dikes.

In general, piping does not apply as the dikes in question are not true dikes, but rather reinforced dunes that are very wide.

Conclusion: the score 'good' is given to all dike profiles considered.

6.5. Inward macrostability

With regard to the sections considered, this failure mechanism was not taken into account for Flanders. The dikes are in fact protected dunes. There is no clear inward slope.

The first step in the LTV assessment mechanism for the inward macrostability comprises the testing of the safe dimensions of the dike. The dikes of type 2 (dike core of sand) are certainly safe, if the inner slope is gentler than 1 in 6. If the average slope of the dikes between Zeebrugge and the Zwin is considered, this is largely complied with.

Conclusion: the score 'good' is given to all dike profiles considered.

6.6. Outward macrostability

6.6.1. Sliding and liquefaction of the foreshore

The results of the sliding and liquefaction assessment are summarised in Table 4. Assuming that no liquefaction-sensitive layers are present, the present soil profiles give a positive result for the sliding criterion. The case that liquefaction-sensitive layers are present, was also taken into account.

profile no.	covering criterion	trough depth H [m]	sliding criterion	liquefaction criterion	final assessment
234	OK	13.27	OK	OK	g
238	OK	12.24	OK	OK	g
239	OK	9.46	OK	OK	g

Table 4 Results for the assessment of covering, sliding and liquefaction criteria.

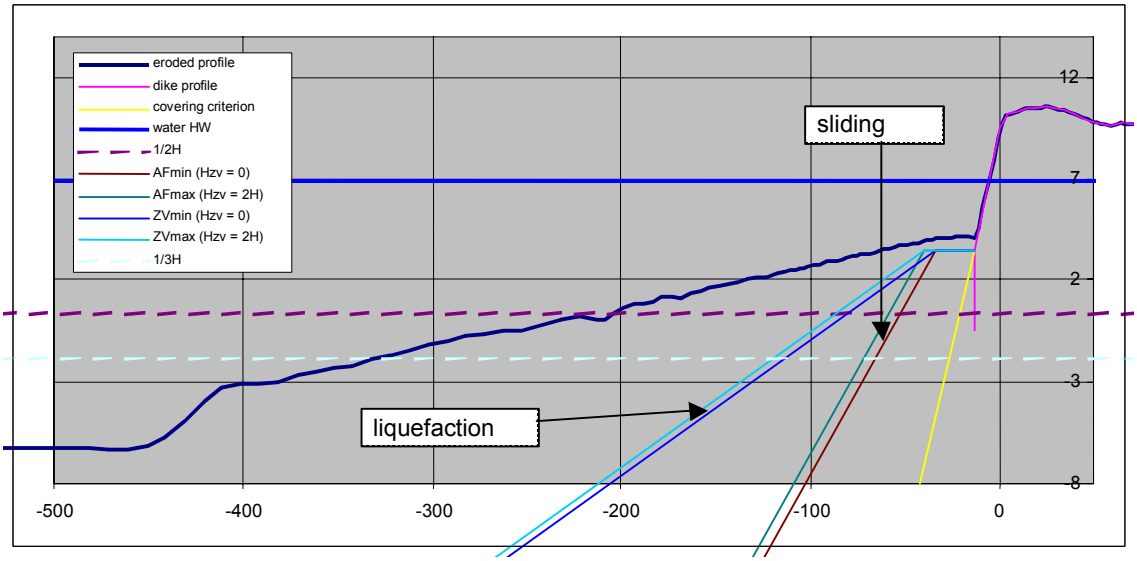

Figure 46 Assessment of sliding and liquefaction of the foreshore for profile 234.

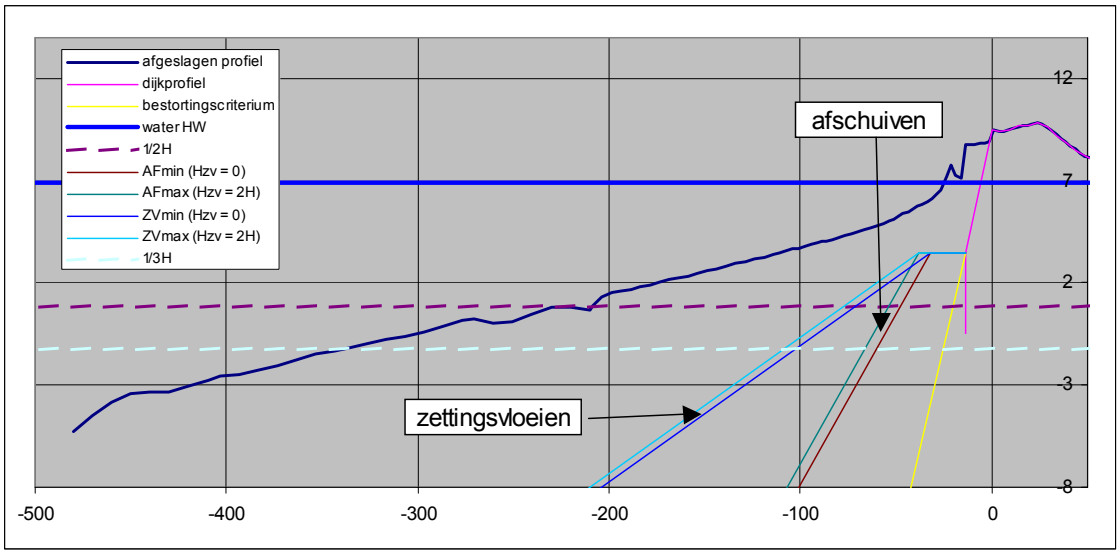

Figure 47 Assessment of sliding and liquefaction of the foreshore for profile 238.

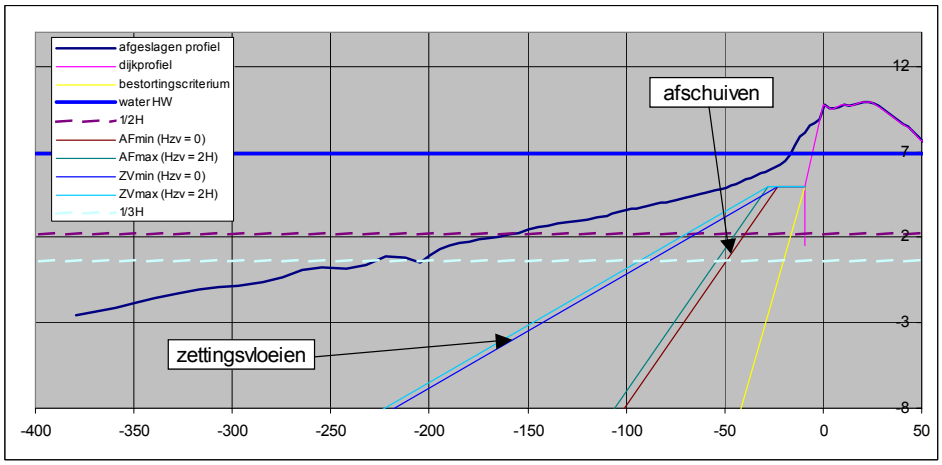

Figure 48 Assessment of sliding and liquefaction of the foreshore for profile 239.

The possible presence of a berm was not taken into account. Because the berm is not taken into account, the covering and signalling profiles are pushed landward. Table 5 gives the 'overwidths' per profile considered. This 'overwidth' is the horizontal distance a berm may take up for compliance with the covering, sliding and liquefaction criteria.

profile	overwidth [m]
p_234	35.00
p_238	85.06
p_239	28.45

Table 5: Overwidth of profiles.

6.6.2. Sliding of outer slope

The sliding of the outer slope at low tide was assessed for the most critical profiles for a 40000-year return period. For the profiles in Flanders it was always assumed that the phreatic line always follows the outer water immediately, as the subsoil always consists of sand. Behind the outer toe of the dike the phreatic level rises parabolically to an average water level (average of high and low water levels).

In the SLOPE-model a low outer water level of 2m TAW was assumed for a return period of 1000 years and 2.72m TAW for 40000 years. The phreatic line in the dike body rises to an average level of 4.43m TAW for the 1000 year return period and to 5.3m TAW for the 40000 year return period.

Figure 49 gives a summary of the results of the stability calculations. The figures below show the most critical slip surface corresponding with the safety coefficient given in Figure 52.

profile	Liqu.	Slid.	sliding (return period of 1000 years)	sliding (return period of 40000 years)	final assessment
			safety coefficient γ regarding sliding equilibrium Return period of 1000y	safety coefficient regarding sliding equilibrium Return period of 40000y	
p_234	g	g	3.94	2.07	g
p_235				1.94	g
p_238	g	g		4.77	g
p_243				1.79	g
p_246				3.56	g

Figure 49: Summary of the results of the outward macrostability assessment.

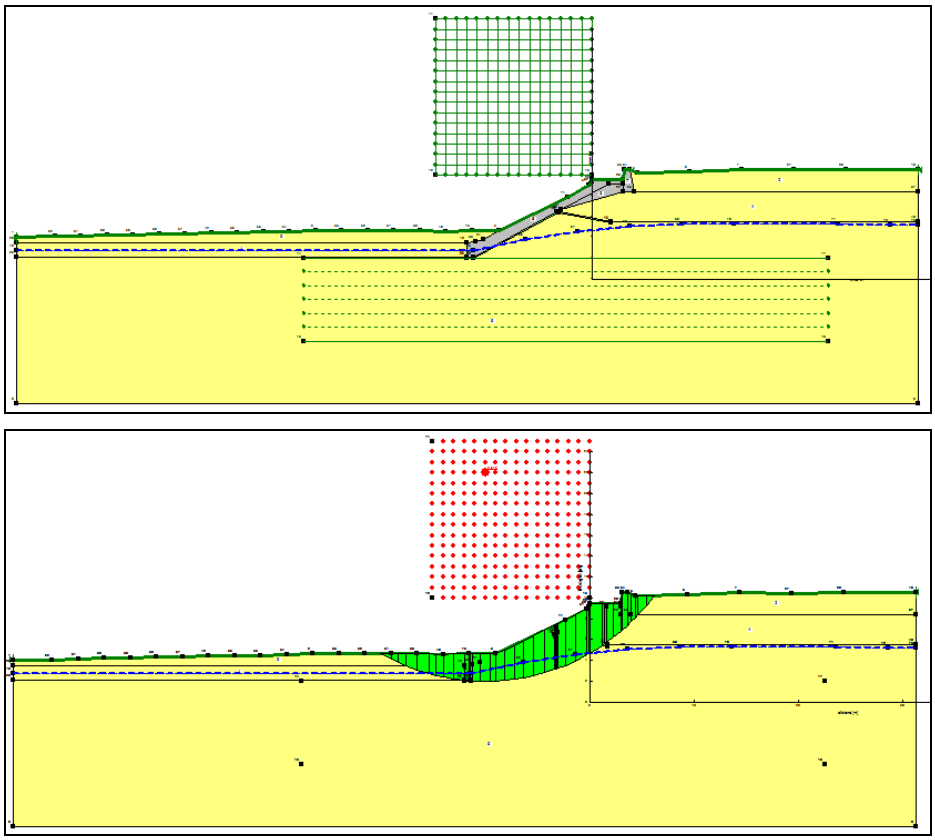

Figure 50 Most critical slip surface for profile 234 for a 40000-year return period.

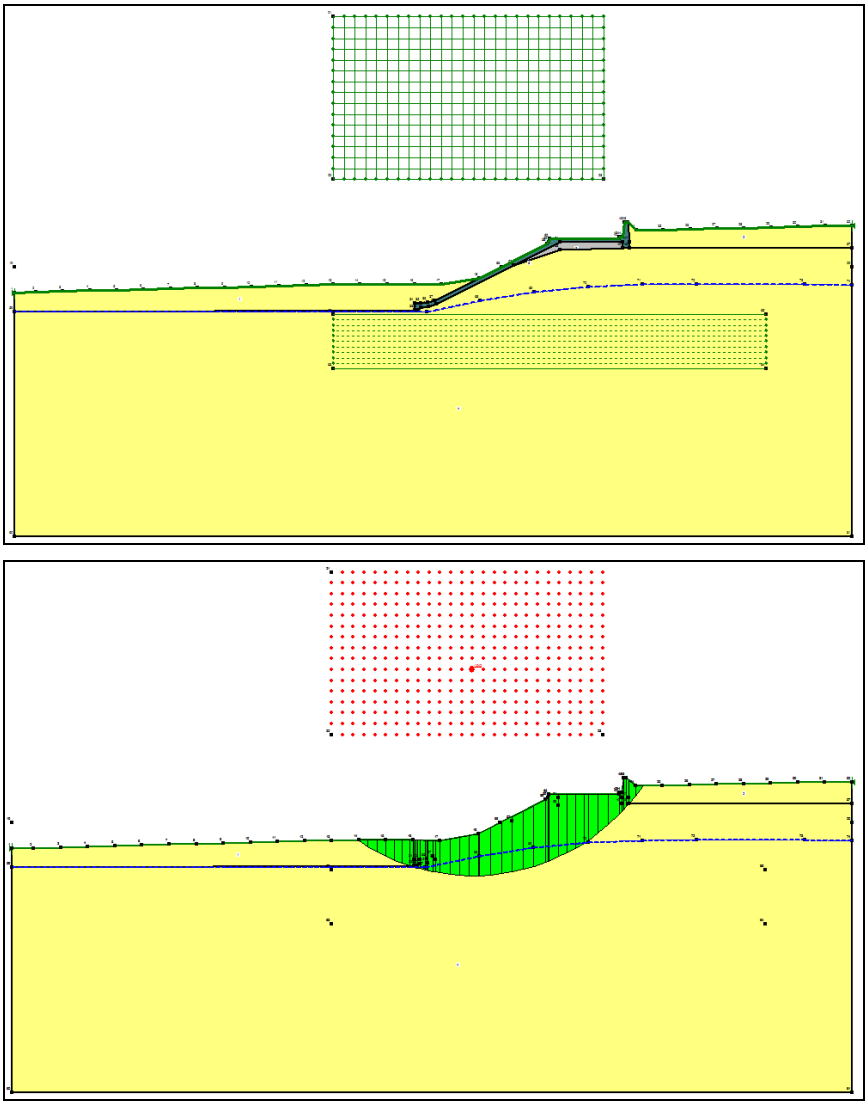

Figure 51 Most critical slip surface for profile 235 for a 40000-year return period.

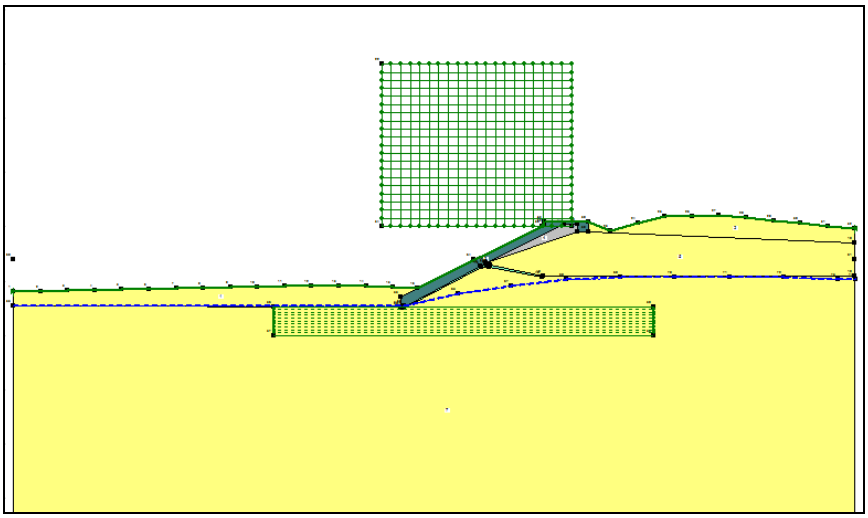

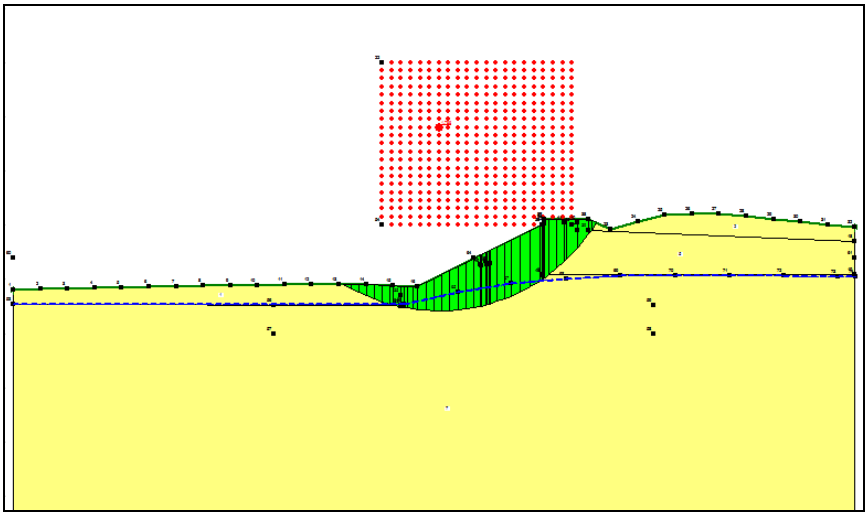

Figure 52 Most critical slip surface for profile 243 for a 40000-year return period.

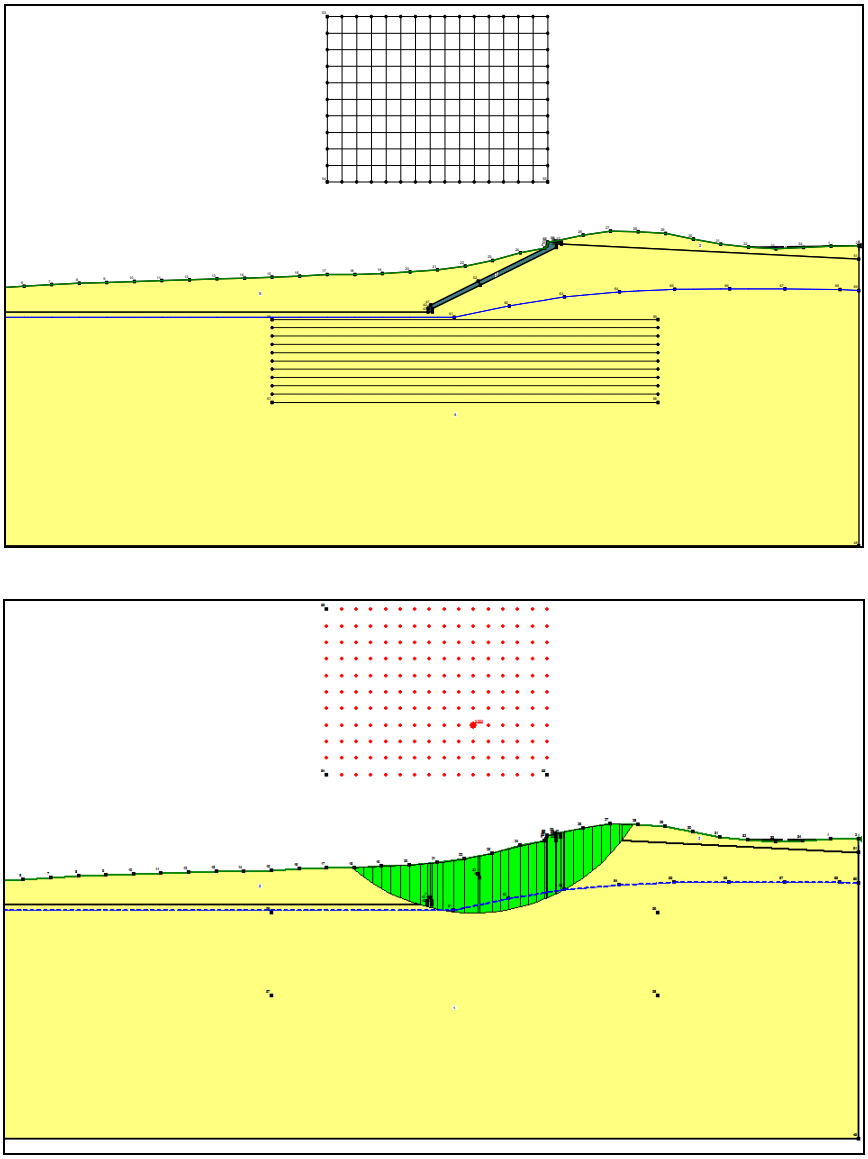

Figure 53 Most critical slip surface for profile 246 for a 40000-year return period.

<u>Conclusion:</u> as the most critical beach profile for a given type of dike profile was consistently used, not a single profile causes problems with regard to the dike stability at low outer water. The score 'good' is given to all dike profiles considered. The different profiles were assessed with an eroded beach profile after a storm with a 40000-year return period. As all profiles complied, an assessment for shorter return periods is not necessary.

6.7. Outward microstability of the slope

With formula (2) $\gamma_{\perp} = \frac{\gamma_g - \gamma_w}{\gamma_w}(\cot\alpha)^2$ and γ_g = 20 kN/m^3, γ_w = 10.26 kN/m^3 and cot α = 2 (virtually all slopes are 1:2) $\gamma_{\perp} = 3.80$ whereby it is required in LTV(1999) that $\gamma_{\perp} > 2$. The perpendicular equilibrium is complied with.

Formula (3) can be used to determine the maximum piezometric fall (difference in water level behind the dike revetment and in front of the dike revetment) to avoid uplift of the top layer. For ρ_g = 2500 kg/m^3, γ_w = 1026 kg/m^3, d = 0.50 m and tan α = 0.5, this amounts to Δh_{max} = 0.84 m. With formula (4) the maximum permissible piezometric fall for the above-mentioned data and tan φ = 27.5° amounts to Δh_{max} = 0.04 m. However, all lateral support of the revetment was ignored in the latter formula.

In all profiles considered for Flanders the impermeable clay layer lies at a great depth; assuming a hydraulic conductivity of k = 10^{-4} m/s for the sand, the phreatic water table never crosses the dike body. This prevents the occurrence of a gradient over the dike revetment. Larger hydraulic conductivities (k > 10^{-4} m/s) are more favourable.

<u>Conclusion:</u> all dikes considered are given a score 'good' for the microstability assessment.

6.8. Revetment

The dikes renewed after 1953 are described in §**6.8.2.1** below. Between Zeebrugge and the Zwin there are still some dikes predating 1953. Dike profiles 217 to 221 in Heist are old dikes built in 1830. At all these locations the dike body is covered with beach sand after erosion by a storm with a 40000-year return period. The dikes in Duinbergen (profiles 221 to 226) are all relatively old, but certain parts were renewed. In this area too there is no direct impact of the waves on the dike body, not even after beach erosion due to a storm with a 40000-year return period. Thus the stone pitching must not be assessed for these areas. The dike profiles between 226 and 232 predate 1953, but they are not directly exposed to waves.

As to the remainder, most dikes were reinforced after 1953 (concrete slab). Dike sections 238, 242 and 245 still have some old constructions predating 1953. Dike section 238 is still protected by a beach in front of it in a 40000-year storm. Profile 242 is directly exposed to wave impact, both after a 4000-year and after a 40000-year storm. Profile 245 is only subjected to a minimal wave height in a 40000-year storm.

Therefore only the revetment of profile 242 must be assessed. Considering the very high overtopping discharges at this profile, the stability of the crest revetment and the residual strength of the sand core were first examined (cfr. §6.9). The profile fails for both return periods (4000 year and 40000 years) in this test, making an additional assessment of the revetment superfluous.

6.8.1. Material transport

We assume that no subsidence or cavities are found under the top layer, neither above nor in the tidal area. Consequently, the score is 'good'. In case of doubt about the presence of cavities under the top layer, the second assessment stage gives a positive result: the slab revetment is fitted on a sub base made of lean concrete (work floor). If geotechnical research were to reveal that cavities are present under the dike revetment, this dike will immediately be given an 'unsufficient' score and the dike will be rejected. Cavities under the dike revetment cannot be tolerated!

6.8.2. Stability of outer slope element

6.8.2.1. Concrete slabs

To do the safety assessment the following initial construction data must be collected:

- slope;
- permeability of the top layer and the filter layer;
- thickness of the top layer and the filter layer;
- concrete strength and representative crack distance in the slab.

This basic assessment is made under the assumption that both the top layer (slab) and the bottom layer (filter) are both somewhat permeable, whereby the permeability of the filter is one order of magnitude larger than that of the top layer (k/k' = 100). This leads to a conservative calculation of the safety. The calculation below is made for a storm with a 40000-year return period.

The leakage length Λ amounts to

$$\Lambda = \sqrt{\frac{bDk}{k'}} = 2.74 \text{ m}$$

whereby

- b = thickness of the filter layer (d = 0.15 m)
- D = thickness of the top layer (D = 0.50 m (average))
- k/k' = 100 (assumption cfr. LTV for lack of information)

The breaker parameter must be calculated for all profiles (Table 6):

$$\xi_{op} = \frac{\tan\alpha}{\sqrt{\frac{H}{L_{op}}}}$$

with $\bullet\ L_{op} = \frac{gT_p^2}{2\pi}$

T_p = peak wave period for deep water (T_p = 13.15 s)

H = 1.4 H_{st} with a maximum of 0.6 times the water depth d at the toe of the construction

H_{st} = the significant wave height at the toe of the construction. This wave height is determined by the water depth, present at a distance $L_{op}/4$ for the crossing of the slope with the water line. Of course the wave height may be limited by possible breaking on the foreshore. The wave heights come from the DUROSTA calculations.

profile	H_{m0} [m]	T_p [s]	ξ_{op} [-]
p_234	2.75	13.15	4.95
p_238	0	13.15	-
p_239	0	13.15	-

Table 6 Iribarren numbers for the various profiles.

On average, the Iribarren number ξ_{op} is about 5. The parameters ϕ_b and tanβ are determined by means of the figure in the 'Safety Assessment Guideline' ('LTV'). These amount to ϕ_b=7.15 m and tan β=1.7 for H = 2.75 m (cfr. p_234). The figures from the 'Safety Assessment Guideline' are used approximatively, as the parameters ϕ_b and the relative thickness of the concrete layer fall outside the range of the figures. As a result, it is calculated that L_{max} will definitely be smaller than 1m (L_{max} = the distance along the slope on which the upward force acts on the top layer) and S_{max} will definitely be smaller than 0.3 (S_{max} = maximum upward force). The distance between the cracks caused by temperature fluctuations (as a rule, this is 5 to 10 m (LTV)) is generally so large that the slabs are not affected. The crack distance L_s is assumed to be L_s/L_{max} > 0.75 so that the assessment must be made by calculating the maximum stress in the concrete. The simple formula

$$\sigma = \frac{Mz}{I}$$

is used and only the concrete cross section is considered (the reinforcement is not taken into account). The maximum moment M_{max} amounts to

$$M_{\max} = \frac{\rho_w g S_{\max} L_{\max}^2}{12}$$

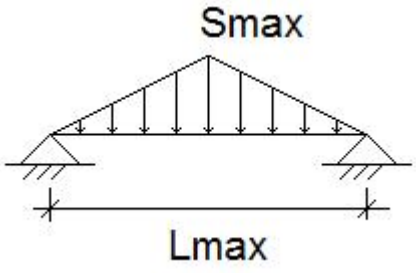

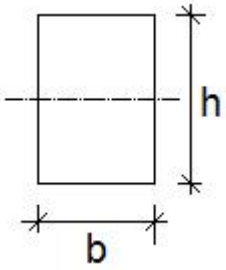

$$I = \frac{bh^3}{12}$$

so that the maximum normal stress in the cross section amounts to 6kPa.

$$\sigma_{\max} = \frac{\frac{\rho_w g S_{\max} L_{\max}^2}{12}\frac{h}{2}}{\frac{bh^3}{12}} = 6 \text{ kPa.}$$

For C25/30 concrete the tensile strength is f_{ctm} = 2.6 MPa, so that $\sigma_{b,toel}$ = 1.3 MPa >> σ_{max}, making the top layer safe and the score 'good'.

6.8.3. Crest element stability

If a stone revetment is placed on the crest and the inner slope, a sizeable overtopping discharge is allowed for. The revetment elements are consequently assessed for wave overtopping, whereby a fictitious wave height H_{crest}, is used, for which the following applies:

$$H_{kruin} = Ru_{2\%} - h_{kr}$$

The score 'unsufficient' is calculated as $H_{crest} > 5D$.

The score 'good' applies if $H_{crest} < 4D$ whereby D = thickness of the element.

In all other cases ($4D < H_{crest} < 5D$) no conclusive decision can be given, necessitating further investigation.

The thickness of the element is on average 50 cm, so that 4D = 2 m. All dikes comply. The most critical dike is p_234, where H_{crest} = 0.99 m.

As the Safety Assessment Guideline dates from 1999 and new insights have been gained in the meantime with regard to the stability of the dike crest, an additional assessment was made. With regard to the Schüttrumpf method (Addendum A), the layer thicknesses and the speed of the overtopping water tongue were calculated.

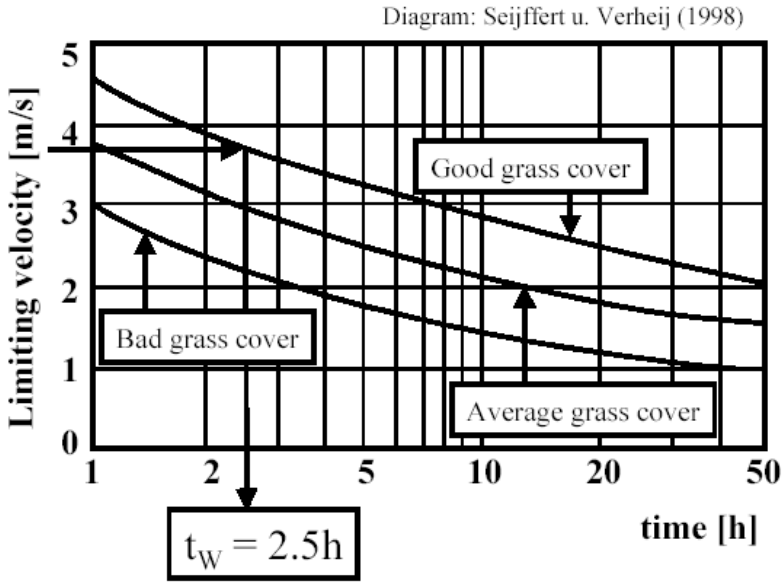

Figure 54: Erosion resistance of grass-covered slopes.

For stone pitching the maximum permissible veolcity on the crest is given by [16]:

$$u_{cr} = \sqrt{\Delta g D}\left(1.19 + 0.5\,.\,P - 1.88\,.\,\sin\alpha\right)^{0.33}$$

whereby

- Δ = relative volumic density of the stone (= 1.58)
- D = thickness of the revetment
- g = acceleration due to gravity (g = 9.81 m/s^2)
- P = factor depending on the positioning of the stones (P = 0.6 for loose stones, P = 1.1 for neatly placed stones and P = 1.25 for stone pitching)
- α = slope (α = 0)

- D [m] voor gezette steen.

The maximum permissible velocity for various layer thicknesses D is given in Figure 55.

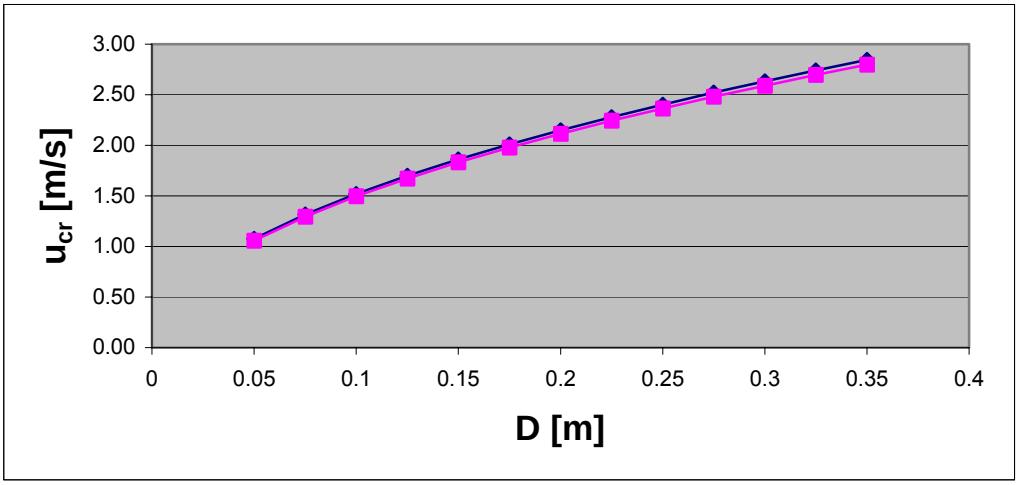

Figure 55: Kritieke stroomsnelheid u_{cr} [m/s] i.f.v. de dikte van de bekleding

In §6.9 the layer thickness of the overtopping layer and the corresponding maximum velocity are calculated for each return period considered. It is assumed that with a velocity of 7m/s no hard dike revement can resist and the sand core will begin to erode.

6.9. Erosion of the dike core by overtopping discharges (=assessment of crest height)

In Flanders the dikes mainly consist of a mass of dune sand protected at the front by a concrete slab (dikes postdating 1953) or by stone pitching (dikes predating 1953). On the landward side protection is provided by paving (asphalt, cobblestones, clinkers, etc.). These dikes have a relatively low crest height (usually 9.5m TAW), but they are very wide.

In some places the low crest height causes very high overtopping discharges. These overtopping discharges may cause very high velocities over the crest. A method was devised to estimate the damage such overtopping discharges may cause on the landward side (damaged paving?) and whether they can cause a breach. If damage to the paving is considered possible, it is obvious that the underlying sand will systematically erode.

Based on the beach erosion profile obtained with a certain return period, the significant wave height in shallow water is calculated per profile (SWAN). Using this significant wave height, an overtopping discharge q and the wave run-up $z_{2\%}$ can be determined for the dike geometry in question. These parameters can then be used to calculate the velocity and layer thickness at the various locations of the dike, by means of the Schüttrümpf method.

It is generally assumed that if the calculated velocities at the crest of the dike on the seaward side exceed 7m/s, the paving on the dike crest will fail. The erosion process of the dike was then estimated in 2 different ways. It is generally assumed that, with such broad dikes with a gentle landward slope, the sand is eroded in horizontal layers. The consequence is that the crest height is systematically reduced from the beginning of the process. Consequently, the overtopping discharges increase.

From the crest height to the water level with the considered return period the amount of sand in the core behind the dike body is determined in layers of 0.5m; the overtopping discharge with the corresponding remaining crest height is also determined. For each layer of sand the time is then calculated which is needed for total erosion. For the initial phase an overtopping discharge is always assumed which corresponds with the crest height of the dike. Higher ground inland is not taken into account for a possible reduction of overtopping volumes. This somewhat conservative approach is

also used to take into account the fact that overtopping water which flows back may also cause erosion of the dike core. Presumably, higher ground inland has a slowing effect which is not taken into account at this point. At the following locations there is a landward higher ground: p233, p236, p241, p242 and p243. The volume of sand above the crest height is of course included in the calculation of the sand volume to be eroded. Another safe approach is to ignore the residual strength of the crest revetment.

To calculate the erosion process 2 methods were evaluated. A first method calculates the erosion capacity with the classic transport formulas: Engelund-Hansen and Ackers-White. The transport formula of Engelund-Hansen gives a transport capacity which is about 20% higher than calculated in accordance with Ackers-White. A second more pragmatic method consists in determining the sand transport based on the product of flow rate and an average concentration. The assumed maximum sediment concentration is 5%, based on tests (Kobayashi et al.,1997).

The calculations above have shown that both methods usually have the same result (failure or not), but that the time needed to erode the dikes up to the water level – calculated in accordance with the classic transport formulas – is unrealistically short. For such non-stationary events such as overtopping discharges, the transport formulas – whereby the velocity is used as a normative parameter – are not suited. That is why the second method is opted for to assess the dikes (average maximum concentration of 5%).

6.9.1. Results for 1000-year return period

For a storm with a 1000-year return period there are 3 profiles with very small overtopping discharges: p233, p234 and p243. These overtopping discharges are so limited (see Table 7) that they certainly do not damage the crest or affect the stability of the dike body.

Profile number	$z_{2\%}$ (m TAW)	q (l/m.s)	H_s (m)
217	-	0.00	-
218	-	0.00	-
219	-	0.00	-
220	9.55	0.80	0.71
221	-	0.00	-
222	-	0.00	-
223	-	0.00	-
224	-	0.00	-
226	-	0.00	-
227	-	0.00	-
228	-	0.00	-
229	-	0.00	-
231	-	0.00	-
232	-	0.00	-
233	9.32	0.15	0.67
234	3.60	0.00	0.11
235	-	0.00	-
236	-	0.00	-
237	-	0.00	-
238	-	0.00	-
239	-	0.00	-
240	-	0.00	-
241	-	0.00	-
242	-	0.00	-
243	8.57	0.18	0.72
244	-	0.00	-
245	-	0.00	-
246	-	0.00	-

Table 7 Wave run-up and overtopping discharges for a storm with a 1000-year return period.

6.9.2. Results for 4000-year return period

For a storm with a 4000-year return period, some locations exists with very high overtopping discharges (cfr. Table 8): p233, p234, p242 and p243. For these profiles – complemented with p235 – the maximum velocities and the layer thickness of the overtopping water near the seaward edge of the crest are calculated. It is then examined whether this may cause damage and to what extent the dike core is eroded (cfr. Table 9).

Profile number	$z_{,2\%}$ (m TAW)	q (l/m.s)	H_s (m)
217	-	0.00	-
218	-	0.00	-
219	-	0.00	-
220	12.12	22.65	1.16
221	-	0.00	-
222	-	0.00	-
223	-	0.00	-
224	-	0.00	-
226	-	0.00	-
227	-	0.00	-
228	-	0.00	-
229	-	0.00	-
231	-	0.00	-
232	-	0.00	-
233	16.35	185.84	2.27
234	14.63	60.90	2.12
235	11.70	0.72	0.91
236	8.14	0.54	0.75
237	-	0.00	-
238	-	0.00	-
239	-	0.00	-
240	-	0.00	-
241	5.98	0.00	0.37
242	15.98	138.82	2.12
243	14.69	184.00	2.28
244	-	0.00	-
245	-	0.00	-
246	-	0.00	-

Table 8 Wave run-up and overtopping discharges for a storm with a 4000-year return period.

Profile number	Maximum speed near seaward crest (v_A m/s)	Layer thickness of overtopping water near seaward crest ($h_{A,50\%}$ m)	Erosion of dike core up to level (m TAW)	Time needed to erode dike core (min)
P233	10.94	1.18	7.5m TAW	104
P234	8.66	0.74	9m TAW	138
P235	5.08	0.25	-	-
P242	10.54	1.09	7.5m TAW	72
P243	9.43	0.87	7.5 m TAW	87

Table 9 Damage of crest and erosion of dike core by overtopping volumes for a return period of 4000 years.

The results in Table 9 imply that for a storm with a 4000-year return period 3 dike profiles fail, i.e. erosion of the dike core up to the assessment level within the high-water peak of about 2h during the storm: p233, p242 and p243. Profile 234 will suffer major damage during the storm, but only a small part of the sand core is eroded here. The overtopping discharges near profile 235 are too small to damage the crest.

The maximum velocity near the crest and the layer thickness of the overtopping water are the same as for the initial condition (original crest height). These values gradually increase as the crest is damaged and lowered.

6.9.3. Results for 40000-year return period

For a storm with a 40000-year return period various locations are subjected to very high overtopping discharges (cfr. Table 10). The profiles that already failed for a 4000-year return period (p233, p242 and p243) are of course not assessed any more. The following profiles must be subjected to a new test: p234, p235, p236, p240, p241 and p246 (cfr. Table 11).

Profile number	$z_{2\%}$ (m TAW)	q (l/m.s)	H_s (m)
217	-	0.00	-
218	-	0.00	-
219	-	0.00	-
220	14.43	195.48	1.55
221	-	0.00	-
222	-	0.00	-
223	-	0.00	-
224	-	0.00	-
226	-	0.00	-
227	-	0.00	-
228	-	0.00	-
229	-	0.00	-
231	-	0.00	-
232	-	0.00	-
233	18.54	682.40	2.77
234	16.96	351.58	2.75
235	19.76	305.09	2.61
236	14.46	437.81	2.40
237	4.12	0.00	0.15
238	-	0.00	-
239	-	0.00	-
240	10.90	58.01	1.37
241	13.96	384.73	2.29
242	18.83	712.74	2.82
243	16.20	706.56	2.82
244	-	0.00	-
245	3.12	0.00	0.10
246	11.52	23.26	1.05

Table 10 Wave run-up and overtopping discharges for a storm wth a 40000-year return period.

The test shows that all profiles tested, except p240 and 246 – where the maximum velocities over the crest remain limited – fail in a relatively short time.

Profile number	Maximum speed near the crest seaward (v_A m/s)	Layer thickness of overtopping water near crest seaward ($h_{A,50\%}$ m)	Erosion of dike core up to level (m TAW)	Time needed to erode the dike core (min)
P234	10.34	1.05	8m TAW	51
P235	12.45	1.52	8m TAW	89
P236	8.73	0.75	8m TAW	81
P240	3.92	0.15	-	-
P241	8.23	0.67	8m TAW	41
P246	5.10	0.26	-	-

Table 11 Damage to crest and erosion of dike core by overtopping volumes for a return period of 40000 years.

6.10. Summary of the results – Conclusions

The Flemish dikes between Zeebrugge and the Zwin only fail as to their height. The dunes reinforced by dikes are relatively low. After storms with a higher return period of 4000 and 40000 years the beach profile before some dikes is eroded and high overtopping discharges occur. These overtopping discharges cause very high velocities over the crest and result in erosion of the sand core after erosion of the crest. In some places this may cause breaches.

For a return period of 1000 years no problems can be expected anywhere. For a storm with a return period of 4000 years there are 4 locations where breach formation can be expected: profile 233 and profile 242 and 243. The residual strength of the sand core at locations 242 and 243 is somewhat greater than at location 233. However, all locations will fail within the second peak of the storm. The times of breach are outlined in Figure 56.

For a return period of 40000 years there are some additional profiles that fail: p235, p236 and p241. The residual strength of p241 is smaller than that of p235 and p236. These three profiles fail during the second peak of the storm. The three profiles which already failed with a return period of 4000 years, fail during the first peak.

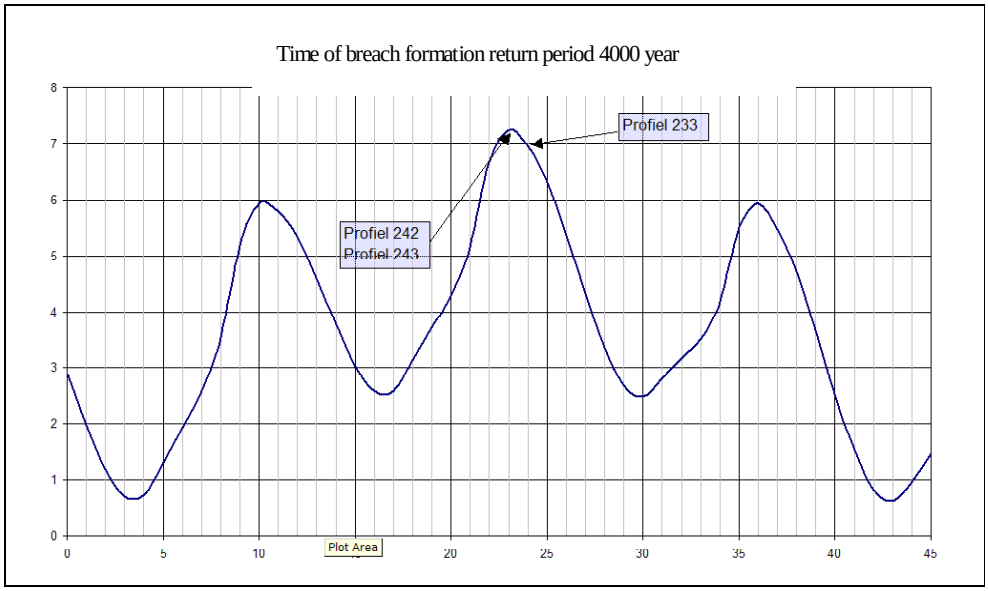

Figure 56 Breach formation of dikes in Flanders (return period of 4000 years).

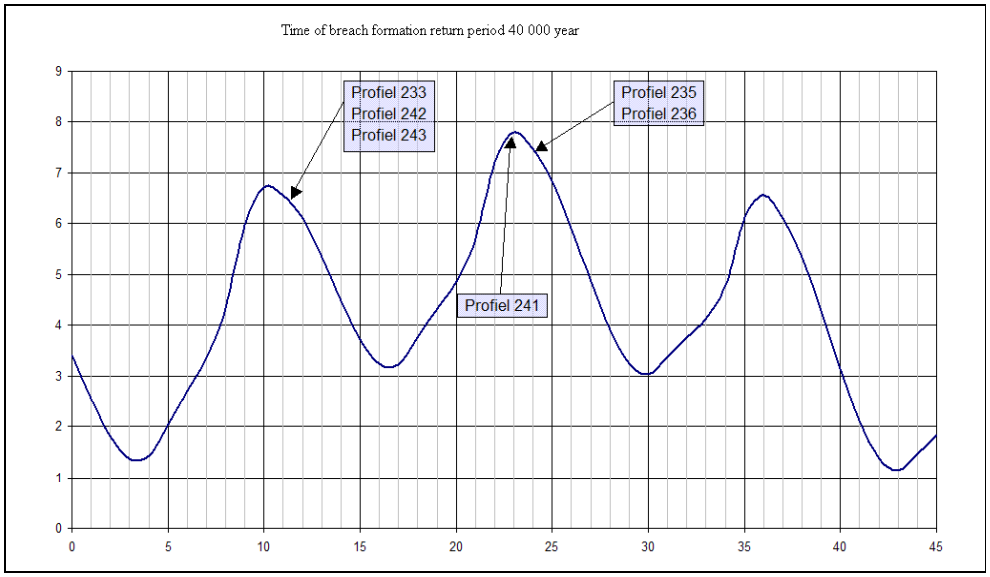

Figure 57 Breach formation of dikes in Flanders (return period of 40000 years)

7. FAILURE OF SEA DEFENCE: RESULTS FOR THE ZWIN

To assess the dikes around the Zwin, the wave penetration within the basin must be known. Two models were tested to know the wave characteristics within the Zwin: the classic SWAN wave model, including depth-induced breaking but no diffraction and the Boussinesq wave model Mike 21 in which diffraction processes were simulated, but not breaking.

With both wave models a run was conducted for a water level of 7m TAW and a peak periods of 8s as boundary conditions. The significant wave height imposed on the edge was chosen in order to obtain a significant wave height of 1 m near the opening of the Zwin in both models. The results of the Mike 21 Boussinesq model (cfr. Figure 58) and the results of the SWAN model (cfr Figure 59) show that wave penetration is similarly simulated by both models.

That is why the SWAN model was further used to obtain the wave characteristics in the Zwin, adjusting the boundary conditions in accordance with the return period considered, and a wind field was imposed in accordance with the return period. The results are discussed below for the various return periods in §7.2.

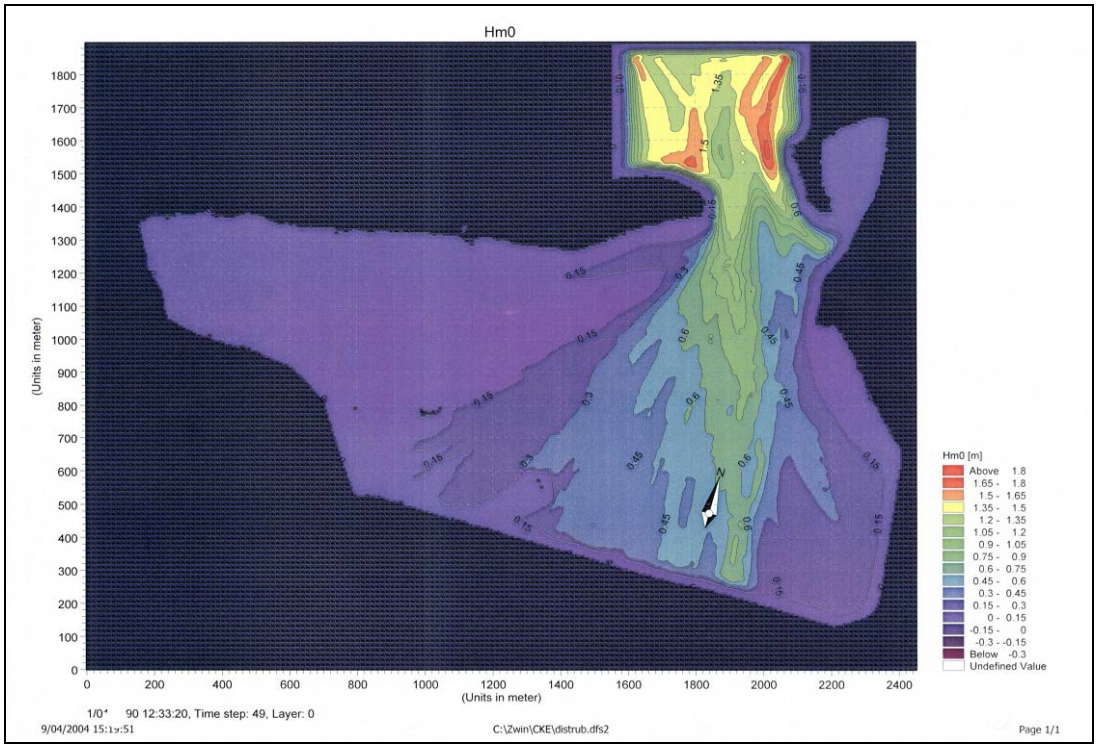

Figure 58 Results of the Boussinesq wave model Mike 21 (significant wave height Zwin)

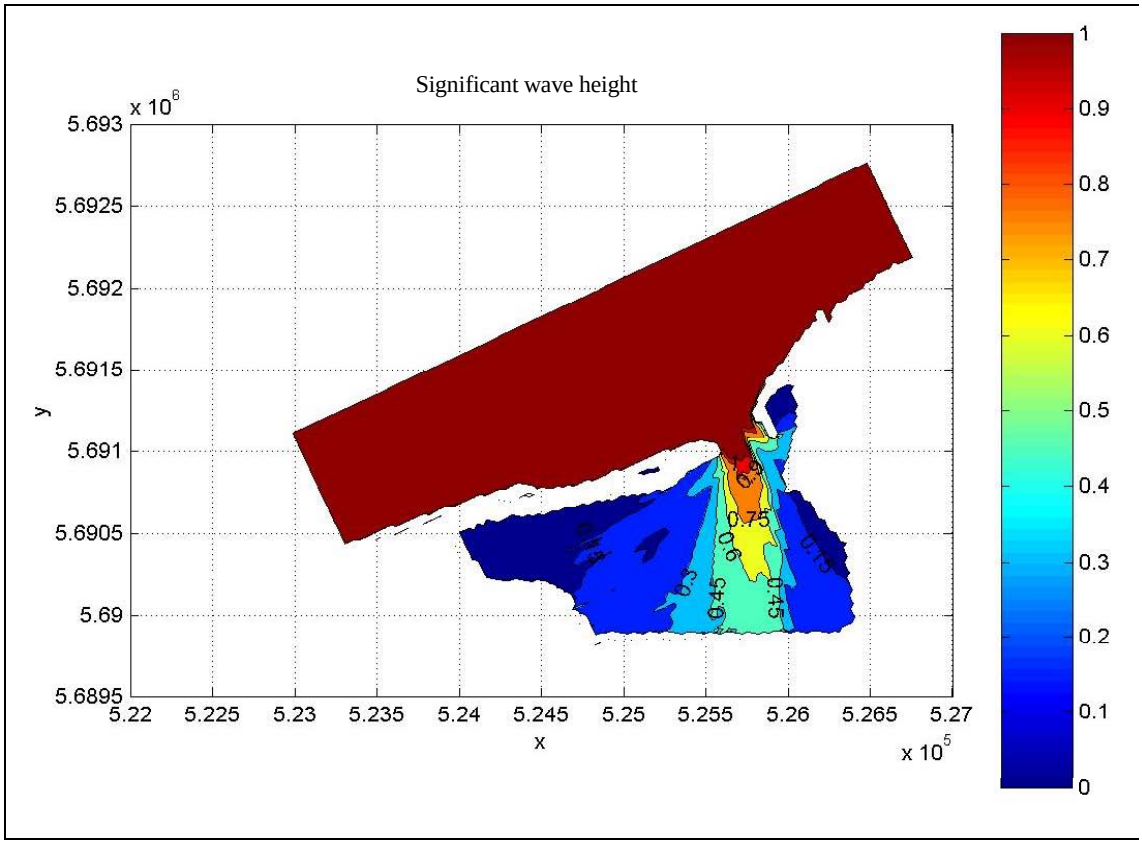

Figure 59 Results of the SWAN model (significant wave height Zwin, return period of 1000 years).

The results do seem to differ greatly from the Dutch Swan calculations, which is probably due to the fact that the latter made use of a schematic bottom.

7.1. Dike structure

According to the plans 'Raising and reinforcing of the dikes around the Zwin' ('Verhogen en versterken van de dijken rond het Zwin', 1958), the Zwin basin is surrounded by 2 types of dikes. The easternmost part of the Zwin is protected by a dike with a height of +11.1m TAW, an outer slope of 16/4 and an inner slope of 10/4 (cfr. Figure 60). The westernmost part of the basin is surrounded by a lower dike with steeper slopes (cfr. Figure 61): crest level at +9.55m TAW, outer slope 12/4 and inner slope 6/4.

The core material consists of sand, covered with a 0.5m thick clay layer broadened to 0.8m below +8m TAW. The inside has a berm with a somewhat gentler slope behind it. The dikes are covered with grass. The quality of the grass cover and clay layer are unknown.

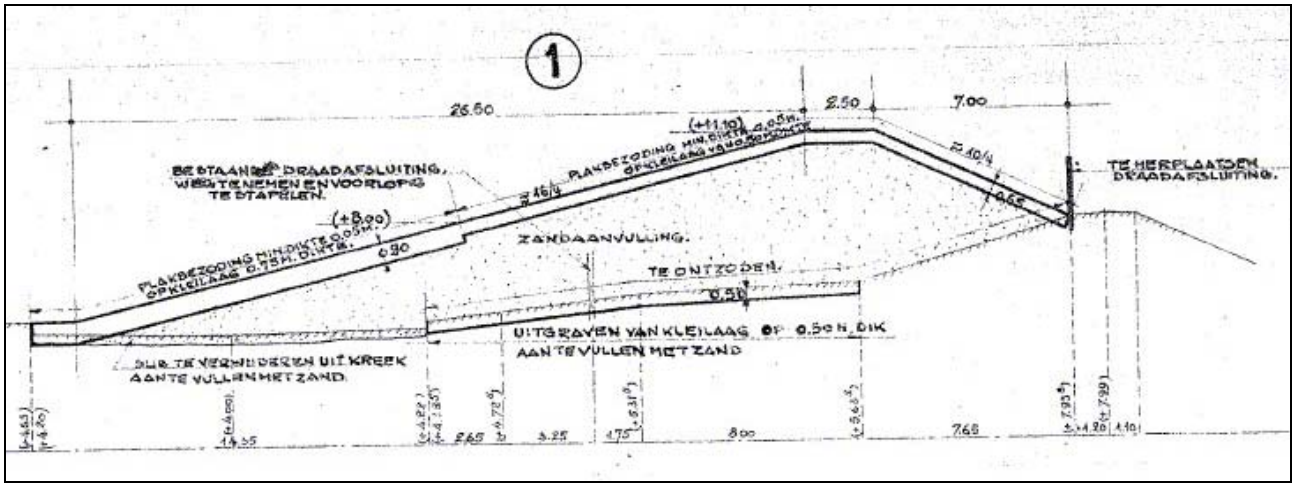

Figure 60 Dike profile at 11.10m TAW (Zwin dike)

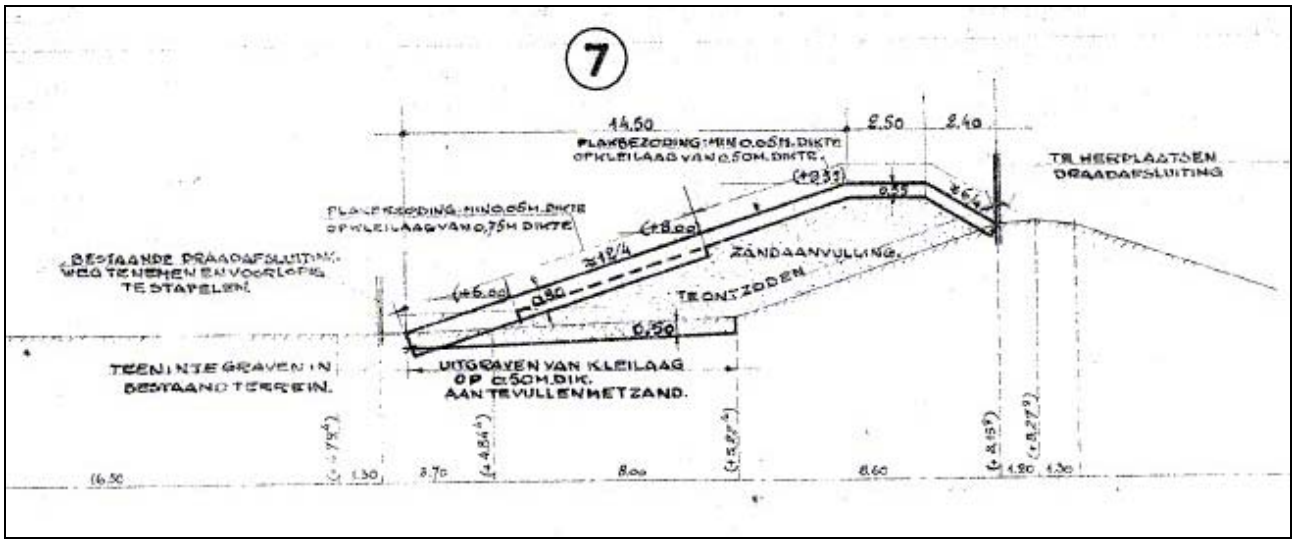

Figure 61 Dike profile at 9.55m TAW (Zwin dike)

According to the DTM, most points around the Zwin are higher than 10.5m TAW. In the area most subjected to waves the crest level is about 10.7m TAW. This level is further assumed as an average height of the Zwin dike for the calculation of the overtopping discharges. The outer slope is assumed to be 1:4 and the inner slope 1:2.5 for the entire Zwin dike.

7.2. Wave model

7.2.1. Boundary Conditions

To determine the boundary conditions for the Zwin, SWAN is thus further used. The wave and wind direction varies between NW and NNE. For each outlet the most critical condition is then assumed in order to calculate the overtopping discharges. Figure 62 gives the bathymetry and the output points of the Zwin.

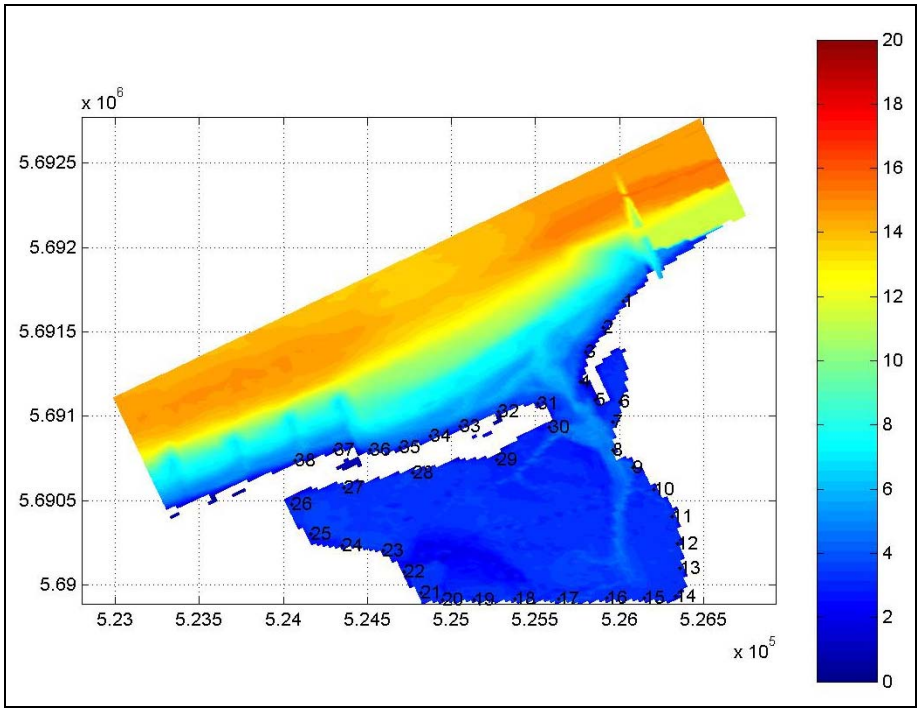

Figure 62 Bathymetry and output points Zwin

As a boundary condition for the different return periods, the characteristics mentioned in Table 12 were imposed.

Return period	Water level [m TAW]	H_{m0} [m]	T_p [s]	Wind [m/s]
1000 years	7.0	5	12	25
4000 years	7.4	5	12.5	34
40000 years	7.9	5	13.1	40

Table 12 Boundary conditions of the SWAN model for the Zwin basin

7.2.2. Results for the 1000-year return period

Figure 63 shows the significant wave height in the Zwin for a storm with a 1000-year return period. The wave direction imposed outside the basin, as well as the wind direction, is NNE.

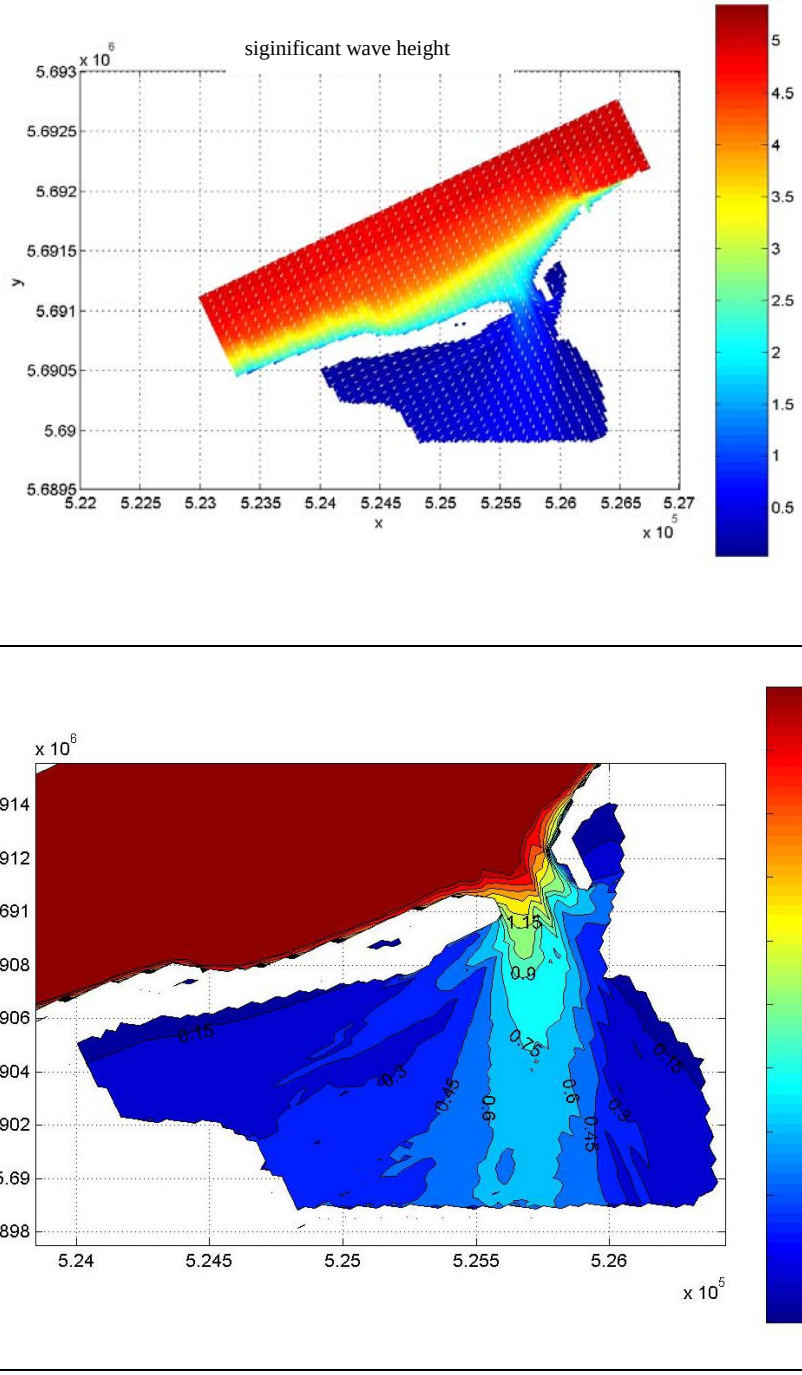

Figure 63 Significant wave height of the Zwin for a return period of 1000 years (NNE wind direction))

Table 13 gives the most critical wave parameters for the output points 6 to 26 of the Zwin. The most exposed area of the basin is the eastern part of the southern dike (between output points 15 and 18). The significant wave height remains limited to 0.67m.

Output point	Wind direction	H_s [m]	T_{peak} [s]	Dir	T_{m01} [s]	T_{m02} [s]
6	NW	0.40	11.91	318.1	5.8	4.0
7	NW	0.18	11.91	295	3.9	2.9
8	NW	0.24	11.91	292	3.2	2.5
9	NW	0.30	2.96	295.7	2.8	2.3
10	NW	0.38	2.96	297.5	2.8	2.3
11	NW	0.43	2.96	302.1	2.8	2.2
12	NW	0.49	2.96	311.9	2.7	2.2
13	NW	0.51	11.91	321.8	2.8	2.3
14	NW	0.40	11.91	318.1	5.8	4.0
15	NW	0.51	11.91	321.8	2.8	2.3
16	NNW	0.67	11.91	349.1	3.3	2.5
17	N	0.65	11.91	10.3	3.8	2.8
18	NNE	0.48	11.91	28.7	3.8	2.8
19	NNE	0.44	11.91	31.2	3.3	2.6
20	NNE	0.43	11.91	33.4	3.2	2.5
21	NNE	0.36	11.91	34.3	3.1	2.4
22	NNE	0.34	11.91	35	3.2	2.5
23	NNE	0.28	11.91	36.3	3.3	2.6
24	NNE	0.27	11.91	43.7	3.4	2.6
25	NNE	0.21	11.91	40.5	3.2	2.5
26	NNE	0.13	11.91	69.6	3.5	2.7

Table 13 Swan output for a return period of 1000 years.

7.2.3. Results for a return period of 4000 year

Figure 64 shows the significant wave height in the Zwin for a storm with a return period of 4000 years. The wave direction imposed outside the basin for the results shown, as well as the wind direction, is NNE.

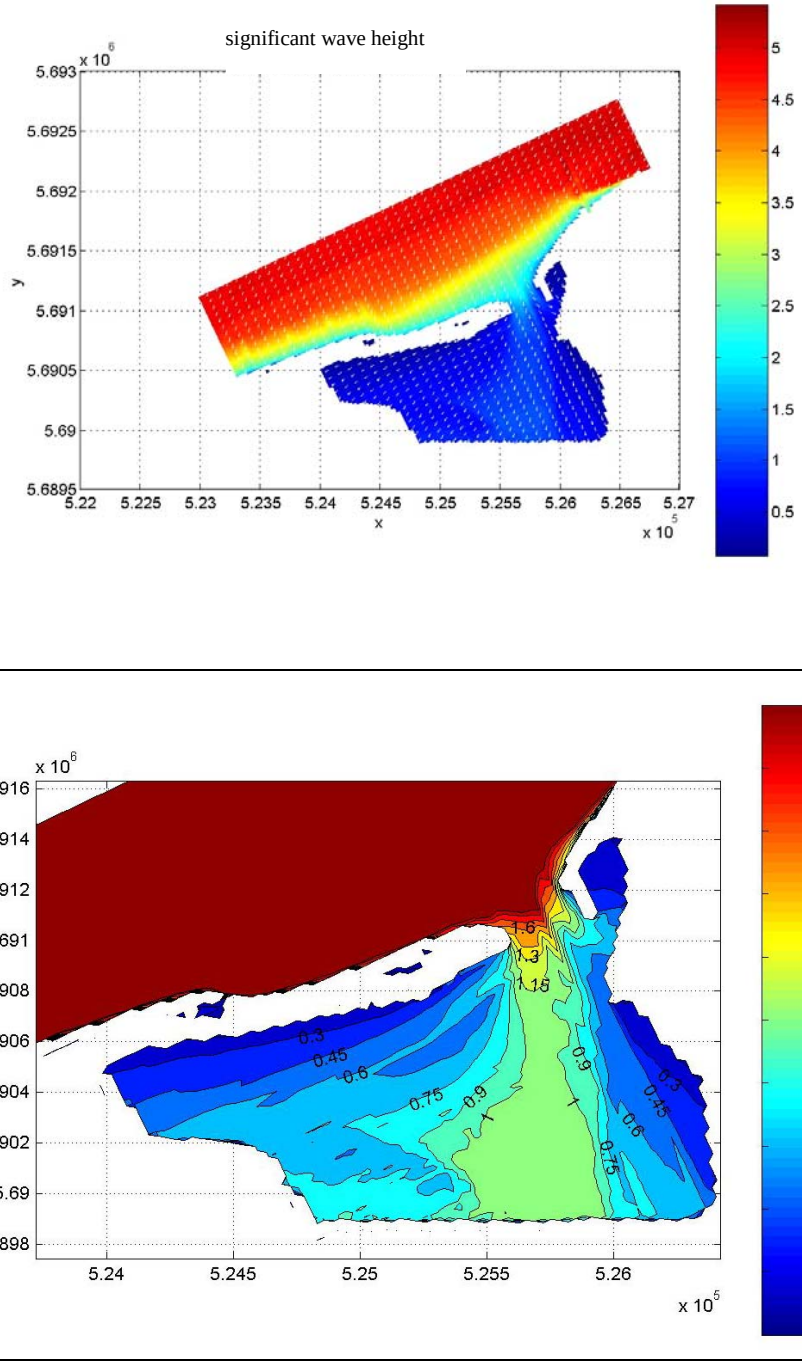

Figure 64 Significant wave height in the Zwin for a return period of 4000 years (NNE wind direction).

Table 14 gives the most critical wave parameters for output points 6 to 26 of the Zwin. The entire southeastern corner of the basin, surrounded by a dike with a crest level of +9.55m TAW, is subjected to wave heights in excess of 1m (between output points 11 and 17). The remainder of the southern dike (western part between output points 18 and 21) with a lower crest level of +9.55m TAW.

Output point	Wind direction	H_s [m]	T_{peak} [s]	Dir	T_{m01} [s]	T_{m02} [s]
6	NW	0.65	13.15	256.7	6.7	4.6
7	NW	0.80	11.91	284.8	5.9	4.1
8	NW	0.73	11.91	318.1	3.5	2.6
9	NW	0.43	2.96	289.3	2.8	2.3
10	NW	0.65	2.96	286.8	2.6	2.2
11	NW	0.89	2.96	292.1	2.5	2.1
12	NW	1.00	2.96	296.8	2.6	2.1
13	NW	1.02	3.27	301.7	2.6	2.2
14	NW	1.00	3.27	309.7	2.7	2.2
15	NW	1.07	2.96	318.7	2.6	2.2
16	NNW	1.11	2.96	343.6	2.8	2.3
17	N	1.07	11.91	8.4	3.0	2.4
18	NNE	0.91	2.96	30.2	2.8	2.3
19	N	0.88	2.96	12.5	2.7	2.2
20	NNE	0.91	2.96	29.9	2.6	2.2
21	NNE	0.87	2.96	32.3	2.5	2.1
22	NNE	0.77	2.96	31.6	2.7	2.2
23	NNE	0.72	2.96	36.8	2.7	2.2
24	NNE	0.67	2.96	43.6	2.8	2.3
25	NNE	0.51	2.96	40.3	2.9	2.4
26	NNE	0.30	2.96	65.3	3.0	2.4

Table 14 Swan output for a return period of 4000 years

7.2.4. Results for a return period of 40000 years

Figure 65 shows the significant wave height in the Zwin for a storm with a 40000-year return period. The wind direction imposed outside the basin for the results shown, as well as the wind direction, is NNE.

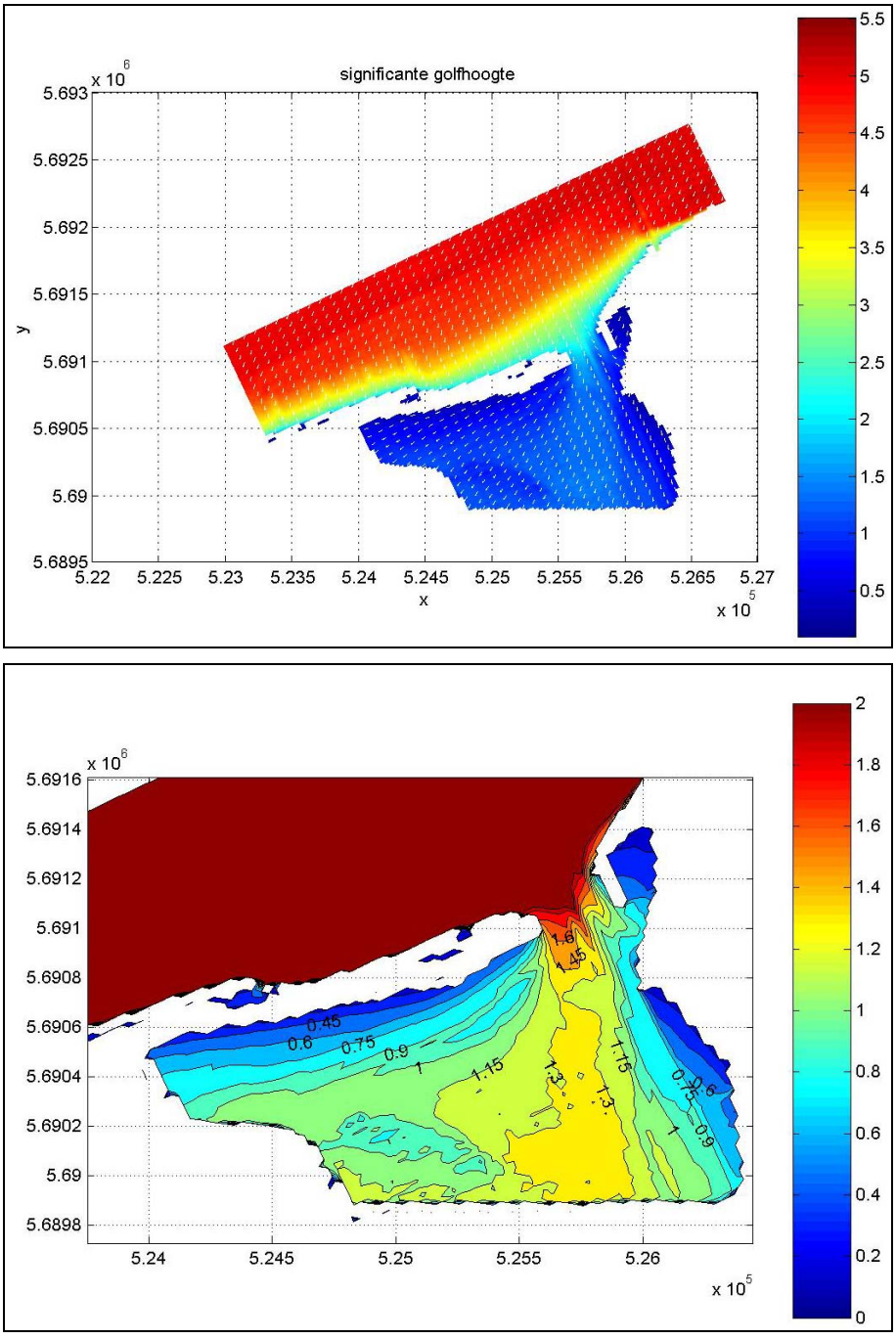

Figure 65 Significant wave height for the Zwin for a 40000-year return period (wind direction NNE)

Table 15 gives the most critical wave parameters for output points 6 to 26 of the Zwin. The entire southern dike is now attacked by waves larger than 1m. The maximum wave impact occurs near output point 16 with a significant wave height of 1.4m.

Output point	Wind direction	H_s [m]	T_{peak} [s]	Dir	T_{m01} [s]	T_{m02} [s]
6	NW	0.82	13.15	271.3	5.2	3.6
7	NW	1.08	13.15	289.2	4.8	3.3
8	NW	1.14	13.15	315.9	3.1	2.4
9	NW	0.79	2.96	285.3	2.6	2.2
10	NW	1.10	2.96	288.1	2.6	2.1
11	NW	1.21	3.27	295.8	2.6	2.2
12	NW	1.28	3.27	300.5	2.7	2.3
13	NW	1.29	3.27	304.7	2.7	2.3
14	NW	1.27	3.27	311.8	2.8	2.3
15	NW	1.34	3.27	319.7	2.8	2.3
16	NNW	1.36	3.27	342.5	2.9	2.4
17	NNW	1.31	3.27	348.5	2.9	2.4
18	NNW	1.22	2.96	344.2	2.6	2.2
19	N	1.19	2.96	8.6	2.6	2.2
20	N	1.22	2.96	7.6	2.6	2.2
21	NNE	1.20	2.96	32.4	2.6	2.2
22	NNE	1.09	2.96	35.5	2.7	2.2
23	NNE	1.12	2.96	38.8	2.7	2.2
24	NNE	1.04	2.96	44.5	2.8	2.3
25	NNE	0.88	2.96	50.1	2.7	2.2
26	NNE	0.60	2.96	75	2.6	2.1

Table 15 Swan output for a return period of 40000 years

7.3. Piping en heave

The dike has an overall structure of type 2 (sand core). The overall structure of the subsoil is type B (sand). Type 2B has no piping if no silt layer was left behind during construction. If it is assumed that this is not the case, the score for this dike is ‘sufficient’.

7.4. Outward slope macrostability

7.4.1. Liquefaction and sliding

Both failure mechanisms do not pose a problem as the foreshore is virtually flat. The score is ‘good’.

7.4.2. Sliding equilibrium at low outer water

For sea dikes the score with low outer water is good if the dike has a berm or foreland of at least 0m NAP (TAW +2.32m) and also an outer slope gentler than 1:3; in addition, the conditions of figure 4.3.3.2 of LTV must also be met (cfr. Figure 66).

The outer slope for the dike profile with a crest level of 11.1m TAW amounts to 1:4, the outer slope with a crest level of 9.55m TAW is somewhat steeper (1:3). In all places, the foreshore of the dikes is higher than +2.32m TAW, so that the first 2 requirements are met.

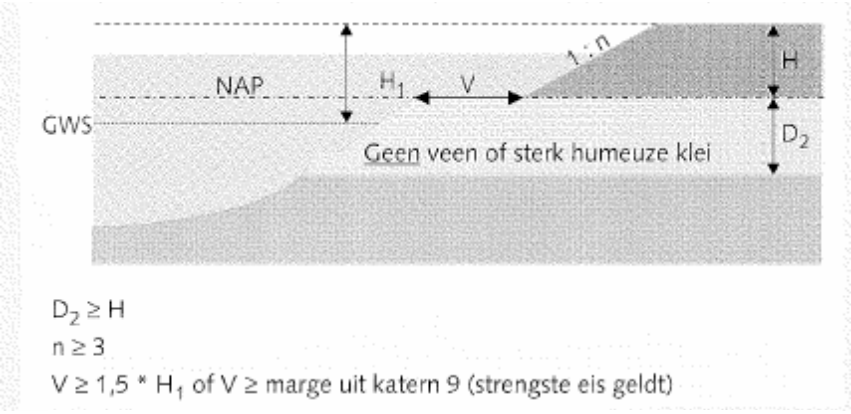

Dutch	English
GWS	MWL
geen veen of sterk humeuze klei	no peat or organic clay

Figure 66 Voorwaarden aan de profielopbouw voor zeedijken (Figuur 4.3.3.2 uit LTV)

Checking of the requirements in figure 4.3.3.2 of LTV(1999):

- $D_2 \geq H$ with D_2 = thickness of the non-peat and non-high-humous clay layer under the dike and H = height of the dike (= 11.60 – 4.97 = 6.63 m). As there are no peat or high-humous clay layers under the dike, D_2 is certainly larger than H.
- $n \geq 3$. OK (see higher)
- $V \geq 1.5\ H_1$ or V ≥ margin (highest requirement applies). As the foreland V is at least 1040 m, H_1 = 11.60 – 3.21 (MWL) = 8.39 m and the margin is virtually non-existent due to the absence of a 'channel', the third requirement is also met.

The score for the outer stability at low water level is 'good'.

The general score for the stability of the outer slope is the lowest score of liquefaction/sliding of the foreshore and the outer stability at low water level and therefore is 'good'.

7.5. Inward slope stability

The dike has an overall structure of type 2 (sand core). The landward slope is 10:4 or 1:2.5. A berm is present on the inward slope. The thickness of the clay layer under the dike D = 0 so that D/H = 0.

The values f_k = 0.85 and f_a = 0.1 as read from the graphs in LTV(1999).

A profile with a berm is certainly safe if the height of the berm above ground level is larger than 0.4 h – 0.15 D with h = water height above the ground level (= +4.97 m TAW) = 6.93 –4.97 = 1.96 m. The height of the berm must therefore be greater than 0.4 * 1.96 = 0.78 m. The berm lies 8 – 4.97 = 3.03 m above ground level (OK).

The overwidth must be greater than f_k * H = 0.85 * (11.60 – 4.97) = 4.65 m and

b > (f_a * H) + (d * n). The overwidth amounts to 0.5 m (k amounts to 2 m for sea dikes) which is smaller than the required 4.65 m. This requirement is not met.

It can be examined whether

$$\left(B_{kr} - o.b.\right) + \left(h_{kr} - h_{dt}\right)\left(n+1\right) \geq k$$

whereby B_{kr} = crest width (B_{kr} = 2.5 m)
o.b. = necessary overwidth (o.w. ≥ f_k.H = 0.85 * (11.60 – 4.97) = 5.64)

h_{kr} = crest level after five years (h_{kr} = +11.60)

h_{dt} = necessary crest level

n = cotangent of the slope (n = 2.5)

k = minimum crest width (k = 2 for sea dikes))

For a wave height of H_{m0} = 0.5 m and a period $T_{m-1,0}$ = 11s ($T_{m-1,0}$ is equal to 10 s on average for point 24; using a correction factor 1.1, $T_{m-1,0}$ = 11 s) the Iribarren number is ξ = 4.86. The maximum permissible overtopping discharge is q = 1 l/ms. Using the formula

$$\frac{q}{\sqrt{gH_{m0}^3}} = \frac{0.06}{\sqrt{\tan\alpha}}\gamma_b\xi\exp\left(-4.7\frac{R_c}{H_{m0}}\frac{1}{\xi_o\gamma_b\gamma_f\gamma_\beta\gamma_v}\right)$$

with a maximum

$$\frac{q}{\sqrt{gH_{m0}^3}} = 0.2\exp\left(-2.3\frac{R_c}{H_{m0}}\frac{1}{\gamma_f\gamma_\beta}\right)$$

whereby γ_b = 1; γ_f = 1 (grass cover); γ_β = 1; γ_v = 1.

The minimum freeboard must be 1.17 m for both dike profiles. The necessary crest level is therefore 6.93 + 1.17 = 8.10 m.

Thus the above-mentioned requirement becomes (2.5 – 5.64) + (11.60 – 8.10)(2.5 + 1) = 9.11 m > 2 m.

When the above-mentioned criterion is met, which is the case, the dike gets a ‘sufficient’ score.

The overall score for the inward slope macrostability is thus also ‘sufficient’.

7.6. Microstability

As to microstability, a dike gets a score ‘good’ if one of the following conditions is met:

- The dike has been subjected to an (almost) normative load, without loss of microstability.
  An almost normative load is understood to mean:
  - a water level which deviates less than half a metre from the normative high water;
  - a comparable high-water duration (at least 90% of the duration).
- The inner toe of the dike has a properly functioning drainage construction: the phreatic line is drawn towards the drain, preventing water from flowing out of the inner slope.
- The dike has an impermeable clay core. In this case as well, no water will flow from the inner slope, nor will uplifting of the top layer occur.
- The dike is sandy and has an inner slope gentler than 1:5. The driving forces in such a case are smaller than the strength of the sand, preventing the occurrence of wash-out.

The dike meets none of the above-mentioned conditions without doubt. Consequently, an advanced assessment will be made.

When a dike is constructed from a sand core with a top layer of sandy material or permeable clay on top (permeability virtually equal to that of sand) the perpendicular and parallel equilibriums must be checked.

The perpendicular equilibrium is assessed with

$$\gamma = \frac{\rho_g - \rho_w}{\rho_w} n^2$$

whereby γ = total safety (γ must be at least 2)

γ_g = soil density (γ_g = 20 kN/m^3)

γ_w = water density (γ_w = 10.26 kN/m^3)

n = cotangent slope (= maximum 2.5)

so that the safety is γ = 5.93 > 2 (OK).

The parallel equilibrium is assessed with

$$\gamma = \frac{\frac{\rho_g \cos\alpha - \rho_w}{\cos\alpha} g \tan\varphi + \frac{c}{d\gamma_c}}{\rho_g g \sin\alpha}$$

whereby γ = total safety factor (γ must be at least 1.5)

ρ_g = soil density (wet) (ρ_g = 20 kN/m^3)

tan α = slope

ρ_w = water density (ρ_w = 10.26 kN/m^3)

g = acceleration due to gravity (g = 9.81 m/s^2)

d = thickness of the top layer (d = 0.5 m)

φ = angle of internal friction (φ = 32.5°)

c = cohesion (c = 0)

γ_c = partial safety coefficient for cohesion (γ_c = 2)

When assessing the parallel equilibrium, two types of dike can be distinguished:

(1) sandy core with a sandy top layer (c = 0);

(2) sandy core (c = 0) with a clay(ey) top layer (c > 0).

The dike considered is of the second type. For the second type it is assessed in first instance whether the equilibrium in the formula above is met by introducing the parameters of the sandy core in the formula (c = 0). When this is complied with, it is also assessed whether the clay layer meets the equilibrium as well.

This results in a safety factor of γ = 2.63 > 1.5 (OK).

The clay layer (with c = 10 kPa) meets (γ = 1.55 > 1.5).

Uplifting of the top layer is verified by means of

$$\gamma = \frac{\rho_g d \cos\alpha}{\rho_w (h_b - z)}$$

whereby γ = total safety factor (γ must be at least 1.3)

ρ_g = soil density (wet) (ρ_g = 20 kN/m^3)

ρ_w = water density (γ_w = 10.26 kN/m^3)

tan α = slope (tan α = 0.25)

d = thickness of the top layer (d = 0.50 m)

h_b = height of the crossing of the phreatic line in the dike with the inner slope

z = height of the underside of the inner slope.

The difference h_b – z must be no more than 0.73 m in order to have the required safety. Addendum 2 of LTV (1999) contains a safe schematic representation of the course of the phreatic water table. The water table flows from the inner slope at a (maximum) height of 0.25 h with h = height of the water in front of the dike. The difference h_b – z can thus be no more than 0.25 * 1.96 = 0.49 m, which is smaller than the maximum permissible height of 0.73 m. So it is OK.

As to microstability, the dike is given the score 'good'.

7.7. Revetment

The revetment consists of sods applied to a clay layer. Grass as dike revetment is capable of resisting considerable wave loads. Waves, such as those in river areas, do not pose a problem for a good grass mat. Waves of up to 0.75 m high (and possibly higher) will not cause any damage to sea and lake dikes with a uniformly closed grass mat with a high rooting density. The management is the decisive factor thereby.

For lack of information a detailed assessment of the grass cover cannot be made. For the assessment of the grass mat a poor quality is thus always assumed.

To investigate the stability of the grass cover the formula of Schüttrumpf can be applied to calculate the maximum wave run-up speeds on the landward side of the dike. For point 16 the significant wave height H_s = 1.36 m in a storm with a return period of 40000 years. These wave heights involve maximum velocities of more than 8m/s at the front of the berm.

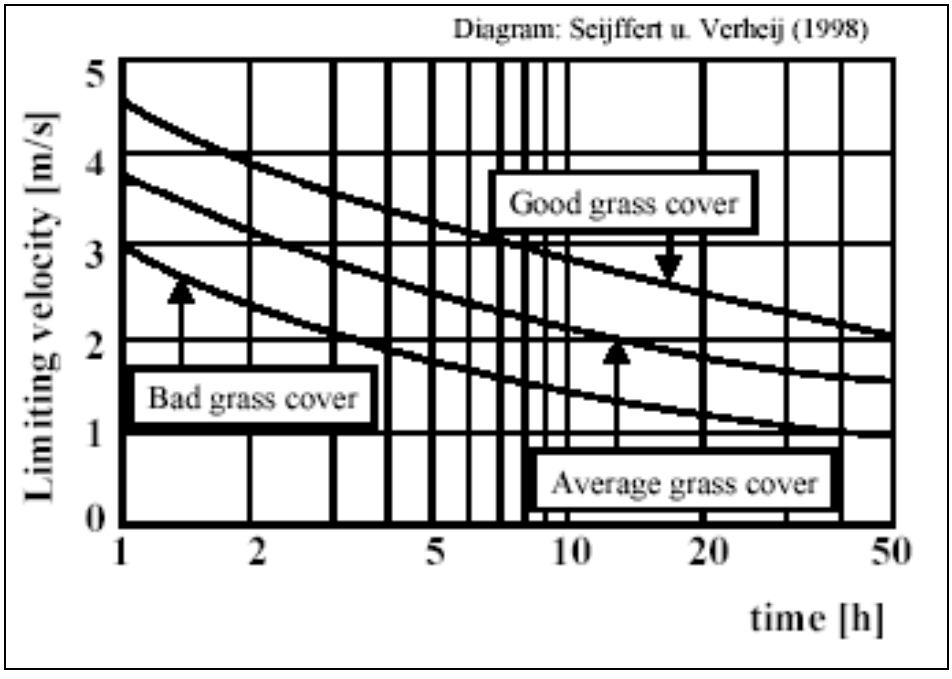

Figure 67 Residual strength of the grass cover (from CIRIA).

A good grass cover can resist an upward current for at least 1 hour and a downward current for at least 3 hours. The graph above (cfr. Figure 67) applies to steady-state conditions instead of irregular and varying boundary conditions. In addition, the above-mentioned velocity is the maximum velocity near the still water line. This velocity drops to v=0 when the maximum wave run-up is reached. Also, the water level varies constantly (tidal action). As a result, not always the same place is exposed to the maximum wave run-up velocity. For a large part of a tidal cycle the Zwin is dry, preventing wave run-up and attack on the dike revetment.

As the load on the grass cover has a pulsating nature, it is better to examine the residual strength of the grass and the underlying clay layer with the method mentioned in Theory Manual PC Ring Version 4.0 ('Theoriehandleiding PC-Ring Versie 4.0') and expounded in §**5.9.1**. Assuming a poor grass and clay quality, the residual strength for location 16 under storm conditions with a return period of 40000 years is 2.5h and 50min, respectively. So, breach formation due to wave impact on the front side of the dike should not be feared.

Consequently, the grass cover on the outer slope is given a score 'good' for all return periods considered.

7.8. Assessment of crest level

To assess the mechanisms of surface erosion of the inner slope due to overtopping water and sliding of the inner slope due to liquefaction, we need information about the overtopping discharges and the corresponding velocities for the various Zwin output points (cfr. Figure 62 in §7.2.1).

To calculate the overtopping discharges, a friction coefficient 1 for grass is used.

7.8.1. Return period of 1000 years

For the results of wave modelling, §7.2.2 is referred to. Table 16 contains the wave run-up heights $z_{2\%}$ and the corresponding overtopping volumes for the various output points in the basin.

Output point	Wave run-up $z_{2\%}$ (m)	Overtopping discharge q (l/m.s)
6	1.9	0.0
7	2.1	0.0
8	1.4	0.0
9	0.7	0.0
10	0.9	0.0
11	1.1	0.0
12	1.4	0.0
13	1.5	0.0
14	1.8	0.0
15	1.8	0.0
16	2.4	0.0
17	2.3	0.0
18	1.8	0.0
19	1.6	0.0
20	1.6	0.0
21	1.3	0.0
22	1.3	0.0
23	1.1	0.0
24	1.0	0.0
25	0.8	0.0

Table 16 Wave run-up and overtopping discharges of Zwin dikes for a return period of 1000 years.

The results for a return period of 1000 years show that the waves in the Zwin basin are too small to cause overtopping discharges. Consequently, the crest height for both mechanisms complies and instability of the inner slope should not be feared.

7.8.2. Return period of 4000 year

For the results of wave modelling, §7.2.3 is referred to. Table 17 contains the wave run-up heights $z_{2\%}$ and the corresponding overtopping volumes for the various output points in the basin.

Output point	Wave run-up $z_{2\%}$ (m)	Overtopping discharge q (l/m.s)
6	2.3	0.0
7	2.8	0.0
8	2.6	0.0
9	1.6	0.0
10	2.3	0.0
11	3.1	0.1
12	3.5	0.3
13	3.5	0.4
14	3.5	0.3
15	3.7	0.6
16	3.8	0.8
17	3.7	0.6
18	3.3	0.1
19	3.2	0.1
20	3.3	0.1
21	3.1	0.1
22	3.1	0.0
23	2.6	0.0
24	2.4	0.0
25	1.9	0.0

Table 17 Wave run-up and overtopping discharges of Zwin dikes for a return period of 4000 years.

For the areas under the greatest loads the average overtopping discharge remains below 1l/m/s. This will definitely not result in any structural damage, so that damage due to surface erosion will definitely not occur. Also, the probability of liquefaction is relatively small, so that sliding of the steep inner slope should not be feared.

7.8.3. Return period of 40000 years

For the results of the wave modelling, §7.2.4 is referred to. Table 18 contains the wave run-up heights $z_{2\%}$ and the corresponding overtopping volumes for the various output points in the basin corresponding with the wave conditions for a return period of 40000 years.

Output point	Wave run-up $z_{2\%}$ (m)	Overtopping discharge q (l/m.s)
6	2.9	0.2
7	3.7	1.8
8	3.9	2.7
9	2.8	0.1
10	3.8	2.1
11	4.2	4.1
12	4.4	5.9
13	4.4	6.2
14	4.3	5.6
15	4.6	7.9
16	4.6	8.7
17	4.5	6.9
18	4.3	4.3
19	4.2	3.6
20	4.3	4.3
21	4.3	3.8
22	3.9	1.9
23	4.0	2.4
24	3.7	1.4
25	3.2	0.3

Table 18 Wave run-up and overtopping discharges of Zwin dikes for a return period of 40000 years.

At the most heavily loaded southeastern part of the Zwin basin (in output point 17) an overtopping discharge of almost 10l/s/m is reached. These high overtopping discharges increase the probability of liquefaction of the inner slope. The steep inner slope of the lower dikes (1:2.5) in combination with the high overtopping volumes, will very likely result in sliding of the inner slope after liquefaction of the core. The berm on level +8m TAW on the inside may provide some stability against sliding, but the critical velocity on the inner slope is also exceeded.

For output point 16 the calculated velocity occurring on the inner slope is 6.3m/s (wave run-up of 4.3m with a water level of 7.9m TAW). Assuming a poor grass quality (c_g=330000ms) and a poor clay quality (c_{RK}=7000ms) and under the assumption that the inner slope is subjected to overtopping water (P_t=0.1) during 10% of the time, the critical speed is 6.9m/s. This critical speed is approached on the inner slope and jeopardises the stability of the inner slope by surface erosion.

7.9. Summary of the Zwin results

For the return periods of 1000 and 4000 years there is no danger of instability and breaching of the Zwin dikes. For higher return periods of 40000 year, the southeastern part of the basin is subjected to waves higher than 1.3m. The grass cover and the covering clay layer will resist the wave impacts. For this part of the basin, however, the overtopping discharges are rather high, almost 10l/s/m. In combination with the steep inner slope (1:2.5) this may cause liquefaction and sliding. The stability of the grass cover and the clay layer on the inner slope is no longer guaranteed due to the high velocities of the overtopping water. Although we are still in doubt about this part (output points 15 to 17), we can safely say – due to uncertainty about some parameters – that this part of the Zwin fails for storms with a return period of 40000 years.

8. FAILURE OF THE SEA DEFENCE: RESULTS FOR ZEEUWS-VLAANDEREN

8.1. Introduction

To examine possible failures, the data available from the Jarkus profiles were used (which not entirely corresponds with the direction lines used in the Dutch assessment). This choice was made because of the necessity of beach profiles and to limit the number of profiles (now 80, otherwise about 150).

The assumed dike profiles were based on the VNK profiles (fitted into the Jarkus profiles). Additional information with regard to the dike profiles did not allow an unambiguous refinement of the VNK profiles.

For the stability calculation, dike sections were sometimes used (such as with VNK); these are indicated in the last column of the table below:

Jarkus profile	X RD	Y RD	x utm	y utm	intermediate distance	type of protection	dike section
11	28016	380443	539215	5694539		dune	
31	27845	380546	539040	5694637	199.92	dune	
51	27674	380649	538865	5694734	199.91	dune	
71	27502	380752	538691	5694831	199.92	dune	
146	26859	381139	538036	5695196	749.67	DIKE	
161	26731	381216	537905	5695269	149.94	DIKE	
171	26639	381249	537812	5695300	98.07	DIKE	d_29
188	26474	381274	537646	5695319	166.92	DIKE (connecting construction)	d_28
208	26281	381304	537453	5695342	194.92	dune	
230	26063	381337	537234	5695368	219.90	dune	
251	25851	381369	537021	5695394	214.91	dune	
271	25653	381399	536822	5695417	199.91	DIKE	d_26
290	25470	381427	536639	5695439	184.92	DIKE	d_25
308	25287	381455	536455	5695461	184.92	DIKE	d_25
324	25129	381479	536296	5695480	159.92	DIKE	d_24
336	25015	381496	536182	5695493	114.95	DIKE	d_23
352	24856	381503	536023	5695495	159.03	DIKE	d_23
373	24642	381489	535809	5695474	214.91	DIKE	d_22
396	24412	381475	535580	5695453	229.90	DIKE	d_22
413	24239	381465	535408	5695436	172.93	DIKE	d_21
421	24177	381428	535346	5695398	72.90	DIKE	d_20
441	24004	381326	535178	5695290	199.92	DIKE	d_18
461	23832	381225	535009	5695183	199.91	dune	
483	23642	381112	534822	5695065	220.91	DIKE (behind)	
496	23531	381047	534713	5694996	128.94	DIKE	d_17
512	23392	380965	534578	5694909	160.93	DIKE	d_17
530	23237	380873	534426	5694813	179.92	DIKE	d_17
558	22980	380771	534173	5694702	276.18	DIKE	
584	22726	380692	533921	5694615	265.88	DIKE	
602	22562	380641	533759	5694559	171.93	DIKE	
619	22392	380589	533591	5694501	177.92	DIKE	
638	22216	380534	533417	5694441	183.92	DIKE	
663	21977	380461	533181	5694359	249.89	DIKE	
684	21771	380397	532977	5694289	215.90	DIKE	

705	21571	380335	532779	5694221	208.92	DIKE	
730	21337	380262	532548	5694141	244.89	DIKE	
751	21139	380201	532352	5694073	206.90	DIKE	
768	20973	380150	532188	5694016	173.93	DIKE	
778	20873	380119	532089	5693982	104.96	DIKE	
791	20753	380082	531971	5693941	124.93	DIKE	
802	20648	380049	531867	5693905	109.96	DIKE and dune	
822	20442	380018	531662	5693867	208.37	dune	
834	20325	380004	531545	5693849	117.93	dune	
851	20163	379985	531384	5693825	162.93	dune	
877	19905	379955	531127	5693787	259.88	DIKE (behind)	
886	19808	379944	531030	5693772	97.95	DIKE (behind)	
903	19642	379924	530865	5693747	166.94	DIKE (behind)	
920	19472	379904	530696	5693722	170.91	DIKE (behind)	
936	19319	379886	530544	5693699	153.93	DIKE	
951	19160	379868	530386	5693675	159.93	DIKE	
962	19056	379855	530282	5693659	104.95	DIKE	
979	18892	379836	530119	5693635	164.93	DIKE	
985	18831	379829	530059	5693626	60.98	DIKE	
993	18753	379820	529980	5693614	78.96	DIKE	
1007	18609	379803	529837	5693592	144.94	DIKE	
1021	18470	379787	529699	5693572	139.94	DIKE	d_12
1032	18365	379774	529595	5693556	104.95	DIKE	d_12
1046	18235	379731	529466	5693509	137.28	DIKE	
1068	18030	379636	529265	5693406	225.91	dune	
1092	17817	379536	529055	5693300	234.89	dune	
1112	17633	379450	528873	5693208	203.91	dune	
1136	17419	379350	528663	5693101	235.89	dune	
1162	17179	379238	528427	5692981	264.89	dune	
1191	16920	379117	528173	5692852	284.87	dune	
1214	16708	379018	527963	5692746	234.89	dune	
1241	16463	378917	527722	5692637	264.61	dune	
1262	16265	378845	527526	5692558	210.91	dune	
1282	16077	378777	527342	5692485	198.91	DIKE and dune	d_9
1300	15908	378716	527175	5692418	179.91	DIKE	d_8
1318	15739	378654	527008	5692351	179.92	DIKE	d_8
1335	15574	378594	526844	5692286	175.92	DIKE	d_8
1354	15401	378532	526674	5692218	183.92	DIKE	d_8
1363	15307	378498	526582	5692181	98.95	dune	
1372	15239	378446	526515	5692126	85.95	dune	
1381	15168	378391	526445	5692070	89.96	dune	
1391	15088	378330	526368	5692006	99.94	dune	
1401	15009	378270	526291	5691943	99.96	dune	
1412	14921	378203	526205	5691874	109.95	dune	
1427	14806	378115	526093	5691782	144.94	dune	
1437	14726	378054	526016	5691719	99.95	dune	
1450	14623	377975	525915	5691636	129.95	dune	
1467	14488	377872	525784	5691529	169.92	dune (behind)	Zwin
1487	14329	377751	525629	5691402	199.90	dune (behind)	Zwin

Table 19 : overview of Zeeuws-Vlaanderen profiles

8.2. Dune erosion

Dune failure was not determined for any of the storms with return periods of 1000 years, 4000 years and 40000 years.

Dune erosion with the 40000-year storm is critical for profile 1363.

8.3. Beach erosion in front of dikes

Many dikes are covered with a sand layer. It is not always known what the dike's position is in relation to the Jarkus profile. With regard to beach erosion, an as good as possible assumption was made. The available information mainly concerns the co-ordinates of some six points describing the dike profile. However, the location (to the front or back of the overall profile) is not known. The dike assumed non-erodable was fitted on the seaward side of the sand dike for the erosion calculations (DUROSTA).

In the figures below, the calculated erosion profiles are given for the profiles failing for the different return periods. The value *Hs 70* mentioned above these figures is the minimum of the significant wave height at 70 m of the toe of the dike and the water depth at the toe of the dike.

By assuming a 'vertical' wall for the dike assumed non-erodable in the erosion calculations, an erosion hole occurred just in front of the 'hard' construction with various profiles, which could not occur in reality because a section of 'hard' dike (toe), covered with sand, may be located at the position of the erosion hole. This erosion hole adversely affects the calculations of the outward macrostability, as the most critical slip surface is always found around the erosion hole and as the presence of the hole influences the safety coefficient of other slip surfaces. In the calculations it was assumed that the formation of an erosion hole cannot occur (toe construction/in-situ cohesive material) and the non-erosion of the in-situ cohesive material on the seaward edge of the dike was taken into account.

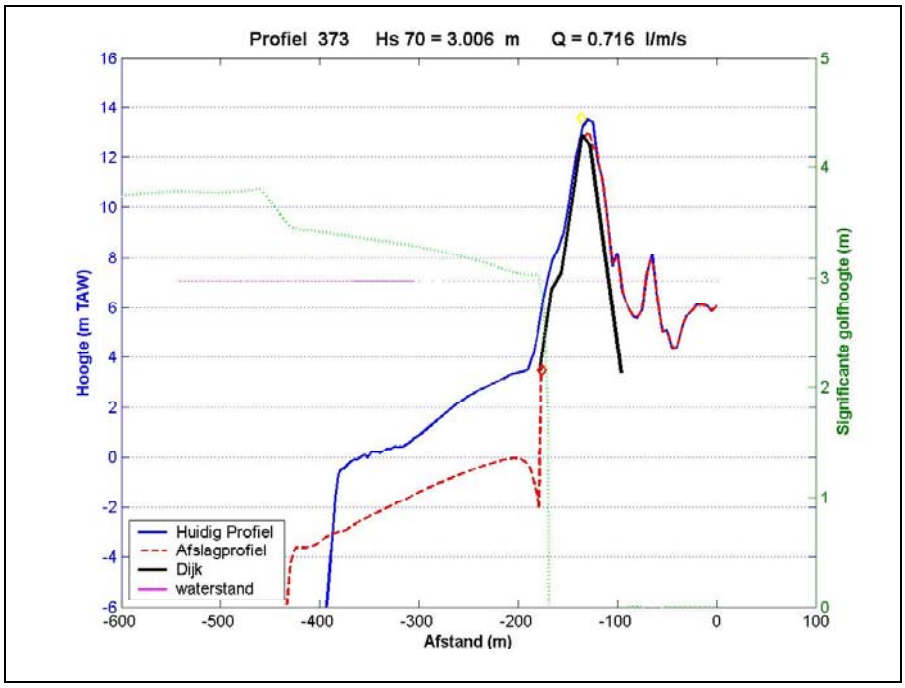

Figure 68 Beach profile of profile 373 after storm with return period 1000 year.

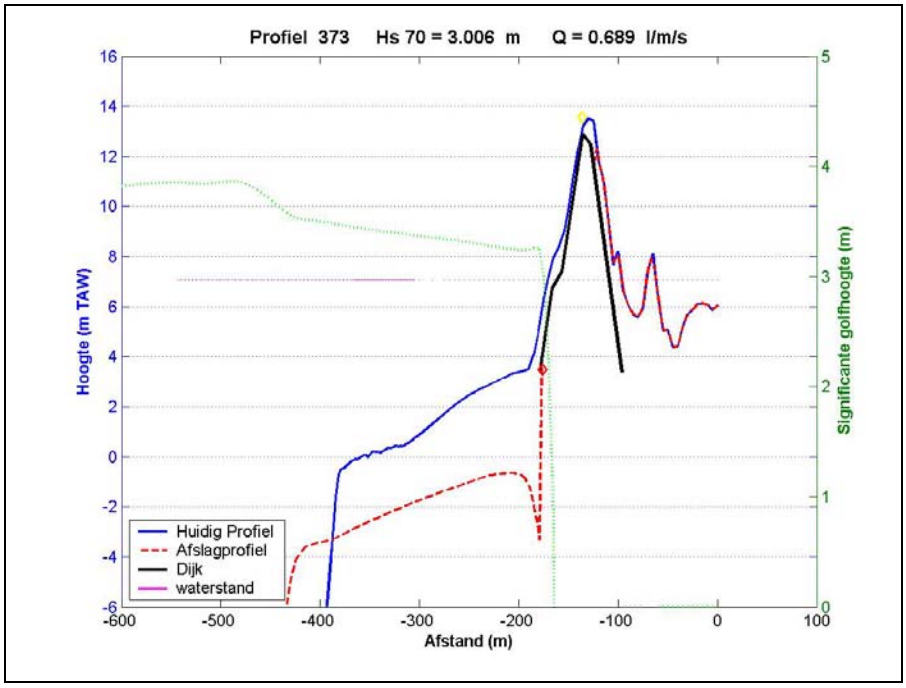

Figure 69 Beach profile of profile 373 after storm with return period 4000 year.

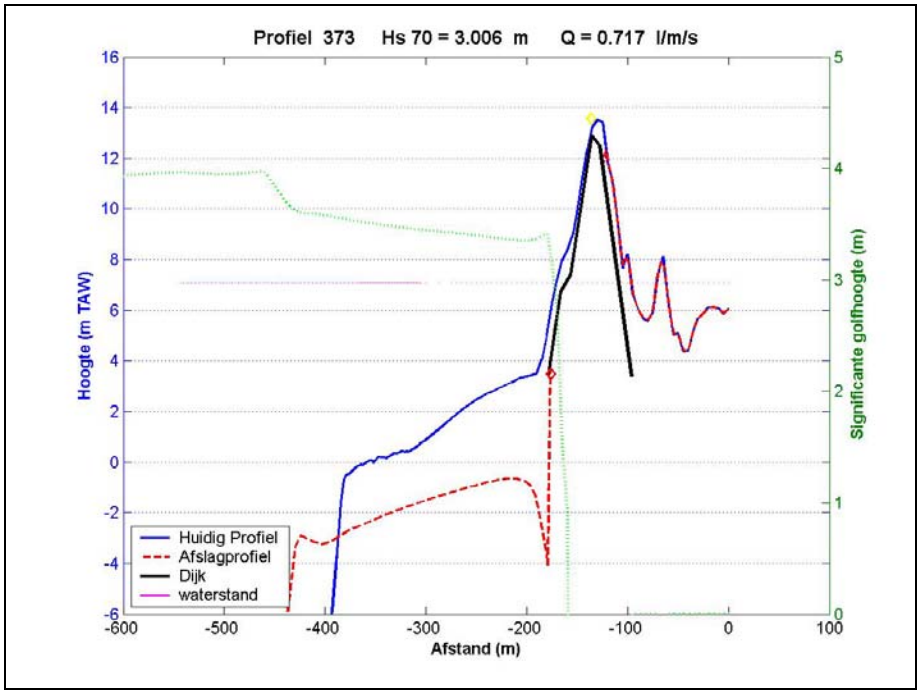

Figure 70 Beach profile of profile 373 after storm with return period 40000 year.

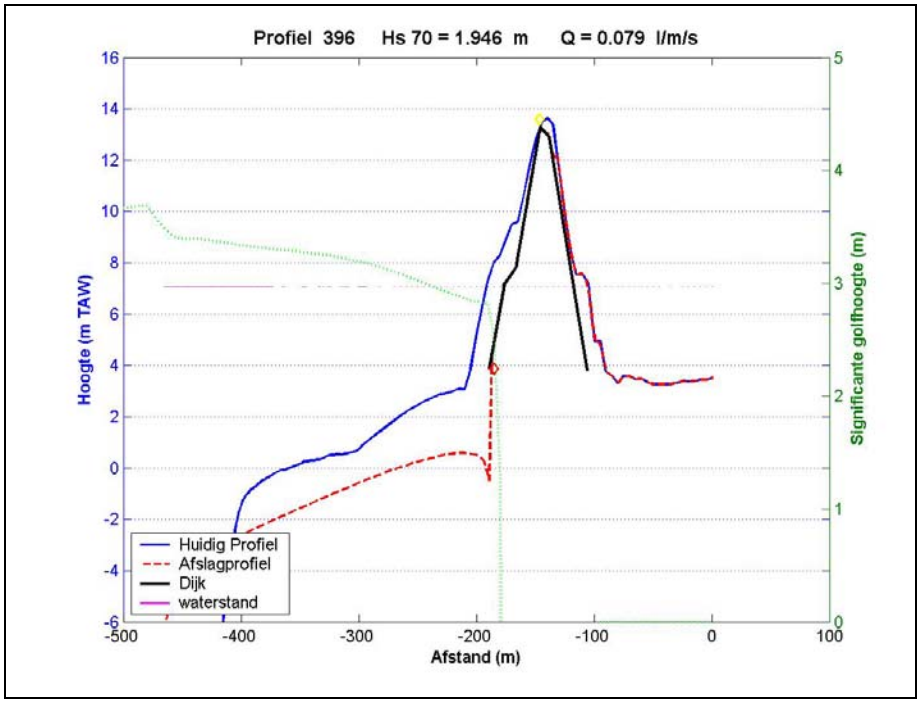

Figure 71 Beach profile of profile 396 after storm with return period 1000 year.

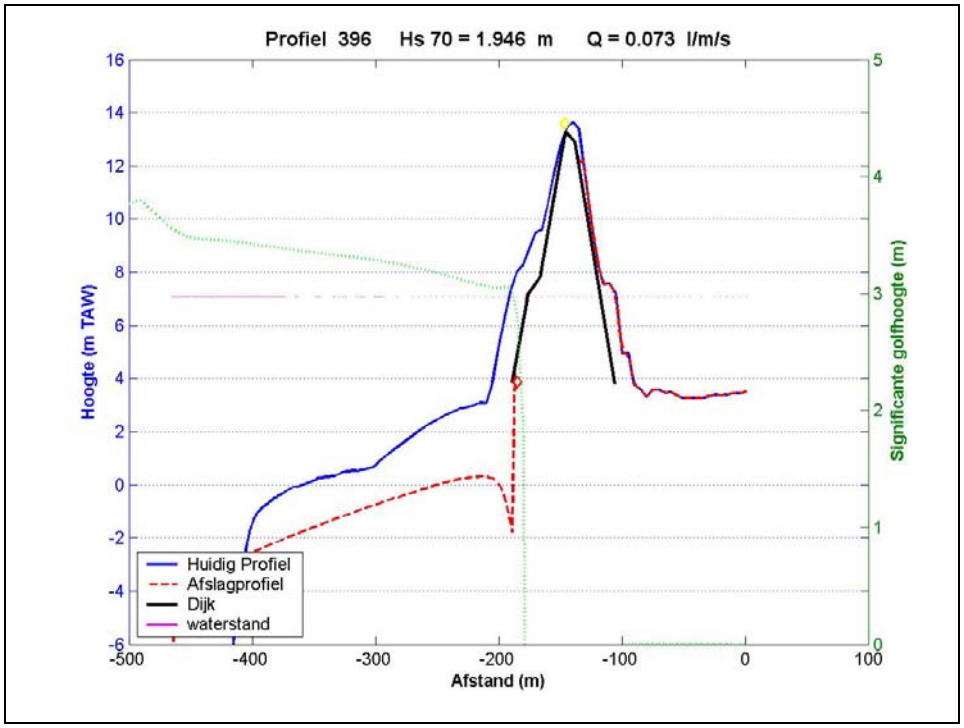

Figure 72 Beach profile of profile 396 after storm with return period 4000 year.

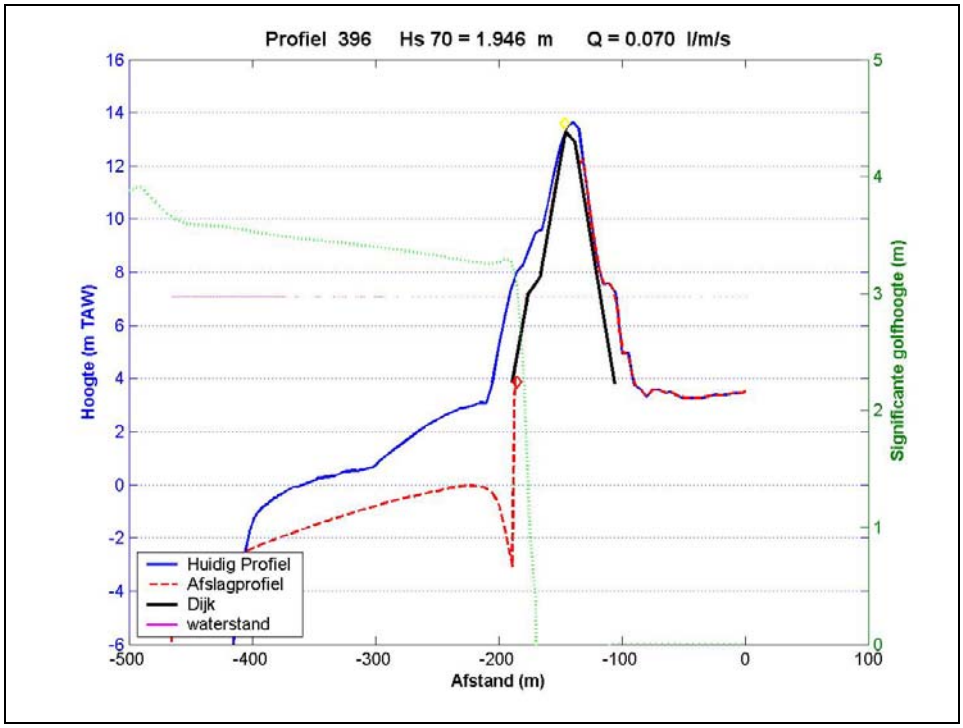

Figure 73 Beach profile of profile 396 after storm with return period 40000 year.

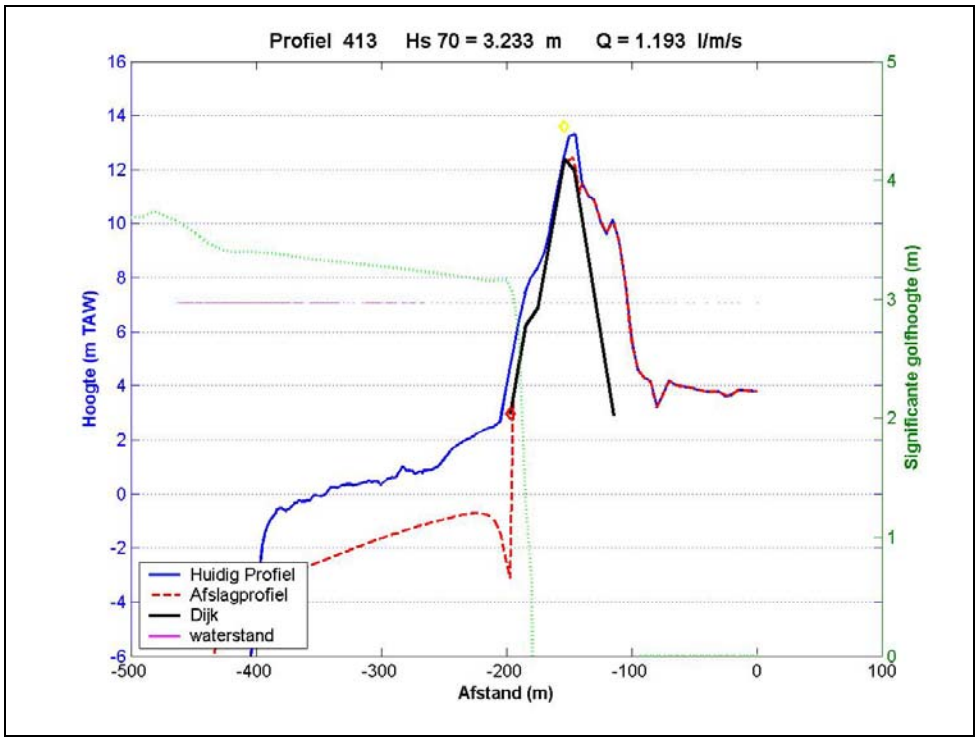

Figure 74 Beach profile of profile 413 after storm with return period 1000 year.

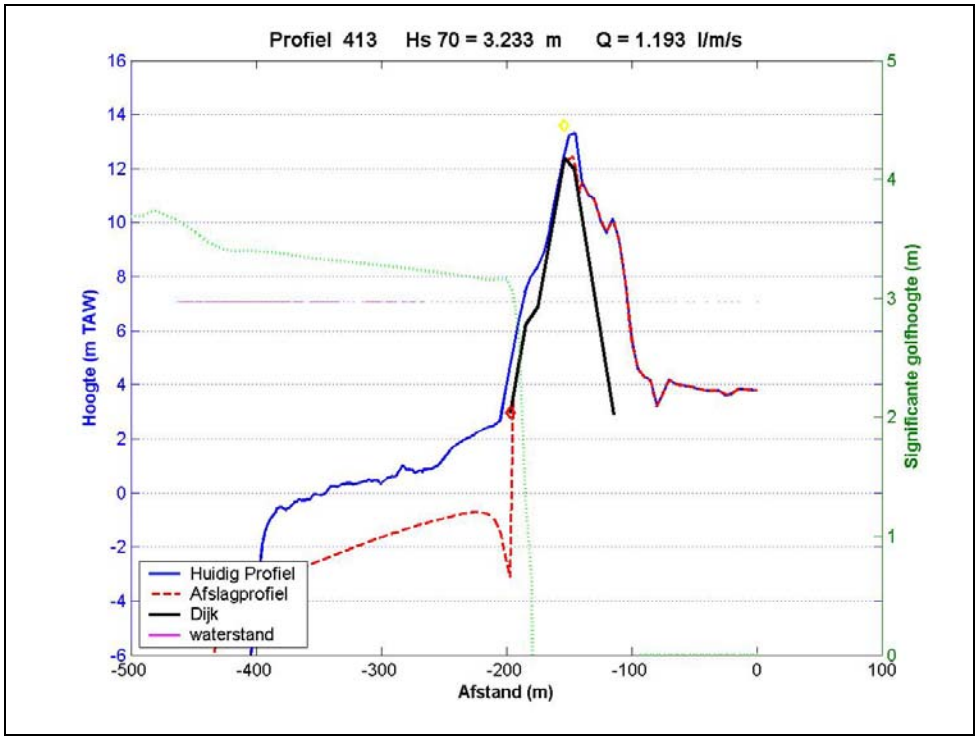

Figure 75 Beach profile of profile 413 after storm with return period 1000 year.

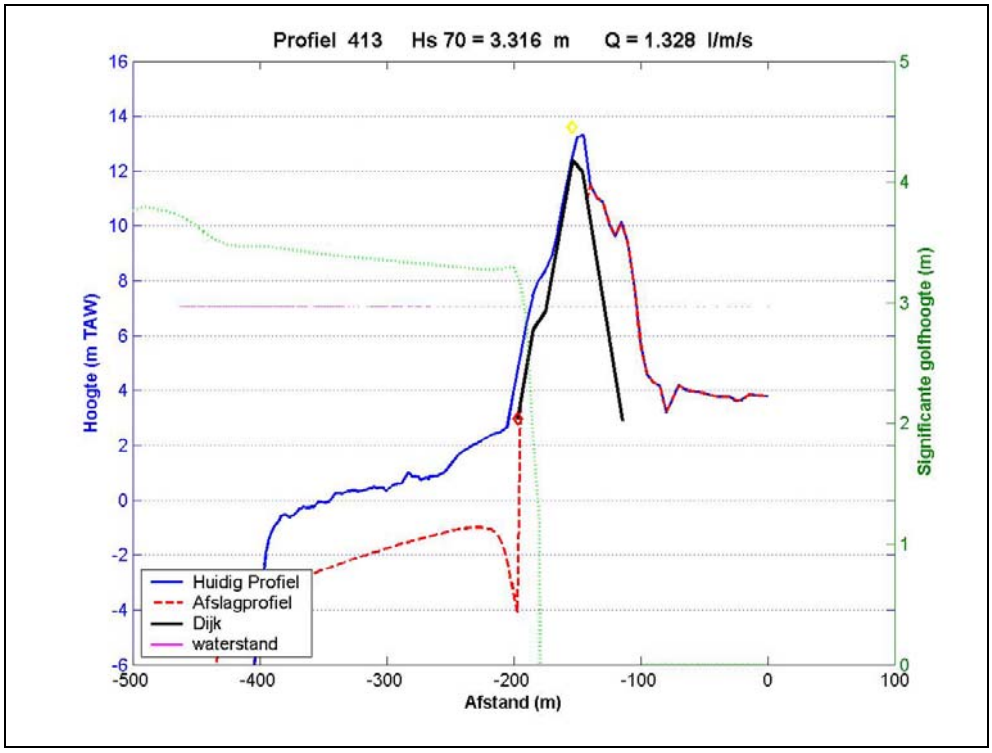

Figure 76 Beach profile of profile 413 after storm with return period 4000 year.

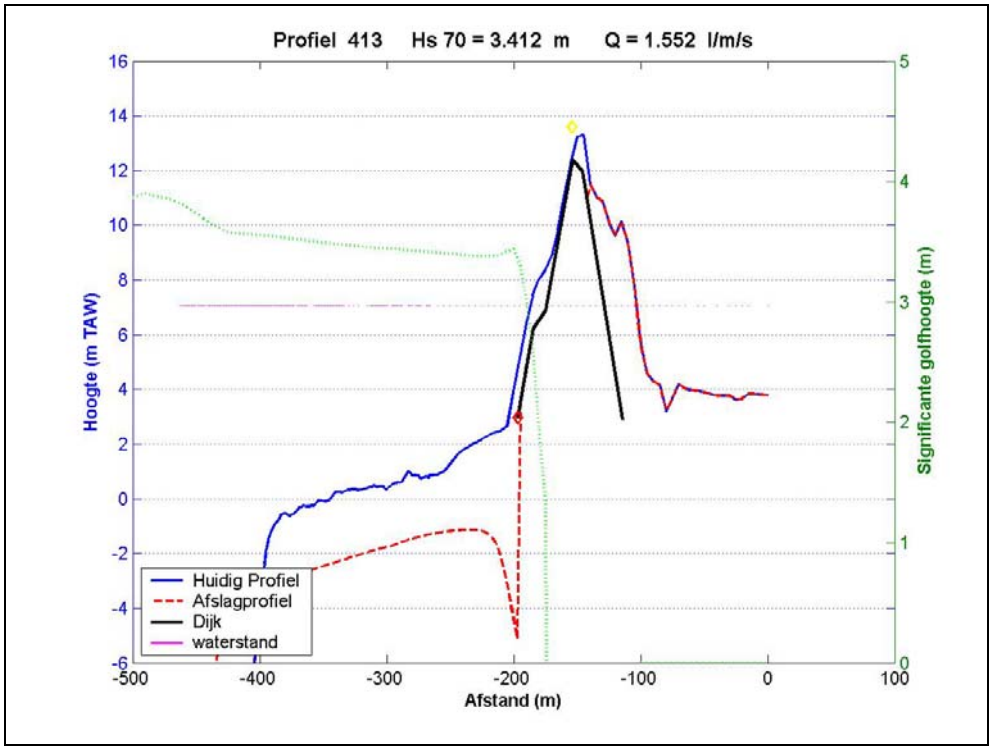

Figure 77 Beach profile of profile 413 after storm with return period 40000 year.

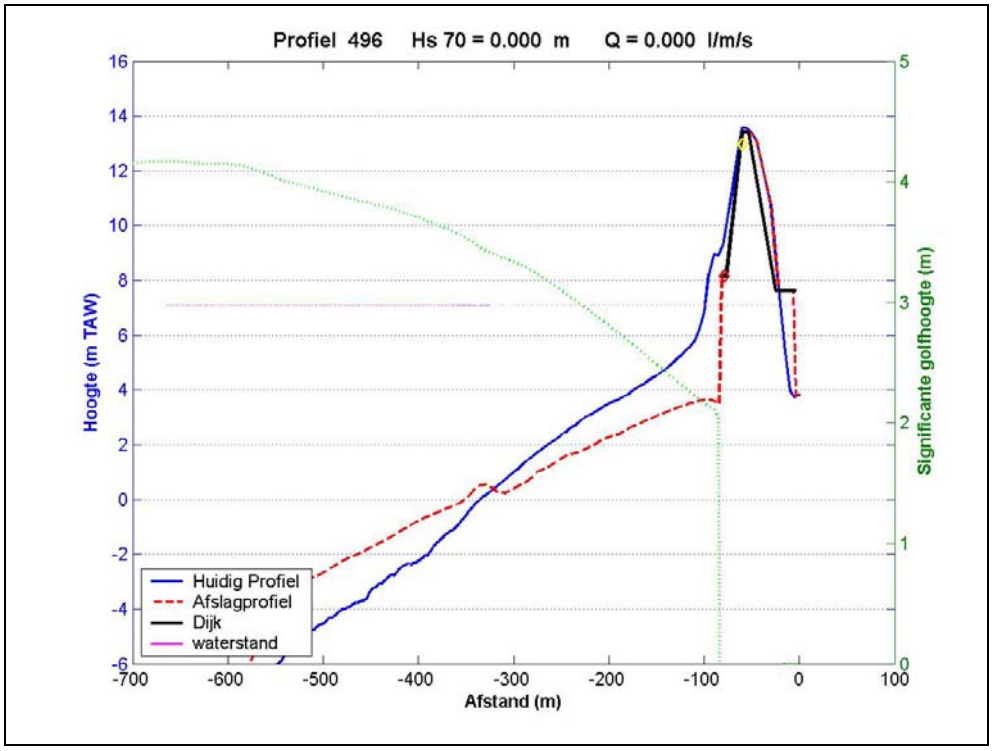

Figure 78 Beach profile of profile 496 after storm with return period 40000 year.

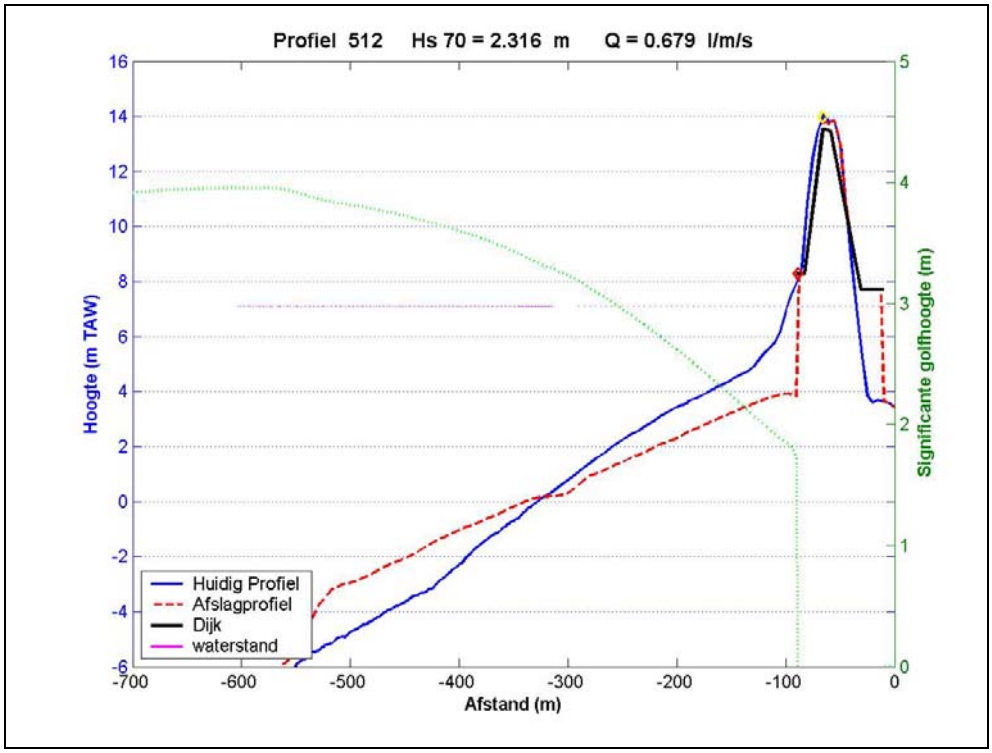

Figure 79 Beach profile of profile 512 after storm with return period 4000 year.

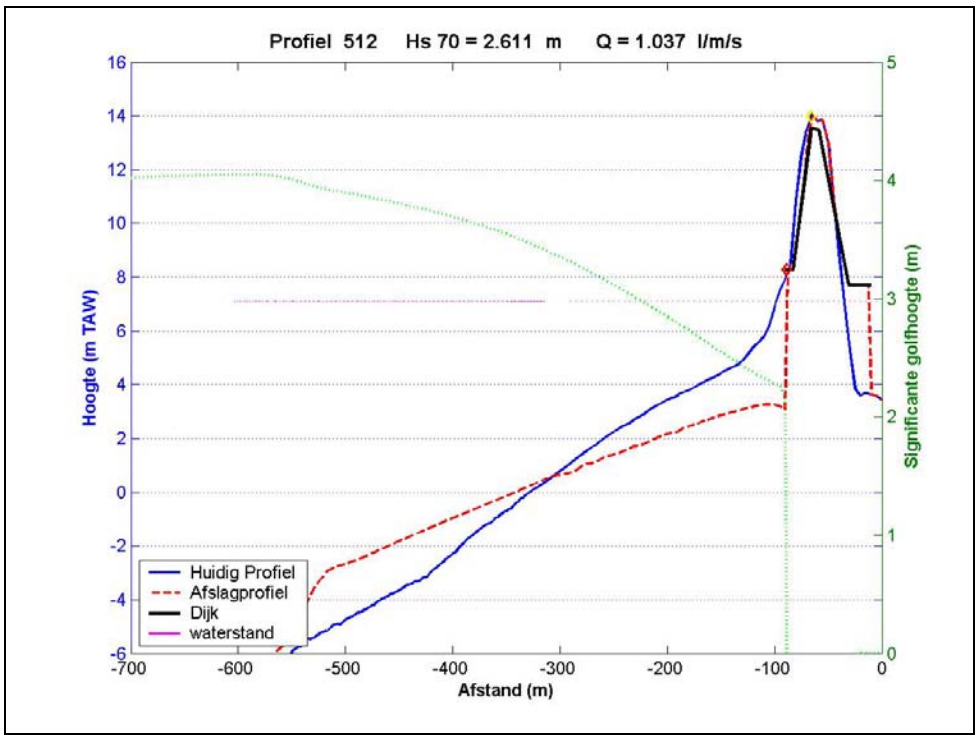

Figure 80 Beach profile of profile 512 after storm with return period 40000 year.

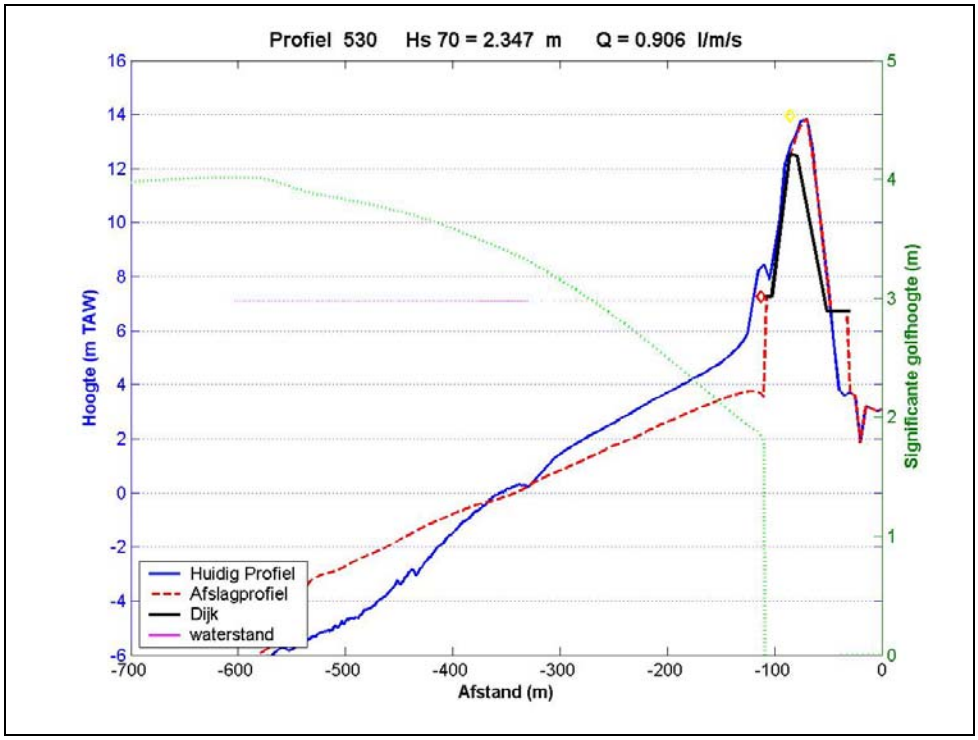

Figure 81 Beach profile of profile 530 after storm with return period 4000 year.

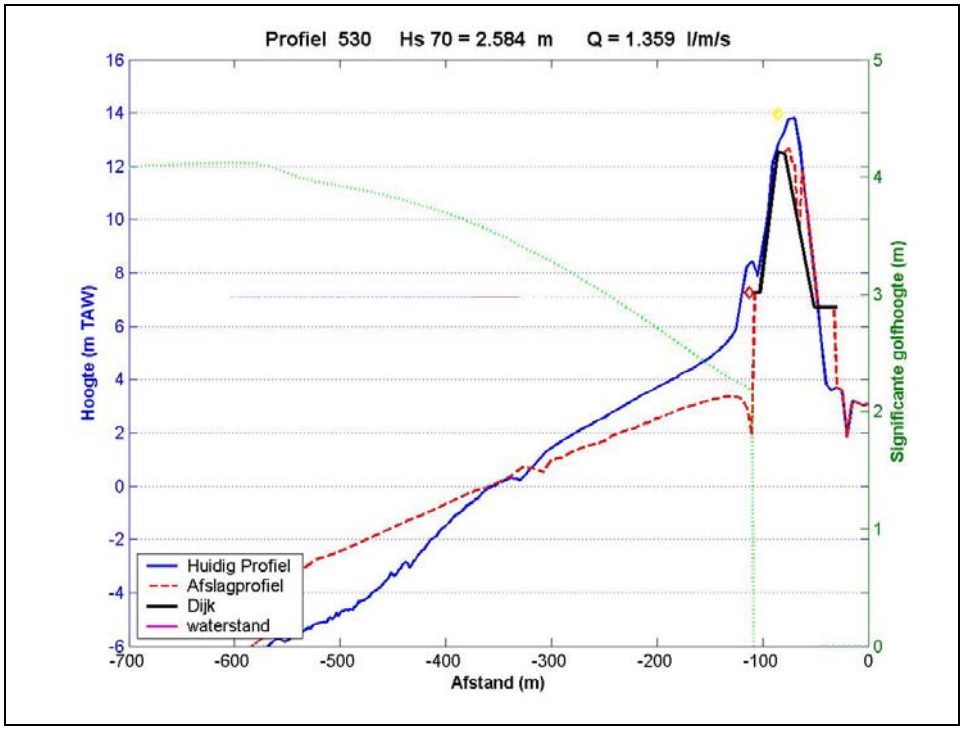

Figure 82 Beach profile of profile 530 after storm with return period 40000 year

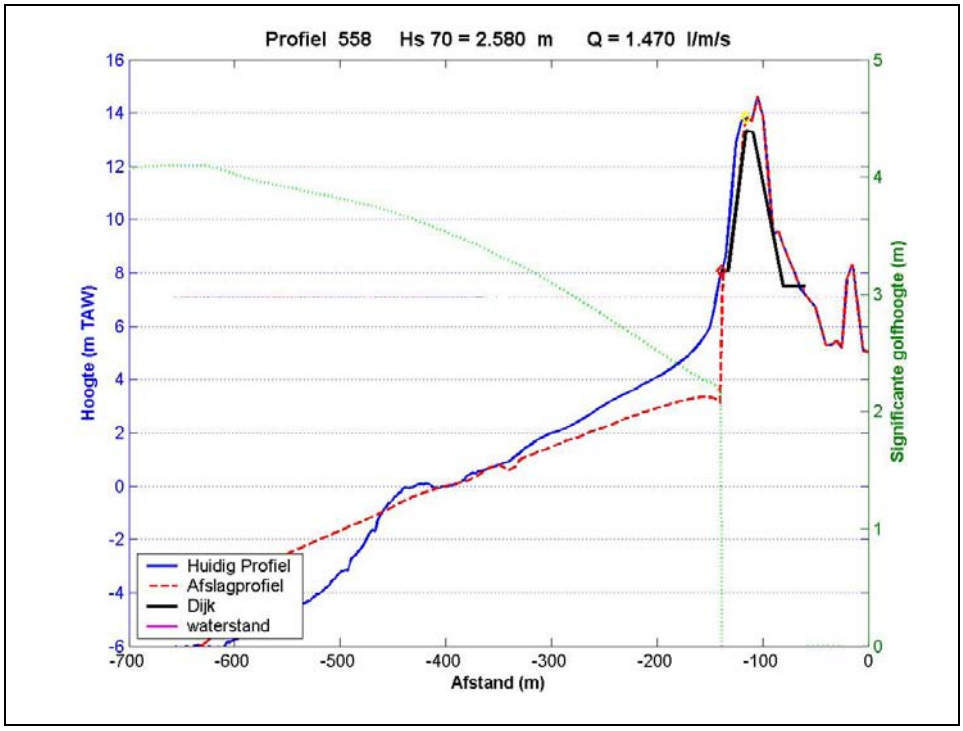

Figure 83 Beach profile of profile 558 after storm with return period 40000 year.

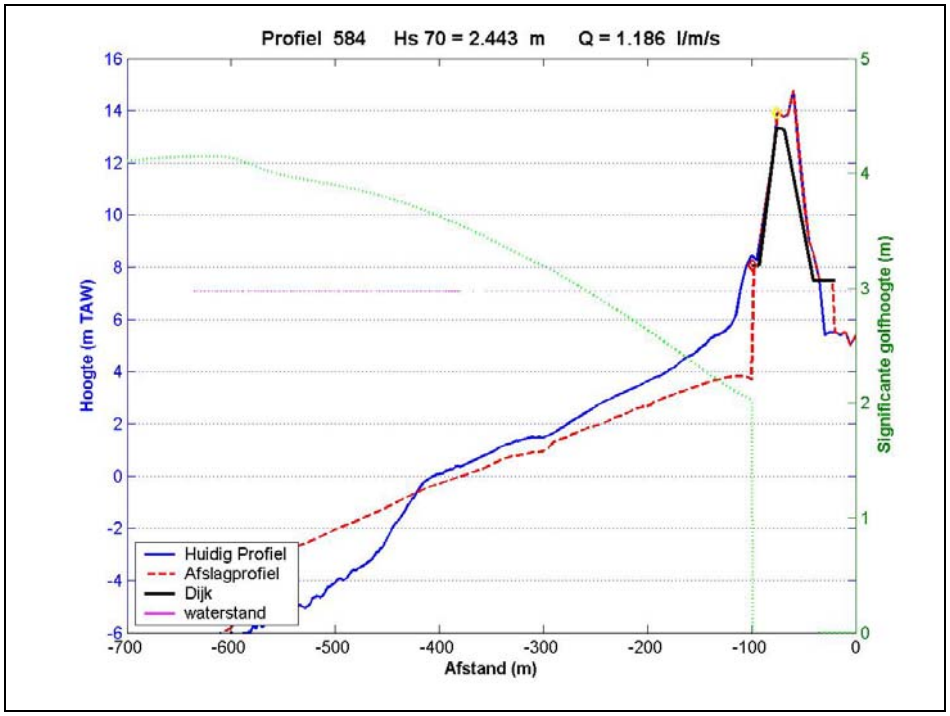

Figure 84 Beach profile of profile 584 after storm with return period 40000 year.

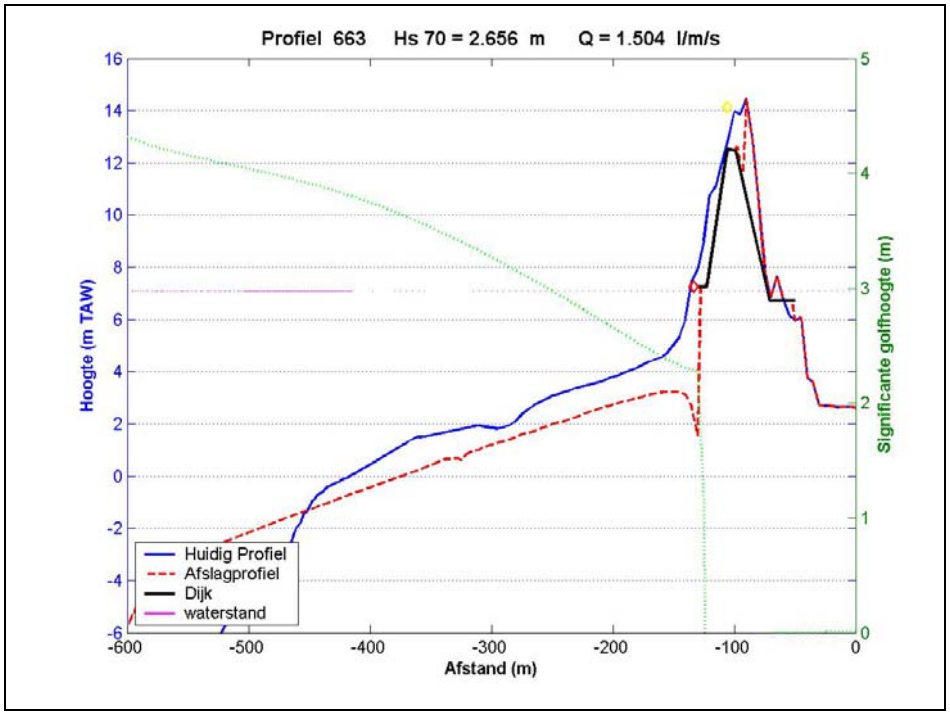

Figure 85 Beach profile of profile 663 after storm with return period 40000 year.

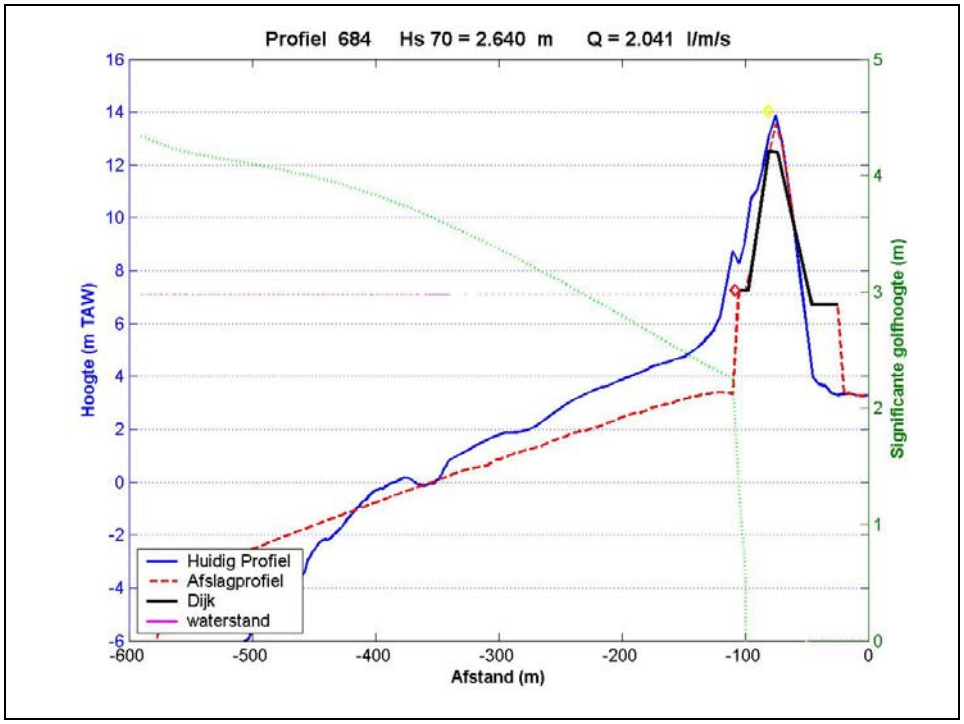

Figure 86 Beach profile of profile 684 after storm with return period 40000 year.

For the return periods considered the following results were obtained:

profile no.	1000 years			4000 years			40000 years		
	H_s (m)	q (l/s.m)	$z_{2\%}$ (m)	H_s (m)	q (l/s.m)	$z_{2\%}$ (m)	H_s (m)	q (l/s.m)	$z_{2\%}$ (m)
171	0	0	N/A	0	0	N/A	0	0	N/A
188	0	0	N/A	0	0	N/A	0	0	N/A
271	0	0	N/A	0	0	N/A	0	0	N/A
290	0.17	0	1.53	0.17	0	1.51	0.38	0	2.19
308	1.60	0.03	4.35	1.60	0.03	4.31	1.60	0.03	4.31
324	1.60	0.02	4.25	1.60	0.02	4.23	1.60	0.02	4.23
336	0.03	0	0.59	0.03	0	0.59	0.03	0	0.59
352	0	0	N/A	0	0	N/A	0	0	N/A
373	3.01	0.72	5.91	3.01	0.69	5.88	3.01	0.72	5.91
396	1.95	0.08	4.87	1.95	0.07	4.84	1.95	0.07	4.82
413	3.23	1.19	6.26	3.32	1.33	6.33	3.41	1.55	6.43
421	2.84	0.81	5.86	2.84	0.79	5.85	2.84	0.78	5.84
441	2.26	0.54	5.63	2.26	0.50	5.59	2.26	0.48	5.57
483	0	0	N/A	0	0	N/A	0.52	0	3.30
496	0	0	N/A	0	0	N/A	0	0	N/A
512	2.10	0.35	5.88	2.32	0.68	6.28	2.61	1.04	6.54
530	2.12	0.52	6.22	2.35	0.91	6.45	2.58	1.36	6.72
558	2.08	0.48	6.06	2.29	0.93	6.39	2.58	1.47	6.69
584	1.88	0.15	5.78	2.13	0.56	6.22	2.44	1.19	6.60
602	0	0	N/A	0	0	N/A	0	0	N/A
619	1.53	0.01	5.17	2.00	0.28	5.84	2.25	0.67	6.26
638	0	0	N/A	0.98	0	4.42	2.07	0.35	6.27
663	2.16	0.49	6.32	2.39	1.08	6.72	2.66	1.5	6.94
684	2.03	0.31	6.28	2.34	1.18	6.80	2.64	2.04	7.11
705	1.26	0	5.02	1.98	0.31	6.20	2.42	2.00	6.92
730	0	0	N/A	0	0	N/A	0	0	N/A
751	0.30	0	2.52	0.30	0	2.47	0.30	0	2.47
768	0	0	N/A	0	0	N/A	0	0	N/A
778	0.10	0	1.53	0.10	0	1.49	0.10	0	1.47
791	0	0	N/A	0	0	N/A	0	0	N/A
802	0	0	N/A	0	0	N/A	0	0	N/A
877	0	0	N/A	0	0	N/A	0	0	N/A
886	0	0	N/A	0	0	N/A	0	0	N/A
903	0	0	N/A	0	0	N/A	0	0	N/A

920	0.01	0	0.30	0.01	0	0.31	0.64	0	0.31
936	0.73	0	2.73	0.92	0	3.13	1.16	0	3.74
951	0	0	0.02	0	0	0.02	0	0	0.01
962	0.48	0	1.99	0.75	0	2.43	0.94	0	3.16
979	0.21	0	1.75	0.21	0	1.74	0.37	0	2.21
985	0.31	0	2.03	0.31	0	2.04	0.31	0	2.01
993	0.41	0	2.34	0.41	0	2.32	0	0	N/A
1007	0.52	0	2.61	0.52	0	2.54	0	0	N/A
1021	0.21	0	1.71	0.42	0	2.28	0.42	0	2.27
1032	1.79	0.24	4.72	1.79	0.21	4.65	1.79	0.20	4.63
1046	0	0	N/A	0.02	0	0.49	0.02	0	0.55
1282	0.23	0	1.80	0.23	0	1.80	0.23	0	1.75
1300	1.67	0.11	4.74	1.67	0.10	4.68	1.67	0.08	4.62
1318	1.58	0.06	4.60	1.58	0.06	4.61	1.58	0.06	4.50
1335	2.45	0.90	5.75	2.45	0.84	5.71	2.45	0.73	5.62
1354	3.76	4.78	6.85	3.96	5.78	7.00	4.12	6.66	7.11

Table 20 Significant wave heights, overtopping discharges, wave run-up heights.

whereby

H_s : significant wave height at the toe of the dike;

q: overtopping discharge;

$z_{2\%}$: wave run-up height in accordance with the 2% largest waves.

8.4. Piping en heave

According to VTV (2004), a dike of type 1 (clay) must be assumed for the assessment in case of uncertainty about the composition of the dike core. For the analysis, dike sections d_8, d_9 and d_12 were consequently assumed to be of type 1B (clay core on an under-layer of sand), for which it must apply that the seepage length $L_b > 18h$ with h = piezometric fall. The other profiles were assumed to be of type 1A (clay core on impermeable subsoil with thickness D). Type 1A is definitely safe if $L_b > 18h - 0.33D$. For the determination of L_b the co-ordinates of the points were used for which the dike geometry is given.

For the 1000-year return period the following results are obtained:

dike section	L_b [m] (*)	D [m]	h [m]	type 1B	type 1A	18h	type 1B: Lb > 18h ?	18h – 0.33D	type 1A: Lb > 18h – 0.33D ?
d_8	89.50	-	2.89	x		52.0	ok		
d_9	90.24	-	2.89	x		52.0	ok		
d_12	69.51	-	2.89	x		52.0	ok		
d_17	80.00	5.58	2.89		x			50.2	ok
d_20	73.24	5.69	2.89		x			50.1	ok
d_21	148.49	6.23	2.89		x			50.0	ok
d_22	82.65	6.28	2.89		x			49.9	ok
d_23	89.47	8.36	2.89		x			49.3	ok
d_24	81.00	8.11	2.89		x			49.3	ok
d_25	80.51	6.41	2.89		x			49.9	ok
d_26	73.97	4.71	2.89		x			50.5	ok
d_28	81.67	7.95	2.89		x			49.4	ok
d_29	65.69	5.61	2.89		x			50.2	ok

Table 21 Basic geometric assessment for a 1000-year return period.

For the 4000-year return period the following results are obtained:

dike section	L_b [m] (*)	D [m]	h [m]	type 1B	type 1A	18h	type 1B: Lb > 18h ?	18h – 0.33D	type 1A: Lb > 18h – 0.33D ?
d_8	89.50	-	3.22	x		57.96	ok		
d_9	90.24	-	3.22	x		57.96	ok		
d_12	69.51	-	3.22	x		57.96	ok		
d_17	80.00	5.58	3.22		x			56.1	ok
d_20	73.24	5.69	3.22		x			56.1	ok
d_21	148.49	6.23	3.22		x			55.9	ok
d_22	82.65	6.28	3.22		x			55.9	ok
d_23	89.47	8.36	3.22		x			55.2	ok
d_24	81.00	8.11	3.22		x			55.3	ok
d_25	80.51	6.41	3.22		x			55.8	ok
d_26	73.97	4.71	3.22		x			56.4	ok
d_28	81.67	7.95	3.22		x			55.3	ok
d_29	65.69	5.61	3.22		x			56.1	ok

Table 22 : Basic geometric assessment for a 4000-year return period.

For the 40000-year return period the following results are obtained:

dike section	L_b [m] (*)	D [m]	h [m]	type 1B	type 1A	18h	type 1B: Lb > 18h ?	18h – 0.33D	type 1A: Lb > 18h – 0.33D ?
d_8	89.50	-	3.76	x		67.7	ok		
d_9	90.24	-	3.76	x		67.7	ok		
d_12	69.51	-	3.76	x		67.7	ok		
d_17	80.00	5.58	3.76		x			65.8	ok
d_20	73.24	5.69	3.76		x			65.8	ok
d_21	148.49	6.23	3.76		x			65.6	ok
d_22	82.65	6.28	3.76		x			65.6	ok
d_23	89.47	8.36	3.76		x			64.9	ok
d_24	81.00	8.11	3.76		x			65.0	ok
d_25	80.51	6.41	3.76		x			65.6	ok
d_26	73.97	4.71	3.76		x			66.1	ok
d_28	81.67	7.95	3.76		x			65.1	ok
d_29	65.69	5.61	3.76		x			65.8	-

Table 23 Basic geometric assessment for a 4000-year return period.

The first step in the assessment scheme gives the result ‘yes’, Consequently, the score is ‘sufficient’. Only dike section d_29 has a borderline score for the basic geometric assessment for the 40000-year return period.

8.5. Outward macrostability

8.5.1. Sliding and liquefaction

Stability loss of the foreshore by sliding or liquefaction in the immediate vicinity of the dike is considered a safety threat.

The geometric assessment was made for the eroded profiles of the storm with a 1000-year return period. The covering criterion was examined for the various profiles. All profiles comply. Both the liquefaction and sliding criteria were then examined. The first four profiles have only 1 trough depth. For other profiles, both the local through depth and the total through depth had to be taken into account.

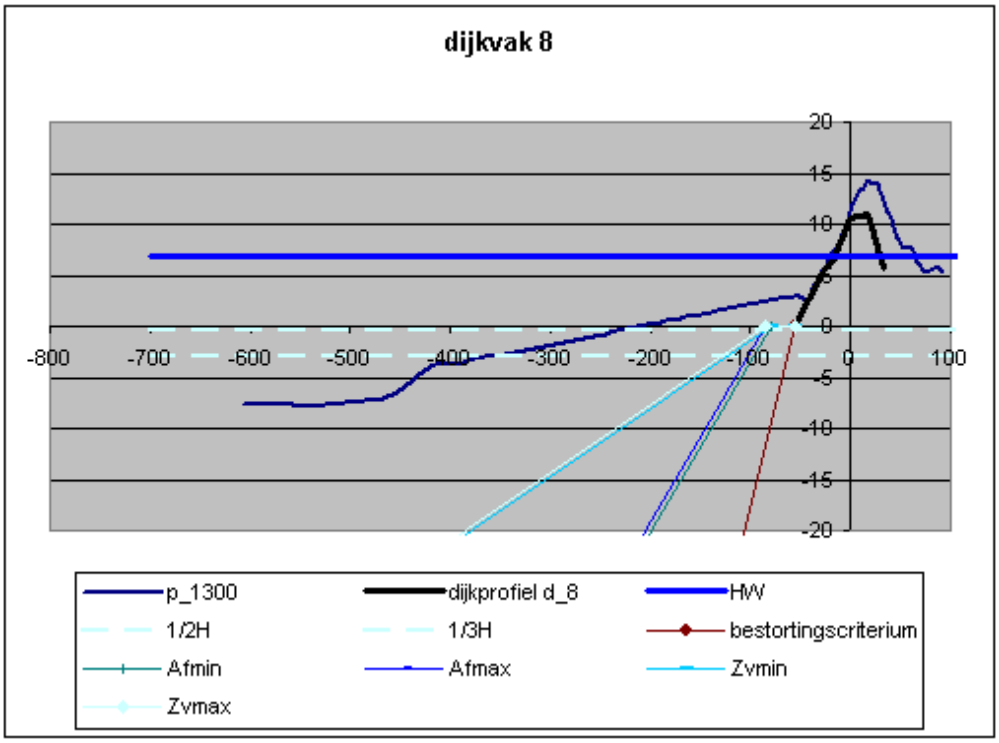

Dutch	English
dijkvak	dike section
bestortingscriterium	covering criterion
Zv	liquefaction
Af	sliding

Figure 87 Covering, liquefaction and sliding criteria for dike section d_8.

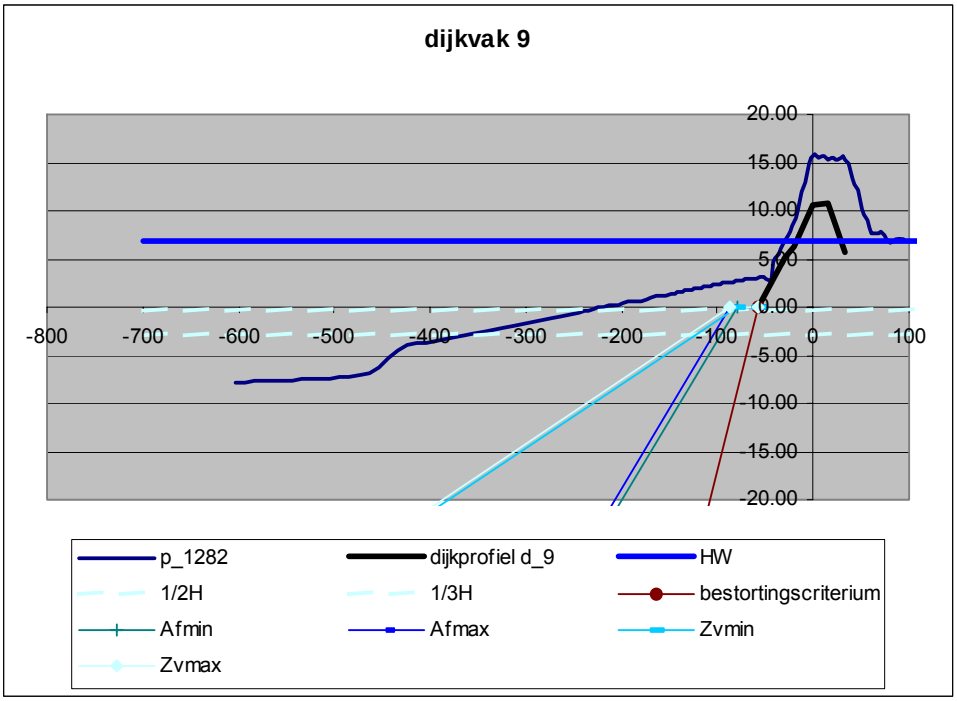

Figure 88 Covering, liquefaction and sliding criteria for dike section d_9.

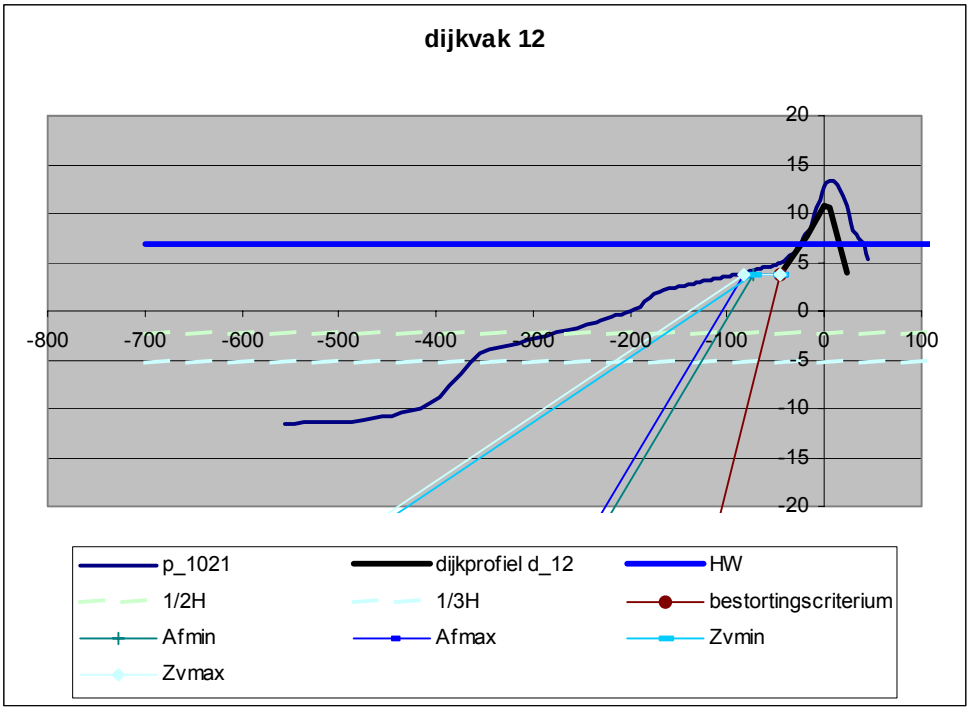

Figure 89 Covering, liquefaction and sliding criteria for dike section d_12.

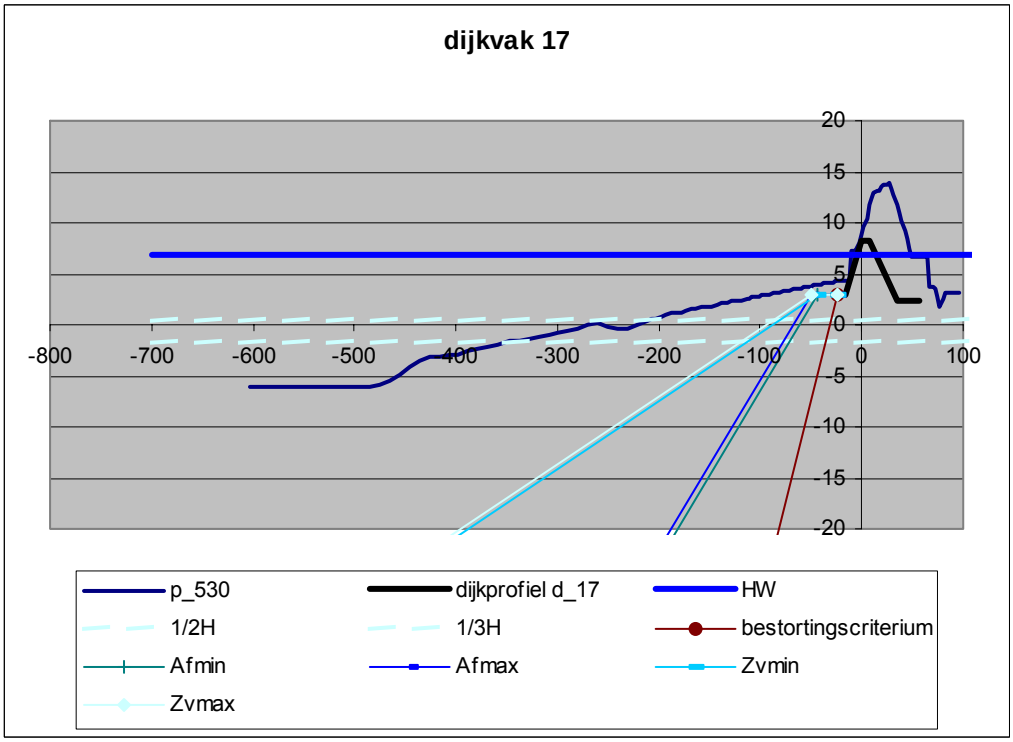

Figure 90 Covering, liquefaction and sliding criteria for dike section d_17.

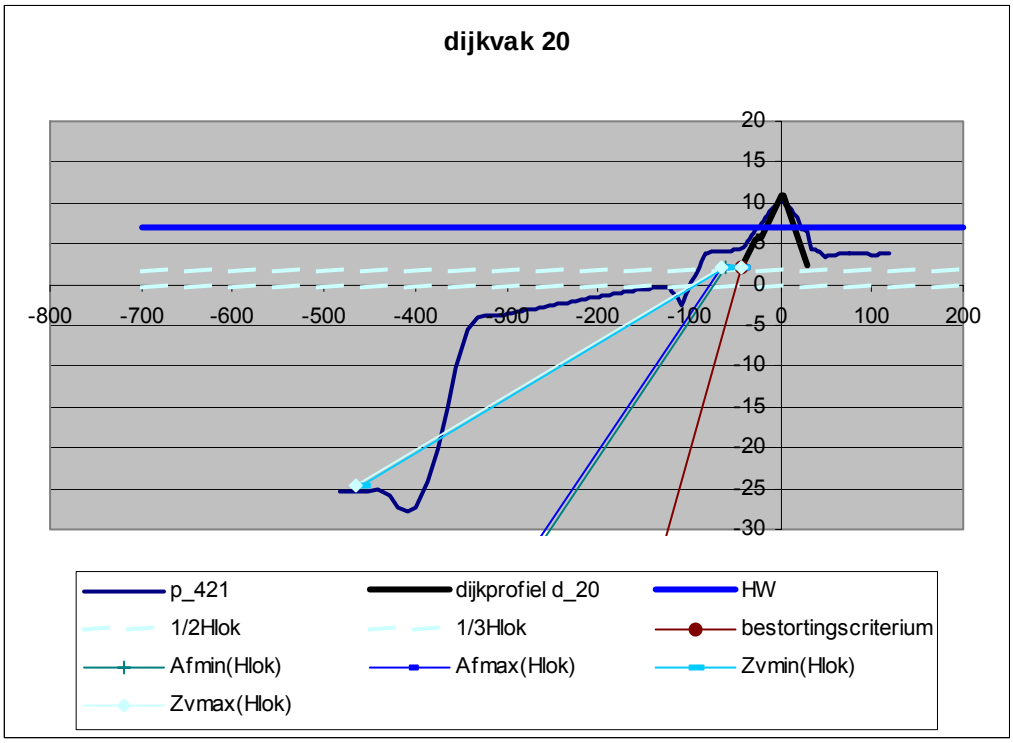

a) local trough depth H_{loc}

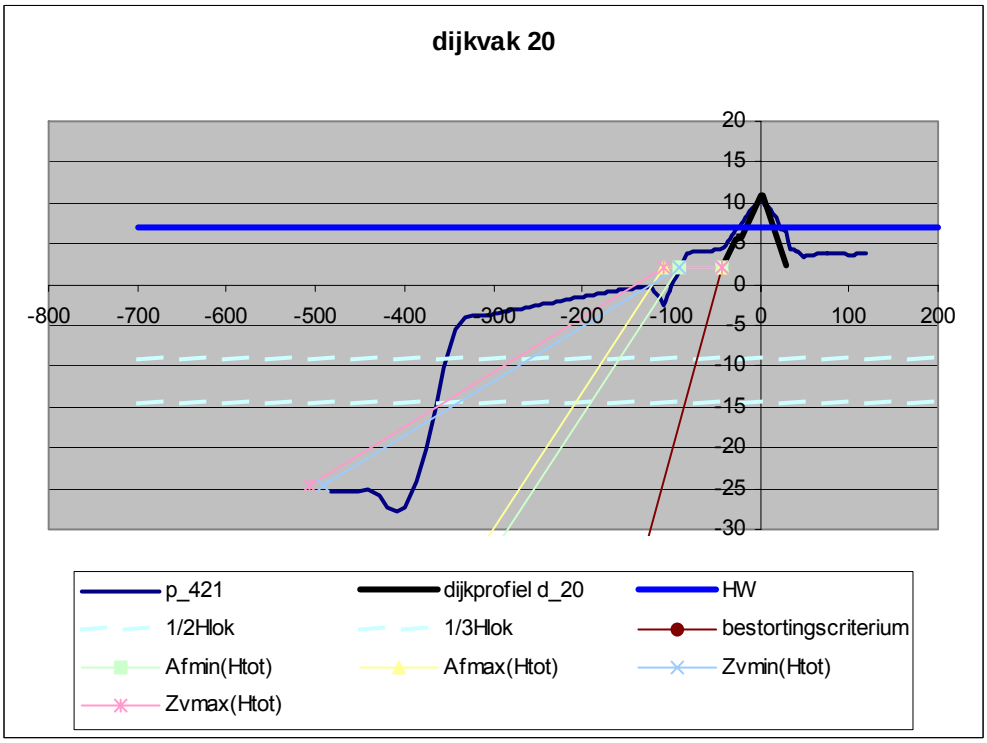

b) total trough depth H_{tot}

Figure 91 Covering, liquefaction and sliding criteria for dike section d_20: (a) local trough depth, (b) total trough depth.

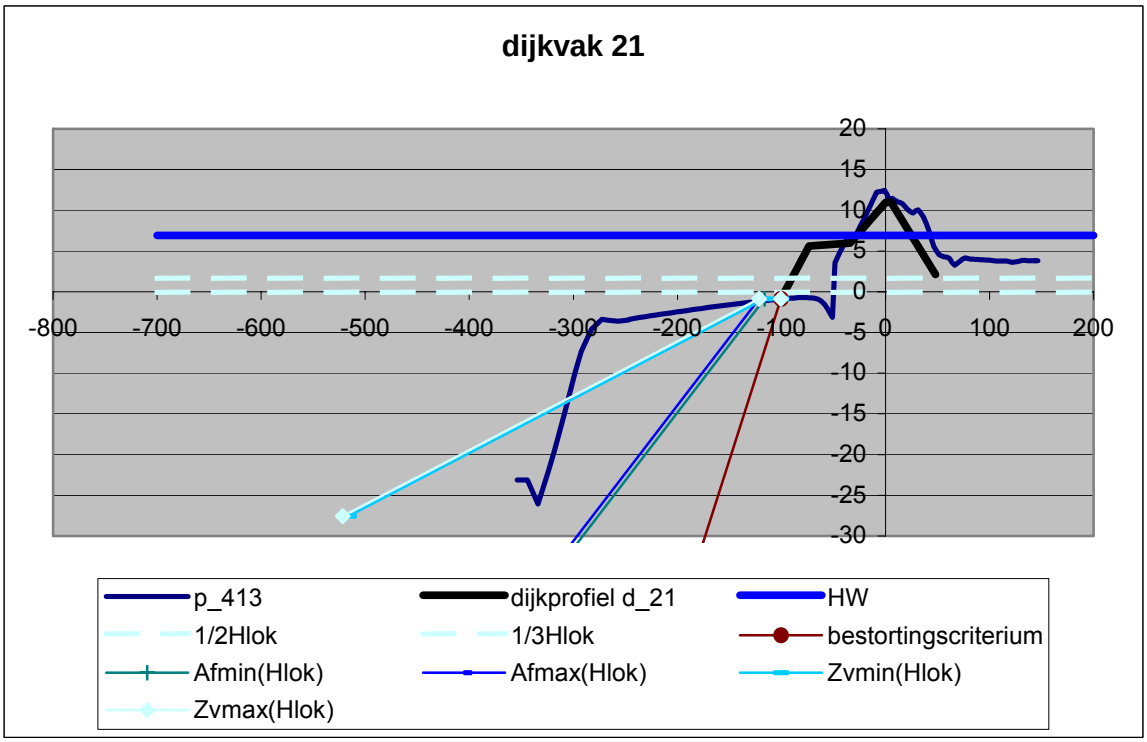

a) local trough depth H_{loc}

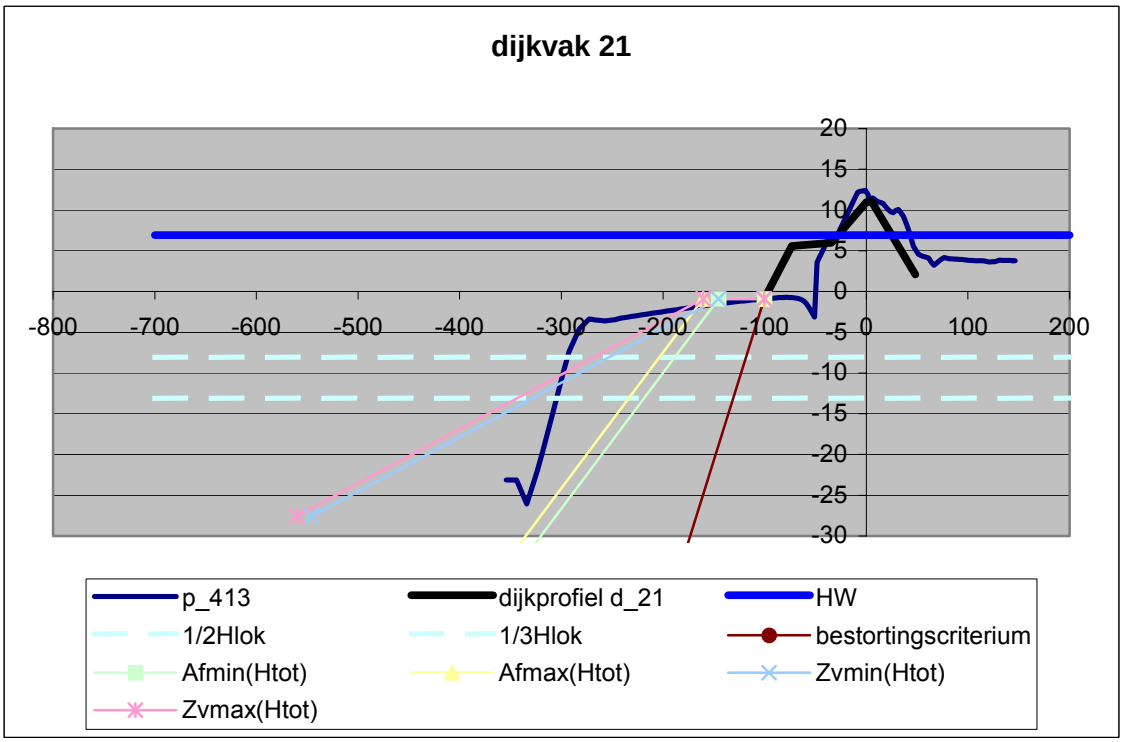

b) total trough depth H_{tot}

Figure 92 Covering, liquefaction and sliding criteria for dike section d_21: (a) local trough depth, (b) total trough depth.

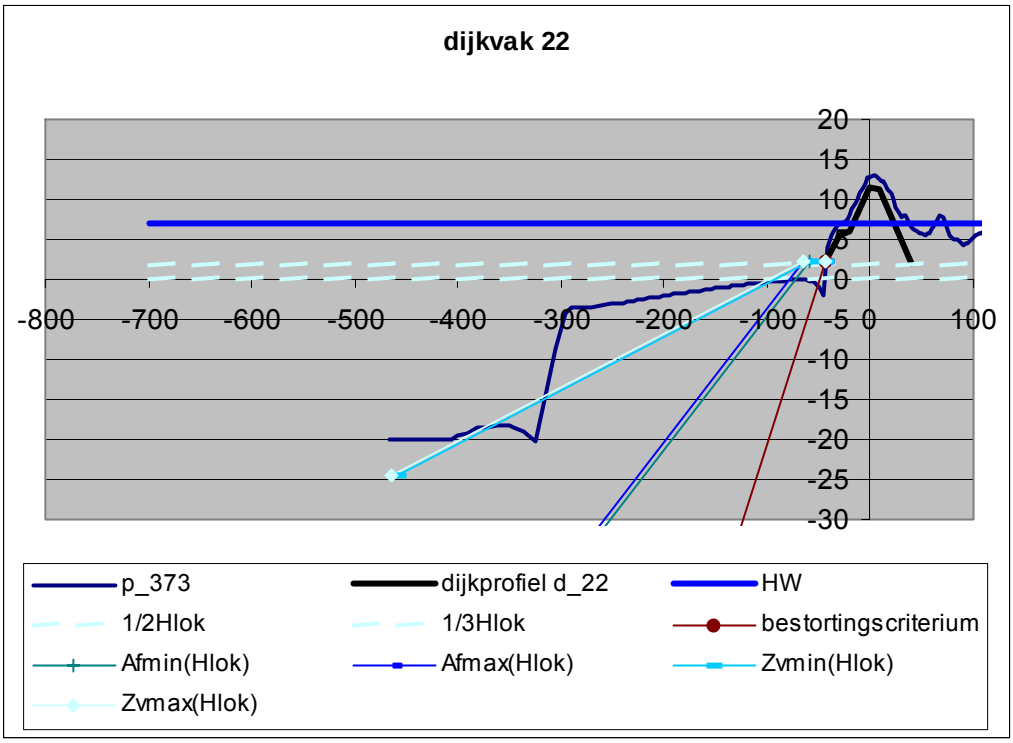

a) local trough depth

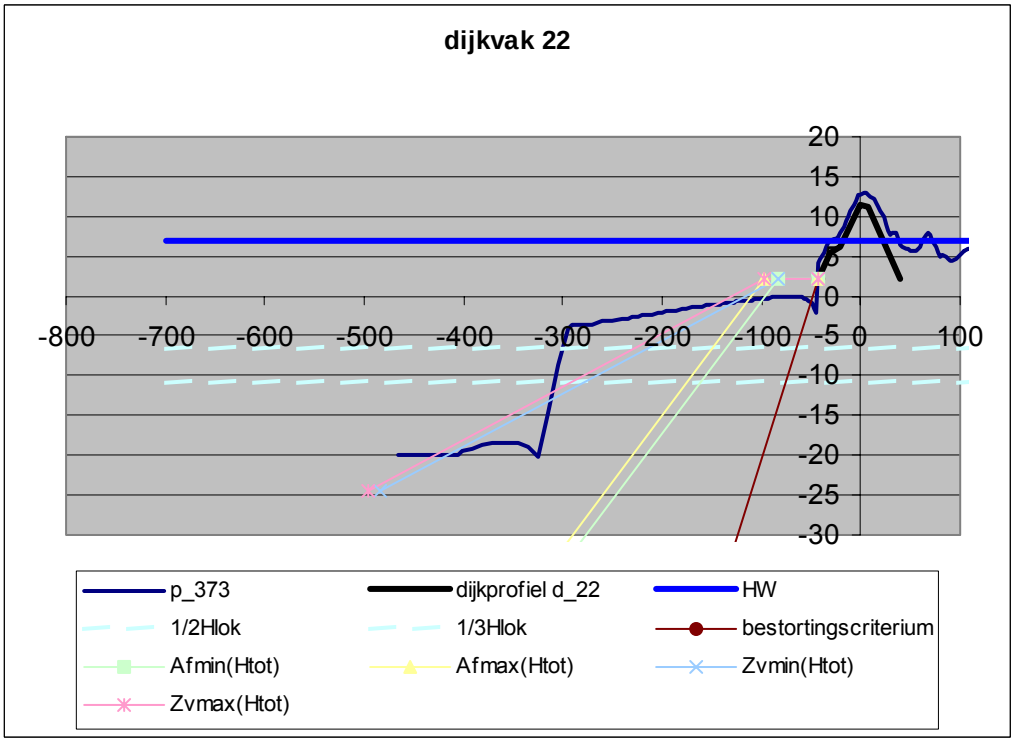

b) total trough depth

Figure 93 Covering, liquefaction and sliding criteria for dike section d_22: (a) local trough depth H_{loc}, (b) total trough depth H_{tot}.

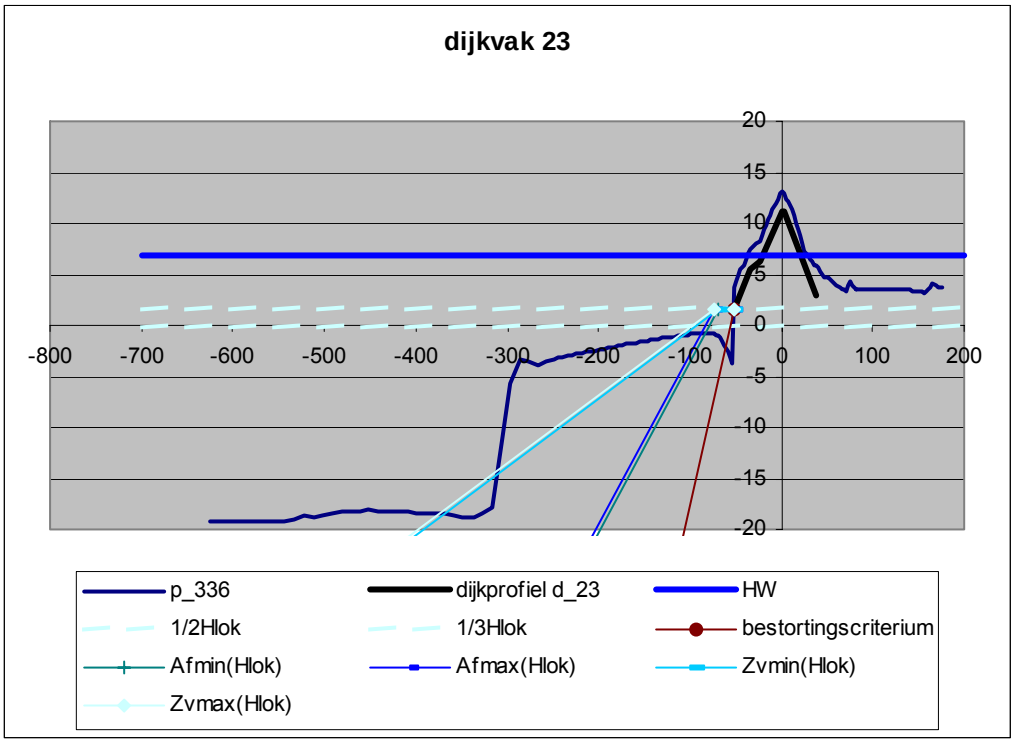

a) local trough depth

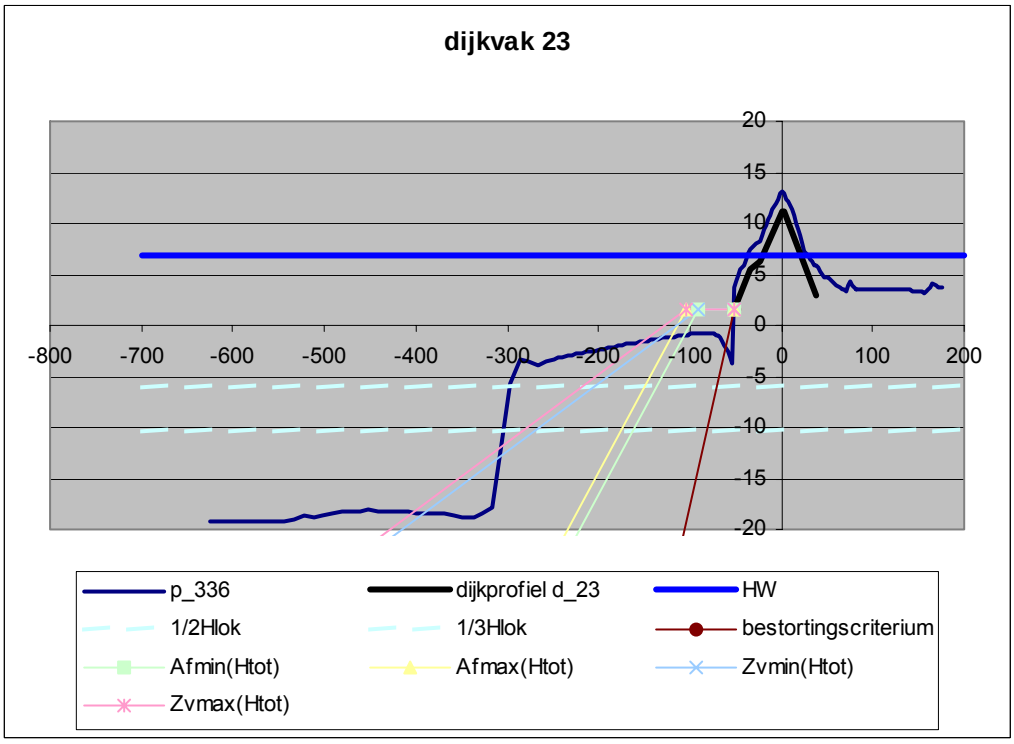

b) total trough depth

Figure 94 Covering, liquefaction and sliding criteria for dike section d_23: (a) local trought depth H_{loc}, (b) total trough depth H_{tot}.

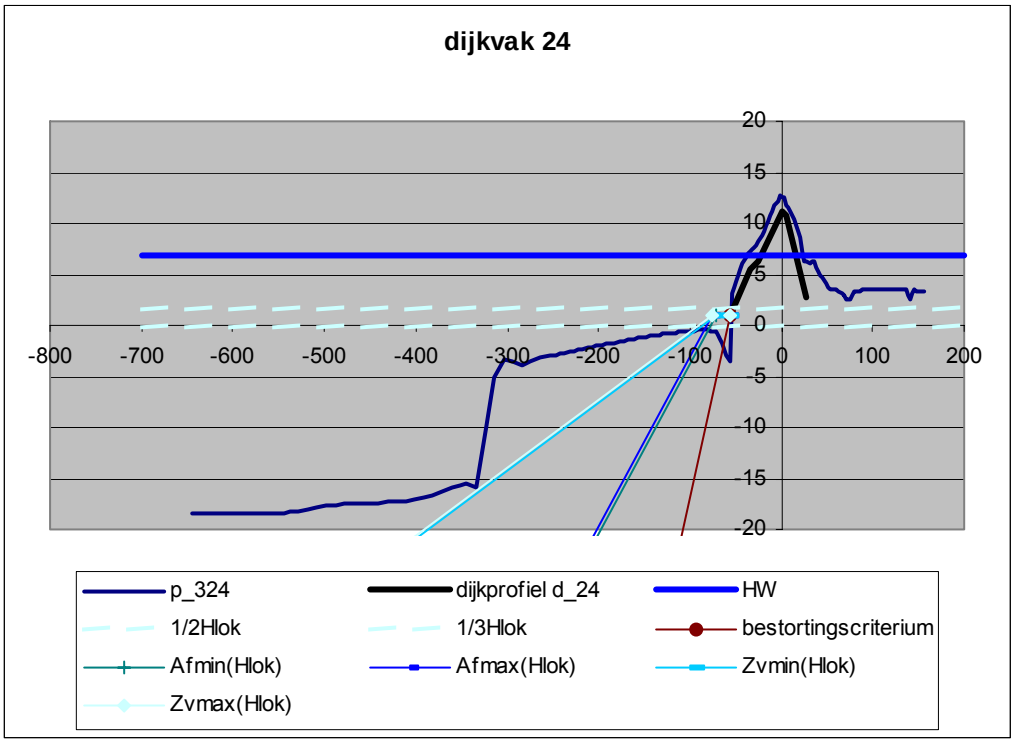

a) local trough depth

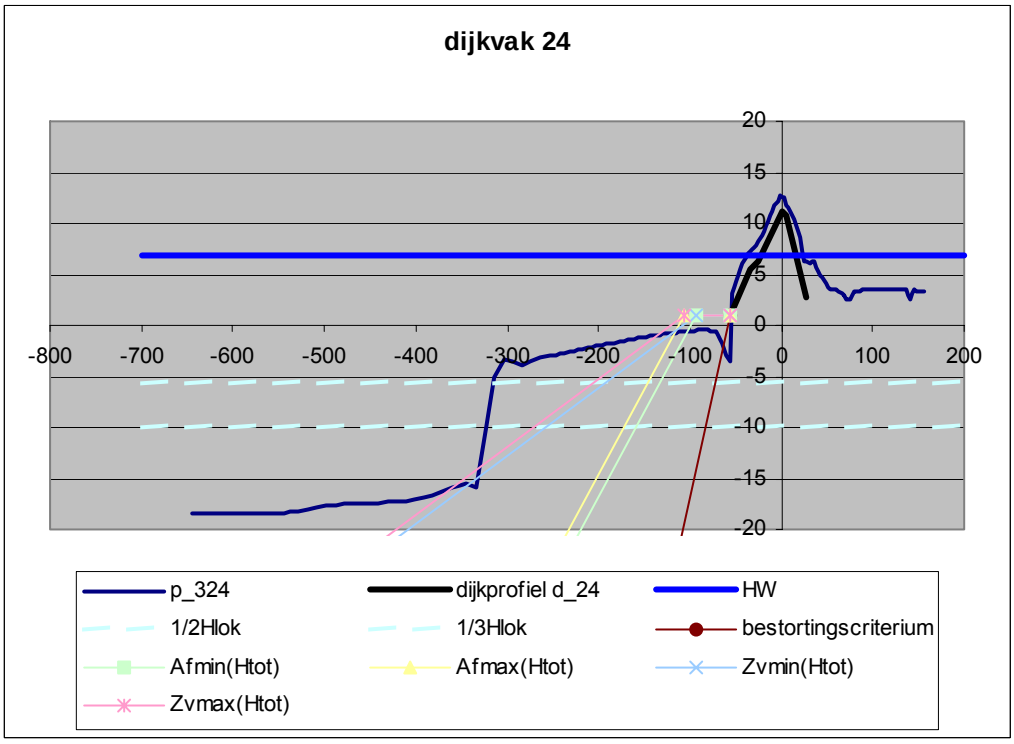

b) total trough depth

Figure 95 Covering, liquefaction and sliding criteria for dike section d_24: (a) local trough depth H_{loc}, (b) total trough depth H_{tot}.

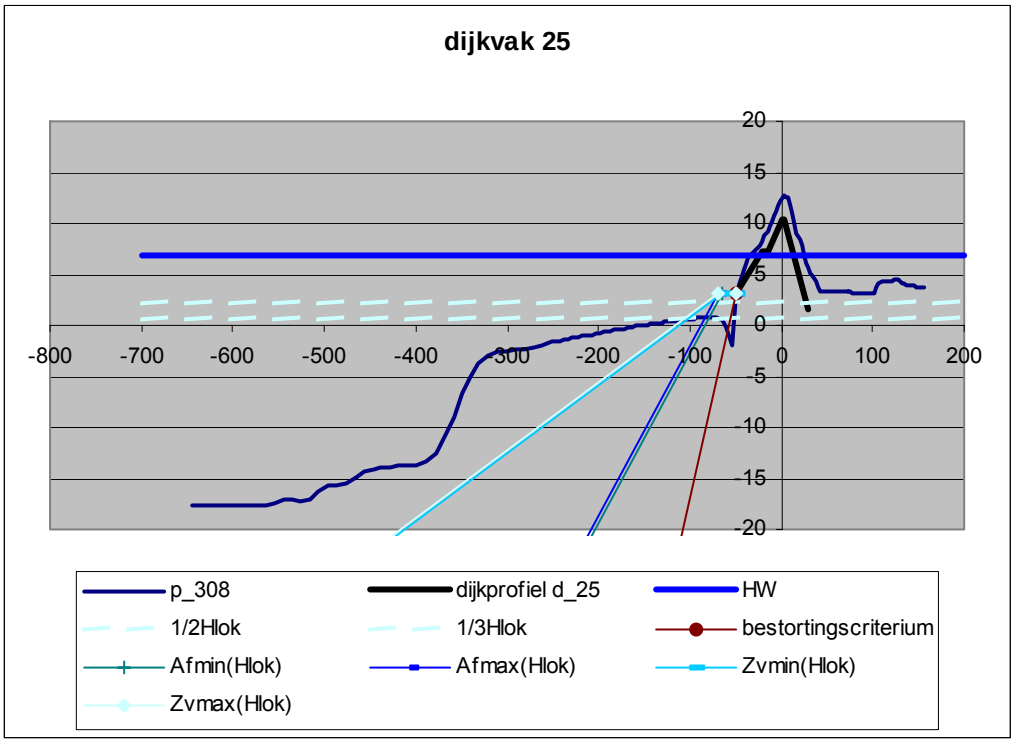

a) local trough depth

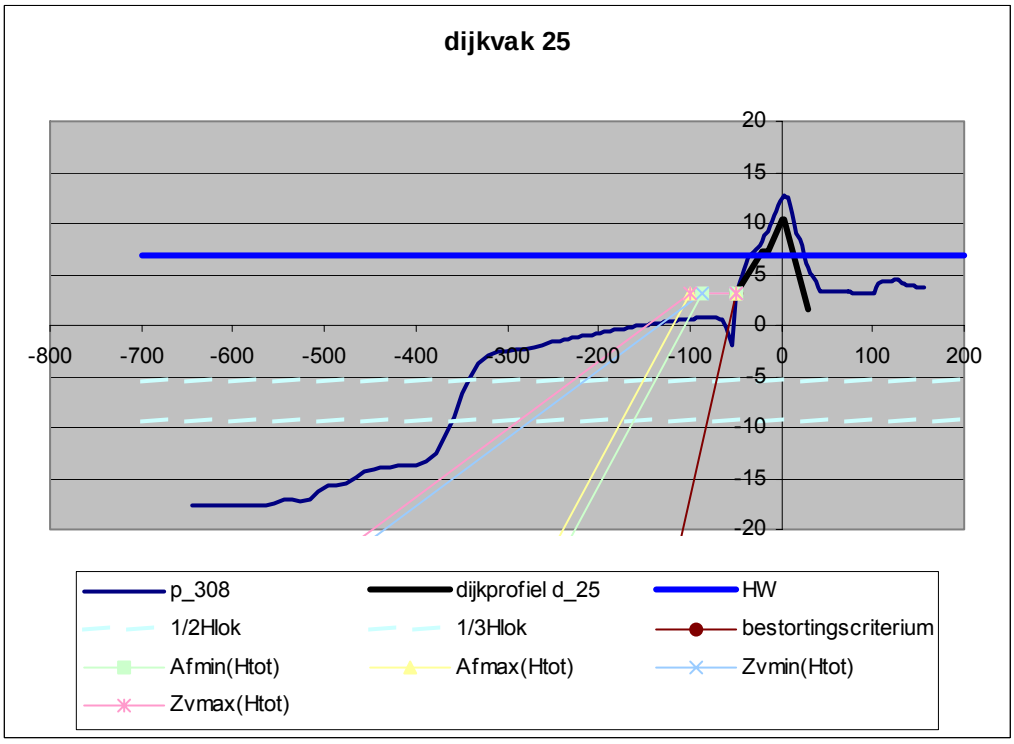

b) total trough depth

Figure 96 Covering, liquefaction and sliding criteria of dike section d_25: (a) local trough depth H_{loc}, (b) total trough depth H_{tot}.

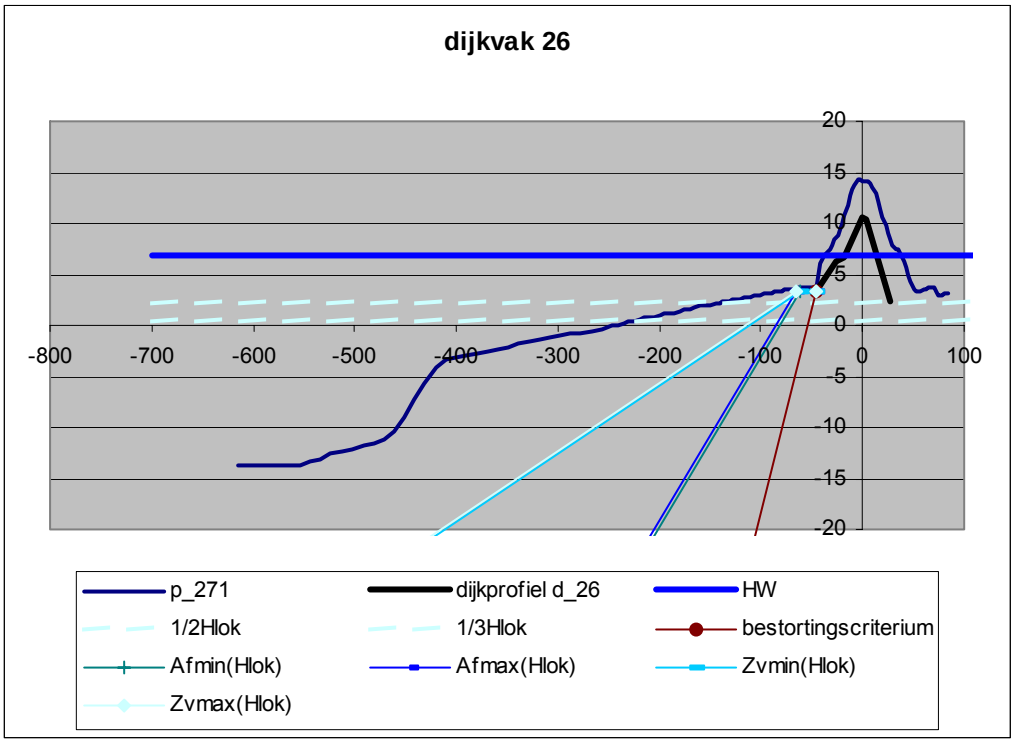

a) local trough depth

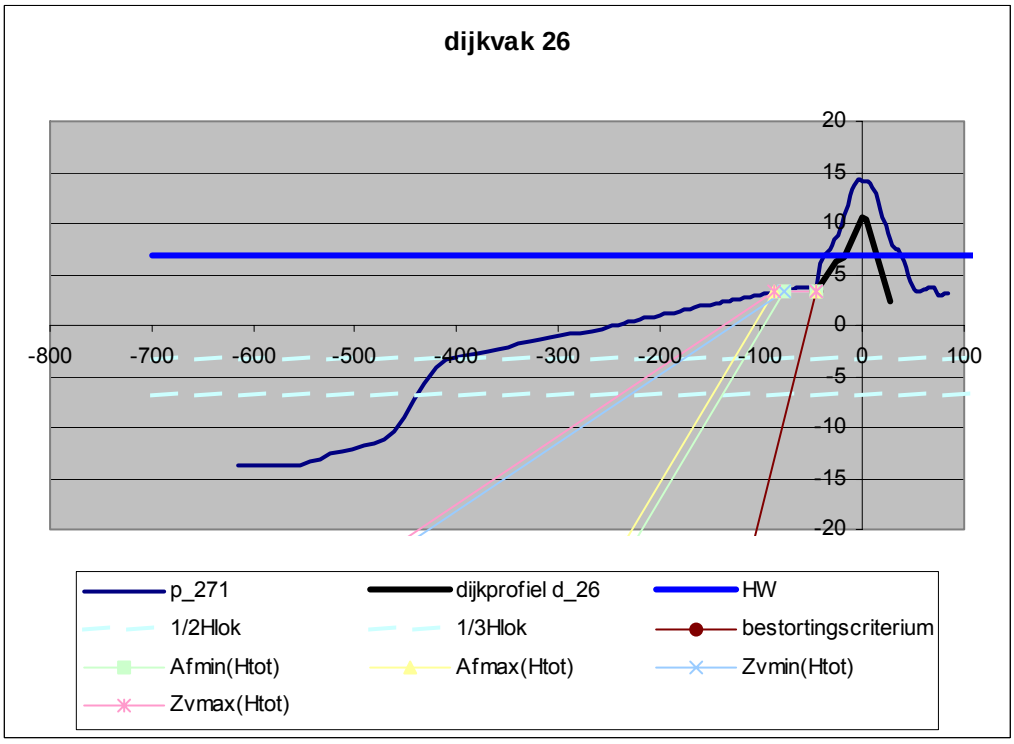

b) total trough depth

Figure 97 Covering, liquefaction and sliding criteria of dike section d_26: (a) local trough depth H_{loc}, (b) total trough depth H_{tot}.

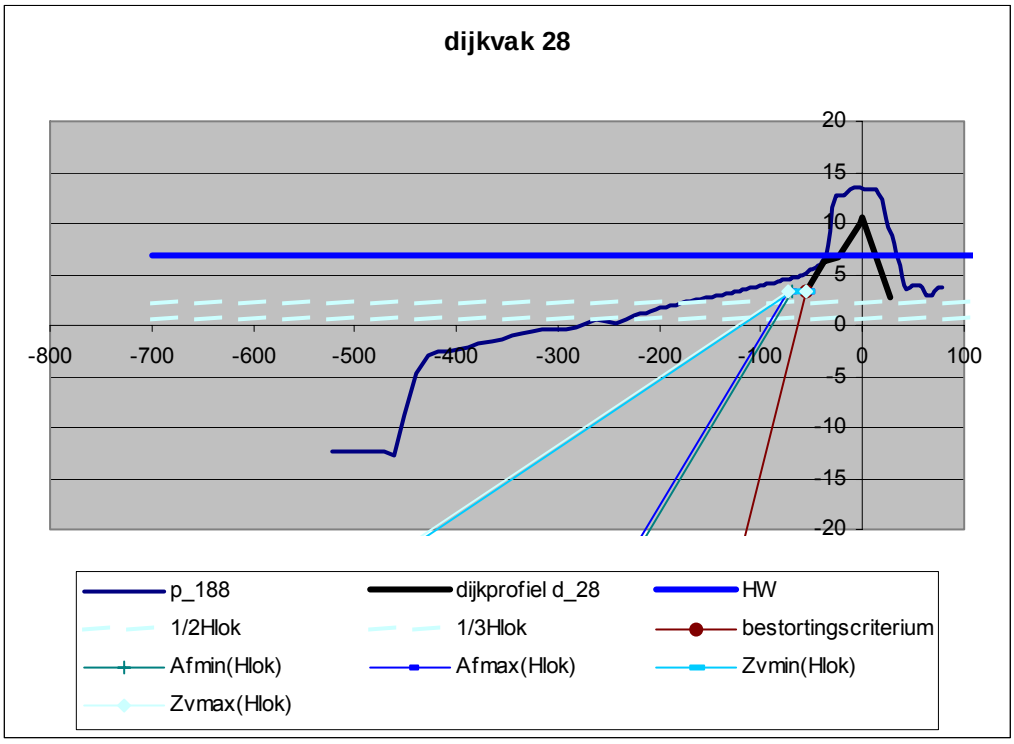

a) local trough depth

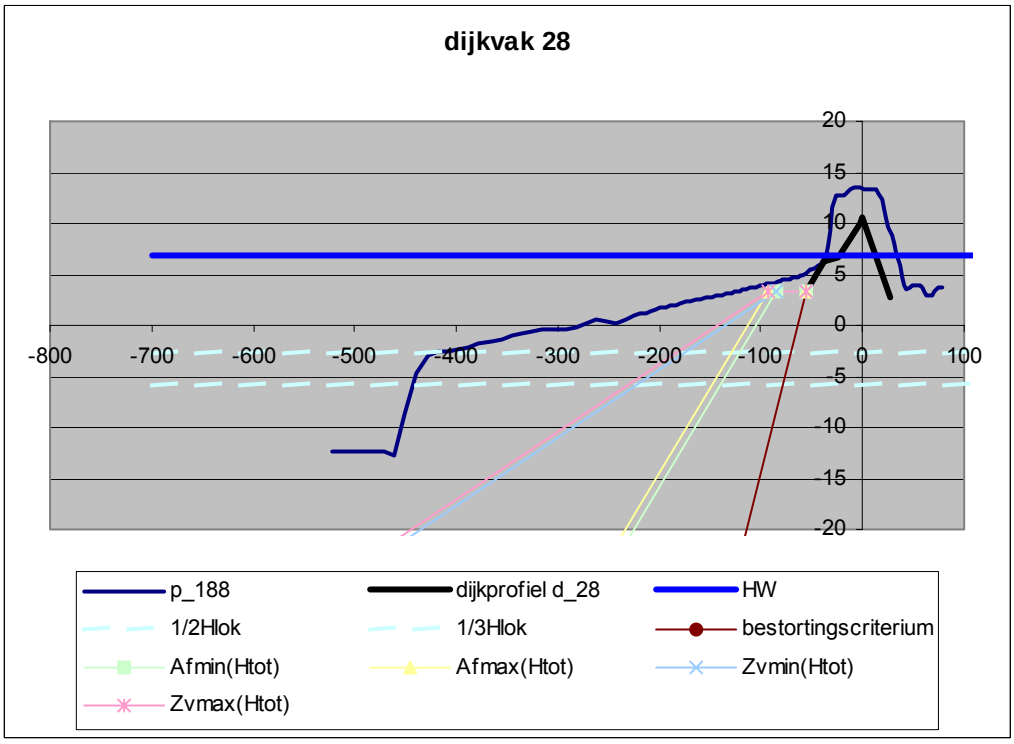

b) total trough depth

Figure 98 Covering, liquefaction and sliding criteria of dike section d_28: (a) local trough depth H_{loc}, (b) total trough depth H_{tot}.

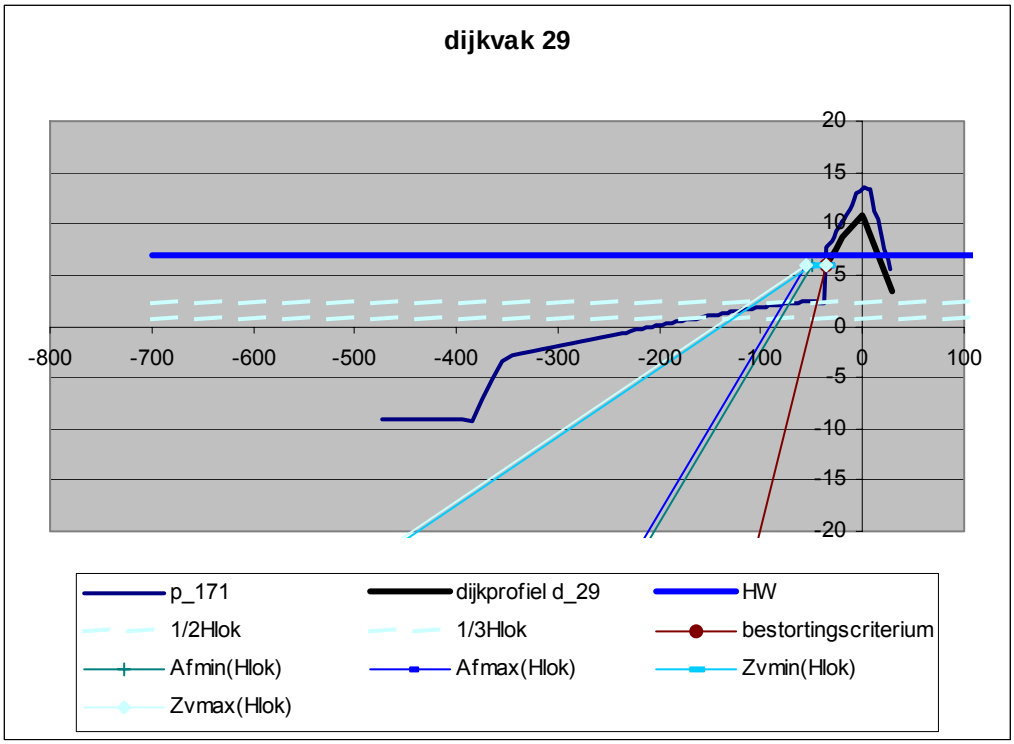

a) local trough depth

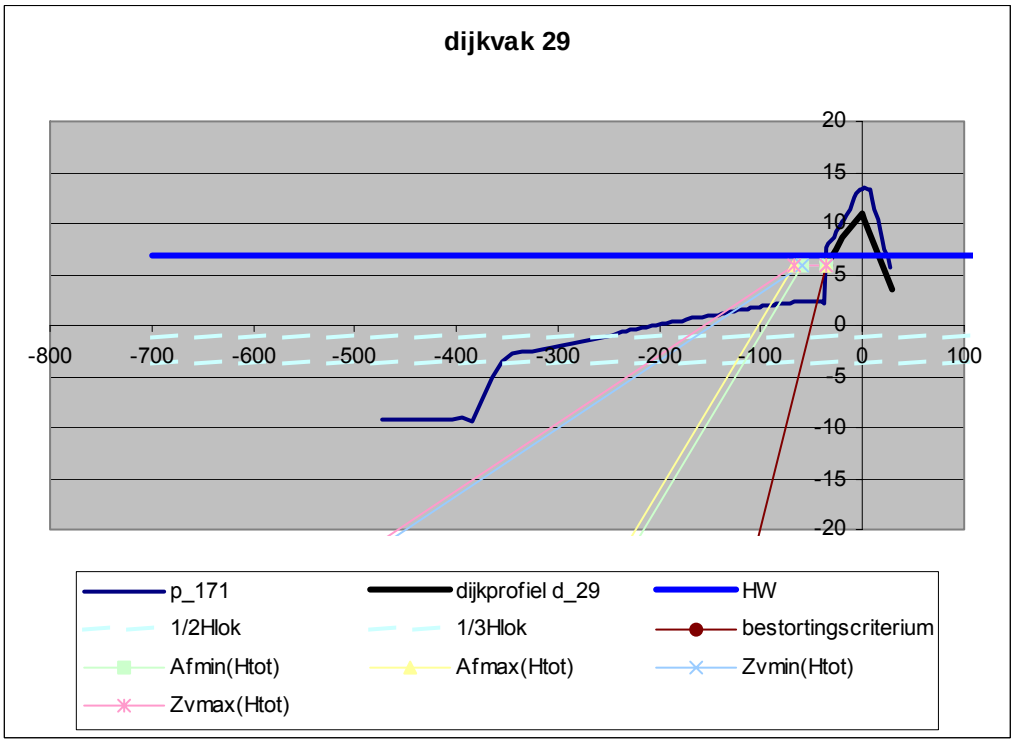

b) total trough depth

Figure 99 Covering, liquefaction and sliding criteria of dike section d_29: (a) local trough depth H_{loc}, (b) total trough depth H_{tot}.

Overview:

profiel	H_{loc}					H_{tot}				
	H_{loc} [m]	$H_{loc}/2$ [m]	$H_{loc}/3$ [m]	peil $H_{loc}/2$	peil $H_{loc}/3$	H_{tot} [m]	$H_{tot}/2$ [m]	$H_{tot}/3$ [m]	peil $H_{tot}/2$	peil $H_{tot}/3$
d_8	14.70	7.35	4.90	-0.42	-2.87					
d_9	14.73	7.37	4.91	-0.44	-2.89					
d_12	18.48	9.24	6.16	-2.31	-5.39					
d_17	13.10	6.55	4.37	0.38	-1.80					
d_20	10.74	5.37	3.58	1.56	-0.23	32.19	16.10	10.73	-9.17	-14.53
d_21	10.55	5.28	3.52	1.66	-0.10	30.06	15.03	10.02	-8.10	-13.11
d_22	10.53	5.27	3.51	1.67	-0.09	26.91	13.46	8.97	-6.53	-11.01
d_23	10.78	5.39	3.59	1.54	-0.26	26.12	13.06	8.71	-6.13	-10.48
d_24	10.79	5.40	3.60	1.54	-0.26	25.41	12.71	8.47	-5.78	-10.01
d_25	9.37	4.69	3.12	2.25	0.68	24.65	12.33	8.22	-5.40	-9.50
d_26	9.74	4.87	3.25	2.06	0.44	20.68	10.34	6.89	-3.41	-6.86
d_28	9.44	4.72	3.15	2.21	0.64	19.22	9.61	6.41	-2.68	-5.88
d_29	9.46	4.73	3.15	2.20	0.62	16.07	8.04	5.36	-1.11	-3.78

Table 24 Overview of local/total trough depths.

Profile	local trough depth	total trough depth
d_8		OK
d_9		OK
d_12		OK
d_17		OK
d_20	OK	OK
d_21	OK	not OK for liquefaction
d_22	not OK(*)	OK
d_23	not OK(*)	OK
d_24	not OK(*)	OK
d_25	not OK(*)	OK
d_26	OK	OK
d_28	OK	OK
d_29	not OK(*)	OK

Table 25 Geometric assessment of sliding/liquefaction of the foreshore

(*) due to lack of information about the precise location of the 'hard' dike core under the dune sand, no well-founded conclusion can be given about the sliding- or liquefaction-sensitive behaviour of the local trough, based on the geometric assessment. Also, the erosion hole in the figures above will not necessarily occur in the manner shown.

With regard to VNK dike section 21, it must be noted that the dike profile of the VNK dike section and the corresponding Jarkus profile do not match.

8.5.2. Sliding of outer slope

For sea dikes the score for sliding at low outer water is 'good' if the dike has a berm or foreshore at least on the N.A.P. level, as well as an outer slope gentler than or equal to 1:3. In addition, the dike must meet the requirements of figure 4.3.3.2 (LTV, 1999). In all other cases, no decisive conclusion is

possible; further research is needed (stability programme) . The calculations were made by means of the SLOPE/W programme.

this could in reality be the course of the “hard” dike so that an erosion hole cannot develop

Dutch	English
harde constructie	hard construction

Figure 100 Diagram of non-erodable profile.

The output of the DUROSTA calculations (eroded beach profiles) is used in the SLOPE/W stability programme. Assuming a 'vertical' wall for the dike assumed non-erodable in the erosion calculations, an erosion hole occurred just in front of the 'hard' construction with various profiles, which could not occur in reality, because a section of 'hard' dike (toe), covered with sand, may be located at the position of the erosion hole. This erosion hole adversely affects the calculations of the outward macrostability, as the most critical slip surface is always found around the erosion hole and as the presence of the hole influences the safety coefficient of other slip surfaces. In the calculations it was assumed that the formation of an erosion hole cannot occur (toe construction/in-situ cohesive material) and the non-erosion of the in-situ cohesive material on the seaward edge of the dike was taken into account.

With regard to the composition of the dike core (sand as opposed to clay), the documents concerning ‘Assessment Dike Ring 32’ (‘Toetsing Dijkring 32’) show contradictory information. An overview table for piping shows that the dikes are of type 2 (sand). An overview table for stone pitching shows that there is no clay core (although there may be a layer of clay, e.g. 0.8m thick). A tabled called ‘inwinspreadsheet VNK 5-3-dijkring 32’ indicates a sandy core (no clay core). An overview table for microstability shows a sandy core or clay core, depending on the location.

The reinforcement works were made using sand. ‘Old’ dikes in the profile cannot be simply assumed to consist of clay (e.g. a clay top layer may be present). Also, part of the ‘old’ dikes was replaced with sand when the reinforcement works were carried out. Consequently, the composition of the dike is uncertain.

For the calculations it is assumed that the dike consists of sand: considering the uncertainty, the calculations use a relatively small internal friction angle for sand (27.5°). Under this assumption the position of the dike in the total profile for the stability calculation is not important (assuming an internal friction angle of 27.5° for beach and dike sand). Average values were assumed for the (other) ground resistance characteristics.

If clay dike cores would actually be present, the (unknown) location (to the front or rear of the overall profile) is important. It could then be assumed that it is at the most disadvantageous position with respect to the outward stability, i.e. on the seaward side of the sand dike. Assuming a saturated clay dike, the low shear resistance and the water pressures cause instability.

With regard to the uncertain composition and location of the dike cores, the reliability of the result of the stability calculations is largely determined by the assumptions, simplifications and extrapolation. The results give an indication of weaknesses in the coastal defence line. The values in the table, however, should not be used to define a 'safety level'. Using the available data, it is not possible to predict which dike will fail when. The odds of being wrong are greater than the odds of being right.

For the phreatic level in the dike the average of the highest water level and the subsequent low water level was calculated. The following phreatic levels in the dikes were thus considered.

return period	phreatic level (m TAW)
1000 years	4.47
4000 years	4.86
40000 years	5.41

Table 26 Phreatic level in dike.

The stability calculations did not take into account traffic loads.
Based on the eroded profiles, stability calculations were made for a number of (critical) dike sections, in first instance for a return period of 40000 years.

For dike sections d_9 (profile 1282), d_23 (336), d_25 (308), d_26 (271) and d_28 (188) there is only a limited failure in the immediate vicinity of the toe. These failures are not considered problematic (the modelling did not take into account the revetment; there is also the effect of the assumed phreatic level).

Safety coefficients ('FS') larger than 1 were obtained for the following dike sections:

dike section/profile no.	FS
d_20 (421)	1.86
d_21 (413)	2.26
d_29 (171)	1.73

Table 27 Safety coefficients (40000 y) for d_20, d_21, d_29.

Profile 496 (d_17) gives the following safety coefficients for the 40000-year and 4000-year return periods:

prof. 496 (d_17)	FS
40000 years	0.87
4000 years	1.11

Table 28 Safety coefficients for profile 496 (d_17).

For a return period of 40000 years the slip circle corresponding with a safety coefficient 1.00 is also given in the figures. For a 40000-year return period, failure is assumed for profile 496. Taking into account the time of exposure (erosion of the overlying sand) of the profile around the first peak, failure is assumed at the second peak of the storm (approximative).

Profiel 512 (d_17) gives the following safety coefficients for the 40000-year and 1000-year return periods:

prof. 512 (d_17)	FS
40000 year	0.66
1000 year	1.09

Table 29 Safety coefficients for profile 512 (d_17).

For a return period of 40000 years the slip circle corresponding with a safety coefficient of 1.00 is also given in the figures. No failure is assumed for the 1000-year return period. Taking into account the time of exposure (erosion of the overlying sand) of the profile around the first peak for the 40000-year return period, failure is assumed at the second peak of the storm and for the 4000-year return period at the third peak of the storm (considering the exposure of the dike profile around the second peak). For profile 530, analogous with profile 512, the failures are considered identical.

Profile 373 (d_22) has similar erosion erosion profiles for the return periods of 1000 years, 4000 years and 40000 years. The slip circle corresponding with a safety coefficient of 1.00 is shown in the figures (already a more limited failure with a smaller FS). Taking into account the exposure of the dike profile around the first peak and the failure of the stone pitching, failure is assumed for the three return periods at the second peak of the storm.

Profile 396 (d_22) has similar erosion profiles for the return periods of 1000 years, 4000 years and 40000 years. The slip circle corresponding with a safety coefficient of 1.00 is shown in the figures (already a more limited failure with a smaller FS). Taking into account the exposure of the dike profile around the first peak for the return periods of 40000 years and 4000 years, failure is assumed at the second peak, for the 1000-year return period the dike profile is exposed around the second peak and failure is assumed from the third peak onwards.

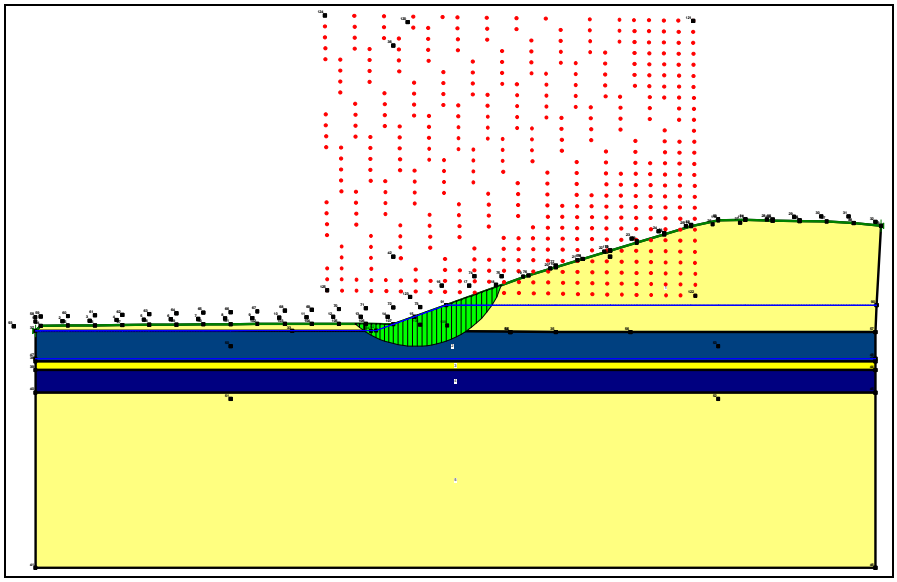

Figure 101 Outward macrostability d_17 (496) ***FS= 0.87***

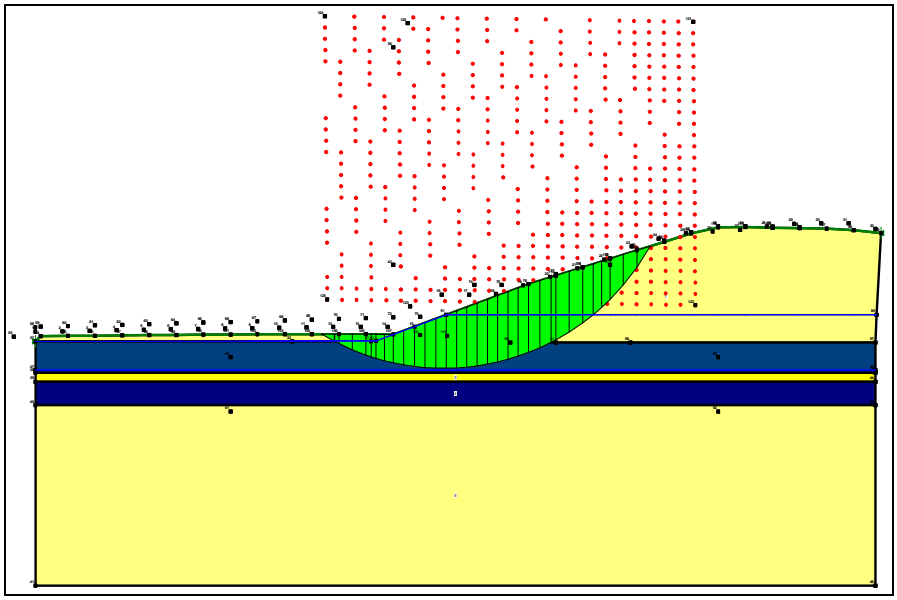

Figure 102 Outward macrostability d_17 (496) ***FS= 1.00***

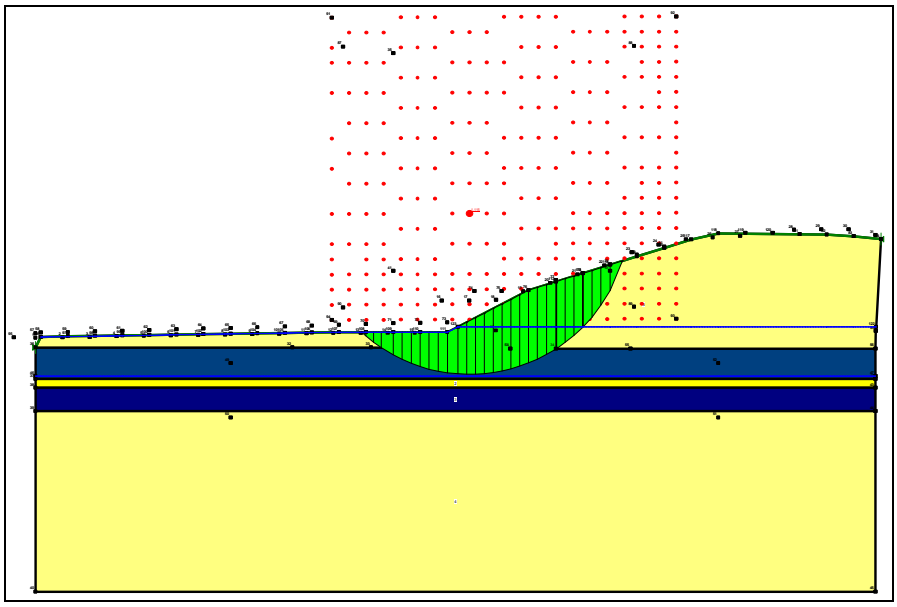

Figure 103 Outward macrostability d_17 (496) 4.000j ***FS= 1.11***

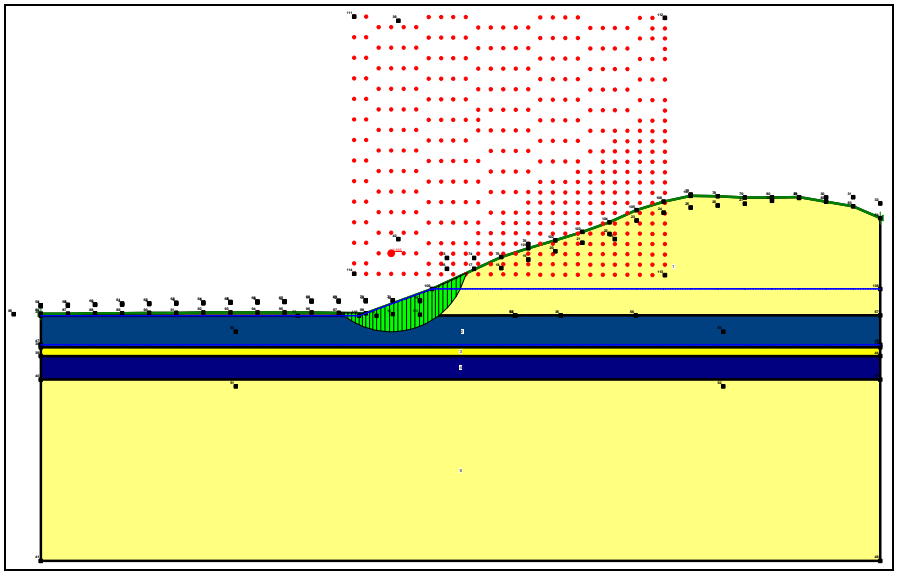

Figure 104 Outward macrostability d_17 (512) ***FS= 0.66***

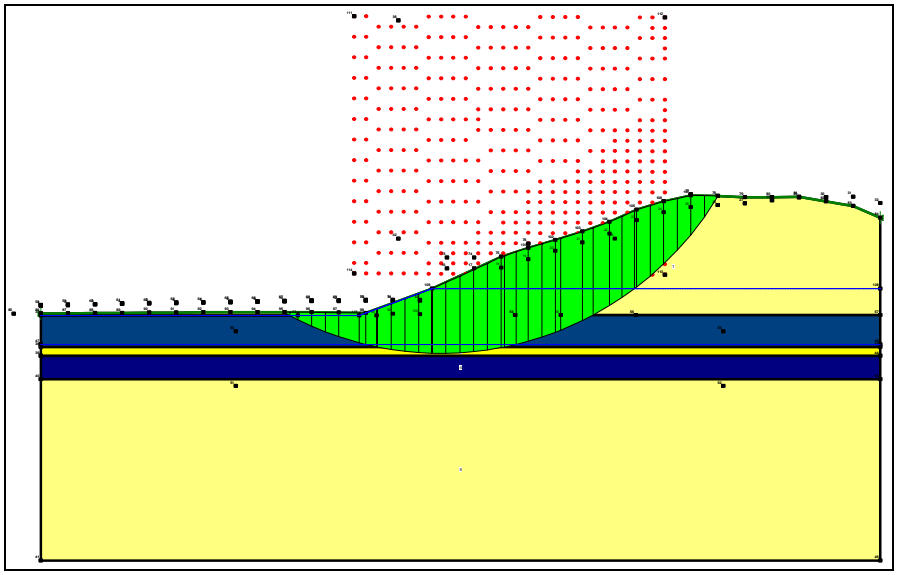

Figure 105 Outward macrostability d_17 (512) ***FS= 1.00***

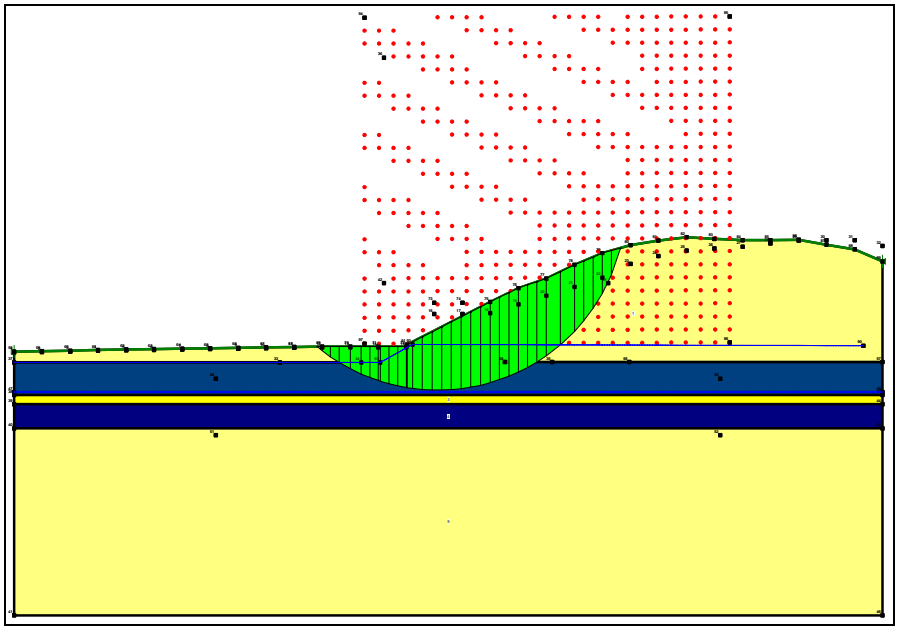

Figure 106 Outward macrostability d_17 (512) 1000j ***FS= 1.09***

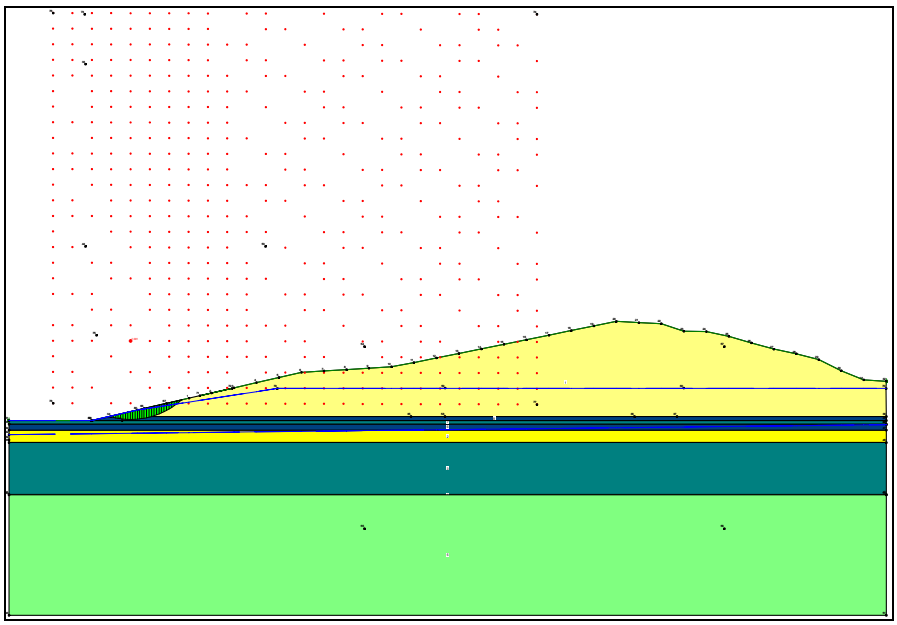

Figure 107 Outward macrostability d_24 (324) ***FS= 1.00***

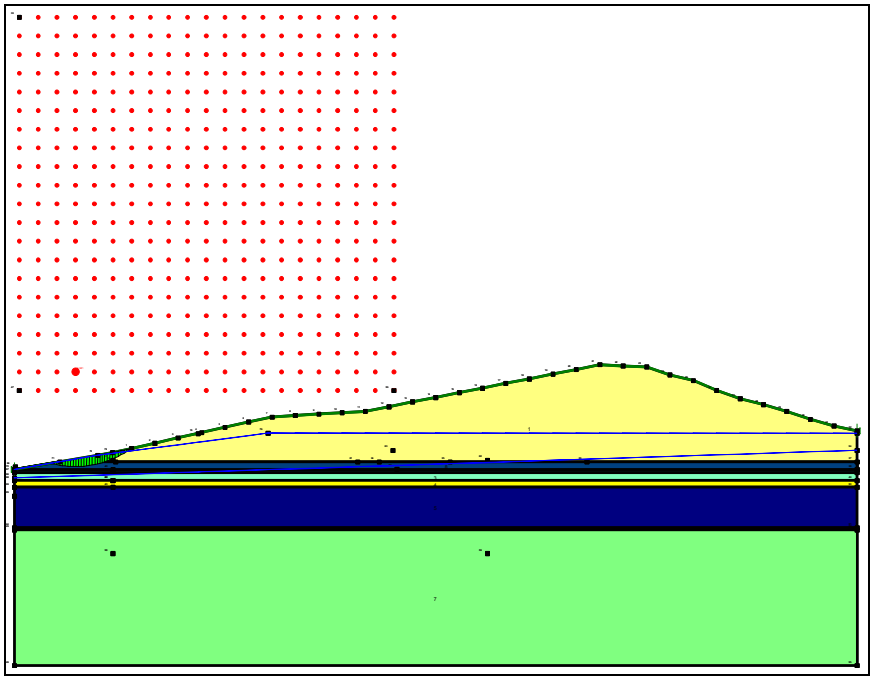

Figure 108 Outward macrostability d_25 (308) ***FS= 1.00***

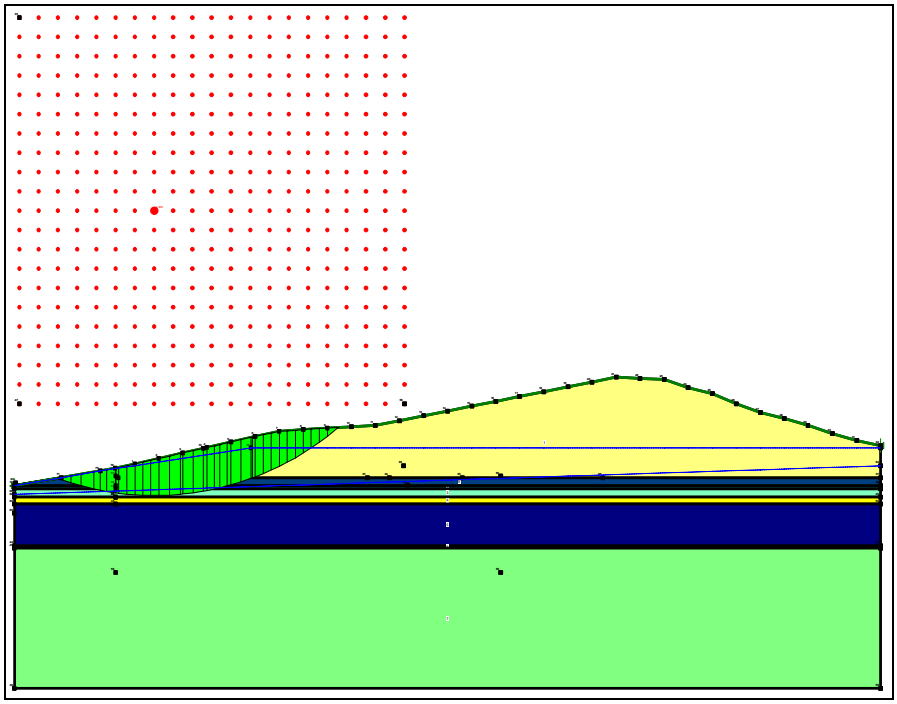

Figure 109 Outward macrostability d_25 (308) ***FS= 1.30***

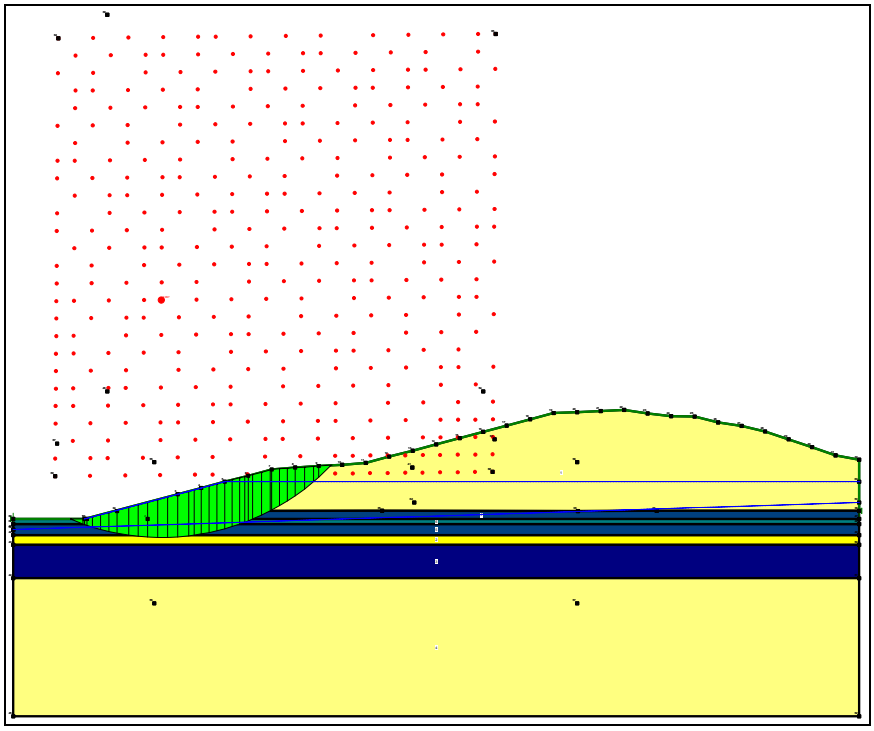

Figure 110 Outward macrostability d_22 (373) ***FS= 1.00***

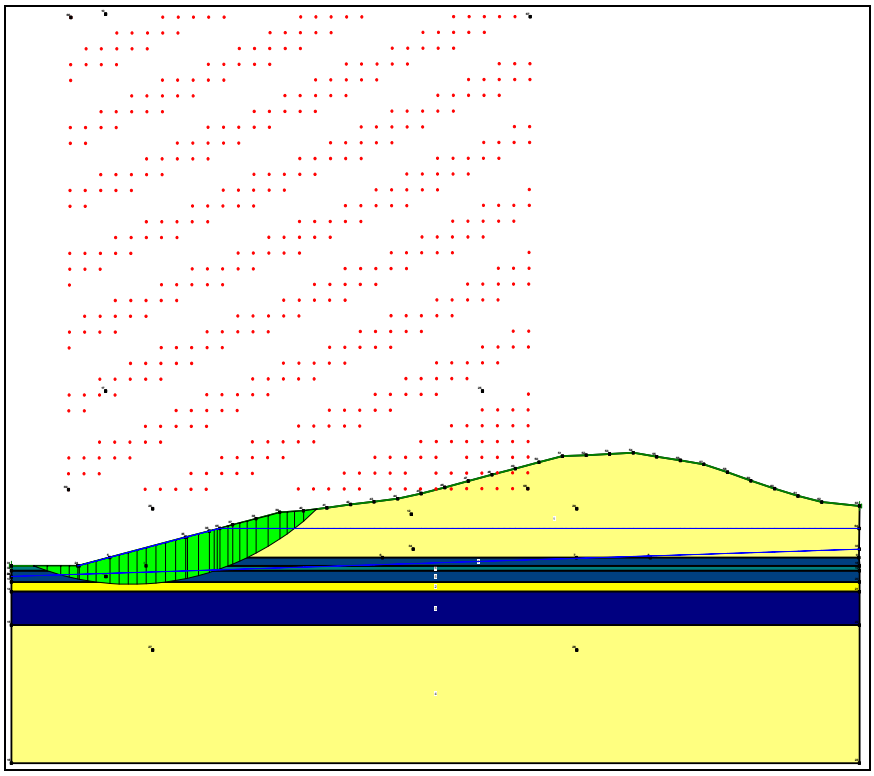

Figure 111 Outward macrostability d_22 (396) ***FS=1.00***

8.6. Inward macrostability (landward slope)

In first instance, a geometric assessment is made whereby the assumption is made that the dikes are of type 1 (clay core). For type 1 f_k must be read from graph X1 (LTV, 1999) and f_a from graph X3 (LTV, 1999).

For sea dikes: k = 2 m.

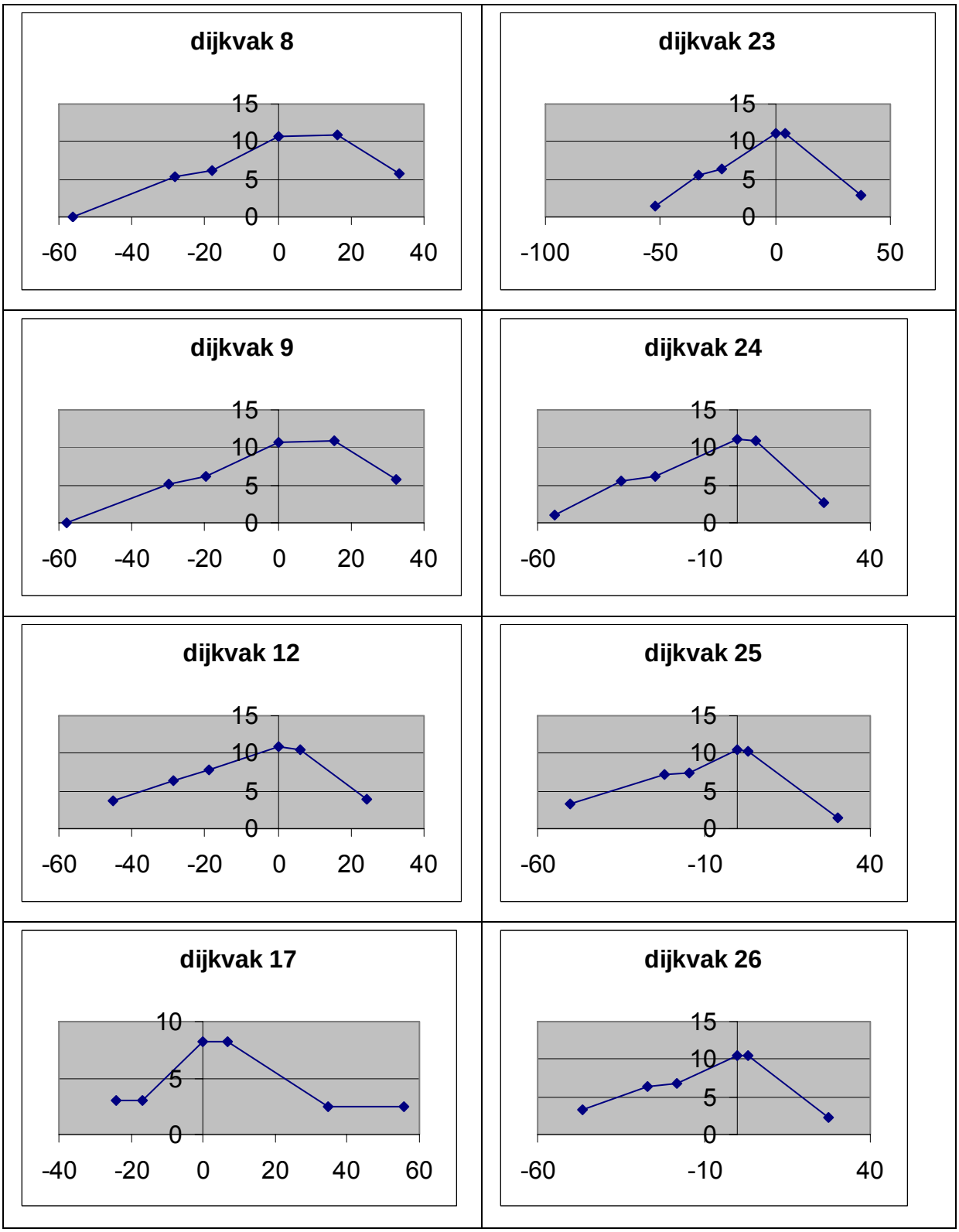

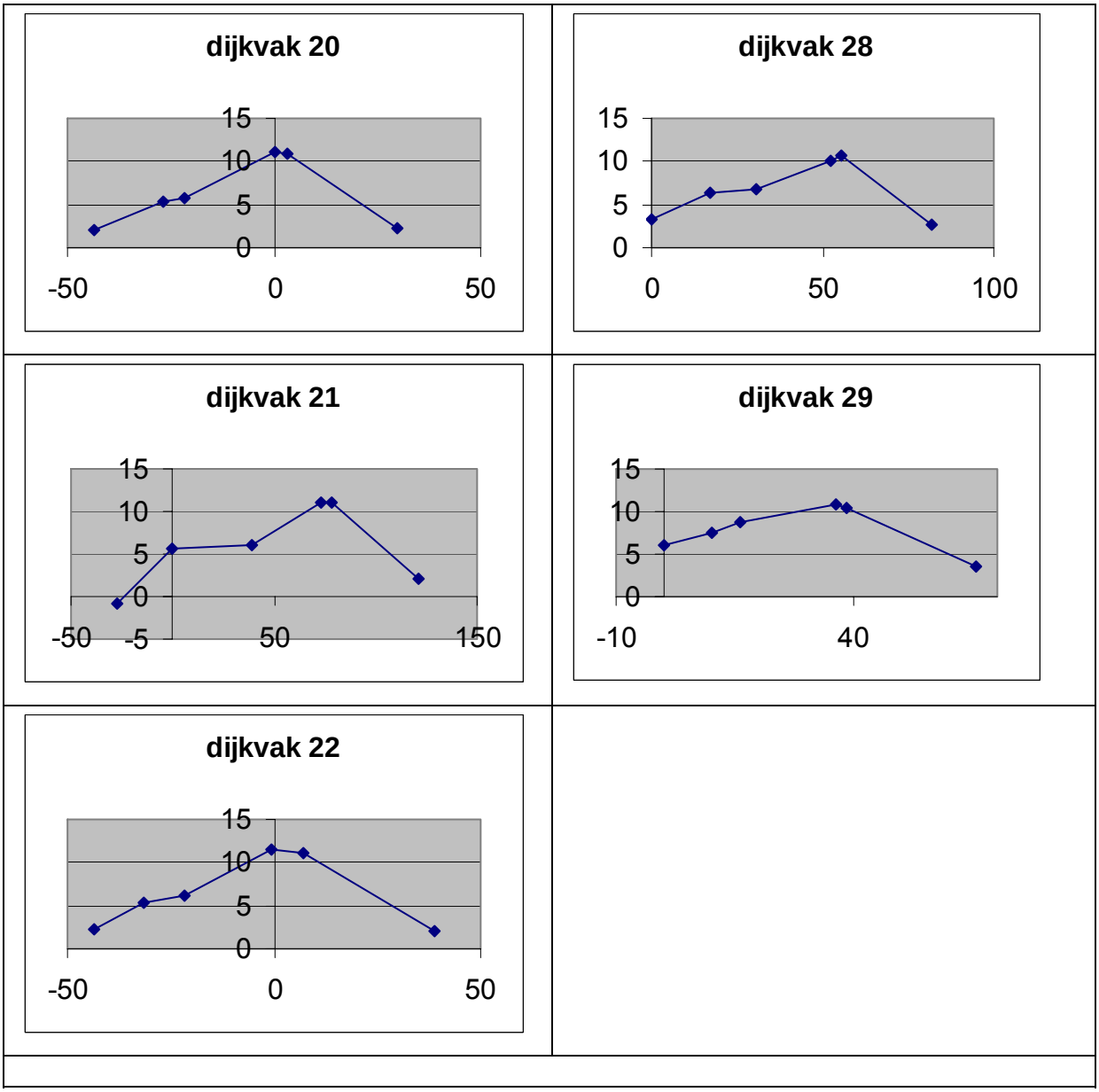

Figure 112 VNK dike sections (dijkvakken)

Dike section	tan α [-]	1:n	D [m]	H [m]	D/H [-]	f_k [-]	f_a [-]	f_k * H [-]	f_a * H [-]	o.w. (dike) [m]	o.w. (core) [m]	o.w. > f_k*H
d_8	0.31	3.2	-	9.00	-							
d_9	0.30	3.3	-	8.75	-							
d_12	0.37	2.7	-	8.95	-							
d_17	0.21	4.8	5.58	5.28	1.06	0	1.5	0	7.92	42	4.92	OK
d_20	0.32	3.1	5.69	9.14	0.62	0.25	0.9	2.29	8.23	1.04	1.04	NOK
d_21	0.21	4.8	6.23	8.96	0.70	2.2	1.6	19.71	14.34	5.5	6.04	NOK
d_22	0.29	3.4	6.28	10.14	0.62	0	0.6	0	6.08	13	6.04	OK
d_23	0.25	4.0	8.36	8.98	0.93	0	1.3	0	11.67	3	2.15	OK
d_24	0.40	2.5	8.11	9.28	0.87	1.3	1.8	12.06	16.70	3	3.48	NOK
d_25	0.33	3.0	6.41	8.92	0.72	0.4	1.1	3.57	9.81	3	1.29	NOK
d_26	0.33	3.0	4.71	7.25	0.65	0.3	1.0	2.18	7.25	12	1.26	OK
d_28	0.30	3.3	7.95	8.38	0.95	0.5	1.6	4.19	13.41	35.5	1.11	OK
d_29	0.26	3.8	5.61	8.58	0.65	0	0.5	0	4.29	5.5	0.36	OK

Table 30 Basic assessment of macrostability of landward slope.

None of the profiles has a berm. Consequently, type 1 is certainly safe if n > 5. This is not the case for any dike. Thus it must be examined whether the overwidth > f_k * H and A > f_a * H. As no information is available for distance A, a conclusion is not possible. A is the length for which a flat ground level must be present. Within this length a berm ditch may be present.

Both for the sand dike (core + sand cover) and for the dike core, the overwidth assessment was made. Dikes with an 'OK' final assessment are given a 'sufficient' final assessment right away. For the other dikes another assessment path must be followed, based on the design method. As the design method used is not known, the dikes are given a '-' assessment (geotechnical research is necessary). Of the dikes with an 'NOK' score, only profile d_25 2 has different dike profiles: 308 and 290. However, p_290 is not more advantageous than p_308 so that d_25 is definitely given the score 'NOK'.

For profile 308 (d_25) a **FS of 1.43** is obtained, assuming a sand dike (angle of internal friction 27.5°) and a normative (high) outer water level for the 40000-year return period by means of a SLOPE calculation.

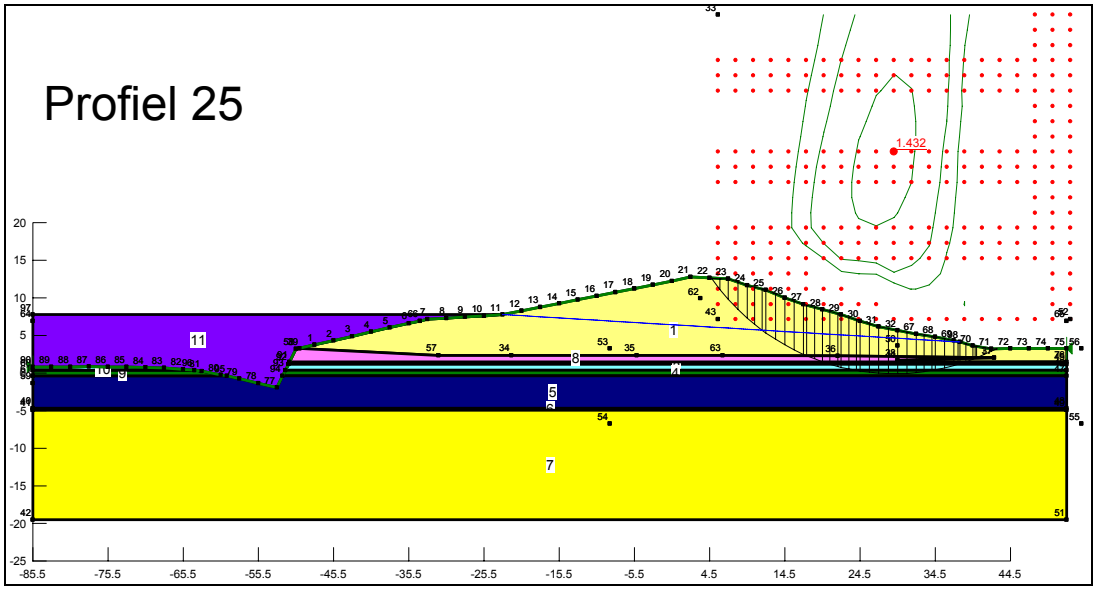

Figure 113 Inward macrostability d_25 (profile 308) ***SF= 1.43***

8.7. Microstability

The results of the 'Assessment Dike Ring 32' ('Toetsing Dijkring 32') show that for the dikes in question:

- there is no certainty that all dikes have an impermeable clay core;
- it may be assumed that the dike has not been subjected to an (almost) normative load;
- the inner toe of the dike has a properly functioning drainage construction.

Consequently, the dikes are given a 'good' score.

8.8. Condition of the revetment

8.8.1. Stone pitching

When assessing the stone pitching, it was assumed that the calculated wave height at the toe of the dike, as given in Table 20, may have an effect on the entire (height of the) stone pitching (also if the stone pitching is lower than the highest still water level). The peak wave periods considered here are given in Table 31.

	1000 year	**4000 year**	**40000 year**
T_p (s)	12	12.5	13.1

Table 31 Peak wave periods for the considered return periods.

Considering the relatively low position of the stone pitching on the slope, this revetment is always at least partially below the 'assessment level + 0.5 H_s' level.

When assessing the stability of the top layer on the outer slope, it was assumed that the normative wave load and strong current on the outer slope do not coincide, allowing a separate assessment of both.

Table 32 indicates the result of the basic assessment of the top layer stability under wave impact for the different return periods. Where the result is 'good' or 'unsufficient', this is the final score for the criterion of top layer stability under wave impact (in case the answer to the question as to the 'good behaviour' is not no). If this basic assessment gives a 'doubtful' result, the further procedure (analytical method, advanced assessment) must be followed. According to the results of the Dutch assessment, there is no experience with space between the top layer and the filter material of the stone pitching.

Table 32 also indicates where the stone pitchings are located on the different profiles (information from the 'Assessment Dike Ring 32' ('Toetsing Dijkring 32') and from digital information obtained from the Water Board Zeeuws-Vlaanderen ('Waterschap Zeeuws-Vlaanderen', 'bekleding3d' file). This information was not always consistent (e.g. with regard to the upper and lower limits of the stone revetment). The analysis was made for the different Jarkus profiles. For profiles 421, 441, 483, 802, 877, 886, 903, 1046 no information is available regarding a possible stone revetment. Profile 1354 is located at a transition point between dike and dune. There is not a 100% consistency between the asphalt levels in Table 35 and the stone pitching levels of Table 32 (in Table 32, by means of the location of the asphalt revetments, the upper levels were adjusted where necessary, as to prevent having both an asphalt revetment and stone pitching on the same level for the same profile).

profile no.	lower level stone pitching (m NAP)	upper level stone pitching (m NAP)	top layer stability wave impact 1000 years	top layer stability wave impact 4000 years	top layer stability wave impact 40000 years
171	1	7.3	g	g	g
188	4.1	5.6	g	g	g
271	0	4	g	g	g
290	-0.3	4	g	g	g
308	-0.4	4	o	o	o
324	-0.4	4	o	o	o
336	0	4	g	g	g
352	0	4	g	g	g
373	0	4	o	o	o
396	0	4	o	o	o
413	0	4	o	o	o
496	0.5	3	g	g	g
512	0.5	3	o	o	o
530	-0.5	3	o	o	o
558	0	3	o	o	o
584	1	3	o	o	o
602	1	3	g	g	g
619	1	3	o	o	o
638	1	3	g	t	o
663	1	3	o	o	o
684	0.6	3	o	o	o
705	0.8	3	o	o	o
730	0.5	3	g	g	g
751	-0.4	3	g	g	g
768	-0.5	3	g	g	g
778	-0.5	3	g	g	g
791	-0.5	3	g	g	g
920	1	3	g	g	g
936	1	3	g	t	o
951	1	3	g	g	g
962	1	3	g	g	t
979	1	3	g	g	g
985	1	3	g	g	g
993	1.5	3	g	g	g
1007	1.5	3	g	g	g
1021	1.5	3	g	g	g
1032	1.5	3	t	t	t
1282	0	3	g	g	g
1300	0	3	o	o	o
1318	0	3	o	o	o
1335	0	3	o	o	o

Table 32 Result of the basic assessment of the top layer instability under wave impact.

whereby

‘g’ : ‘good’;

‘o’ : ‘unsufficient’;

‘t’ : ‘doubtful’.

Table 33 shows the result of the basic assessment of the top layer stability under current attack for the different return periods. Where the result is 'good' or 'unsufficient', this is the final score for the criterion of top layer stability under current attack (in case the answer as to 'good behaviour' is not no). If this simple assessment gives a 'doubtful' result, the advanced assessment must be followed.

profile no.	lower level stone pitching (m NAP)	upper level stone pitching (m NAP)	top layer stability current attack 1000 years	top layer stability current attack 4000 years	top layer stability current attack 40000 years
171	1	7.3	g	g	g
188	4.1	5.6	g	g	g
271	0	4	g	g	g
290	-0.3	4	t	o	o
308	-0.4	4	o	o	o
324	-0.4	4	o	o	o
336	0	4	g	g	g
352	0	4	g	g	g
373	0	4	o	o	o
396	0	4	o	o	o
413	0	4	o	o	o
496	0.5	3	g	g	g
512	0.5	3	o	o	o
530	-0.5	3	o	o	o
558	0	3	o	o	o
584	1	3	o	o	o
602	1	3	g	g	g
619	1	3	o	o	o
638	1	3	g	o	o
663	1	3	o	o	o
684	0.6	3	o	o	o
705	0.8	3	o	o	o
730	0.5	3	g	g	g
751	-0.4	3	o	o	o
768	-0.5	3	g	g	g
778	-0.5	3	t	t	t
791	-0.5	3	g	g	g
920	1	3	g	g	g
936	1	3	t	o	o
951	1	3	g	g	g
962	1	3	t	t	o
979	1	3	t	t	t
985	1	3	t	t	t
993	1.5	3	t	t	g
1007	1.5	3	t	t	g
1021	1.5	3	t	t	t
1032	1.5	3	o	o	o
1282	0	3	o	o	o
1300	0	3	o	o	o
1318	0	3	o	o	o
1335	0	3	o	o	o

Table 33 Result of the basic assessment of the top layer instability under current attack.

whereby

‘g’ : ‘good’;

‘o’ : ‘unsufficient’;

‘t’ : ‘doubtful’.

In the ‘Assessment Dike Ring 32’ (‘Toetsing Dijkring 32’) a significant part of the stone pitchings received an ‘unsufficient’ final score and were consequently included in the ‘Sea Defence Improvement Project’ (‘Project Zeeweringen verbeteringsbestekken’) in this regard. Any improvements from these works were not taken into account in this study.

With regard to the ‘sliding’ criterion, the diagram of **Figure 38** is followed. As it is unclear whether or not the revetment and granular layer are located directly on the clay core of the dike, a decisive conclusion cannot be reached with regard to this criterion. According to the results obtained from the Dutch assessment, there is no experience with sliding. According to LTV (1999), the following satisfactory condition applies for a ‘good’ score: a slope not steeper than 1:4 and no observation of geotechnical instability at previous wave loads.

With regard to the criteria of ‘material transport from the subsoil’ and ‘material transport from the granular layer’, a decisive conclusion cannot be reached without knowing the composition of the subsoil. However, it is important that there is no experience with material transport according to the results obtained from the ‘Assessment Dike Ring 32’.

Considering the ‘unsufficient’ score for top layer stability under wave impact and/or current attack, failure is assumed for the following profiles. For these profiles the residual strength of the dike body is assessed under ‘erosion of dike body’.

profile no.	40000 years	4000 years	1000 years
290	X	X	
308	X	X	X
324	X	X	X
373	X	X	X
396	X	X	X
413	X	X	X
512	X	X	X
530	X	X	X
558	X	X	X
584	X	X	X
619	X	X	X
638	X	X	
663	X	X	X
684	X	X	X
705	X	X	X
936	X	X	
962	X		
1032	X	X	X
1300	X	X	X
1318	X	X	X
1335	X	X	X

Table 34 Failure of stone pitching for the different return periods.

With regard to profiles 936 and 962, it must be noted that the stone pitchings in fact do not fail, as they are not exposed to the wave actions. For profiles 751 and 1282 the residual strength of the dike body largely suffices, considering the limited significant wave height.

8.8.2. Asphalt revetment

According to the 'Assessment Dike Ring 32', asphalt revetments are located at the following profiles (all type 1, lower slope, flat berm, upper berm):

profile no.	lower slope	flat berm	upper berm	
	lower level (m NAP)	lower level (m NAP)	lower level (m NAP)	upper level (m NAP)
271	4	5.6	6.3	7.5
290	4	5.6	6.3	7.5
308	4	5.6	6.3	7.5
324	4	5.6	6.3	7.5
336	4	5.6	6.3	7.5
352	4	5.6	6.3	7.5
373	4	5.6	6.3	7.5
396	4	5.6	6.3	7.5
413	4	5.6	6.3	7.5
496	3	5.6	6.3	7.5
512	3	5.6	6.3	7.5
530	3	5.6	6.3	7.5
558	3	5.6	6.3	7.5
584	3	5.6	6.3	7.5
602	3	5.6	6.3	7.5
619	3	5.6	6.3	7.5
638	3	5.6	6.3	7.5
663	3	5.6	6.3	7.5
684	3	5.6	6.3	7.5
705	3	5.6	6.3	7.5
730	3	5.6	6.3	7.5
751	3	5.6	6.3	7.5
768	3	5.6	6.3	7.5
778	3	5.6	6.3	7.5
920	3	5.6	6.2	7.5
936	3	5.6	6.2	7.5
951	3	5.6	6.2	7.5
962	3	5.6	6.2	7.5
979	3	5.6	6.2	7.5
985	3	5.6	6.2	7.5
993	3	5.6	6.2	7.5
1007	3	5.6	6.2	7.5
1021	3	5.6	6.2	7.5
1032	3	5.6	6.2	7.5
1046	3	5.6	6.2	7.5
1300	3	5.6	6.2	7.5
1318	3	5.6	6.2	7.5
1335	3	5.6	6.2	7.5

Table 35 Location of asphalt revetment.

The significant wave height considered in the wave impact assessment is the (maximum) significant wave height at the toe of the dike (conservative assumption).

When

Figure 114 (VTV, 2004) is used to determine the layer thickness needed for the wave impact (hydraulic engineering asphalt concrete), it must be determined which subsoil is present. Considering the uncertainty about the composition of the dike core, it is assumed conservatively that the subsoil consists of clay.

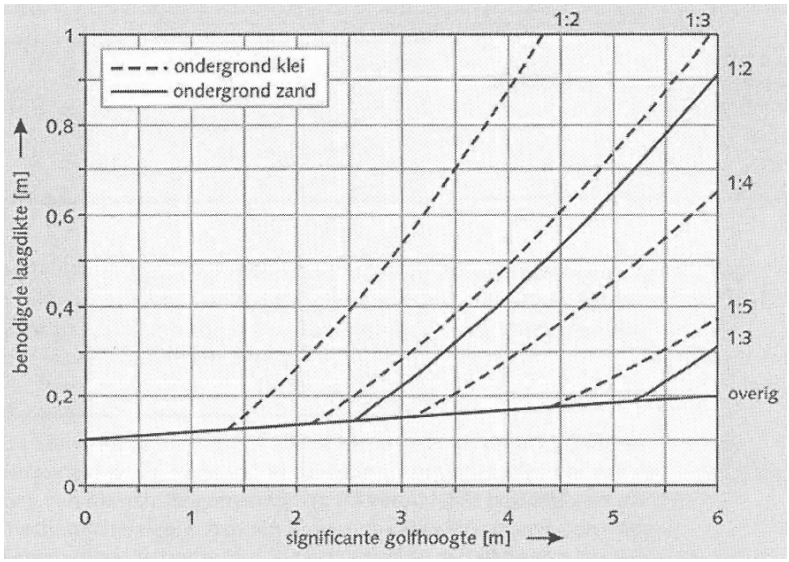

Dutch	English
benodigde laagdikte	required layer thickness
significante golfhoogte	significant wave height
ondergrond klei	clay base
ondergrond zand	sand base

Figure 114 Basic wave impact assessment.

When considering the profiles with asphalt revetment, the largest significant wave heights in a storm with a 40000-year return period are obtained for the following profiles:

Profile nr.	$H_{s,40000}$ [m]	$D_{required}$ [m]
373	3.01	0.15
413	3.41	0.19

Table 36: necessary asphalt layer thickness for largest wave heights.

To assess the layer thickness under wave impact, the layer thicknesses that are given in the 'Assessment Dike Ring 32' are assumed present. It can be deduced that the minimum layer thickness present is 0.20 m. Consequently, the layer thickness required for wave impact is present in accordance with the basic method. It can be deduced from the 'Assessment Dike Ring 32' that a significant part of the profiles received a 'doubtful' score during visual inspection. Advanced assessment is thus needed.

Advanded assessment is needed for the material transport criterion, when visual inspection results in a 'doubtful' score.

8.8.3. Erosion of dike body

In case of the 'revetment damage and dike body erosion' mechanism, the dike fails because the revetment is first damaged by the wave impact; the cross section of the dike core is then reduced by erosion.

It is assumed that the stone pitchings giving an 'unsatisfactory' score for the assessment of top layer stability under wave impact/current attack, fail. Considering the satisfactory scores of asphalt thickness for wave impact and considering that advanced assessment is needed to reach a decision, no initial failure of the asphalt revetments is assumed.

The occurrence or non-occurrence of failure due to erosion, will depend on the entire water level and wave height course, after failure of the revetment. The erosion model mentioned in Theory Manual

PC-Ring (version 4.0, 2003 TNO report 2003-CI-R0020, April 2003) does not take into account the full course water level and wave height.

Two models are proposed in PC-Ring for calculating the residual strength of the dike core. The 'erosion model without mixing' whereby the erosion is not influenced by mixing of the dike core and revetment. In the other model, the so-called 'rudimentary erosion model', mixing of the dike core and revetment is assumed.

As the residual strength of the failed stone pitching can be considered 0, considering the fact that the formula for the residual strength of a covering top layer is similar to that of the 'erosion model without mixing', considering the uncertain composition of the dike core and considering that only 1 type of revement can be assumed per slope with the 'rudimentary erosion model', the residual strength of the dike core was calculated in this report by means of the formula for the residual strength of the dike core mentioned in PC-Ring, in accordance with the 'erosion model without mixing'.

As to the level on which the width of the dike core is considered, the value of the upper level of the (failing) stone pitching was used, except where the top of the stone pitching is higher than the normative water level – $0.25.H_s$ (the normative water level – $0.25.H_s$ was considered there to determine the width of the dike core). The level on which the width of the dike core is considered, is called the 'failure level' in the tables below.

As the eroding effect of waves is also felt on levels above or below the still water level (depending on wave height and wave run-up), considering the varying water level, the simplified assumption was made that the wave heights mentioned, after failure of the stone pitching, act on the dike core for the entire remaining duration of the storm and thus sollicit the residual strength of the dike core for the entire remaining duration of the storm. This is a highly simplified assumption.

Considering the uncertain composition of the dike core, the calculations were made on the basis of a c_{RB} value of 30.10^3 m.s (a c_{RB} value corresponding with mediocre clay and which approximately corresponds with the average of the c_{RB} values for sand and good clay). It can be deduced from the above-mentioned formula that the residual strength linearly depends on the assumed erosion resistance (c_{RB} value) of the core material. This assumption is largely arbitrarily, but it must be seen in the context of the uncertain composition of the dike core (and the corresponding residual strength) and the fact that the detailed water level and wave height course are not taken into account.

VTV (2004) gives the following calculation rule for the residual strength of the top layer and the underlying granular layer for stone pitchings:

$$t_{rg} = 163000 \cdot T_p \cdot \exp\left[-0.74 \cdot \sqrt{H_s \cdot L_{0p}}\right] \cdot \frac{1}{3600}$$

whereby

t_{rg} : residual strength of top layer and granular layer [u];

T_p : peak wave period [s];

H_s : significant wave height [m];

L_{0p} : wave length in deep water related to peak period T_p ($L_{0p} = g.T_p^2/2.\pi$) [m].

The residual strengths obtained in accordance with the formula are negligibly small compared to the residual strengths needed for the failing stone pitchings and are ignored compared to the residual strengths of the dike core. In addition, this residual strength for top layer and granular layer can only be applied under certain conditions (regarding wave height, condition of the top layer elements, sliding, material transport from the subsoil, material transport from the granular layer).

For the storm with a 40000-year return period the following results are obtained, for the profiles for which the stone pitching is exposed.

profile no.	H_s (m)	failure level (m TAW)	L_B (m)	$t_{exposed}$ (h)	$t_{res, 30000}$ (h)	$t_{res, 30000, net}$ (h)
290	0.38	6.4	18	30	415	385
308	1.60	6.3	45	30	59	29
324	1.60	6.3	45	30	59	29
373	3.01	6.5	41	30	15	-15
396	1.95	6.3	45	30	39	9
413	3.41	6.0	40	30	11	-19
512	2.61	5.3	41.5	30	20	-10
530	2.58	5.3	38	30	19	-11
558	2.58	5.3	42	30	21	-9
584	2.44	5.3	44.5	30	25	-5
619	2.25	5.3	60	30	40	10
638	2.07	5.3	53.5	20	42	22
663	2.66	7.1	45	30	21	-9
684	2.64	4.6	41	20	19	-1
705	2.42	5	40.5	20	23	3
1032	1.79	5.3	46.5	30	48	18
1300	1.67	5.3	63	30	75	45
1318	1.58	5.3	69	30	92	62
1335	2.45	5.3	57.5	30	32	2

Table 37 Residual strength calculation of dike core for 40000-year return period.

whereby

$t_{exposed}$: rudimentary determination of the duration of the storm in which the stone pitching is exposed [h];

$t_{res, 30000}$: residual strength of the dike core with c_{RB} = 30000 m.s [h];

$t_{res,30000, net}$: difference between the residual strength of the dike core and the necessary residual strength [h] (negative value indicates that the residual strength of the dike core is insufficient).

For profiles with an insufficient residual strength of the dike core for the 40000-year storm, the assessment was made for the storm with a 4000-year return period (in case of failing stone pitching).

profile no.	H_s (m)	failure level (m TAW)	L_B (m)	$t_{exposed}$ (h)	$t_{res, 30000}$ (h)	$t_{res, 30000, net}$ (h)
373	3.01	6.5	41	30	15	-15
413	3.32	6.0	40	30	12	-18
512	2.32	5.3	41.5	30	26	-4
530	2.35	5.3	45.5	20	28	8
558	2.29	5.3	42	20	27	7
584	2.13	5.3	44.5	30	33	3
663	2.39	6.7	45	20	26	6
684	2.34	4.6	41	20	25	5

Table 38 Residual strength calculation of dike core for 4000-year return period.

For a storm with a 1000-year return period the following profiles fail:

profile no.	H_s (m)	failure level (m TAW)	L_B (m)	$t_{exposed}$ (h)	$t_{res, 30000}$ (h)	$t_{res, 30000, net}$ (h)
373	3.01	6.2	49	30	18	-12
413	3.23	6.0	42	30	13	-17

Table 39 Residual strength calculation of dike core for 1000-year return period.

It must be noted that the assumption of the dike position in the sand profile is important with regard to the time of exposure of the dike profile during the storm.

8.8.4. Grass cover

With regard to the crest and the landward side of the dike, overtopping discharges are obtained in the range from 0 to approx. 2 l/m.s (see Table 20). For profile 1354 located in the transition point between dike and dune, an overtopping discharge of 6.66 l/s.m is obtained with a 40000-year storm. The precise revetment and condition of the revetment on the upper part of the seaward side of the dike, the crest and the landward side of the dike is not known. In Goda (1970, estimation of the rate of irregular overtopping of seawalls, report of port and harbour institute, Vol 9, No 4) the following overtopping discharges (in l/s.m) are mentioned for dikes:

- q < 5 : no damage;
- 5 < q < 20: damage in case of unprotected crest;
- 20 < q < 50: damage in case of unprotected inner slope.

According to reference... ('Rijkswaterstaat, Dienst Weg- en Waterbouwkunde, 1993, Het ontwerpen van een bekleding voor een zeedijk') for an inner slope of 1:3 (good grass mat, guaranteed water drainage, special attention to concentrated water flows), a limit value of 10 l/s.m is assumed (comparable to the transition from 'start of damage' to 'damage' according to reference (CEM, 2001).

Considering the relatively low values of the calculated overtopping discharges and the uncertainty about the revetment, no damage to the (grass) cover is assumed at the upper part of the seaward side of the dike, the crest and the landward side of the dike due to overtopping discharges. Assuming failure of the (crest) revetment and an assumed 5% soil transport of the overtopping discharge, a rather limited eroded volume of 0.6 m^3/h.m would be obtained for an overtopping discharge of 2 l/s.m.

8.9. Conclusions

For the return periods of 1000 years, 4000 years and 40000 years there is no dune erosion problem anywhere.

However, with regard to the dikes, the revetment on a significant part of the profiles does result in a doubtful score (or further research is needed). Failure of a significant number of stone pitchings also occurs, whereby the erosion of the dike body was examined. With regard to the revetments, it is important to take the most recent data into account in future analyses (e.g. improvements made to the stone pitchings).

Due to the uncertain position of the dikes in the Jarkus profiles and the uncertainty about the dike's composition, the results of the dike's seaward macrostability must be considered merely indicatively. For the profiles 373, 396, 496, 512 and 530 the macroinstability of the seaward slope is held (partly) responsible for the profile's failure. A better knowledge of the dike composition is required to reach better-founded conclusions about the macrostability of the dikes and the erosion velocity, for instance.

Dike section 21, profile no. 413 is given a failure score (due to liquefaction). It must be noted that the VNK dike profile and the corresponding Jarkus profile do not match.

For the flood calculations it was assumed that breaches evolve at the following profiles and from the times indicated in Table 40. It must be noted that the time of failure was determined rudimentarily at the top of a peak.

	1000 years		4000 years		40000 years	
profile no.	**breach**	**time of failure**	**breach**	**time of failure**	**breach**	**time of failure**
373	x	top 2nd peak	X	top 2nd peak	x	top 2nd peak
396	x	top 3rd peak	X	top 2nd peak	x	top 2nd peak
413	x	top 2nd peak	X	top 2nd peak	x	top 2nd peak
496					x	top 2nd peak
512			X	top 3rd peak	x	top 2nd peak
530			x	top 3rd peak	x	top 2nd peak
558					x	top 3rd peak
584					x	top 3rd peak
663					x	top 3rd peak
684					x	top 3rd peak

Table 40 Breaches and times of failure.

9. FLOOD MODELLING

9.1. Introduction

This chapter describes the floods due to failure of the seawall between Breskens and Zeebrugge. For the purpose, a series of simulations were carried out which show the consequences of possible failures of the seawall between Zeebrugge and Breskens.
These flood simulations were carried out by means of DHI's MikeFlood (2D model). The model allows the simulation of inundation speeds and water depths as a consequence of dike breaches. The results are used in economic damage calculations and the estimation of the number of possible casualties.

The present chapter gives an exposition on the objectives of the flood model, a comprehensive description of the development of the flood model, an overview of the flood calculations followed by the results.

9.2. Objective and study area

9.2.1. Study area

The study area included in the hydrodynamic 2D model comprises a limited part of the North Sea, including the coast between the port of Zeebrugge and Breskens on Dutch soil. The hinterland extends about 15 km inland.

Figure 115: Situation of the study area[1]

[1] © mappy.com

The study comprises a two-dimensional flood model from Zeebrugge to Breskens for the present situation (2004).

The results are used as basis for the economic damage and casualty calculations (Chapter X) .

The flood model used is developed by means of Mike21. The software consists of various modules. In this project the Mike21 Flow Model will be used for hydrodynamic modelling of the flood areas. For the modelling of dike breaches, Mike Flood will be used, an addition to the model, allowing a link between the 1D-model (Mike11) and the 2D-model (Mike21). This allows simultaneous hydrodynamic simulations, whereby the dike overflow or dike breaches can be calculated by means of the specific formulas available in Mike11.

9.3. Development of the flood model

The flood model is developed in Mike21 Flow Model for currents over land (2D-model) and Mike11 (1D-model) for dike breaches. The 1D- and 2D-model are combined by using the MikeFlood module.

9.3.1. The 2D-model

9.3.1.1. The model grid

The grid consists of rectangular cells. For the area between Zeebrugge and Breskens a model is developed which includes the topography of the area. Considering the extensiveness of the model and a clear relief in the study area, it is recommended to use a grid with a cell size of 20 by 20m.

To limit the calculation time, the model grid can be limited depending on the scenarios. The number of grid cells in the Y-direction (North-South) varies to a maximum of 1125 cells (22,500m). The number of grid cells in the X-direction (East-West) varies to a maximum of 1550 cells (31,000m).

The basic grid uses UTM coordinates (ED50).

9.3.1.2. Topography

The terrain data included in the 2D-model for Flanders are derived from the DTM of WLH-OCGIS Flanders (2003) and from the AHN files for Zeeland Flanders (Actueel Hoogte bestand Nederland 2000, Rijkswaterstaat Meetkundige dienst, Present Height File for the Netherlands 2000, Department of Public Works, Survey Department). The buildings have already been removed from the Flanders DHM for the coastal area.

To make the topography of the 2D-model, the xyz data of the DHM's were interpolated to the model grid of 20 by 20m. A graphic representation of the bathymetry is given in Figure 116.

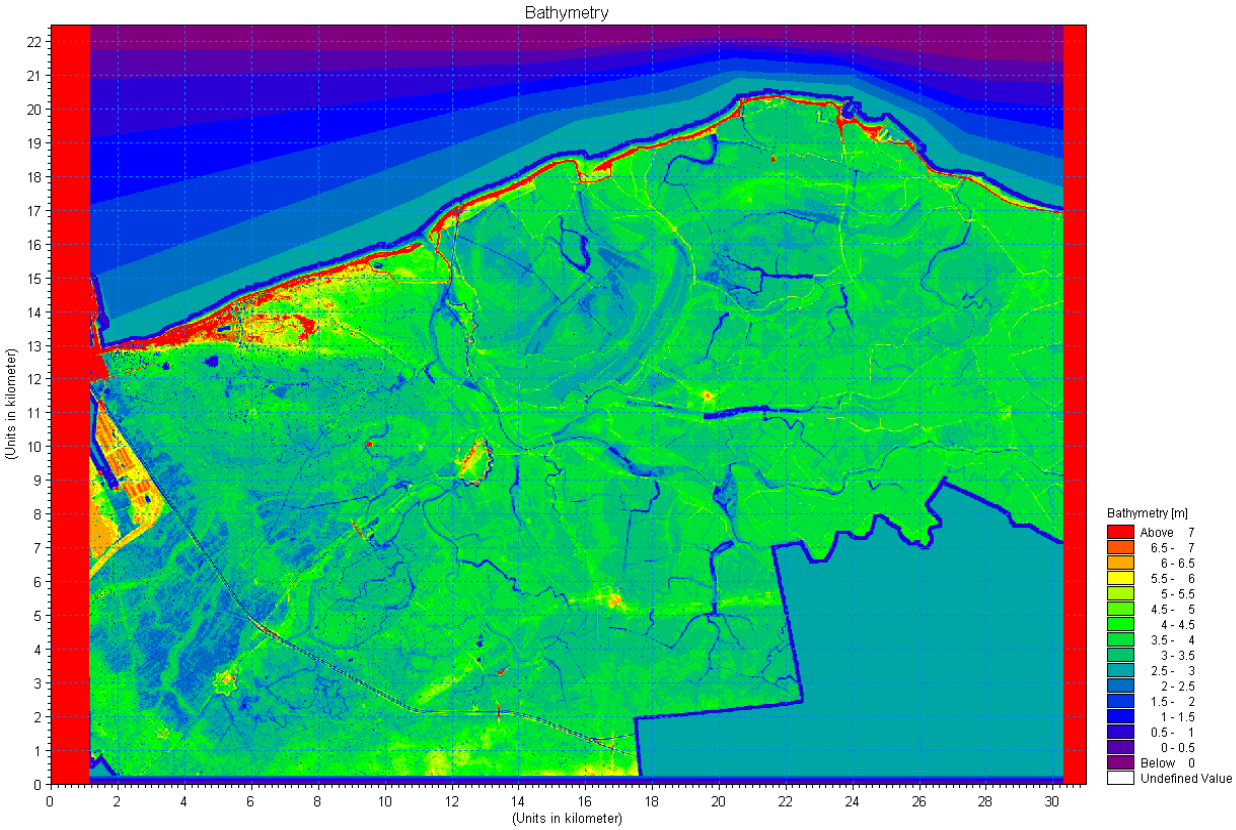

Figure 116: Topography model for Zeebrugge-Breskens

The altitudes of inner dikes, channel dikes, etc. were inspected and, if necessary, inserted into the model topography, using the measurements of the Coastal Waterways department (2003) for the inner dikes on Belgian soil (Damme Waterway and the Leopold Canal) (see Figure 117). The altitudes of the Dutch secondary dikes are included in the AHN.

The secondary retaining structures, inner dikes and dikes along channels can overflow during a simulation if the water level rises above the crest height of the secondary retaining structure in question. The model assumes that these dikes will not fail. In reality, the secondary retaining structures can fail if they overflow for a longer period of time. This may also cause breaches.

The model features a number of watercourses or ponds. The altitudes of these bodies of water are not included in the AHN or the Flanders DHM. When floods commence, the storage of these bodies of water is already used up, so that the actual bottom level of these bodies of water is not a necessary datum for the flood model.

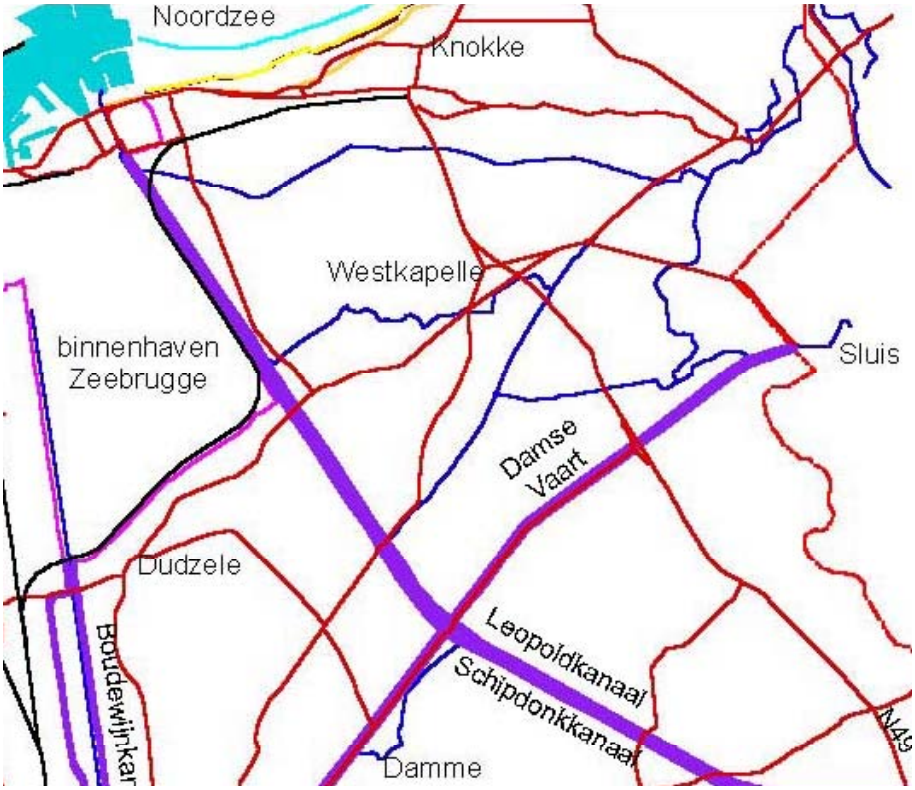

Figure 117: Inner dike of Damme Waterway and Leopold Canal.

9.3.1.3. Roughness and viscosity:

The Strickler coefficient (1/Manning (n)) is of the order of 20-40.

The higher the Strickler coefficient, the lower the resistance, in city centres it is recommended to use a lower Mannings number. A small sensitivity analysis with 1/20, 1/32 (recommended value in manual Mike21) and 1/40 shows that a shift of the water rise is limited to several minutes. The maximum water level reached hardly depends on the roughness .(cf chapter 11)

A homogeneous roughness (value of 1/32) is imposed for the entire model.

The Eddy viscosity value used in the model amounts to 1.1m²/s, this corresponds with water with a temperature of 15 °C.

9.3.1.4. The model borders

Near the North Sea, the northern border of the model, and inland, the southern border of the model, open boundary conditions were defined in the model. This allows hydrodynamic boundary conditions to be imposed (water level). The eastern and western parts of the model are delimited by a closed border.

9.3.2. The 1D-model

Dike breaches are modelled with Mike11, using a “Dambreak”. The moment of failure and the evolution of the breach in time, up to the eventual width and depth of the breach, are integrated in the model.

The 1-dimensional modelling of breaches has the advantage that the breach size can vary over time and that a life-size width of the breach can be shown. If the breaches are modelled 2-dimensionally they have a width equal to the dimensions of a 2D grid cell or a multiple thereof. The dike breach is present initially and no scenario with breach development can be taken into account.

Open borders are defined up and down the “dam break”, allowing the seawater level to be imposed as upward boundary condition and allowing a downward link with the 2D height model.

9.3.3. Link between 1D and 2D-model

The 1D-model is linked to the 2D-model, which together form one flood model. The calculation link is made by means of the MikeFlood module. For this purpose the downward section (open border) of the 1D-model is linked to a series of cells of the 2D-model, allowing water exchange between both model elements. This link is made at the various dike breach locations modelled.

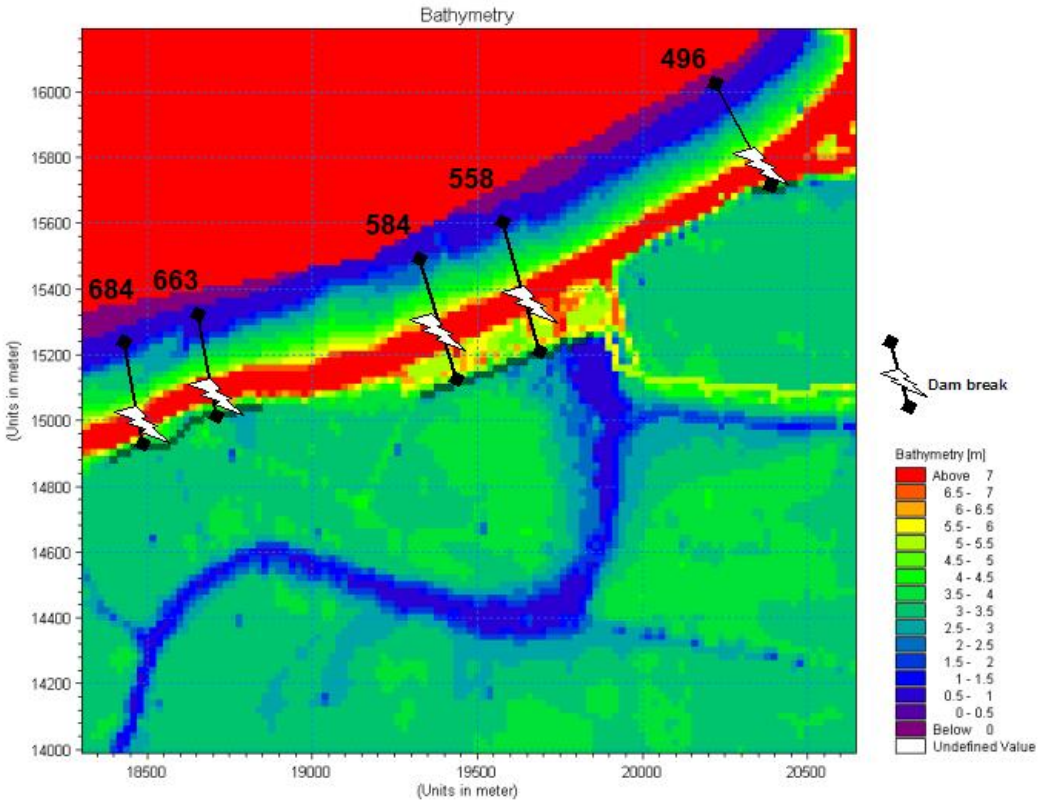

Figure 118: Schematic representation of the link between the 1D-model and the 2D-model

9.3.4. Calculation time and calculation transient of the model

The calculation time of a model strongly depends on various factors. The most important are

- The number of active grid cells,
- The duration of the simulation and the transient used for calculations;
- The hardware configuration used.

To guarantee the stability of the model, the Courant number must be taken into when determining the calculation transient.

For the 2D-model Mike21 with a cell size of 20 by 20 m a calculation transient of 4 seconds is recommended (if the breaches are included by lowering the topography at the dike). If, however, as was done for the present calculations, the breach development is integrated via Mike Flood, a maximum transient of 2 seconds is necessary to achieve a stable model.

9.4. Scenarios: dike breach

The flood model was used to calculate four dike breach scenarios. Below is an overview of the assumptions made and the boundary conditions used. These assumptions pertain to, among other things, the location of the breach, the breach development and the water level where the breach occurs. The analysis and selection of the locations with a potential seawall failure risk was extensively clarified in chapters 6, 7 and 8.

For a 10000-year return period no analysis of the failure points was made. However, considering the large difference in the number of breaches between the 4000- and the 40000-year return periods, it was examined for all places where a breach occurred with the 40000-year return period and a breach did not occur with the 4000-year return period (based on how 'close' the breach occurred with a 40000-year return period or how 'close' the breach did not occur with the 4000-year return period) where it is likely that breaches occurred with a 10000-year storm. This showed that for Flanders the failure locations coincide with the 40000-year return period; for the Zwin and the Netherlands they coincided with the 4000-year return period, except for profile 496 in the Netherlands.

The boundary conditions and the number of dike breaches per scenario are summarised in Table 41 and are shown in Figure 119.

Table 41: Scenarios for dike breaches

Simulation	***North Sea water level: return period***	***Number of dike breaches in Flanders***	***Breach in the Zwin***	***Number of dike breaches in Zeeland Flanders***
Scenario 1	1000 years	0	0	3
Scenario 2	4000 years	3	0	5
Scenario 3	"10000 years"	7	0	6
Scenario 4	40000 years	7	1	10

Figure 119: Situation of the Zeebrugge- Breskens study area, including an indication of the places where breaches occur

The background consist of photos from OCGis – West-Vlaanderen and from the AHN-The Netherlands

9.4.1. Boundary conditions

9.4.1.1. Water levels

For the North Sea water level, time series (hourly values) were imposed, cf. water level evolution of storm tides with a return period of 1000, 4000, 10000 and 40000 years (see chapter 3).

The water level evolution, used with the flood modelling of dike breaches, is given in Figure 120. These water levels are imposed on the upward edge of the dike which will fail during the storm, particularly upwards of the “Dambreak” in the 1D-model (Mike11).

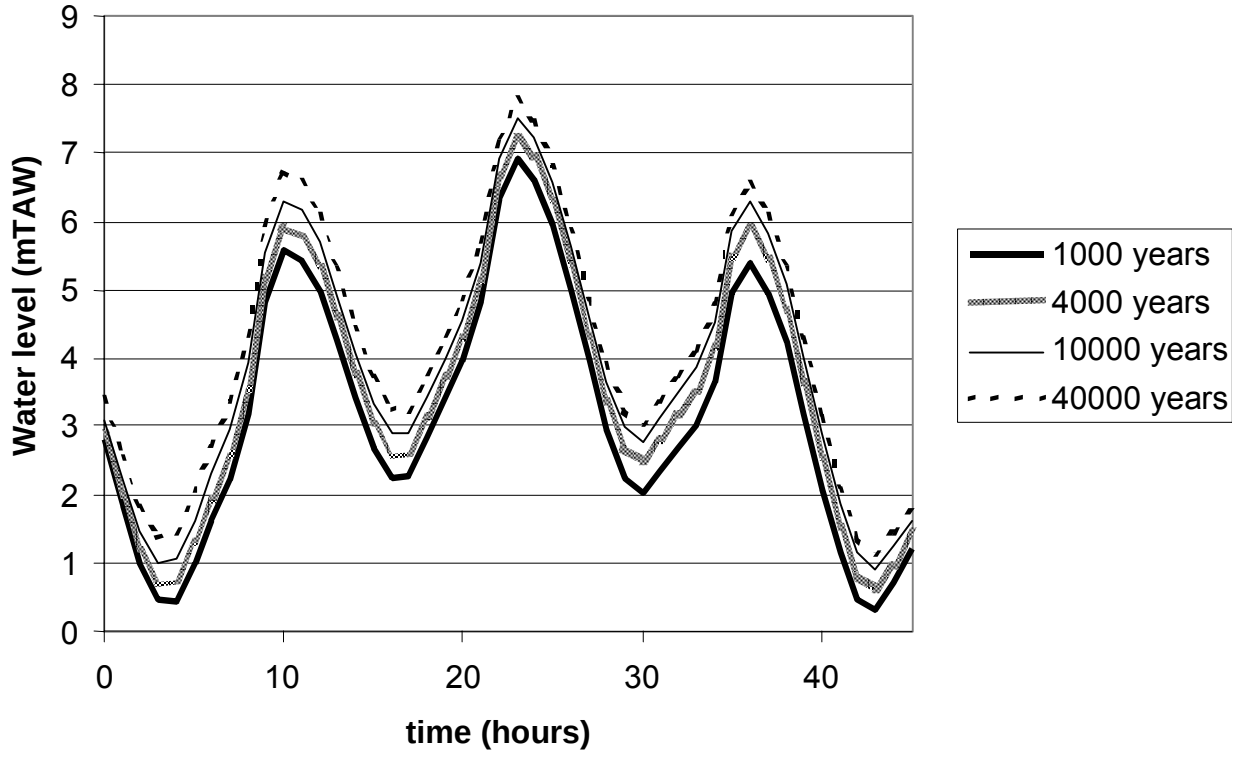

Figure 120: Water level evolution of storm tides with a return period of 1000, 4000, 10000 and 40000 years

9.4.1.2. Wind

The calculation of the scenarios with the flood model does not take into account wind effects.

9.4.2. Dike breach: breach evolution

The number of seawall failures, the extent and locations of the breaches have a great impact on the evolution of the floods. That is why it is important to correctly schematise the breaches.

In Mike11 breach evolution is modelled by means of 2 time series, entered by the user. The first time series gives the evolution of the breach depth in time. At the moment of breaching it is assumed that the dike height is equal to the water level, the maximum depth is reached after 1 to 2 hours. (Steetzel, H.J., 1993.). An evolution in 1 hour was opted for, with regard to breach depths smaller than 2m, and in 2 hours with regard to breach depths greater than 2 m. The second time series gives the evolution of the breach development as to width.

Width-wise breach development correlates with the erosion of the water-retaining structure located on both sides of the breach. The width development depends on a large number of parameters, including momentary hydraulic boundary conditions, geometry of the retaining structure and the material the water-retaining structure is made of. For the modelling of the breach development, the width evolution speed in phase II of the process is particularly important. In the above-mentioned study this (unilateral) speed is indicated with the so-called ß-value (see Figure 121with the schematic evolution in case of a constant outer water level).

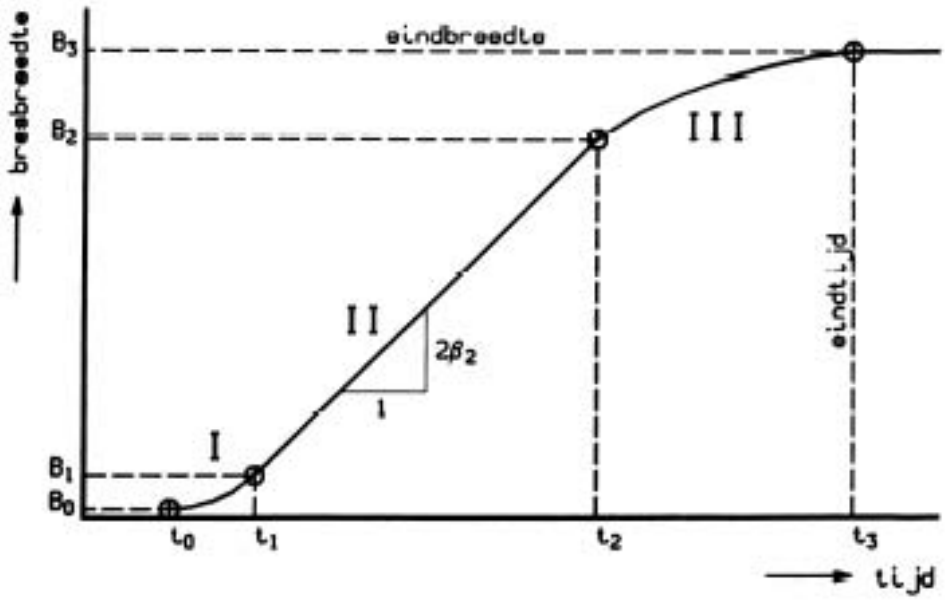

Figure 121: Schematic representation of the width evolution

Table 42 gives an overview of the (unilateral) ß-value as deduced from a short inventory of relevant data. These results imply a large spread of the results. It must be noted that the information regarding the hydraulic conditions, the geometry and the material properties are often lacking. As the breaches in this project occur under very severe hydrodynamic circumstances, including a high wave stress (which is usually not the case in the historic breaches), it was decided to do the calculations using a breach development of 30m/h (=2 ß). As an initial breach size, 20 m was used. For Flanders, where dikes fail due to erosion of the crest as a consequence of wave overtopping (which can be assumed to be uniform over the entire dike section), it is usually assumed that the breach is immediately formed over the entire length of the dike section, excluding the places where apartments are located (cf.Figure 122) (actually, breach development does not really occur, the overtopping water causes continuous erosion until the water level is higher than the dike, and the erosion will continue at an accelerated pace. If an apartment were to collapse (which is hardly likely), the rubble would automatically close the breach. So, it must be assumed conservatively that nothing occurs at the site of the apartments.

Figure 122: locations of breaches (red arrows)(situation in Flanders)

Table 42: Overview of result of short inventory.

Source	Observation	Estimate of β-value
Scheldebak survey (TAW)	Breach widening speed decreases from 0.25 to 0.45 m/min initially to approx. 0.05 m/min	Max. 15-25 m/hour Min. 3 m/hour
Japanese tests	Decrease from 0.4 m/min to 0.1 m/min	0.5 – 4.0 m/hour
Zwin test (TAW)	During linear growth phase 25 m in 18 minutes	42 m/hour (!)
DBW/RIZA	Tidal waters: 500 m / 12 days River dikes: from 40 m/36 hours (min) to 200 m/24 hours (max) Lake dikes: from 150 m/36 hours (min) to 200 m/24 hours (max)	1 m/hour 0.6 – 1.0 m/hour 2.1 – 4.2 m/hour
Zalk dike breach (1926)	Decreasing width development of 50 m per 3 hours to 30 m in 20 hours	0.8 – 8 m/hour
Dalfsen dike breach (1926)	Decreasing from 12 m in 9 hours to 8 m in 27 hours	0.15 – 0.7 m/hour
Wieringermeer dike breach	Estimate of 160 to 200 m in 50 hours	1.6 – 2.0 m/hour
Northern Y-polder	15 m in 7.5 hours	1.0 m/hour
Walcheren bombardment	West-Kapelle: from 130 m to 600 m in 12 days Vlissingen: from 50 to 350 m in 8 days Veere: from 450 to 975 m in 4 days	0.8 m/hour 0.8 m/hour 2.7 m/hour

The maximum extent of the breaches as modelled in the flood model, is determined by the distance between the failing profile and the up- and downward dike profile for the width of the breach. The maximum depth of the breach extends to ground level in the vicinity of the dike.

The moment of seawall failure comes from the analysis of the seawall failure (Chapters 6, 7 and 8).

An overview of the parameters used for dike breaches for the 4 scenarios are included in Table 43 to Table 48. The potential locations of dike breaches are given in Figure 119

Table 43: Parameters for breach development with seawall failure during a storm tide with a 1000-year return period: scenario 1

Parameter	***Unit***	***Profiles for seawall failure in Zeeland Flanders***		
		373	**396**	**413**
Breach location		Nieuwe Sluis (Jong Breskens polder)		
Moment of seawall failure		HW tide 2	HW tide 3	HW tide 2
Initial width of the breach	m	20	20	20
Speed of width-wise breach development	m/hour	30	30	30
Maximum width of the underside of the breach	m	222	201	123
Duration of the maximum width of the breach	hour	7	7	4
End height of the underside of the breach	m T.A.W.	4	4	4
Duration of the maximum depth of the breach	hour	2	2	2

Table 44: Parameters for breach evolution with seawall failure during a storm tide with a 4000-year return period: scenario 2

Parameter	***Unit***	***Profiles for seawall failure in Zeeland Flanders***					***Profiles for seawall failure in Flanders***		
		373	***396***	***413***	***512***	***530***	***242***	***243***	***233***
Breach location		Nieuwe Sluis (Jong Breskens polder)			Walen dike		Het Zoute (Zwinlaan)		Knokke
Initial moment of dike breach		HW tide 2	HW tide 2	HW tide 2	HW tide 3	HW tide 3	HW tide 2	HW tide 2	HW+1 hour tide 2
Initial width of the breach	m	20	20	20	20	20	60	60	90
Speed of width-wise breach development	m/hour	30	30	30	30	30	30	30	-
Maximum width of the underside of the breach	m	222	201	123	170	228	150	150	90
Duration of the maximum width of the breach	uur	7	7	4	5	7	3	3	0
End height of the underside of the breach	m T.A.W.	4	4	4	3.5	3.5	5	5	6
Duration of the maximum depth of the breach	hour	2	2	2	2	2	1	1	0

Table 45: Parameters for breach evolution with seawall failure during a storm tide with a 10000-year return period in Zeeland Flanders : scenario 3

Parameter	***Unit***	***Profiles for seawall failure in Zeeland Flanders***					
		373	***396***	***413***	***512***	***530***	***496***
Breach location		Nieuwe Sluis (Jong Breskens polder)			Walen dike		
Initial moment of dike breach		HW tide 2	HW tide 2	HW tide 2	HW tide 3	HW tide 3	HW tide 3
Initial width of the breach	m	20	20	20	20	20	20
Speed of width-wise breach development	m/hour	30	30	30	30	30	30
Maximum width of the underside of the breach	m	222	201	123	170	228	145
Duration of the maximum width of the breach	hour	7	7	4	5	7	5
End height of the underside of the breach	m T.A.W.	4	4	4	3.5	3.5	3.5
Duration of the maximum depth of the breach	hour	1	1	1	2	2	2

Table 46: Parameters for breach evolution with seawall failure during a storm tide with a 10000-year return period in Flanders: scenario 3

Parameter	***Unit***	***Profiles for seawall failure in Flanders***						
		233	***234***	***235***	***236***	***241***	***242***	***243***
Breach location		Knokke				Het Zoute (Zwinlaan)		
Initial moment of dike breach		HW+1 hour tide 2	HW tide 2	HW+1 hour tide 2	HW+1 hour tide 2	HW tide 2	HW tide 2	HW tide 2
Initial width of the breach	m	90	90	90	90	60	60	60
Speed of width-wise breach development	m/hour	-	-	-	-	30	30	30
Maximum width of the underside of the breach	m	90	90	90	90	150	150	150
Duration of the maximum width of the breach	hour	0	0	0	0	3	3	3
End height of the underside of the breach	m T.A.W.	6	6	6	6	5	5	5
Duration of the maximum depth of the breach	hour	0	0	0	0	1	1	1

Table 47: Parameters for breach evolution with seawall failure during a storm tide with a 40000-year return period in Zeeland Flanders: scenario 4

Parameter	***Unit***	***Profiles for seawall failure in Zeeland Flanders***									
		373	***396***	***413***	***512***	***530***	***496***	***558***	***584***	***663***	***684***
Breach location		Nieuwe Sluis (Jong Breskens polder)			Walen dike			Zeeweg (Zwarte Gat)			
Initial moment of dike breach		HW tide 2	HW tide 2	HW tide 2	HW tide 2	HW tide 2	HW tide 2	HW tide 3	HW tide 3	HW tide 3	HW tide 3
Initial width of the breach	m	20	20	20	20	20	20	20	20	20	20
Speed of width-wise breach development	m/hour	30	30	30	30	30	30	30	30	30	30
Maximum width of the underside of the breach	m	222	201	123	170	228	145	271	219	233	212
Duration of the maximum width of the breach	hour	7	7	4	5	7	5	8	7	7	7
End height of the underside of the breach	m T.A.W.	4	4	4	3.5	3.5	3.5	3.5	3.5	3.5	3.5
Duration of the maximum depth of the breach	hour	1	1	1	2	2	2	2	2	2	2

Table 48: Parameters for breach evolution with seawall failure during a storm tide with a 40000-year reuturn period in Flanders: scenario 4

Parameter	***Unit***	***Profiles for seawall failure in Flanders***							
		233	***234***	***235***	***236***	***241***	***242***	***243***	***Zwin dike***
Breach location		Knokke				Het Zoute (Zwinlaan)			Inner dike Zwin dike
Initial moment of dike breach		HW+1 hour tide 1	HW tide 2	HW+1hour tide 2	HW+1 hour tide 2	HW tide 2	HW tide 1	HW tide 1	HW tide 2
Initial width of the breach	m	90	90	90	90	60	60	60	20
Speed of width-wise breach development	m/hour	-	-	-	-	30	30	30	30
Maximum width of the underside of the breach	m	90	90	90	90	150	150	150	300
Duration of the maximum width of the breach	hour	0	0	0	0	3	3	3	9
End height of the underside of the breach	m T.A.W.	6	6	6	6	5	5	5	4
Duration of the maximum depth of the breach	hour	0	0	0	0	1	1	1	1

9.4.3. Wave overtopping

The effect of wave overtopping can be modelled by including the calculated overtopping discharges in the flood model.

The overtopping discharges can be added to the Mike21 model by means of the definition of a “Source”. A Source gives the possibility to inject a flow rate into a grid cell in a certain direction. To do so, a time series can be used. However, sudden changes (overtopping discharges are momentary peak flow rates) cause instability in the model. That is why it is recommended to convert the overtopping discharges into an average flow rate over a longer period. For the moment no overtopping discharges were included in the model, considering their negligible share compared to the water volumes flowing in through breaches (seawall failure). For studies into local effects this may be important, though.

9.5. Dike breach results

In this paragraph the results of the four scenarios are discussed: flooding due to dike breaches which may occur during storm tides with a return period of 1000, 4000, 10000 and 40000 years, respectively.

The necessary results from the 2D-model for the implementation of economic damage calculations and the number of casualties are:

- Maximum water level occurring during the simulation.
- Maximum water rise (the water levels occurring every 30 min were taken into account).
- Maximum velocity occurring during the simulation.

The results are represented by means of a figure showing the maximum water depth and the maximum velocities occurring. A graph also shows the flood depth evolution in time for a limited number of locations.

These locations are given in Figure 123 and Figure 124. The altitudes of the corresponding grid cells are given in Table 50and Table 49. It is not the average soil height of the area.

Figure 123: Locations of flood depths in Zeeland Flanders

Table 49: Altitudes of the locations for the results of flood depths in Zeeland Flanders

Point	Location	Altitude mTAW
A	Niewe Sluis	2.92
B	Niewe Sluis below Walendike	3.22
C	Het Heem	3.35
D	Breskens	3.57
E	Groede	3.46
F	Agricultural area between Baarzandsche Kreek – Nieuwkerksche Kreek	3.00
G	Puijen dike	3.31
H	Zeeweg (Zwarte Gat)	3.23

Figure 124: Locations for the results of flood depths in Flanders

Table 50: Altitude of the locations for the results of flood depths in Flanders

Point	Location	Altitude mTAW
I	Knokke centre	4.37
J	Het Zoute	5.00
K	The Zwin outside the International Dike	3.54
L	Sint Anna Ter Muiden	3.56
M	Westkapelle	2.75
N	Ramskapelle	3.01
O	Oostkerke	3.08

9.5.1. Scenario 1: Dike breach for a return period of 1000 years

The results of scenario 1 show the effect of a dike breach during a storm tide with a 1000-year return period. Dike breaches at dike profiles 373 and 413 near Nieuwe Sluis occur when the storm tide is at its peak. A third breach at profile 396 occurs during the nevxt flood period. In the Jong Breskens polder, adjacent to the dike breach, the water depth increases to more than 3 metres within two hours (Figure 125). The polder behind it, protected by the secondary retaining structure (Walen dike), is flooded 3 to 4 hours after the dike breach. The water level in the Jong Breskens polder reaches a water level resulting in overflow at the Walen dike. The water depth in the polder behind it (Oud Breskens polder) remains limited to 20cm (Figure 126).

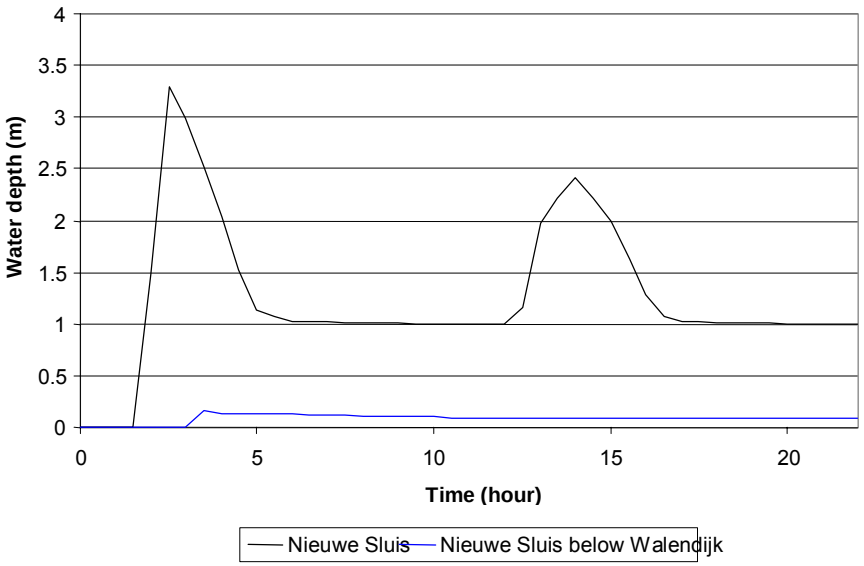

Figure 125: Flood depth during a storm flood with a 1000-year return period at dike profiles 373, 396 and 413 near Nieuwe Sluis.

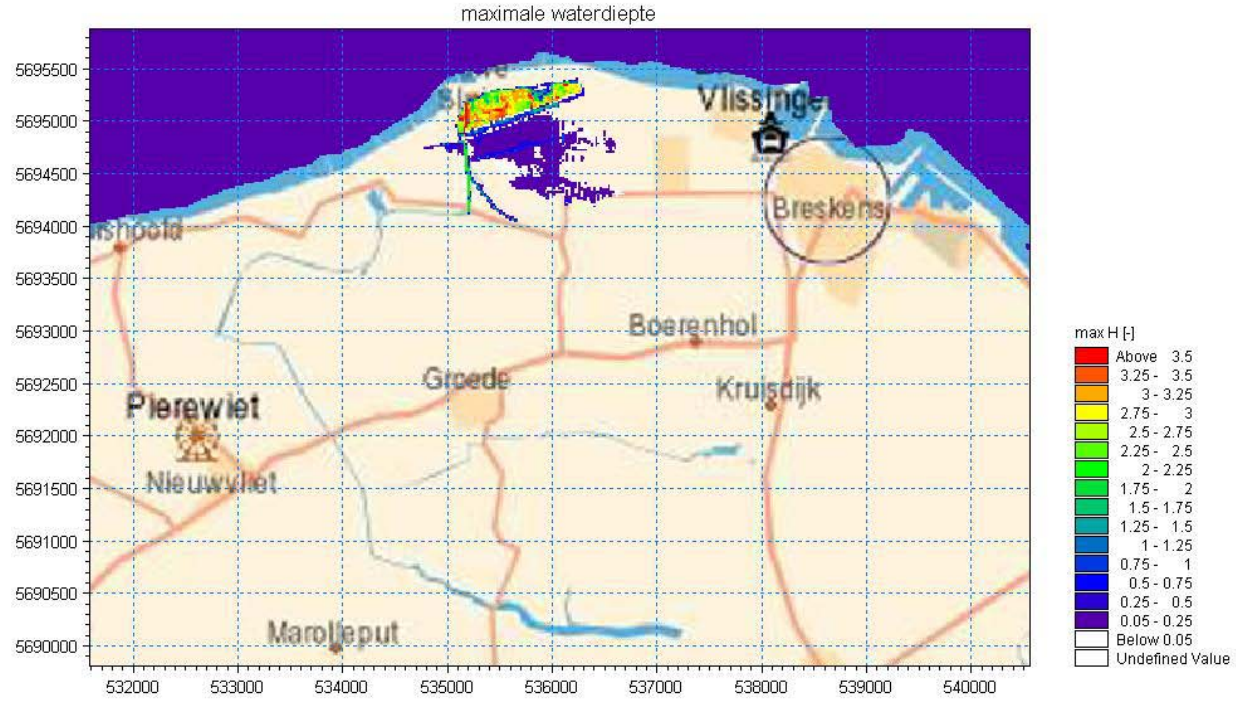

Figure 126: Maximum water depth (m) for scenario 1 during a storm tide with a 1000-year return period.

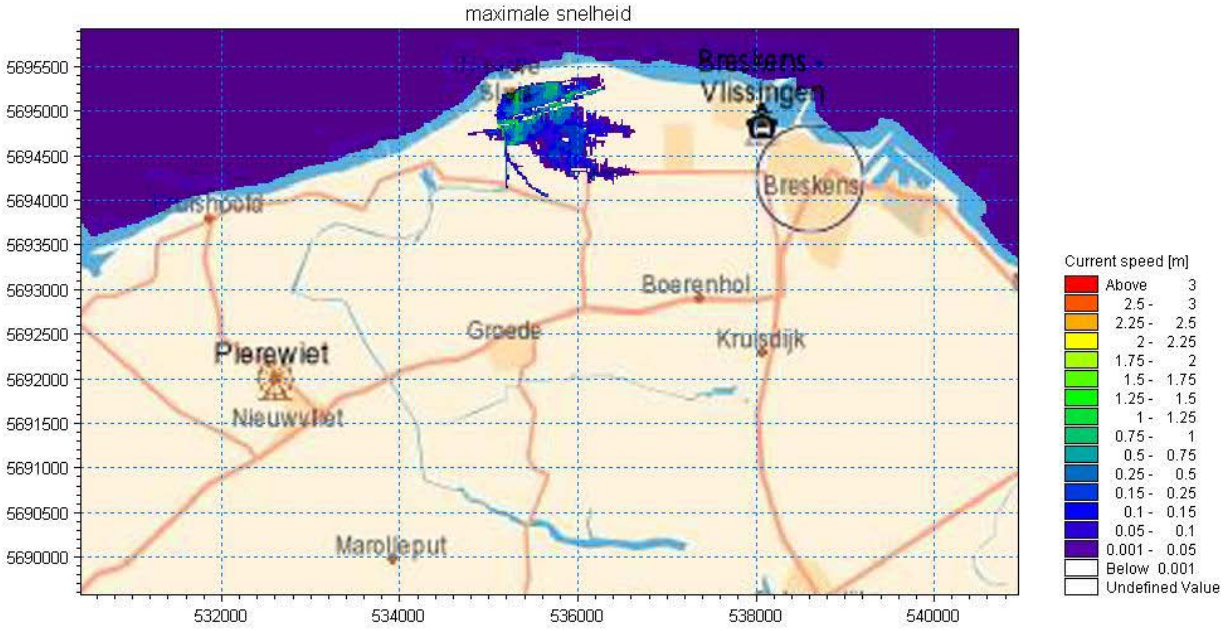

Figure 127: Maximum velocities (m/s) for scenario 1 during a storm tide with a 1000-year return period.

9.5.2. Scenario 2: Dike breach for a 4000-year return period

The results of scenario 2 show the effect of dike breach during a storm tide with a 4000-year return period. In Zeeland Flanders dike breaches occur at dike profiles 373, 396 and 413 near Nieuwe Sluis. These occur when the storm flood is at its peak. During the next flood period additional dike breaches occur at profiles 512 and 530 near Walen dike.
In Flanders dike breaches also occur at the height of the storm at dike profiles 242 and 243 near Het Zoute; 1 hour later a dike in Knokke fails (profile 233).

In Zeeland Flanders, in the Jong Breskens polder, adjacent to the dike breach, the water depth increases to more than 3.5 metres within two hours (Figure 128). The water level in the Jong Breskens polder reaches a water level resulting in overflow at the Walen dike. The polder behind it, protected by the secondary retaining structure (Walen dike), is flooded 1 hour later. The water depth in the polder behind it (Oud Breskens polder) increases to 0.5 to 1m. A next secondary retaining structure holds the water, keeping the Gerard de Moor polder and the Heeren polder free from flooding. The flooded area extends eastward to the Het Heem residential area and westward to the Puijen dike.

On Belgian soil, the floods in Knokke centre remain limited. The dike breach at the Het Zoute allows a high velocity, the flat hinterland is slowly flooded. The floods extend to 5 km inland up to the Nieuwe Hazegra polder dike and the Graaf Jan dike.

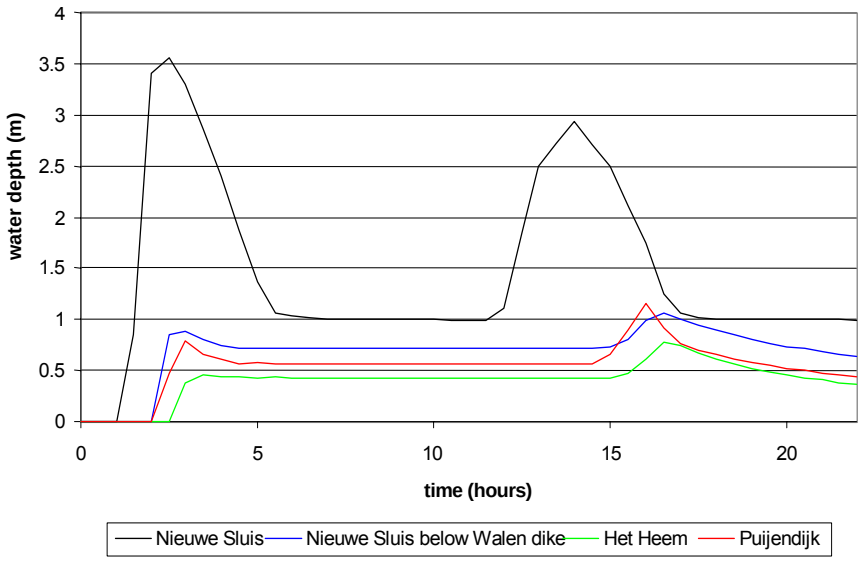

Figure 128: Flood depth during a storm flood with a 4000-year return period with a dike breach at dike profiles 373, 396 and 413 near Nieuwe Sluis and profile 512 and 530 near Walen dike.

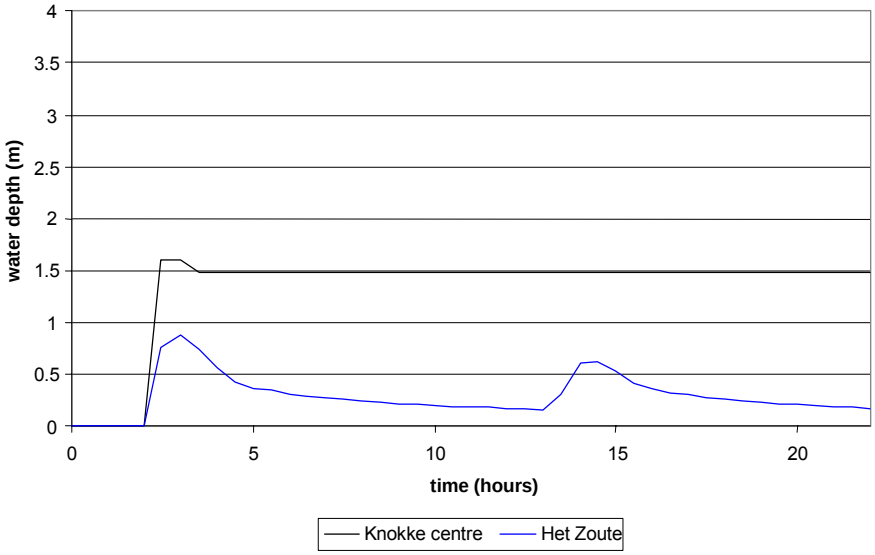

Figure 129: Flood depth during a storm flood with a 4000-year return period with a dike breach at dike profiles 242 and 243 near Het Zoute and profile 233 in Knokke.

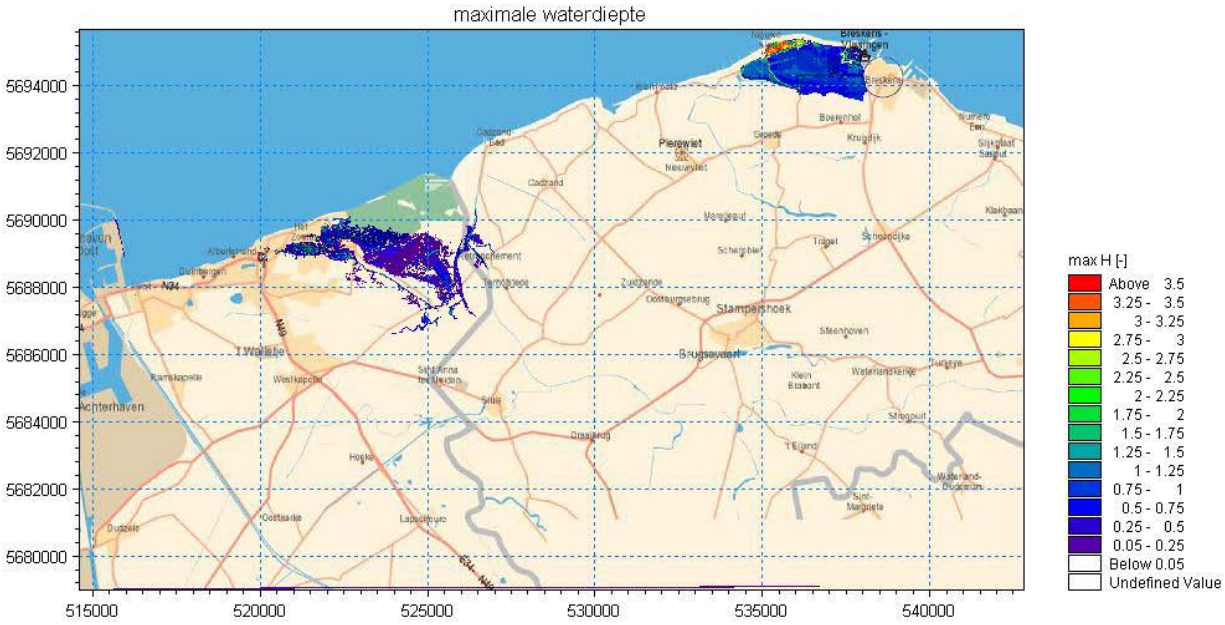

Figure 130: Maximum water depth (m) for scenario 2 during a storm tide with a 4000-year return period.

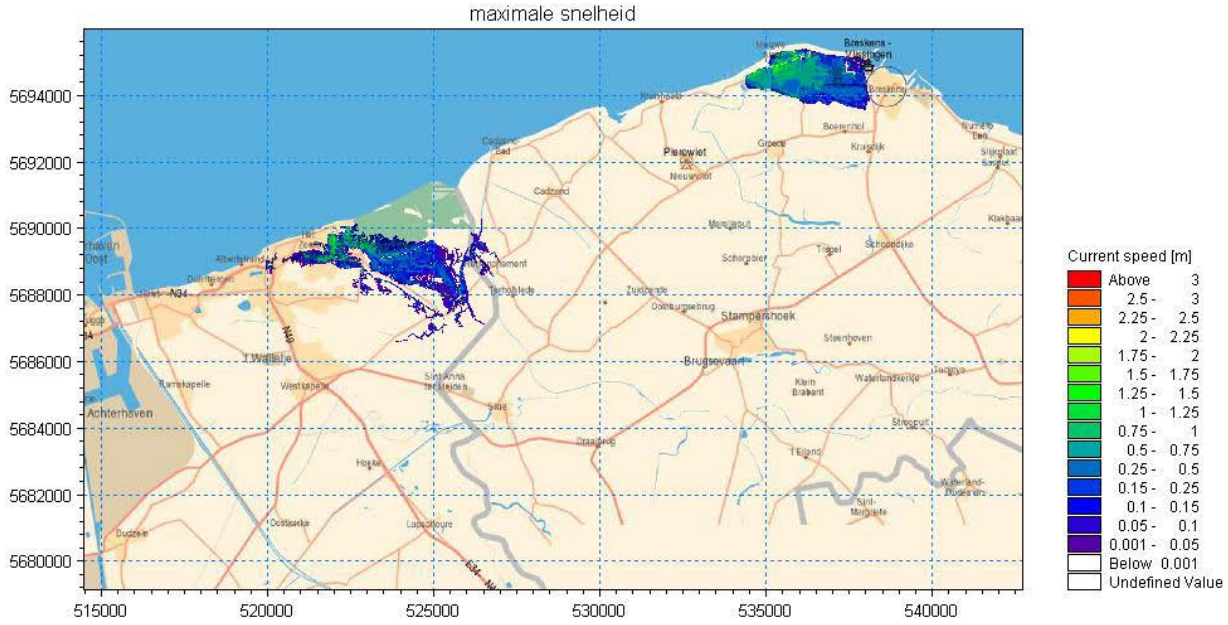

Figure 131: Maximum velocities (m/s) for scenario 2 during a storm tide with a 4000-year return period.

9.5.3. Scenario 3: Dike breach with a 10000-year return period

The results of scenario 3 show the effect of a dike breach during a storm tide with a 10000-year return period. In Zeeland Flanders dike breaches occur at dike profiles 373, 396 and 413 near Nieuwe Sluis. These occur when the storm flood is at its height. During the next flood period additional dike breaches occur at profiles 512, 530 and 496 near Walen dike.
In Flanders, at the height of the storm, dike breaches also occur at dike profiles 241, 242 and 243 near Het Zoute, dike profile 234 near Knokke and 1 hour later a number of dikes in the vicinity also fail (dike profiles 233, 235 and 236).

In Zeeland Flanders, in the Jong Breskens polder, adjacent to the dike breach, the water depth increases to more than 3.5 metres within half an hour. The polder area behind the Walen dike is flooded. The water depth in the polder rises to more than 1m. A next secondary retaining structure (Puijen dike and Hoge dike) holds the water. The flood area corresponds with the areas flooded during a storm tide with a 4000-year return period.

On Belgian soil the floods in Knokke centre remain limited, the water depth rises 2 to 3m. The dike breach at Het Zoute allows a high velocity, the flat hinterland is slowly flooded. The floods extend to the Grevening dike near Sint anna Termuiden and the Kalvekeet dike in Westkapelle.

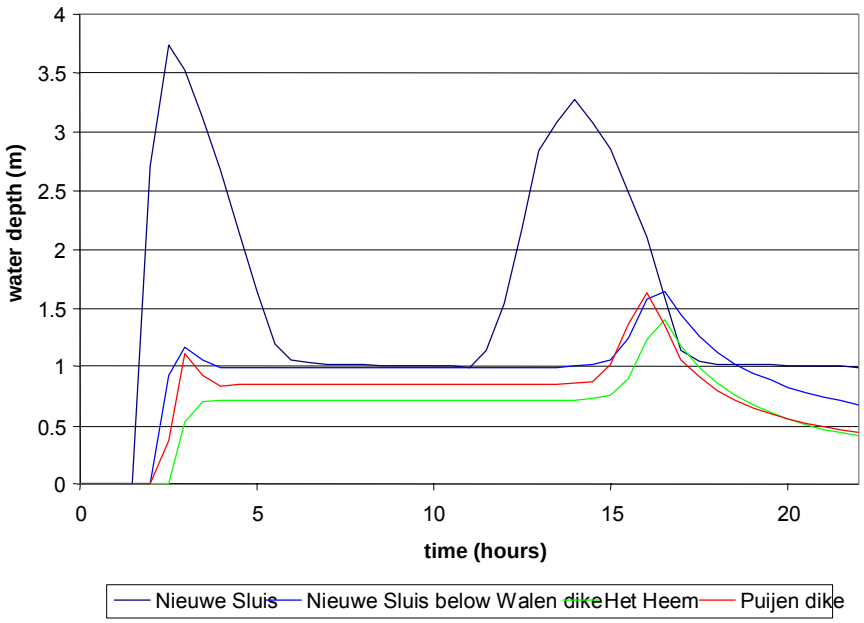

Figure 132: Flood depth during a storm flood with a 10000-year return period with a dike breach at dike profiles 373, 396 and 413 near Nieuwe Sluis and profiles 512, 530 and 496 near Walen dike.

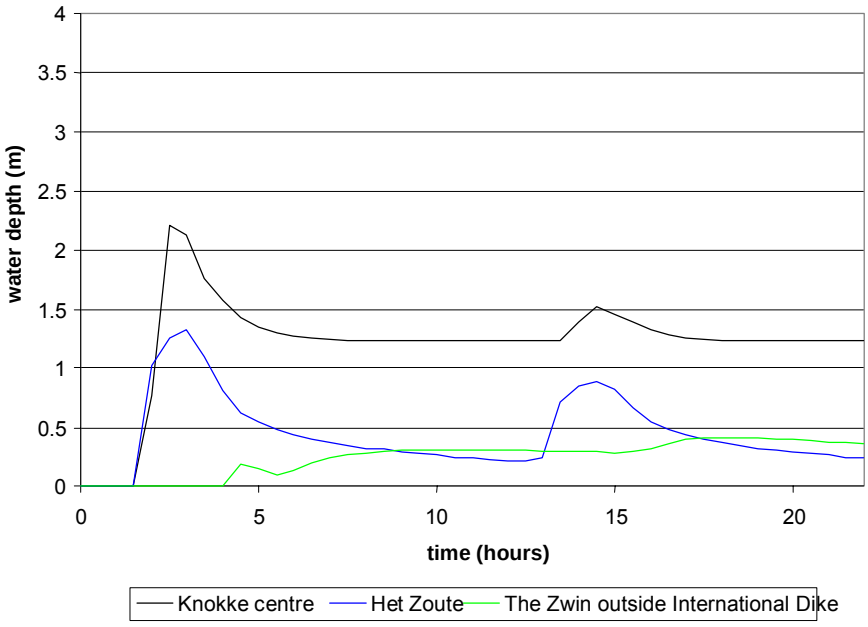

Figure 133: Flood depth during a storm flood with a 10000-year return period with a dike breach at dike profiles 241, 242 and 243 near Het Zoute and profiles 233, 234, 235 and 236 in Knokke

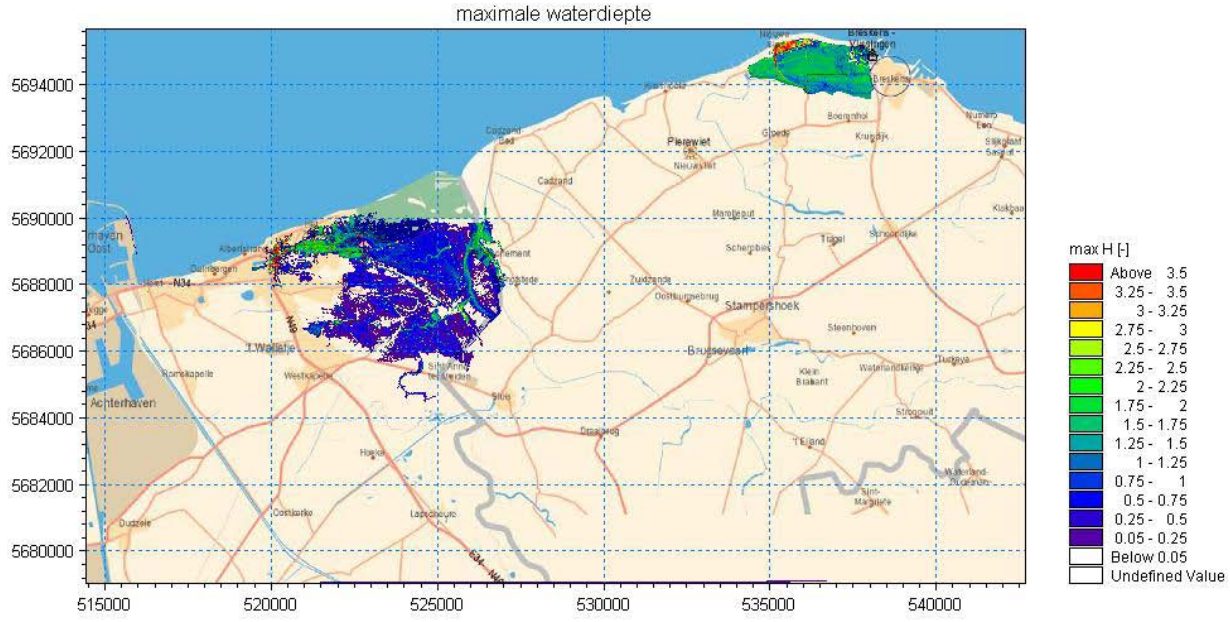

Figure 134: Maximum water depth (m) for scenario 3 during a storm tide with a 10000-year return period.

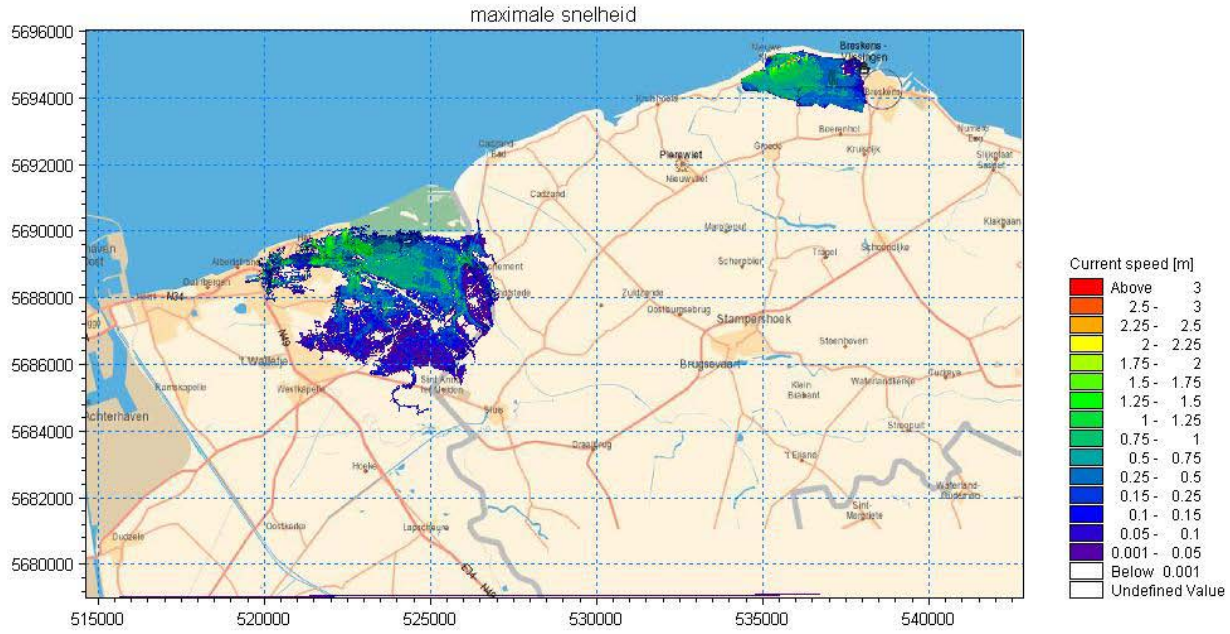

Figure 135: Maximum velocities (m/s) for scenario 3 during a storm tide with a 10000-year return period.

9.5.4. Scenario 4: Dike breach with a 40000-year return period

The results of scenario 4 show the effect of a dike breach during a storm tide with a 40000-year return period. In Zeeland Flanders dike breaches occur at dike profiles 373, 396 and 413 near Nieuwe Sluis and profiles 512, 530 and 496 near Walen dike. These occur at the height of the storm flood. During

the next flood periods additional dike breaches occur at dike profiles 558, 584, 663 and 684 at the Zeeweg near Zwarte Gat.

In Flanders, dike breaches occur during the first tide of the storm near Knokke (profile 233) and Het Zoute (profile 242 and 243). At the height of the storm dike breaches also occur at dike profiles 241 and 243 near Het Zoute, dike profiles 234, 235 and 236 near Knokke and the Zwin dike inner dike (International Dike).

In Zeeland Flanders, in the Jong Breskens polder, the water depth rapidly increases to 4 metres. The dike braches at the Walen dike virtually immediately cause overflow of the dikes along the Zoete Kreek. The polder behind it (Oud Breskens polder) is flooded, velocities of more than 3m/s occur. The water depth also fairly rapidly increases to a depth of more than 3 metres. The same rising speed is found at the Het Heem residential area and near the Puijen dike.

A next secondary retaining structure, Puijen dike and Hoge dike, holds the water temporarily. The flooded area extends eastward to Number One. In the centre of Breskens the water rises to more than 1 metre. To the south, the water is held by the Krabbe dike to the south, and by the Sint Bavo dike to the west.

On Belgian soil, the floods are even more extensive, reaching to the dikes of the Leopold Canal and the Damme Waterway. The water depth in the urbanised areas of Westkapeele, Ramskapelle and Oostkerke amounts to 0.5 to more than 1m locally.

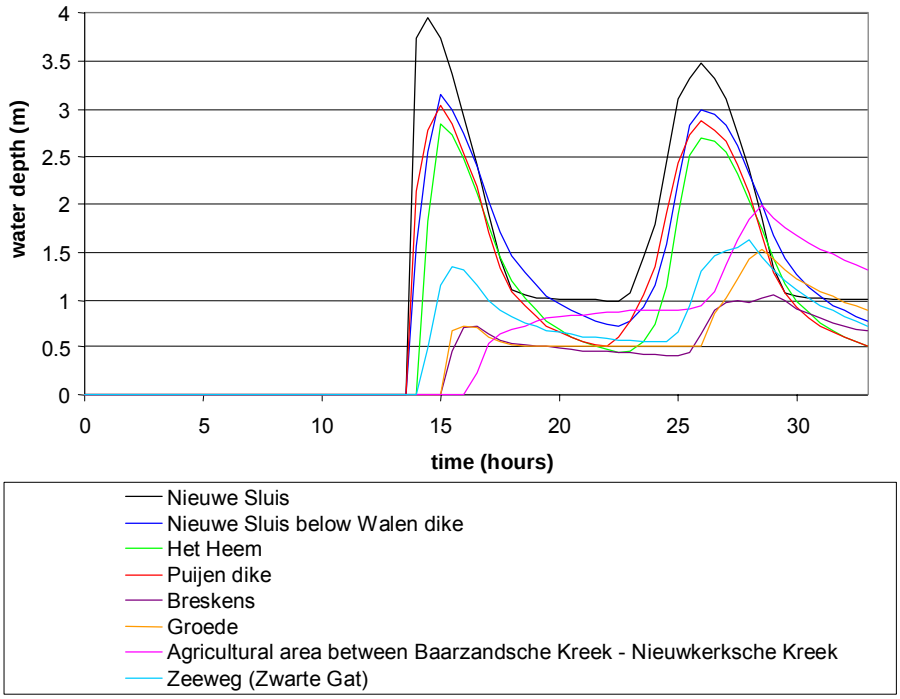

Figure 136: Flood depth during a storm flood with a 40000-year return period with a dike breach at dike profiles 373, 396 and 413 near Nieuwe Sluis, profiles 512, 530 and 496 near Walen dike and profiles 558, 584, 663 and 684 near Zeeweg (Zwarte Gat).

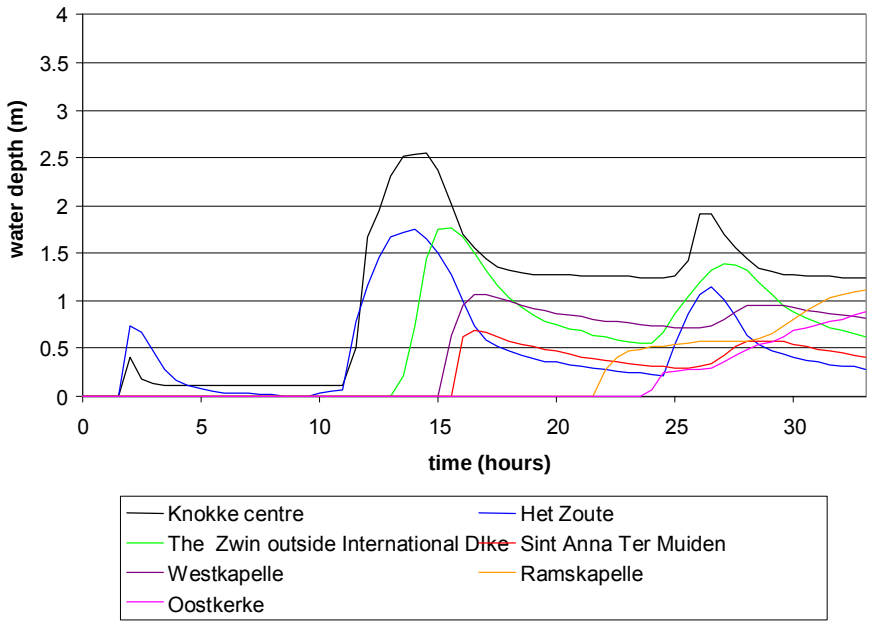

Figure 137: Flood depth during a storm flood with a 10000-year return period with a dike breach at dike profiles 241, 242 and 243 near Het Zoute, profiles 233, 234, 235 and 236 in Knokke and the inner Zwin dike (International Dike).

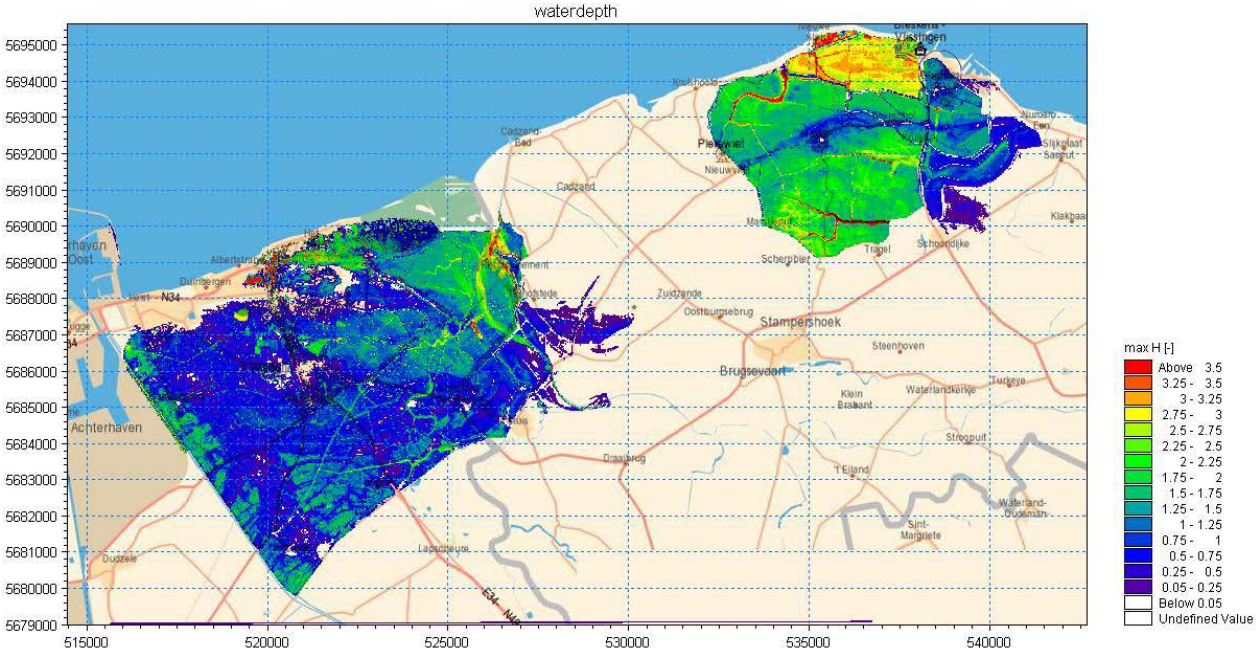

Figure 138: Maximum water depth for scenario 4 during a storm tide with a 40000-year return period.

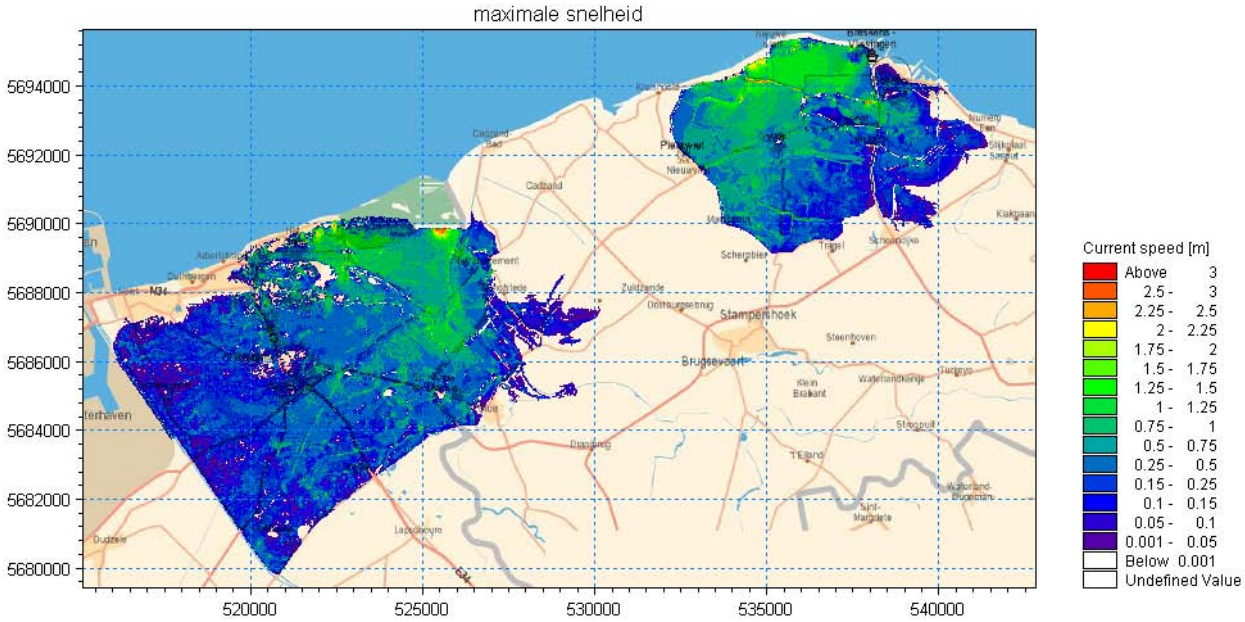

Figure 139: Maximum velocities for scenario 4 during a storm tide with a 40000-year return period.

10. DAMAGE AND CASUALTIES

10.1. Methodology

Both in the Netherlands and in Flanders, a methodology was developed to calculate the damage and casualties based on the flood characteristics (water depth, water speed). Both methods have a similar set-up. This report describes the Flemish method and, where the differences between the Flemish and Dutch methods are relevant, the Dutch equivalent is given.

The Flemish method was developed by the Hydraulic Engineering Laboratory and Hydrological Research department in co-operation with the geography department of the University of Ghent. More information about the Flemish method can be found in Vanneuville et al. (2002, 2003a,b,c). More information about the Dutch method can be found in DWW(2002)

10.1.1. Damage definition

Damage is usually defined by means of three different categories.
Damage can be categorised as monetary damage (which can be valued in terms of money) and non-monetary damage (e.g. cultural value, natural value, landscape value, etc.). In addition, a distinction is made between primary, secondary and induced damage. This distinction is made on the basis of the location where the damage occurs. Primary damage is the damage in the flood area; secondary damage is damage outside the flood area (e.g. damage to transport companies because motorways are damaged) and induced damage is damage which cannot be directly attributed to the area (e.g. salvage costs). Finally, a distinction can be made between direct and indirect damage due to flood. Direct damage is understood to mean damage to capital goods; non-direct damage includes production loss and loss of income.

As regards the damage, the Flemish method only concerns monetary damage and the number of casualties. Next, the damage to capital goods (direct damage), production loss and loss of income (indirect damage) are taken into account. Indirect damage is determined as a share of the direct damage. The method is limited to damage within the flooded area (internal damage).
In the Netherlands, separate damage functions are used for indirect damage as well.

The occurrence or non-occurrence of damage *only* depends on the actual flooding or not of a section of land. Flooding is thereby defined as the occurrence of the situation whereby the land is covered by a minimum water depth.
Depending on the availability and accuracy of geographical area data, the various elements in an area where damage may occur are categorised. These are the so-called damage categories (for instance, roads, agriculture, single-family dwellings, etc.). For each damage category a damage amount is determined.

10.1.2. Procedure

The overall method comprises the following steps:

1. the making of flood maps, so that the maximum water depth is known for each point, as well as the probability of occurrence[2];
2. the making of land use maps in the flooded area, based on data uniformly available for Flanders;

[2] To make flood maps, the composite hydrogram method is used. This method has already been amply discussed in previous notes.

3. the combination of flood maps with land use maps;
4. the determination of the maximum damage at every location in the flood area and the determination of the relation between this damage and the water depth;
5. the making of damage maps per return period;

The total damage in an area is the sum of the damage in all categories. Examples of categories are agriculture, houses, vehicles, infrastructure, etc. The categories have units in the form of the number of hectares, objects, kilometres and jobs. The damage per category is determined by the product of a so-called damage factor, the number of units and a maximum damage amount. The so-called damage factor is deduced from a damage function. This function gives the influence of the hydraulic conditions, such as the flood depth and weather, on the damage factor. In principle, every category has a different damage function. The number of casualties can be determined in the same way, using a casualty function instead of a damage function, however.
The damage and casualty calculations follow the total damage and the number of casualties in a (dike ring) area per flood scenario. In combination with the conditional probability per flood scenario, they are used to calculate the risk.

10.1.3. Damage functions and maximum damage

To make the land use maps, the CORINE Land Cover land use file was used (with a resolution of 30*30 metres) as well as the Small-scale land use file for Flanders and Brussels (with a resolution of 20*20 metres). Both files are combined, keeping the advantages of the various files.
15 different categories can be distinguished:

- Buildings I, II and III
- Industry I and II
- Infrastructure I and II
- Airport I and II
- Recreation
- Arable farming
- Pasture
- Forest
- Water

For roads and railways, a separate GIS database (top50v) is used, to assess the damage.
The following choices have been made to to compile the collection of damage functions:

1) a distinction is made between the damage due to fresh and salt water floods (not in the Netherlands)
2) the maximum damage amounts are based on the replacement value. When using the replacement value as basis for the maximum damage amount, it is assumed that an 'identical' object can be obtained. A 6-year-old car is replaced with an 'identical' 6-year-old car.
3) no distinction is made between high- and low-frequency flooded areas.
4) the damage is determined by the (maximum) water depth.

Damage calculation method
The general expression used to determine damage due to floods is (Vrisou van Eck et al 1999):

$$S = \sum_{i=1}^{n} \alpha_i n_i S_i$$

whereby:

n the number of damage categories

α_i damage factor category i, this depends on the flood depth (the waves and velocity) deduced from a damage function

n_i number of units in category i

S_i maximum damage (based on the replacement value) per unit in category i

The damage functions are based on observations made during the storm of 1953, but adjusted afterwards. These adaptations are limited as to the damage, but are quite significant as to the casualties, thanks to advances in warning possibilities.

The calculation is generally made on the basis of a grid. For each grid cell the damage per category is determined and then the total damage in the area is calculated by summing the damage of all grid cells. The accuracy of the calculated damage of course depends on the cell size chosen. The smaller the cell size, the more accurate the result. However, the calculation time increases if the cell size decreases. An excessively large cell size, however, does not result in loss of information. If an area is highly fragmented, the use of grid cells may result in an excessive simplification of the reality.
An alternative method would be to use vectors instead of a grid. The disadvantage, however, is that this results in much longer calculation times.

The flood maps were categorised conservatively into categories of 25 cm. This means that all water levels are replaced by the larger multiple of 25. All water is assumed to be salt water.

Furthermore, thresholds have been implemented for houses and industry. With these land uses it is assumed that the objects sustaining damage are higher than the ground level. For houses a threshold of 1 category was used (25cm), for industry it is 2 categories (50cm). Because a conservative categorisation into depth categories was first made of the flood map, the actual threshold for houses lies between 1 and 25 cm and for industries between 26 and 50 cm. With regard to roads, it is assumed that a small water depth does not cause any significant damage. So, after categorisation of the water depth, a threshold of 50 cm is determined (in reality, this is 26 to 50 cm).

10.1.3.1. Damage to houses

For the number of houses, the data of the last census were used, as available on the level of the static industry. This is the census of 1991. The houses are spread homogeneously over the built-up area, taking into account the various building density categories. The density in the “Buildings I” category was assumed three times greater than the “Buildings III” category and the density in the “Buildings II” category twice as great as the “Buildings III” category.

The value of houses was split up in accordance with the categorisation from the “Trends Real-estate Guide” and are recalculated to the mid-2002 situation. For household effects, a maximum amount of 50% of the value of the house in a certain area was considered.

With regard to the damage functions, the functions were used household effects as described in Vanneuville et al. (2002), p. 32-33. For the houses themselves, the adjusted damage function for salt water was used (Vanneuville et al. 2003a, p. 6-7).

For indirect damage, the functions were used as described in Vanneuville et al. (2002, p. 21-22). These range from 15% of the direct damage with an initially small direct damage to 1% of the direct damage with a direct damage equal to the potential direct damage.

10.1.3.2. Damage to industry

With regard to the number of employees, the data were used which were made available by the Social Security Service (RSZ) including the employees per municipality for 2003. This list contains the employees in the municipality where the company's registered offices are located, and not the actual location of employment.

For the calculation of the damage using the number of employees as key, the damage is assumed to be twice as great in places with an "Industry I" land use than in places with an "Industry II" land use.

The damage to industry is determined on the basis of the number of employees and on the basis of the surface area, whereby the eventual damage is determined by means of the maximum of both calculations.[3]

For the maximum damage per employee and per industrial surface area, the data were used as determined in Vanneuville et al. (2002) and recalculated in accordance with the consumer index based on the mid-2002 situation. For the damage functions, the functions were used as described in Vanneuville et al. (2002, p. 32-33). The maximum (direct) damage per employee amounts to € 175820. The maximum (direct) damage according to the method depending on the surface area is € 96.2267 / m².

The indirect damage was calculated on the basis of the formulas from Vanneuville et al. (2002, p. 24). These range from 45% of the direct damage with an initially small damage to 35% with a direct damage equal to the potential damage.

10.1.3.3. Infrastructure and airport

The "Infrastructure I" and "Infrastructure II" categories have the same damage and damage function as the direct damage to industry, calculated in accordance with the surface area method.

For the "Airport I" category, damage and damage function are equal to those of the "Infrastructure" category. For the "Airport II" category, the damage is considered equal to € 0 / m². Thus there is no damage function.

The maximum direct damage in Flanders is € 96.2267 / m² everywhere. There is no indirect damage.

10.1.3.4. Recreation

For damage to recreation, the maximum damage is used as described in Vanneuville et al. (2003a, p. 9). This is € 0.054 / m² everywhere in Flanders.

The damage function is identical to the damage function for salt water and described in Vanneuville et al. (2002, p. 32-33).

10.1.3.5. Orchards, arable farming and meadow

For arable farming and meadow, hereafter called agriculture, the maximum damage is taken from Vanneuville et al. (2003a, p. 9). It is equal to twice the maximum damage with a fresh water flood plus a fixed amount of € 0.05 / m².

[3] In reality, the damage is determined in 2 ways for every return period considered in the project, after which these damage amounts are combined into to 2 risk maps (1 on the basis of the industrial surface area and 1 on the basis of the employees for damage and risk to industry). These 2 risk maps are used to calculate the maximum.

The maximum damage for arable farming thus depends on the agricultural region (Vanneuville et al. 2004: addendum B), the maximum damage for pasture is equal to € 0.146 / m² + € 0.05 / m². The damage functions and the indirect damage (10% of the direct damage) are identical to those of salt water and are described in Vanneuville et al. (2002, p. 26, 32-33).

For orchards the damage function is equal to the damage function for arable farming, but the maximum damage differs. In the "Damage functions for forests and orchards" (Vanneuville et al. 2004: addendum C) note, a price of € 2.96 /m² + € 0.05 / m² for the addition of lime is determined for a salt water flood.

10.1.3.6. Vehicles

To determine the number of vehicles, the most recent available data are used on the level of the statistical sector, i.e. the census of 1991. The vehicles aggregated to municipality level. The value of the vehicles is the value calculated in Vanneuville et al. (2002), i.e. € 4627 per vehicle. The vehicles are distributed homogeneously over the "Buildings I, II, III", "Industry I, II" and "Infrastructure I, II" categories.

Of all the vehicles, it is assumed that only 30% is located in the floodable area at the moment of flooding, and that the rest has been evacuated. The damage function used is the damage function described in Vanneuville et al. (2003a, p. 8).

10.1.3.7. Water, nature and forests

For these land use categories the damage is considered equal to € 0 / m², thus there is no damage function (see Vanneuville et Al. 2002 and 2004: addendum C).

10.1.3.8. Roads and railways

The damage function for roads and railways is $f = MIN(0{,}28 * d; 0{,}18 * d + 0{,}1; 1)$ (shown in Figure 140)

The maximum damage for railways was obtained from the Belgian railway company (NMBS), for roads the information was obtained from the Ministry of the Flemish Community, Roads and Traffic Administration.

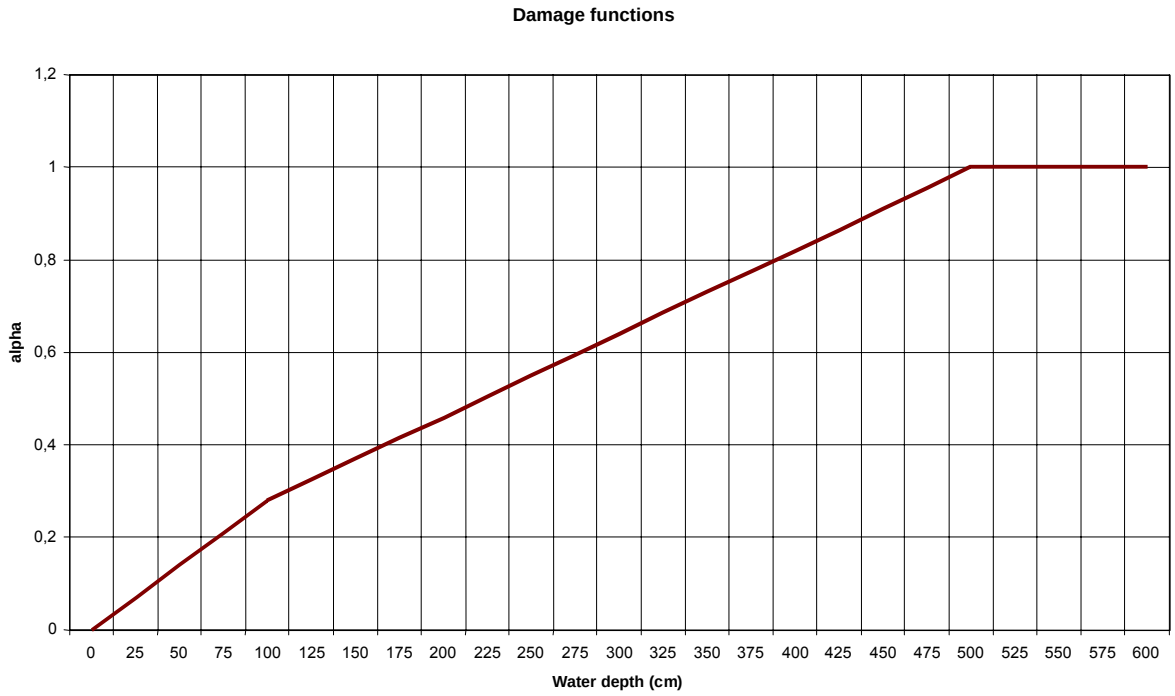

Figure 140: Damage function, damage factor alpha depending on the water depth for roads and railways (Source: Technical Advisory Committee for Water-retaining Structures (TAW), Vrisou van Eck et.al., 1999, p. A-6).

In the table below, the damage functions as applied in the Flemish method are compared with those of the Dutch method. The damage functions from the Dutch method are usually shown as different branches, while the damage function of the Flemish method consists of a line.

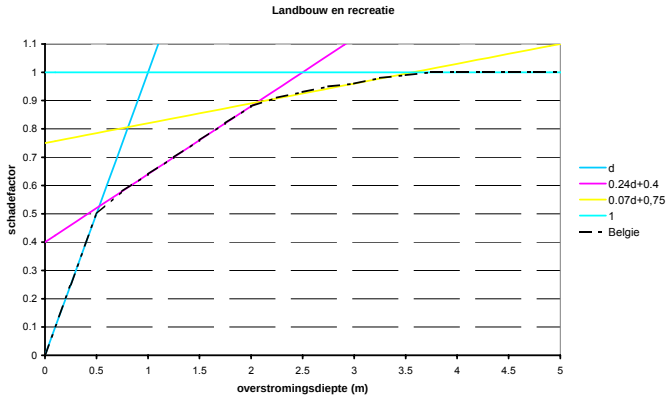

Agriculture

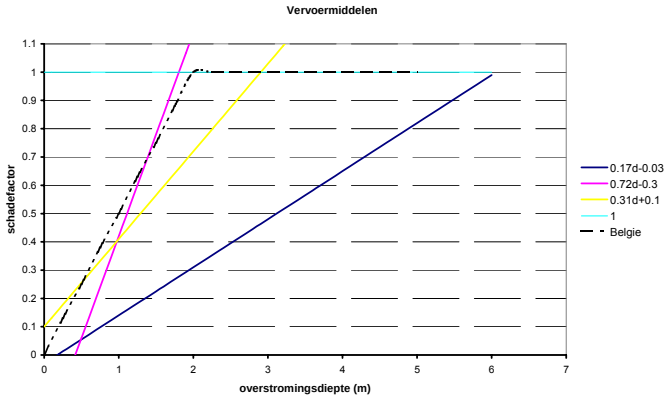

means of transport

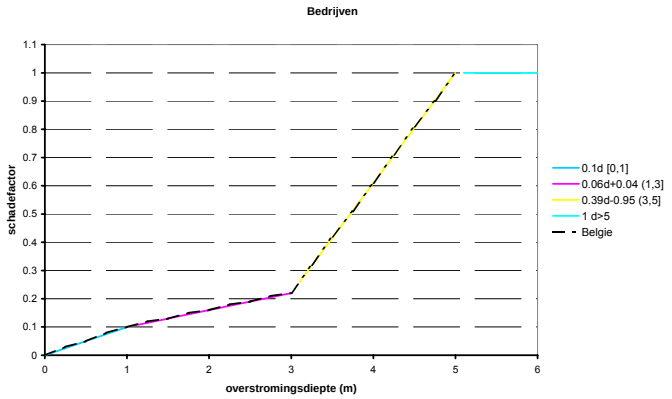

companies

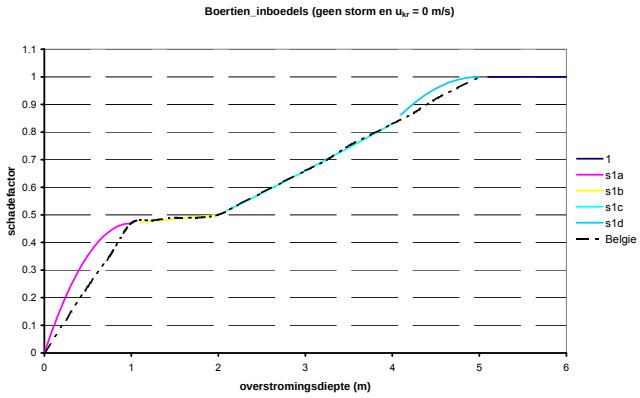

furniture

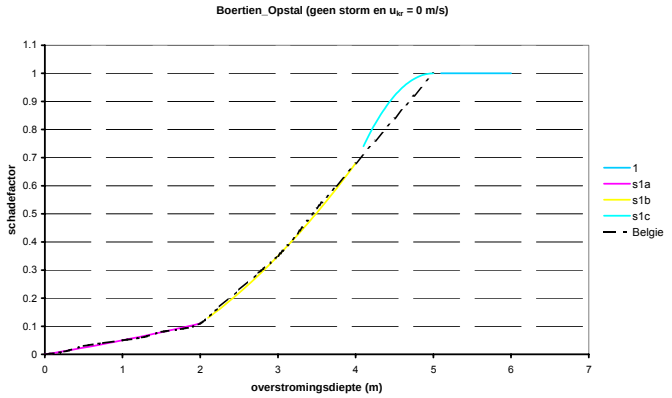

buildings

For buildings in the Netherlands, a collapse of houses due to a high velocity is also taken into account. Depending on the typical building, it amounts to 4 to 8 m/s. However, these velocities are reached nowhere.

The indirect damage in Flanders depends on the direct damage. In the Netherlands separate damage functions are drawn up, consisting of two categories:

- damage to suppliers and purchasers outside the dike ring area due to the (partial) loss of turnover. This damage is calculated on the basis of the added value per job or hectare multiplied with a sector-specific multiplier. The multiplier, calculated on a national scale, does not take into account substitution effects outside the dike ring area and suppliers in

the dike ring area (these have already been processed in the direct damage of a dike ring area). This means that the application of the multiplier may be an overestimation of the actual damage. This overestimation is greater as the flooded area is greater. For these reasons a reduction factor can be given in the Standard method for indirect damage. The standard value for this reduction factor with indirect damage is set at 0.25;

- damage due to the cutting of transport lines, approximated by means of loss of travel time.

10.1.4. Land use

10.1.4.1. Flanders

Three different source documents were used as land use maps. To determine the land use of areas, “CORINE Land Cover” (CLC) was used (NGI, distributed by OC GIS Flanders) and the “Small-scale land use file for Flanders and Brussels” (KBG) (OC GIS Flanders). For CLC the version issued in 1995 (1989 records) was used, for KBG the version issued in 2003 (2001 records) was used. These data were combined as indicated in the contingency table (Table 51).

Top50-v GIS files (NGI) were used for the line elements, particularly the “roadnet” and “railnet” data layers. The combination of the attribute data in these files into different railway and road types with the potential damage is described in Vanneuville et al. (2003c).

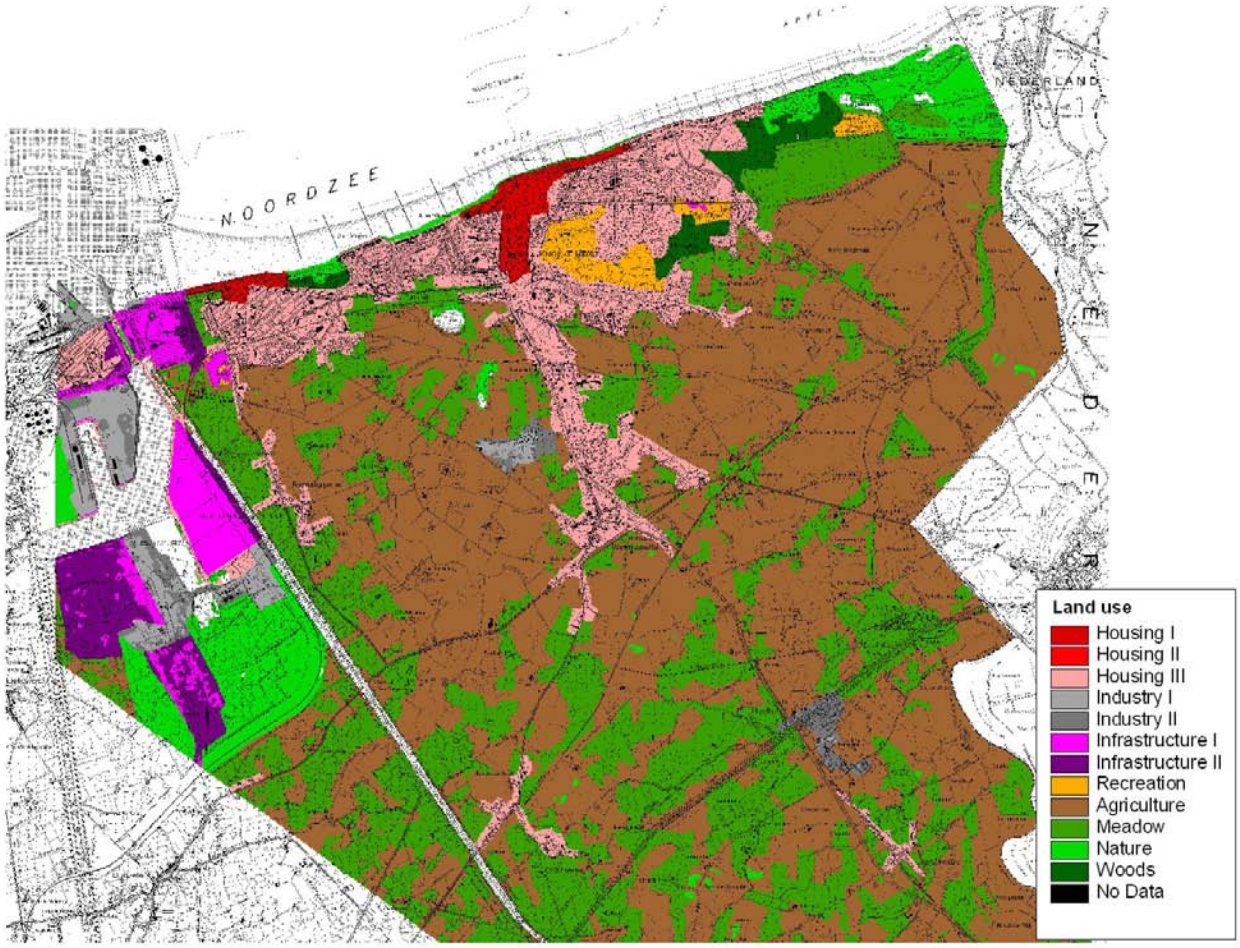

Figure 141Land use map for Flanders (background: topographic map 1:10000 c NGI Belgium)

To calculate the damage, a grid was used of 20 by 20 metres.

KBG

			0 Background	1 Nucleated city building	Buildings	3 Industry and trade	4 Infrastructure	5 Seaport	6 Airport	10 Open-space development	21 Arable farming	23 Pasture (+ crops	28 Wet pasture	29 Orchard	31 Deciduous	32 Coniferous	33 Mixed forest	Beach/dune	52 Freshwater surface	201 Motorway	202 Regional road
		CODE:	0	1	2	3	4	5	6	10	21	23	28	29	31	32	33	37	52	201	202
	111 Continuous building	111	Buildings I	Buildings I	Buildings II	Industry I	Buildings II				Buildings I	Buildings I				Buildings II		Nature	Buildings I		Buildings I
	112 Discontinuous building	112	Buildings III	Buildings I	Buildings III	Industry I	Buildings III	Industry I		Buildings III	Buildings III	Buildings III	Buildings III	Buildings III	Buildings III	Buildings III	Buildings III	Nature	Buildings III	Buildings III	Buildings III
	121 Industrial or commercial areas	121	Industry I	Industry I	Industry I	Industry I	Industry I	Industry I		Industry II	Industry II	Industry II	Industry II	Industry II	Industry II	Industry II	Industry II	Nature	Industry II	Industry I	Industry I
	122 Roads and railways with corresponding surfaces	122	Infrastructure I		Infrastructure I	Infrastructure I	Infrastructure I	Industry I		Infrastructure I	Infrastructure II	Infrastructure II	Infrastructure II	Infrastructure II	Infrastructure II	Infrastructure II		Nature	Infrastructure II	Infrastructure I	Infrastructure I
	123 Port areas	123	Industry I		Industry I	Industry I	Industry I	Industry I			Industry II	Industry II		Industry II	Industry II	Industry II		Nature	Industry II		Industry I
	124 Airports	124			Airport I				Airport I		Airport II	Airport II		Airport II	Airport II	Airport II					
	131 Exploitation sites	131			Recreation						Recreation	Recreation	Recreation	Recreation	Recreation	Recreation		Nature	Recreation		Recreation
	132 Landfills	132			Infrastructure II						Infrastructure II	Infrastructure II		Infrastructure II		Infrastructure II		Nature	Infrastructure II		
	133 Construction areas	133	Infrastructure II		Infrastructure I	Infrastructure I	Infrastructure I	Infrastructure I			Infrastructure II	Infrastructure II		Infrastructure II	Infrastructure II	Infrastructure II		Nature	Infrastructure II		Infrastructure I
	141 Green urban areas	141		Buildings II	Buildings III		Buildings III			Buildings III	Arable farming	Pasture		Fores	Fores	Fores			Water		Infrastructure II
	142 Sports and recreation areas	142	Recreation	Infrastructure I	Infrastructure I	Infrastructure I	Infrastructure I				Recreation	Recreation	Recreation	Recreation	Recreation	Recreation	Recreation		Water	Recreation	Recreation
CORINE	211 Non-irrigated arable land	211	Arable farming		Arable farming	Arable farming	Arable farming				Arable farming	Arable farming	Arable farming	Orchard	Arable farming	Arable farming	Arable farming	Nature	Arable farming	Arable farming	Arable farming
	222 Orchards	222	Orchards		Orchards						Orchards	Orchards								Orchards	
	231 Pasture	231	Pasture	Pasture	Pasture	Pasture	Pasture	Pasture			Pasture	Pasture	Pasture	Pasture	Pasture	Pasture	Pasture	Nature	Pasture	Pasture	Pasture
	242 Agricultural area with complex parcelling	242	Arable farming		Arable farming	Arable farming	Arable farming	Arable farming			Arable farming	Pasture	Pasture	Pasture	Pasture	Pasture	Pasture	Nature	Pasture	Arable farming	Arable farming
	243 Agricultural area with presence of natural vegetation	243	Nature		Pasture	Pasture	Pasture				Arable farming	Pasture	Pasture	Pasture	Nature	Nature	Nature	Nature	Nature	Nature	Nature
	311 Deciduous	311	Fores		Fores	Fores	Fores			Fores	Fores	Fores	Fores	Fores	Fores	Fores	Fores		Water	Fores	Fores
	312 Coniferous forest	312			Fores	Fores	Fores		Fores		Fores	Fores	Fores	Fores	Fores	Fores	Fores		Water	Fores	Fores
	313 Mixed forests	313			Fores	Fores					Fores	Fores	Fores	Fores	Fores	Fores	Fores		Water	Fores	Fores
	321 Natural grassland	321			Pasture						Pasture	Pasture						Nature			
	322 Heath and bush	322	Nature	Nature	Nature	Nature	Nature	Nature			Nature	Nature	Nature	Nature	Nature	Nature		Nature	Water	Nature	Nature
	324 Transitional forest	324	Fores	Fores	Fores						Bos	Bos			Fores	Fores			Water		
	331 beach, dunes and sand surfaces	331	Nature		Nature			Nature			Nature	Nature						Nature	Natuur		
	411 Marshland	411	Nature		Nature			Nature			Nature	Nature		Nature	Nature	Nature			Water		
	421 Salt marshes	421	Nature		Nature						Nature	Nature						Water	Water		
	423 Mud flats	423	Nature		Nature						Nature	Nature							Water		
	444 Non-categorised / unknown	444	Water																		
	511 Waterways	511	Water	Buildings II	Buildings III	Industry I	Infrastructure I	Infrastructure I			Arable farming	Pasture	Pasture	Orchard	Fores	Fores			Water	Water	Water
	512 Water surfaces	512	Water		Buildings III		Infrastructure I	Infrastructure I			Nature	Nature	Nature	Nature	Nature	Nature	Nature	Water	Water	Water	Water
	522 Estuaries	522	Water		Buildings III	Industry I	Infrastructure I				Nature	Nature			Nature	Nature			Water	Water	Water
	523 sea	523	Water		Water			Water			Water	Water						Water	Water		

Table 51Contingency table for land use

10.1.4.2. The Netherlands

In the Netherlands the use of the 1996 CBS land file, codes bg_93, is opted for. This file was made on December 16, 1999. The following CBS categories are used: agricultural land, built-up land, forests, recreation and traffic.

In the Netherlands a grid of 100 by 100 m is used.

10.1.5. Casualties

To determine the casualties, the maximum water depth and maximum rise speed are used. For the maximum water depth, the flood map is used.

The project includes flood maps giving the situation every 30 minutes. Using these flood maps, the rise speed is determined for every situation in the previous hour, after which the maximum is selected per pixel.

The data used to determine the number of persons per statistical sector, are the tables from the most recent census for which these data are already available, i.e. the census of 1991.

It is assumed that 50% of the people were able to leave the flooded area and that everyone is in the areas with “Buildings I, II, III” land use category, in accordance with the same distribution key for the concentration as for the houses. This means that per surface unit 3 times more people are located in the “Buildings I” category than in the “Buildings III” category and that twice as many people are located in the “Buildings II” category than in the “Buildings III” category.

The formulas used to determine the number of casualties on the basis of maximum water depth and maximum rise speed are those described in Vanneuville et al. (2003 b, p. 5-7).
The risk of casualties is largely determined analogous to the determination of the material risk. The maximum number of casualties (expressed here in m²) is the number of people present[4].

The number of casualties N for a certain event with a return period T is then:

$$N = f_d * f_w * A$$

whereby
- A the number of people present per surface area (here m²)
- f_d drowning factor depending on the flood depth
- f_w drowning factor depending on the rise speed

(Vrisou van Eck, 1999b, p. 5-1, 5-3)

The drowning factor on the basis of the water depth can be obtained with the formula (Vrisou van Eck et. al. 1999b, p. 5-1):

$$f_d = \exp(1{,}16 * d - 7{,}3)$$

[4] This number of people present is an average, assuming a homogeneous density over the entire built-up area (see Vanneuville et.al. 2002)

with *d* as water depth (flood depth) in metres (also see figure 1).

As in Vanneuville et.al. (2002, p. 30), the water depths are categorised conservatively in 25 cm categories. The same threshold value is entered as for the damage to houses (where all persons are assumed to be), i.e. 1 category (25cm, in reality between 1 and 25cm).
Figure 1: drowning factor for water depth

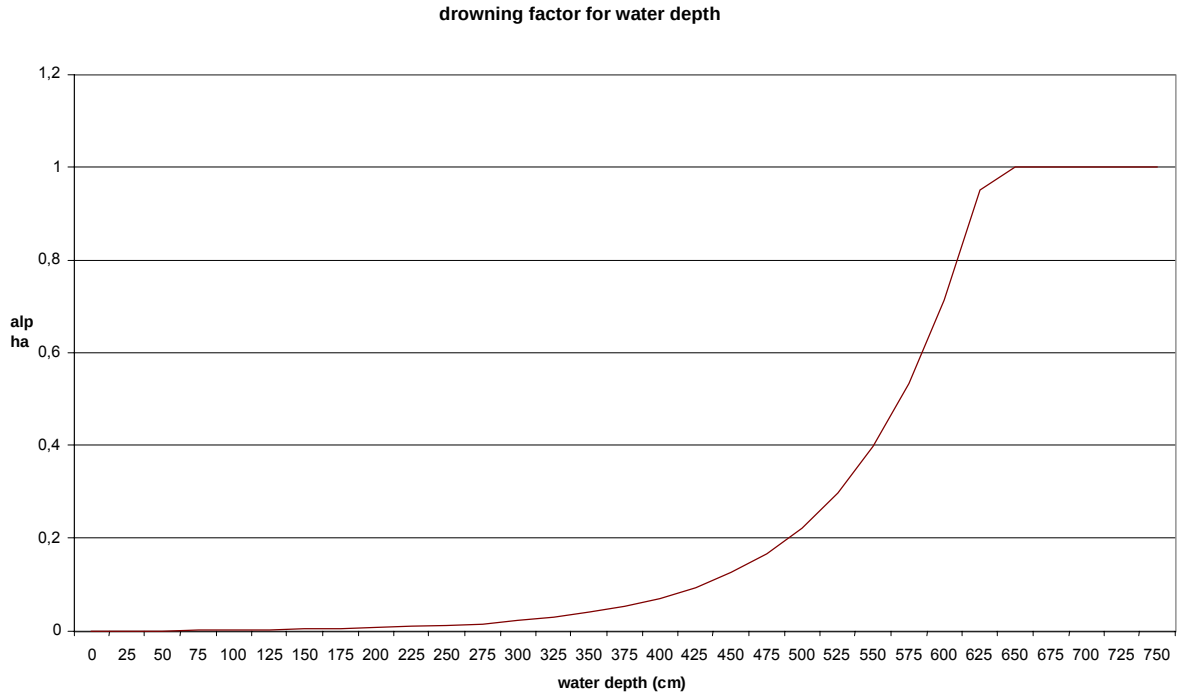

The drowning factor resulting from the rise speed can be defined as follows (Vrisou van Eck et. al. 1999b, p. 5-3):

$f_w = 0$ for $w \le 0{,}3$

$f_w = 0{,}37 * w - 0{,}11$ for $0{,}3 < w < 3{,}0$

$f_w = 1$ for $w \ge 3{,}0$

whereby the rise speed *w* is expressed in m/hour!

In the Netherlands a method with and without evacuation exists.

In this method the number of casualties solely depends on the maximum flood depth.

$$N_d = f_0 N_i = \exp(1.16d - 7.3) N_i$$

with: N_d = number of casualties resulting from flood

f_0 = drowning factor

N_i = number of people present in the area during the flood

d = flood depth (m)

The drowning factor f_0 in function of the flood depth can be read from Figure 142.

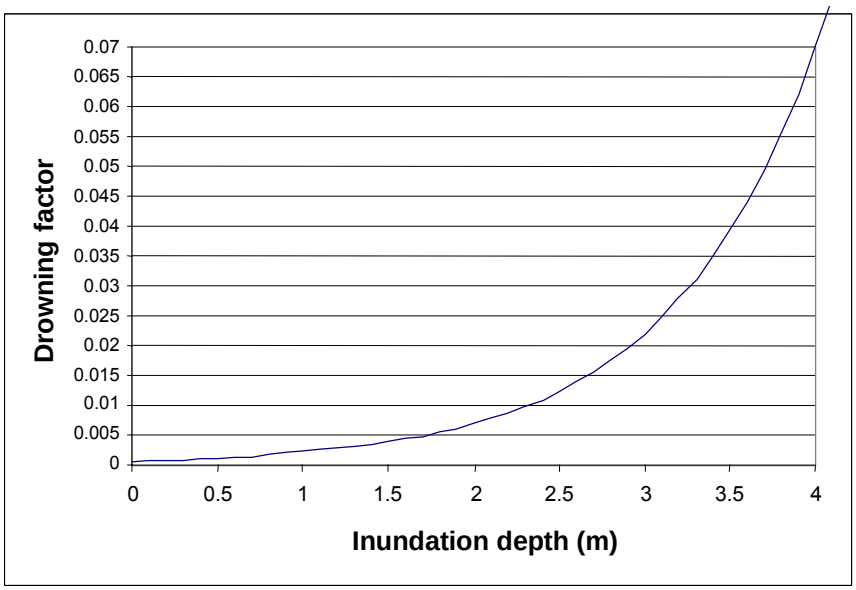

Figure 142 Drowning factor, numbering not yet uniform

Alternatively, evacuation can also be taken into account. f is then a function of the rise speed (w) and the water depth (d):

$f = 0 \; if \; d < 3m \, or \, w < 0.3m/h$

$f = 1 \; if \; d > 6.25m \, and \, w > 2.0m/h$

$f = \min(\max(8.5\exp(0.6d - 6) - 0.15,0),1) * \min(\max(8.5 * \exp(1.2w - 4.3) - 0.15,0),1)$

The factor f_{ng} does not take into account the influence of high-rise flats on the number of people, who are not saved. In case of flood, residents of high-rise flats will have a greater chance of being rescued. After all, they can get to safety on higher levels. The standard method does not take into account the influence of high-rise flats on the number of casualties, because it is expected that the influence is low and because there is no knowledge regarding the effect of high-rise flats on the number of casualties.

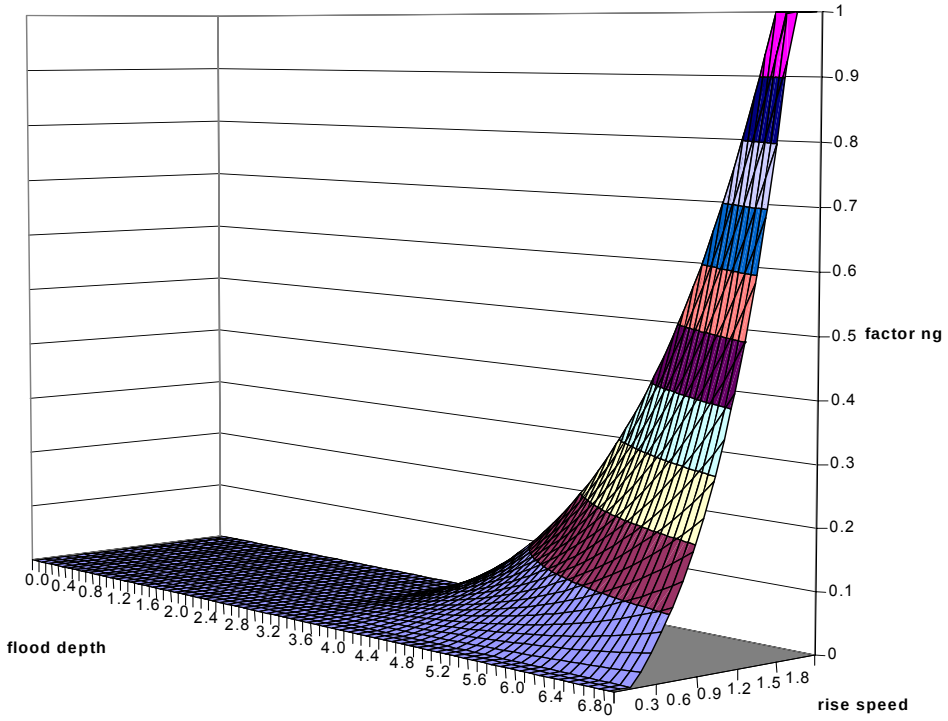

Figure 143the factor fng

10.2. Results

The results for the 4 scenarios are summarised in tables below for Flanders and the Netherlands.

	T=1000	T=4000	T=10000	T=40000
Buildings	0	35730	196446	295606
Furniture	0	38992	176130	303110
Means of transport	0	1133	2703	6735
Companies	0	0	0	51951
Infrastructure	0	392	1015	5087
Recreation	0	9	24	50
Arable agriculture	0	498	2248	9931
Meadow	0	123	371	2231
Orchards	0	0	1	8
Railway	0	0	0	1716
Roads	0	1559	6648	25684
Total excl casualties	0	78436	385586	702108
casualties	0	0	2	4

Table 52 Damage in Flanders (x1000 euro)(evacuatie factor: 50%)

		T=1000	T=4000	T=10000	T=40000
agriculture	direct	280	3558	5046	42240
Cultivation under glass	direct	0	0	0	0
Urban area	direct	0	491	1451	43226
Recreation Extensive	direct	117	213	274	1845
Recreation Intensive	direct	1549	4628	5967	10098
airports	direct	0	0	0	0
National roads	direct	0	344	569	3459
High ways	direct	0	0	0	1974
Other roads	direct	248	972	1629	10365
Railways	direct	0	0	0	0
Means of transport	direct	8	17	31	428
Pump stations	direct	747	747	747	747
Sewage treatment plant	direct	0	0	0	0
Single family house	direct	1787	6512	11528	133852
Low rise building	direct	0	0	0	2116
High rise building	direct	0	0	0	242
Medium rise building	direct	0	0	0	5015
farms	direct	0	478	621	6056
minerals	direct	0	0	0	189
Building industry	direct	0	0	1	57
trade/Horeca	direct	26	72	121	818
Transport/Communication	direct	0	95	142	1596
Banks/assurance	direct	0	44	82	1604
administration	direct	0	4	7	47
Industry	direct	0	0	36	1427
Public utilities	direct	0	0	0	0
others	direct	0	0	0	21
agriculture	indirect	76	961	1362	11405
Cultivation under glass	indirect	0	0	0	0
National roads	indirect	0	39	64	388
Railways	indirect	0	0	0	0
minerals	indirect	0	0	0	3
Building industry	indirect	0	0	0	37
trade/Horeca	indirect	1	3	5	36
Transport/Communication	indirect	0	0	1	6
Banks/assurance	indirect	0	1	2	31
administration	indirect	0	0	0	0
Industry	indirect	0	0	2	90
Public utility	indirect	0	0	0	0
others	indirect	0	0	0	2
Airports	b.u.	0	0	0	0
Railways	b.u.	0	0	0	0
Minerals	b.u.	0	0	0	9
Building industry	b.u.	0	1	3	256
Trade/Horeca	b.u.	10	27	45	307
Transport/Communication	b.u.	0	14	21	238

Banks/assurance	b.u.	0	7	13	249
administration	b.u.	0	1	1	7
Industry	b.u.	0	0	8	317
Public utility	b.u.	0	0	0	0
others	b.u.	0	0	0	4
Total		4849	19229	29779	280807
casualties	direct	4	6	8	24

Table 53Schade in Nederland (x1000 euro)(evacuatiefactor: 50%)

This results in:

	Flanders	Zeeuws-Vlaanderen	Total
T=1000	0	4849	4849
T=4000	78436	19229	97665
"T=10000"	385586	29779	415365
T=40000	702108	280807	982915

Table 54total damage (x1000euro)

	Vlaanderen	Nederland	Totaal
T=1000	0	4	4
T=4000	0	6	6
"T=10000"	2	8	10
T=40000	4	24	28

Table 55 total number of casualties

The following maps give an overview of the locations of failure in resp. Flanders and Zeeuws-Vlaanderen for different return periods.

10.2.1. T=1000jaar

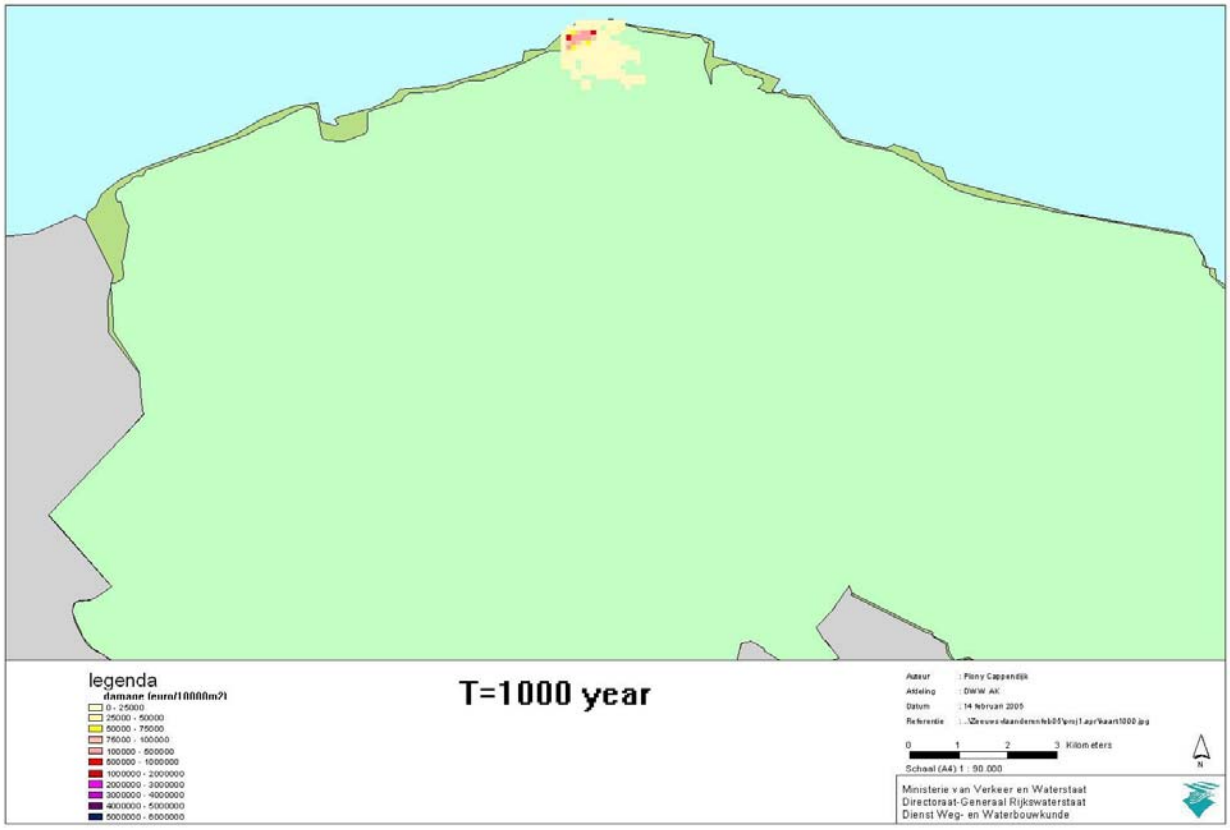

No damage in Flanders

10.2.2. T=4000 jaar

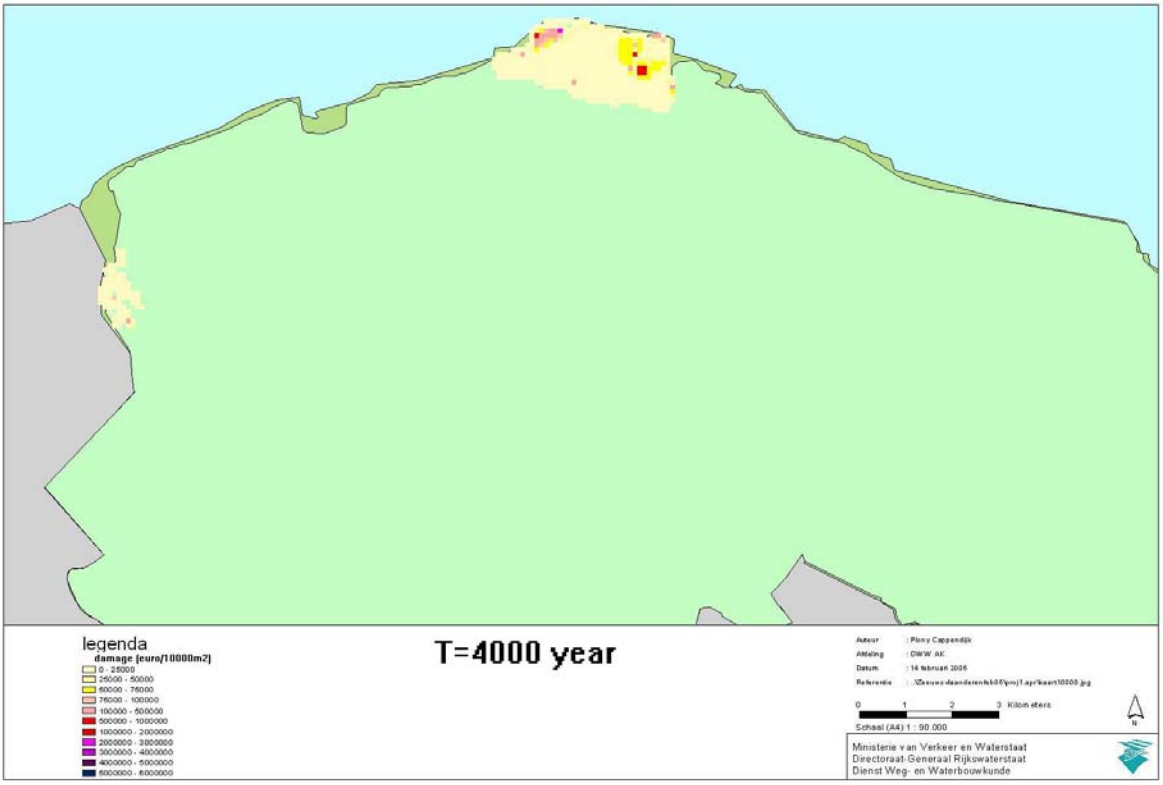

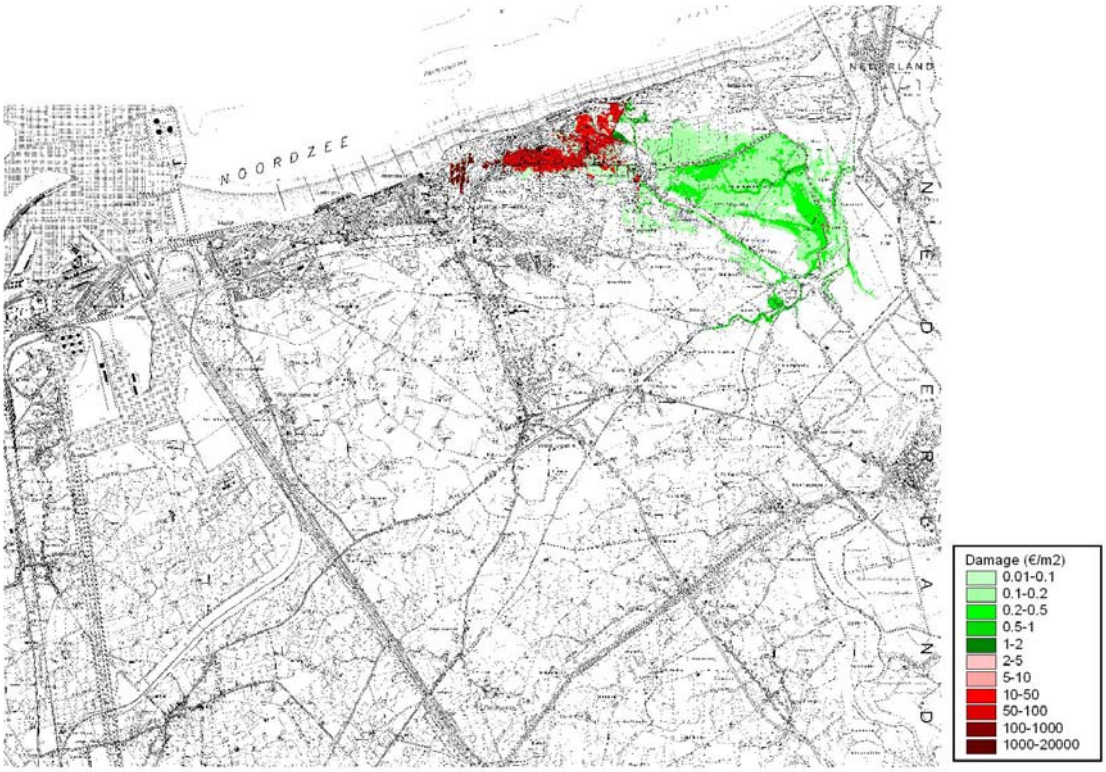

10.2.3. T=10000 jaar

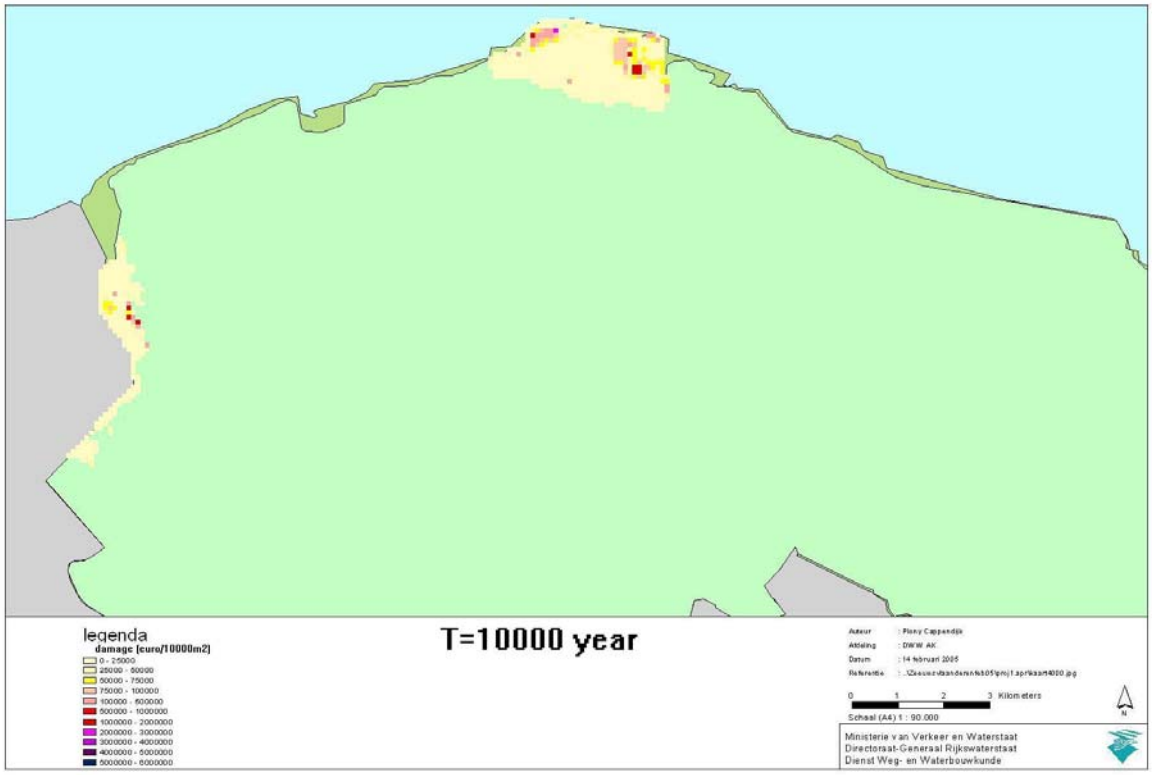

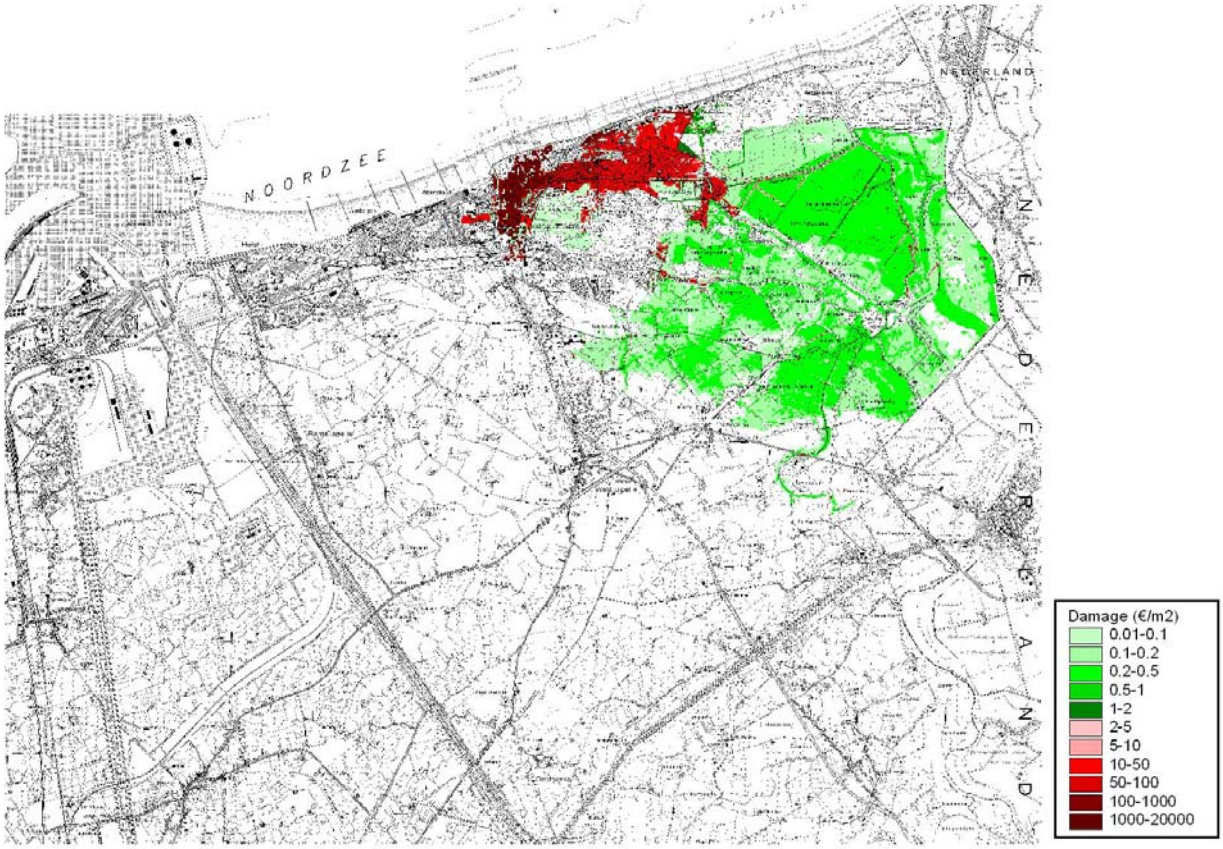

10.2.4. T=40000 jaar

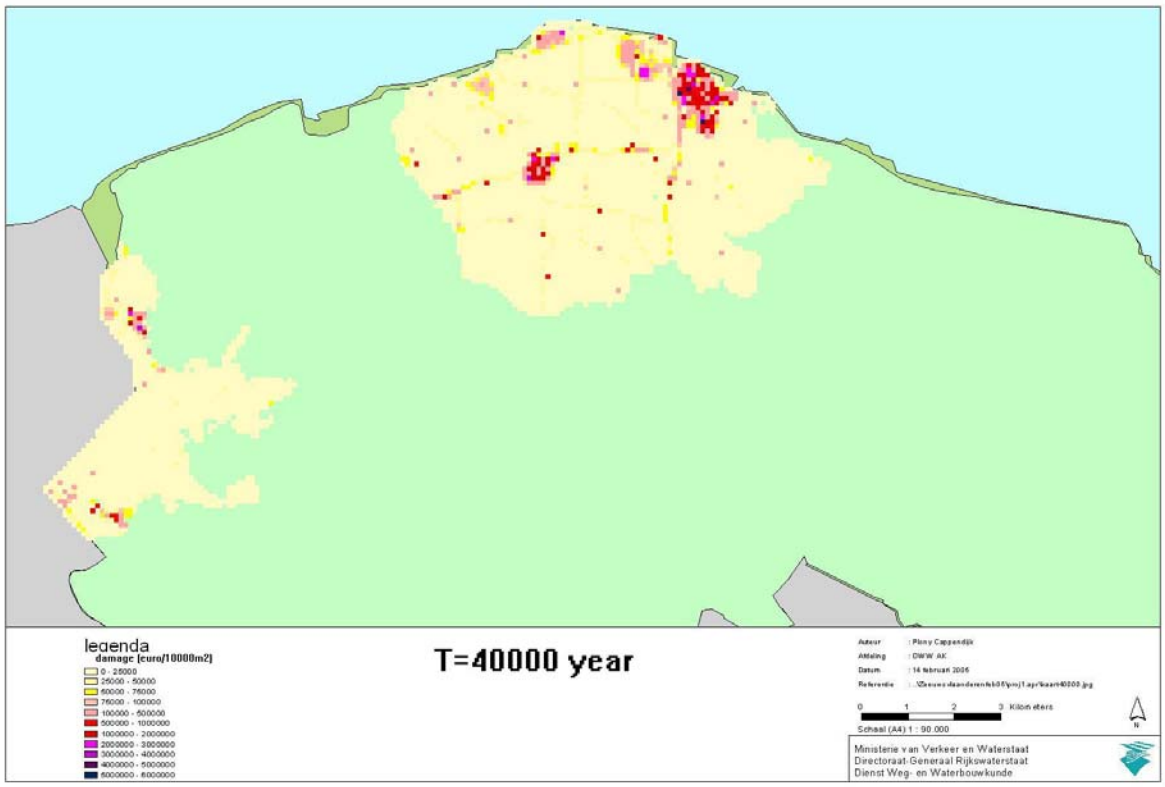

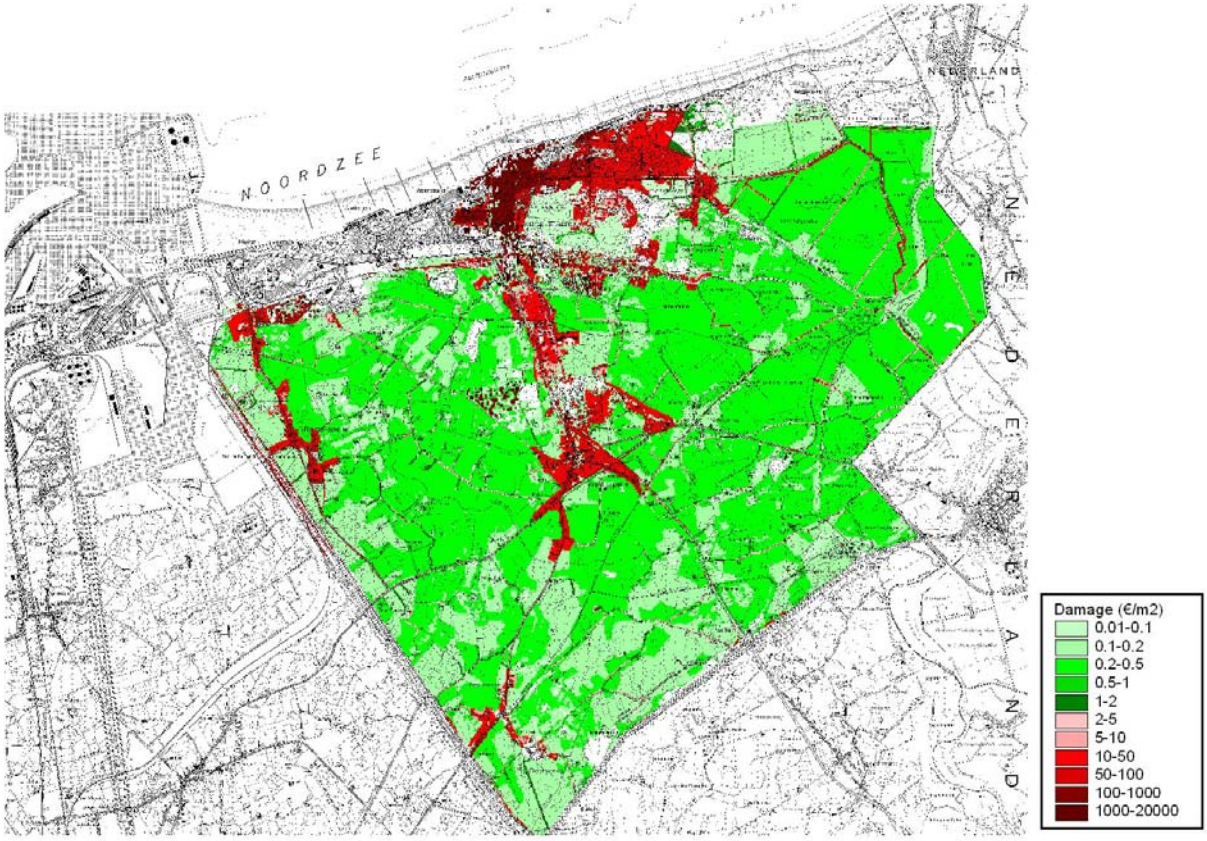

11. SENSITIVITY ANALYSIS

In this chapter the basic parameters are varied, if known the variation is taken equal to its standard deviation.

11.1. Dike failure Flanders

11.1.1. Sensitivity analysis of Durosta calculations

The overtopping discharge is strongly determined by the wave height in front of the toe of the dike and thus the beach profile in front of the dike. The erosion profile was always calculated by means of Durosta. There is always some uncertainty about the input parameters entered in Durosta: significant wave height, peak period, water level and grain diameter of the sand.

These parameters vary, whereby the variation is equal to the uncertainty about the parameter in question. For the grain diameter, the calculation diameter was used, as for the assessment of dunes (reduction of the grain diameter from 280 μm to 225μm). The sensitivity analysis was made for profile 238 for a return period of 4000 years. Using the original calculation, an overtopping discharge of <1l/s/m was calculated for the location. In other words, there was no risk of breach formation due to erosion by high overtopping discharges.

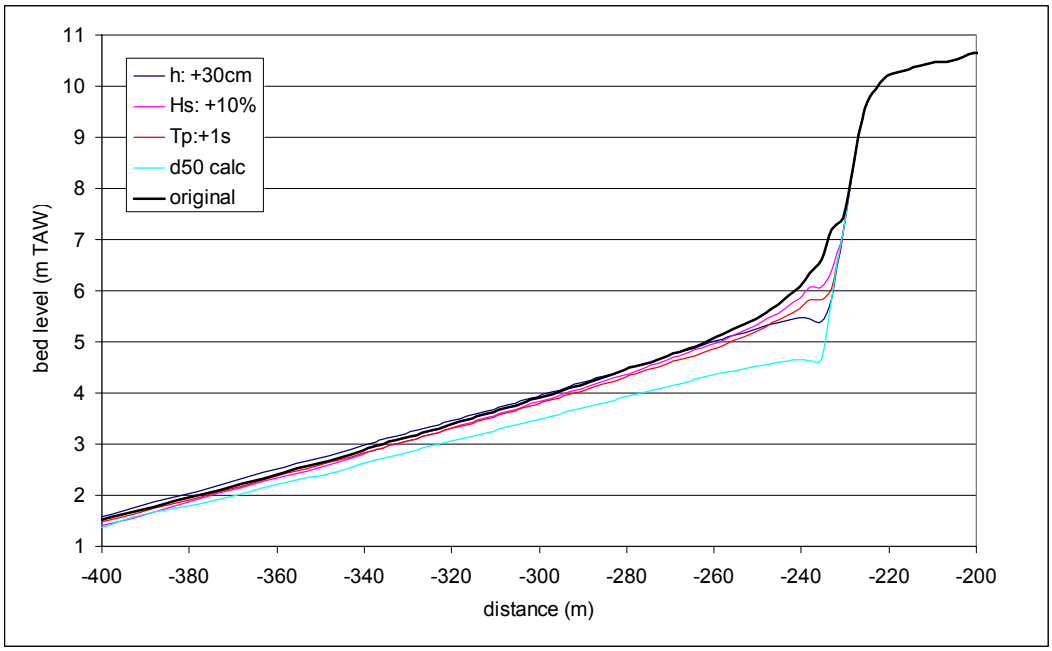

Figure 144 Sensitivity analysis for Durosta calculations p_235 (4000 years).

	$H_{s,70}$	H_s=0.9 d	q (l/s/m)
Original	2.3	0.9	0.7
H_s +10%	2.35	1.07	3.8
T_p +1s	2.4	1.3	10.5
h +30cm	2.39	1.88	72.2
$D_{50,calc}$	2.41	2.34	121.2

Figure 145 Sensitivity analysis of Durosta input parameters for overtopping discharges.

It is clear that for profile 235 (return period of 4000 years), some small variations of the input parameters have a significant effect on the overtopping discharges. The reason was that the original calculations included a small stretch of beach in front of the dike at a level of approx. +7m TAW. Especially a rise in water level and a smaller grain diameter cause a critical increase of the overtopping discharge for this profile.

Variation during the storm in case of a reduced grain diameter.

In a 4000-year storm the water level is 7.25m and the ground level at the toe of the dike is 6m, at the peak of the storm, resulting in a wave height of 1.1m. The following peak has a water level of 5.93 m and a ground level of 4.83 m, or a wave height of 1m. For the calculations, however, the deepest ground profile during the storm is used, combined with the highest water level. It is as if the highest peak occurs again at the end of the storm. It is conservative, but on the other hand it is justified, because the storm analysis shows that the storm can be highly asymmetric, whereby the peak in water level at the high water following the peak has only decreased slightly. A wave height of 2.34 m is thus used, whereas strictly theoretically the wave height at the toe of the dike is 1.1m at the most.

11.2. Dike failure The Zwin

11.2.1. Wave period

For the calculation of overtopping discharges the spectral wave period $T_{m-1,0}$ is always used. For the overtopping discharges to be calculated in the Zwin basin, this period is calculated based on the relation $T_p = 1.1 T_{m-1,0}$. In the Zwin basin a significant part of the wave energy is generated locally by the wind field. The consequence is that the peak period in the basin, calculated with Swan, can strongly vary (cf. Figure 146). The relation above would result in a much too low spectral wave period for some output points, giving an underestimation of the overtopping discharges. This is why the offshore wave period imposed was always used for T_p (for instance, 13.15s for a return period of 40000-years).

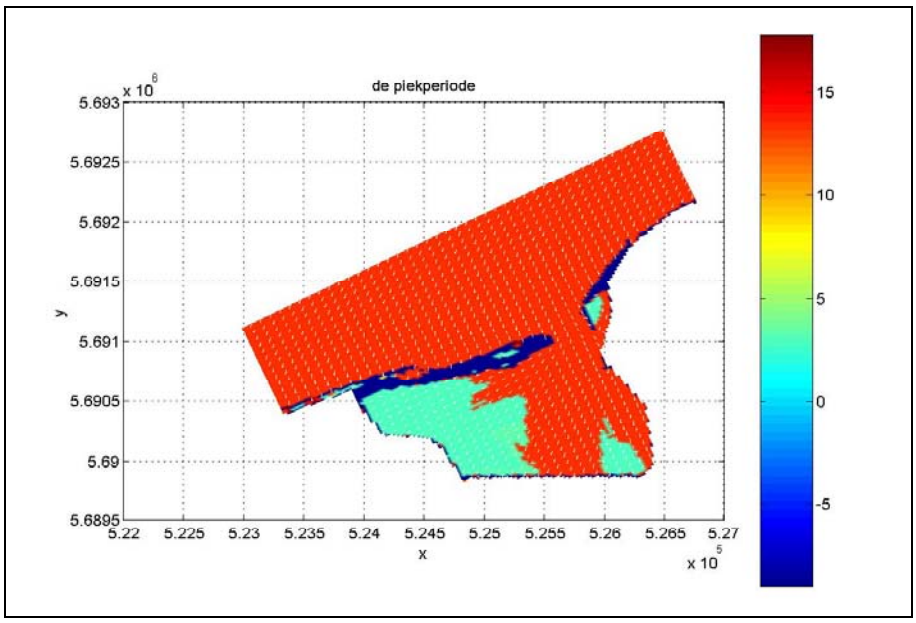

Figure 146 Peak period in the Zwin basin (wind direction NNE for 40000-year return period)

The method followed may imply an overestimation of the wave period $T_{m-1,0}$. But on the other hand, the SWAN calculations do not take into account the possible occurrence of long waves in the closed basin.

Nevertheless, the sensitivity analysis examines the effect of a longer wave period on the overtopping discharges. The most critical output point for the Zwin was nr. 16 with an overtopping discharge of 8.7l/s/m for a return period of 40000-years.

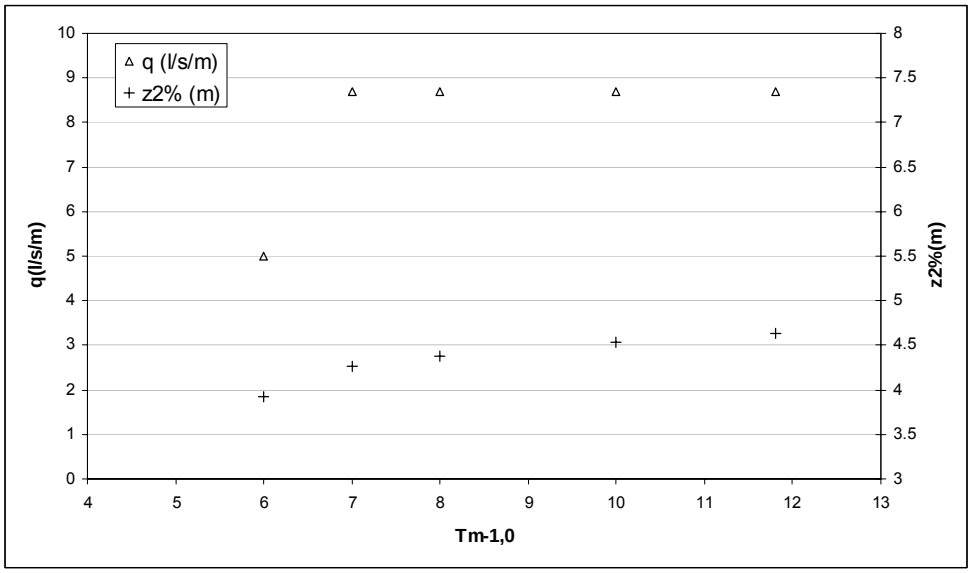

Figure 147 Sensitivity analysis of wave period for overtopping discharge q and wave run-up height z2% (Zwin output point 16 for a 40000-year return period).

Figure 147 shows the variation of the wave run-up and the overtopping discharge with a varying spectral wave period for outlet 16 in the Zwin basin for a 40000-year return period (h_s=1.36m). The wave run-up height gradually decreases as the wave period becomes smaller. Up to a wave period of 7s the calculated overtopping discharge is limited by the maximum criterion in the formulas, i.e. a variation of the wave period has no effect on the overtopping discharge with wave periods in excess of 7s in the calculations. For smaller wave periods the calculated overtopping discharge is strongly reduced.

11.2.2. Roughness factor of grass cover

For the calculation of the wave run-up height $z_{2\%}$ a roughness value is assigned to the covers on the outer slope. For dikes covered with grass (such as the Zwin), the literature gives a roughness factor γ_f =0.9 to 1.0. A value of 1.0 was assumed for the calculations made during the assessment. Below, the effect on the wave run-up heights and the related overtopping discharges are examined for all output points in the Zwin for a 40000-year return period.

Figure 148 and Figure 149 show the effect on the wave run-up height and the overtopping discharge for a variation of the roughness factor from 1 to 0.9 for the grass cover. This shows that the overtopping discharges decrease to 40% and more for Zwin dikes for a return period of 40000 years. The overtopping discharge at the most critical point could thus be limited to 5.7l/s/m.

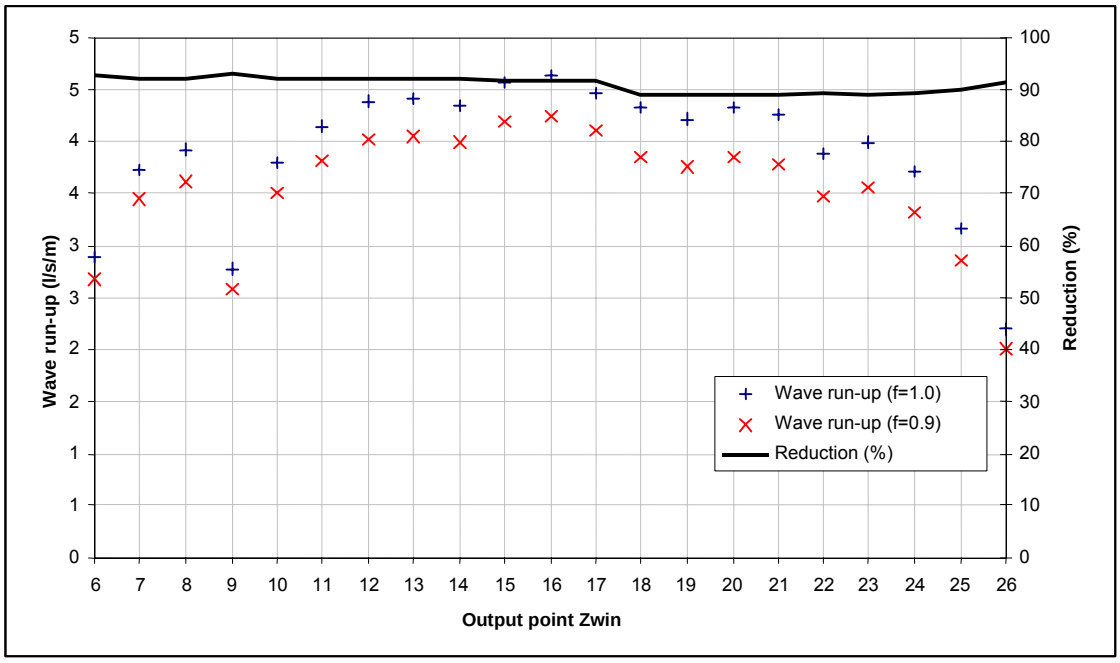

Figure 148 Sensitivity of wave run-up height with variation of roughness factor of the outer slope grass cover.

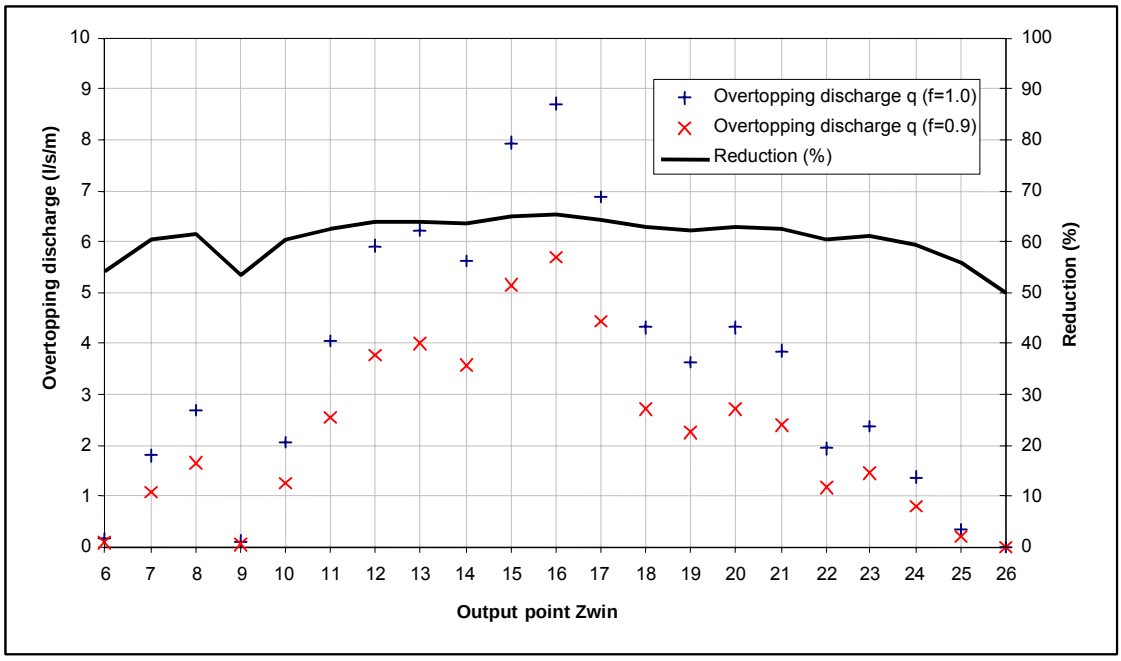

Figure 149 Sensitivity of overtopping discharge with variation of roughness factor of the outer slope grass cover.

11.2.3. Clay and grass quality

For the inner slope of the dikes around the Zwin a critical velocity is calculated under Assessment of the crest height (see §) which is barely resisted by the grass mat and the underlying clay layer for the entire duration of the storm. In the calculation method used, a quality value must be assigned to the grass cover and the clay. The erosion resistance c_g for a grass cover is between $3.3^{E}05$ (poor) and

1^E06 (good), the erosion resistance c_{RK} for clay is between 7000 (poor) and 54000 (good). For lack of detailed data about the quality, a poor quality was always taken into account, for both the grass and the clay.

For the Zwin dike a critical velocity of 6.9m/s was calculated for the overtopping water stability of the inner slope. Figure 150 clearly shows that the acceptable velocities over the steep inner slope of the Zwin dikes quickly increase with increasing grass and/or clay quality. For lack of proper quality data, a conservative calculation approach was opted for.

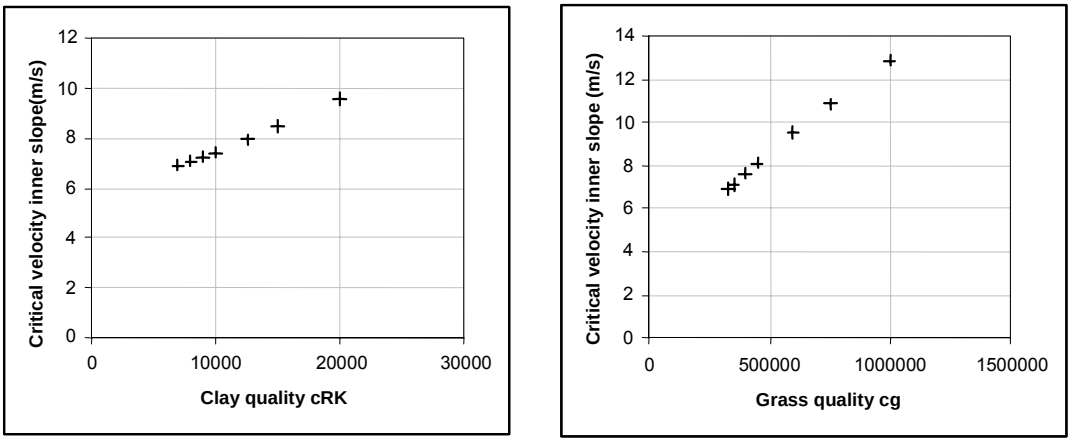

Figure 150 Sensitivity of critical velocity of the inner slope with varying clay and grass quality.

11.2.4. Crest height

For the Zwin dikes an average dike height of 10.7m TAW was defined, based on the available DTM, and used in the calculations. Nevertheless, it is possible that a lower or higher crest height may be present locally in some locations. For the most critical output point 16 in the Zwin basin, the effect of small crest height variations on the overtopping discharges is examined for a return period of 40000 years.

Figure 151 shows that for the case in question (Zwin output point 16, return period of 40000 years) a local 0.5m reduction results in a tripling of the calculated overtopping discharge. On the other hand, a somewhat higher crest height has a strongly reducing effect on the critical overtopping discharges.

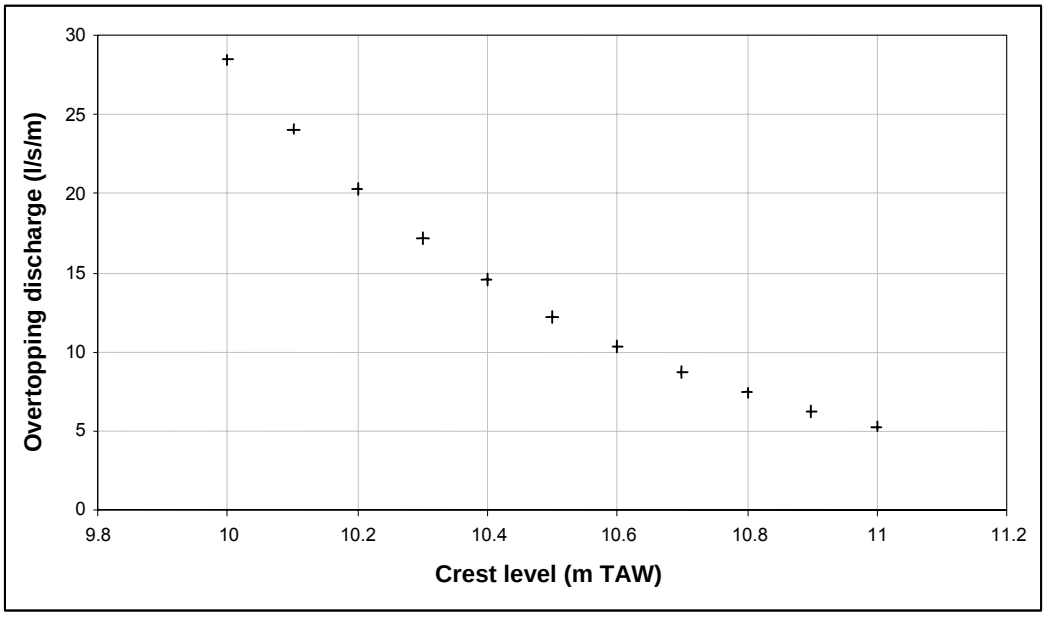

Figure 151 Sensitivity analysis: effect of crest height on overtopping discharges.

11.3. Dike failure Zeeuws-Vlaanderen

11.3.1. Macrostability of seaward slope

Some variants were considered for profile 512 (d_17). These were summarised in the table below:

name	φ	Phreat. level	FS	remarks
Basic case	27.5°	+5.4	0.66	Figure 67; FS=1: Figure 68
Variant 1	27.5°	**+3**	1.03	Figure 69
Variant 2	**32.5°**	+5.4	0.71	Figure 70; FS=1: Figure 71
Variant 3	**32.5°**	**+3**	1.10	Figure 72
Variant 4	**17.5°**	+5.4	0.5	**(weak) clay** assumed in dike: Figure 73 FS=1: Figure 74

Table 56: sensitivity analysis of macrostability of seaward slope

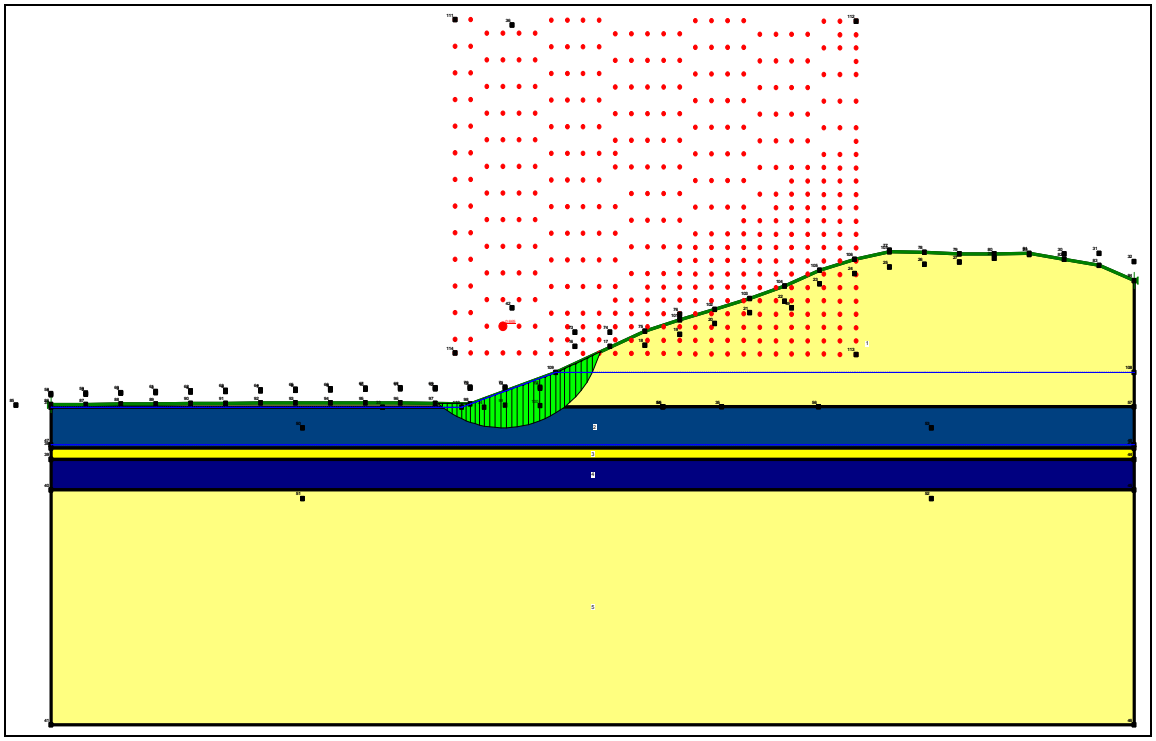

Figure 152 basic case ***FS=0.66***

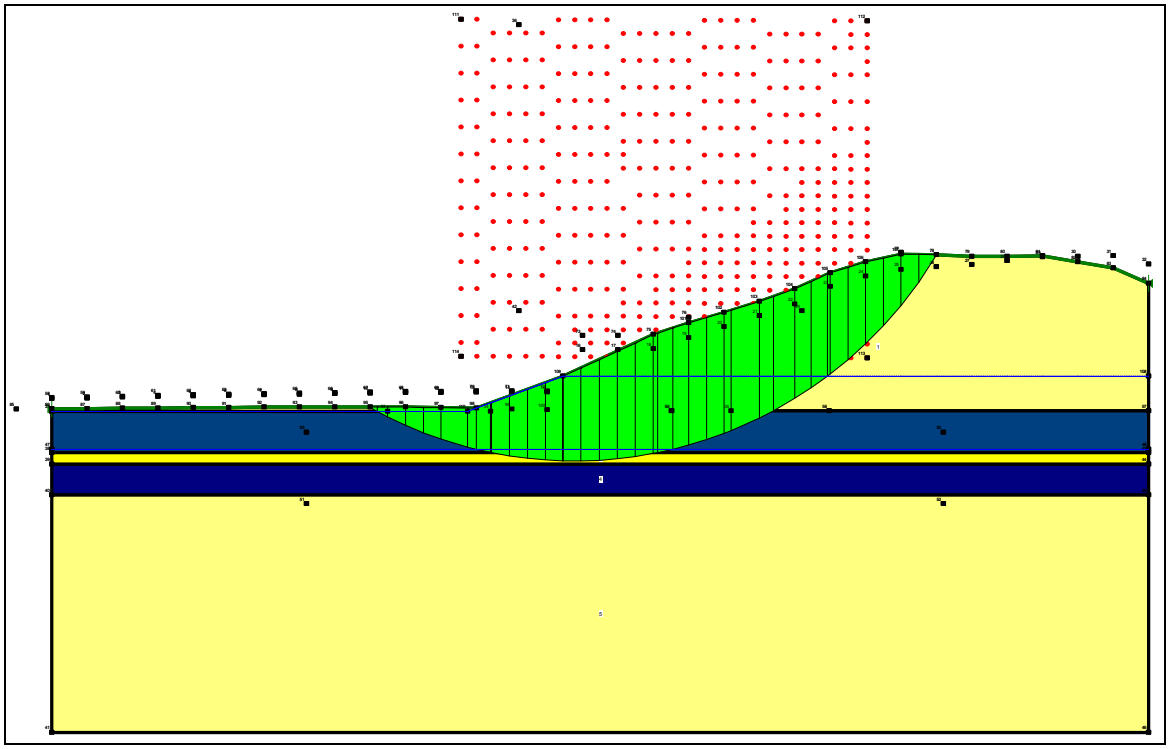

Figure 153 basic case ***FS=1.00*** *(already slip circle with FS=0.66).*

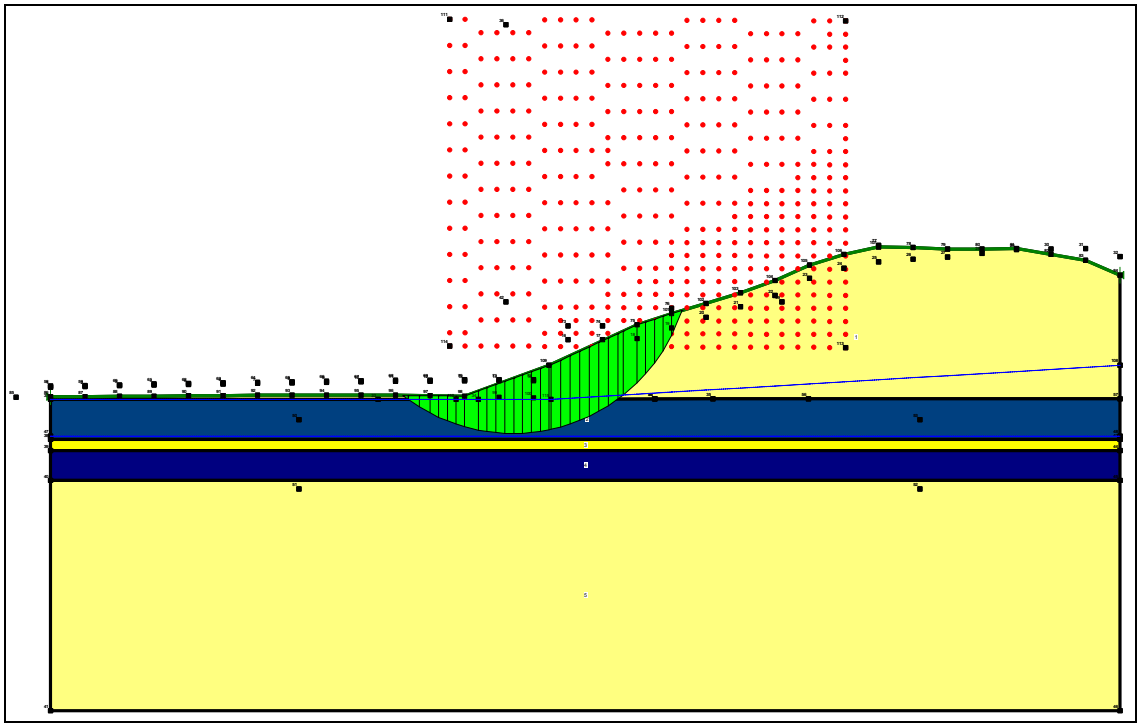

*Figure 154 variant 1 (phreatic level at +3) **FS=1.03** (compared to 0.66 in basic case).*

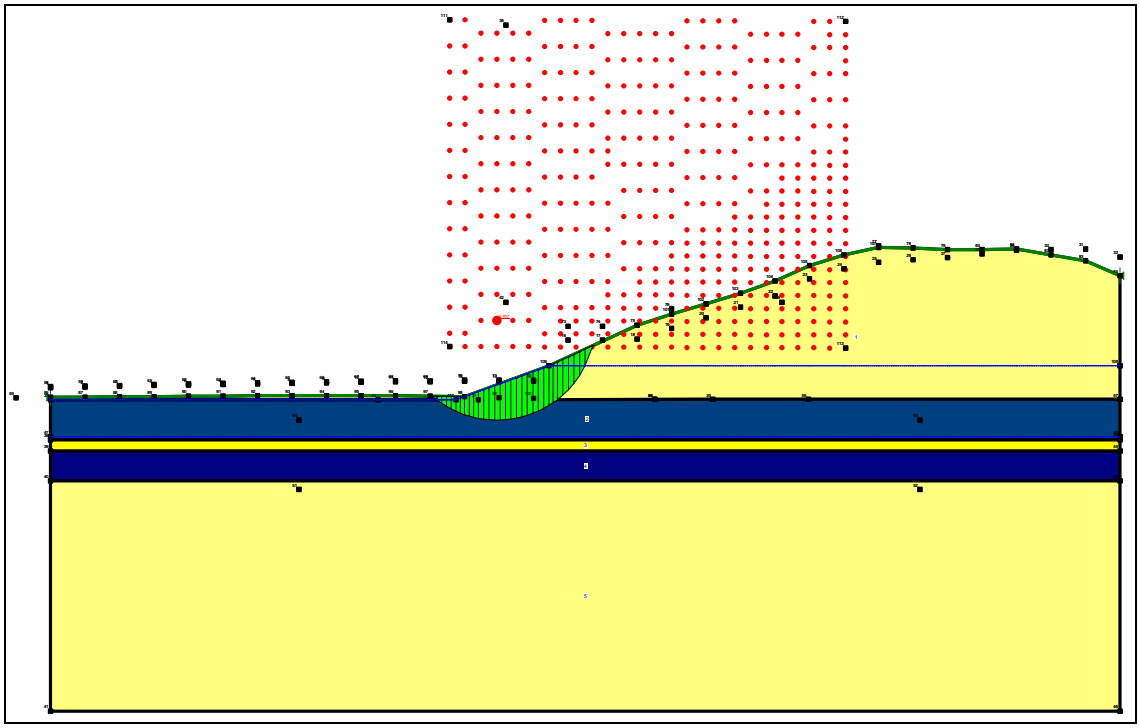

*Figure 155 variant 2 ($\varphi_{dike\ sand}$ 32.5°) **FS=0.71** (compared to 0.66 in basic case).*

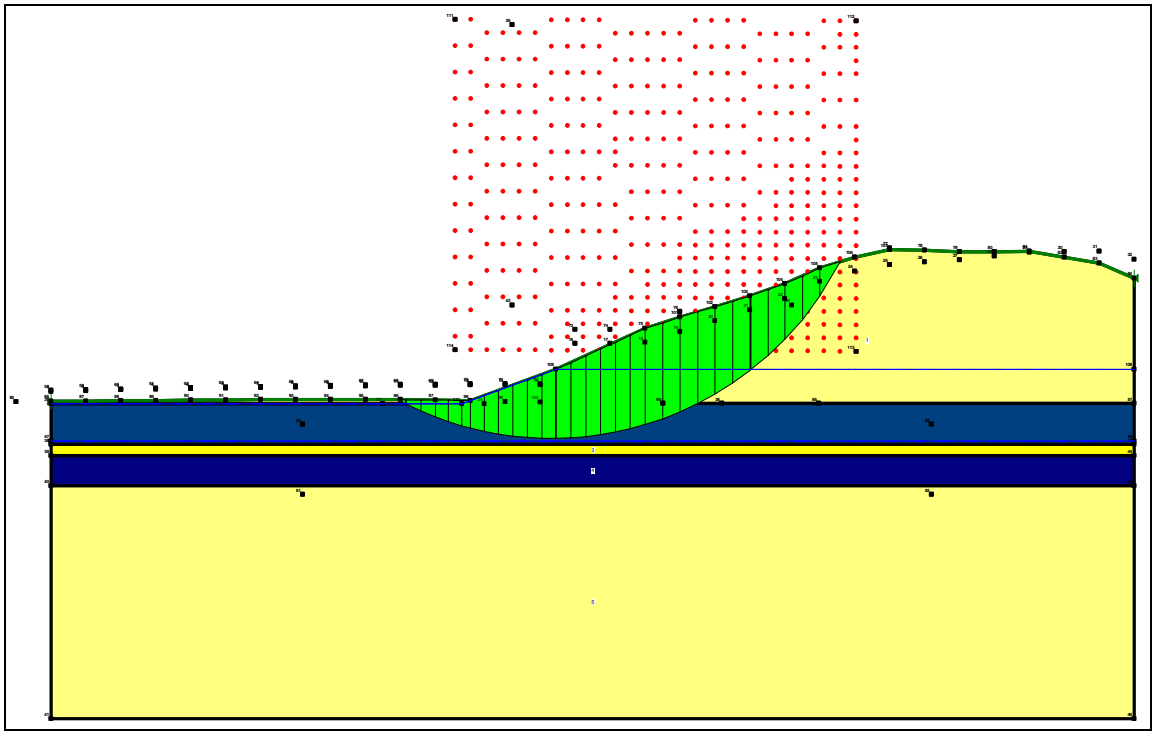

*Figure 156 variant 2 ($\varphi_{dike\ sand}$ 32.5°) **FS=1.00** (already slip circle with FS=0.71).*

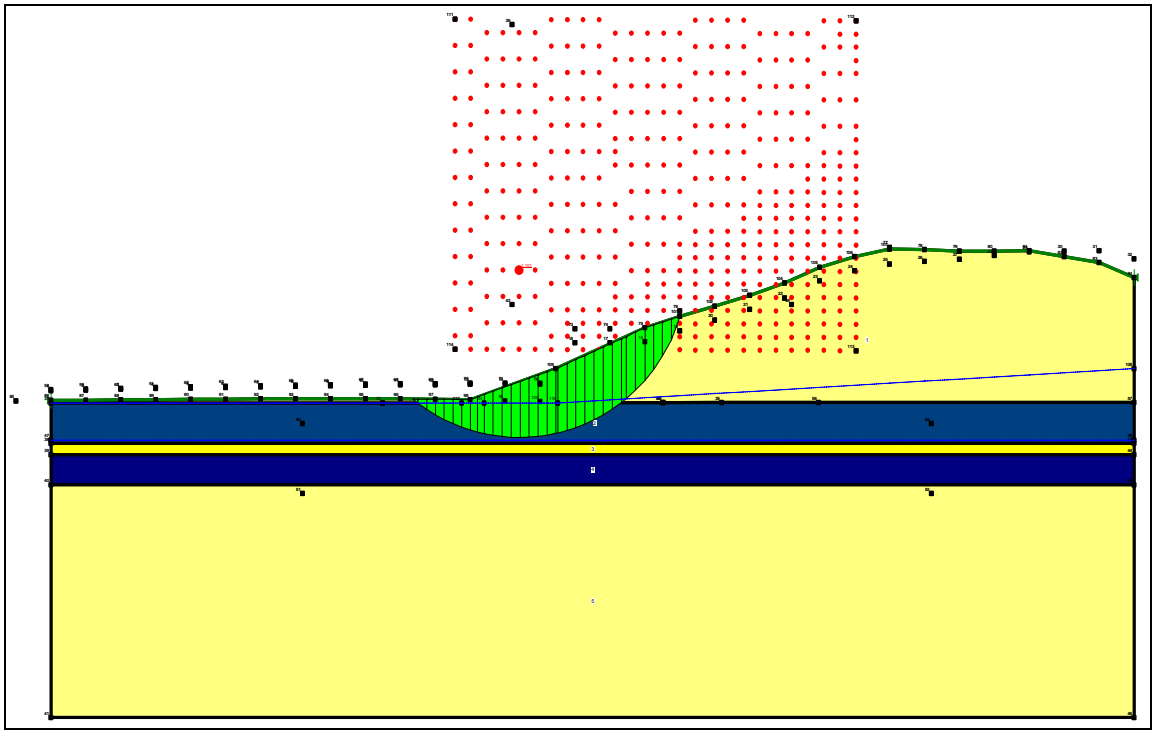

*Figure 157 variant 3 ($\varphi_{dike\ sand}$ 32.5°, phreatic level +3) **FS=1.10***

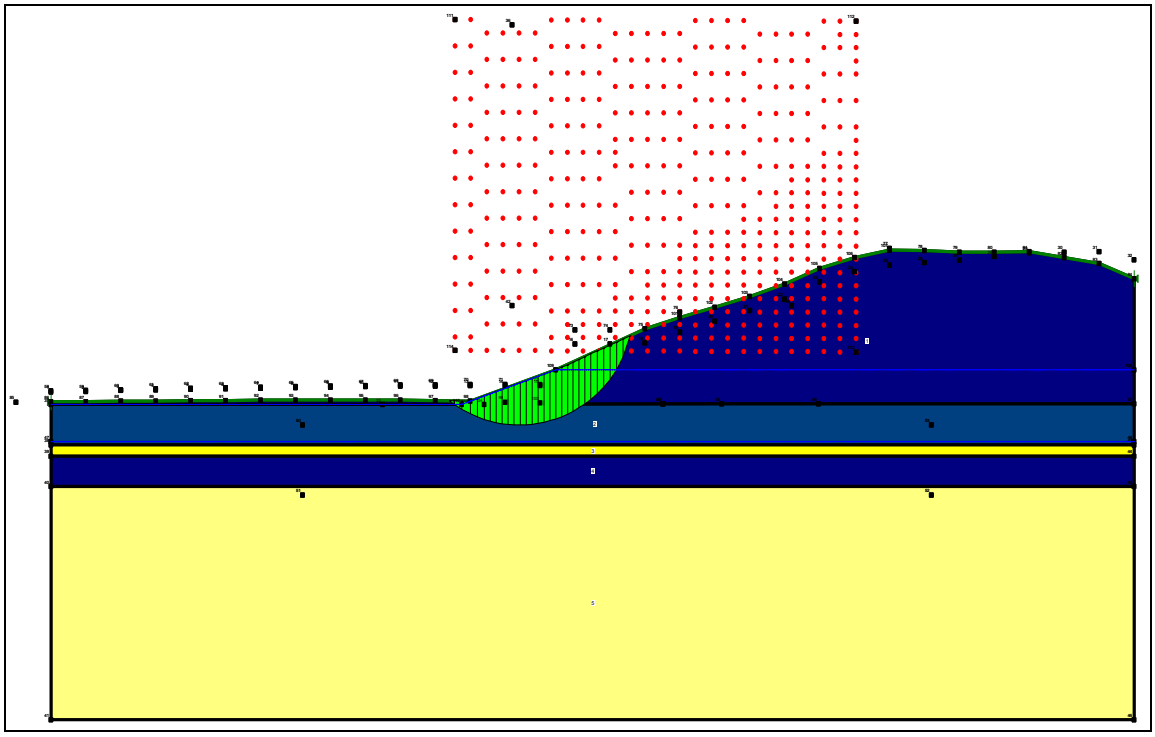

Figure 158 variant 4 ($\varphi_{clay\ dike}$ 17.5°, phreatic level +5.4) ***FS=0.50*** *(compared to 0.66 in basic case).*

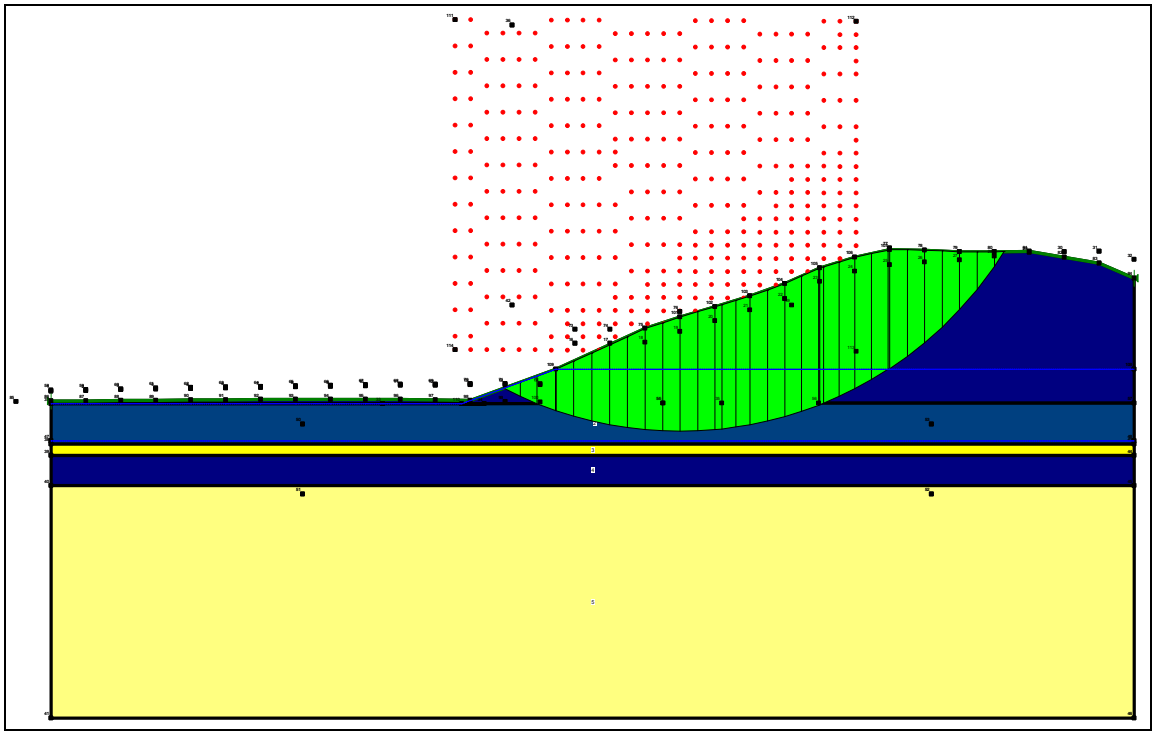

Figure 159 variant 4 ($\varphi_{clay\ dike}$ 17.5°, phreatic level +5.4) ***FS=1.00*** *(already slip circle with FS=0.50).*

The following can be deduced from the sensitivity analysis for the case in question:

- effect of phreatic level +3 compared to +5.4: FS 1.03 compared to 0.66;
- effect of φ 32.5° compared to 27.5°: FS 0.71 compared to 0.66: effect relatively limited;
- effect of weak clay (φ 17.5°, c=0) compared to sand in dike: FS 0.50 compared to 0.66.

The analysis shows the significant influence of the phreatic level in the dike and the composition of the dike material.

11.3.2. Stability of landward slope

By means of SLOPE calculations an SF of 1.43 is obtained for profile 308 (d_25), assuming a sand dike (angle of internal friction 27.5°) and a normative (high) outer water level for the 40000-year return period. For this profile the stability was also examined in the case of some (fictitious) steeper slopes.

landward slope	FS
real slope	1.43
1:3 (fictitious)	1.28
1:2.5 (fictitious)	1.18
1:2 (fictitious)	0.98

Table 57: stability of landward slope of profile 308 (d_25)

For dike section d_24 the inward slope for profile 324 is approx. 1:3.5, for profile 290 it is approx. 1:2.

For dike section d_21 the inward slope for profile 421 is approx. 1:4, profile 413 has a gentler inward slope.

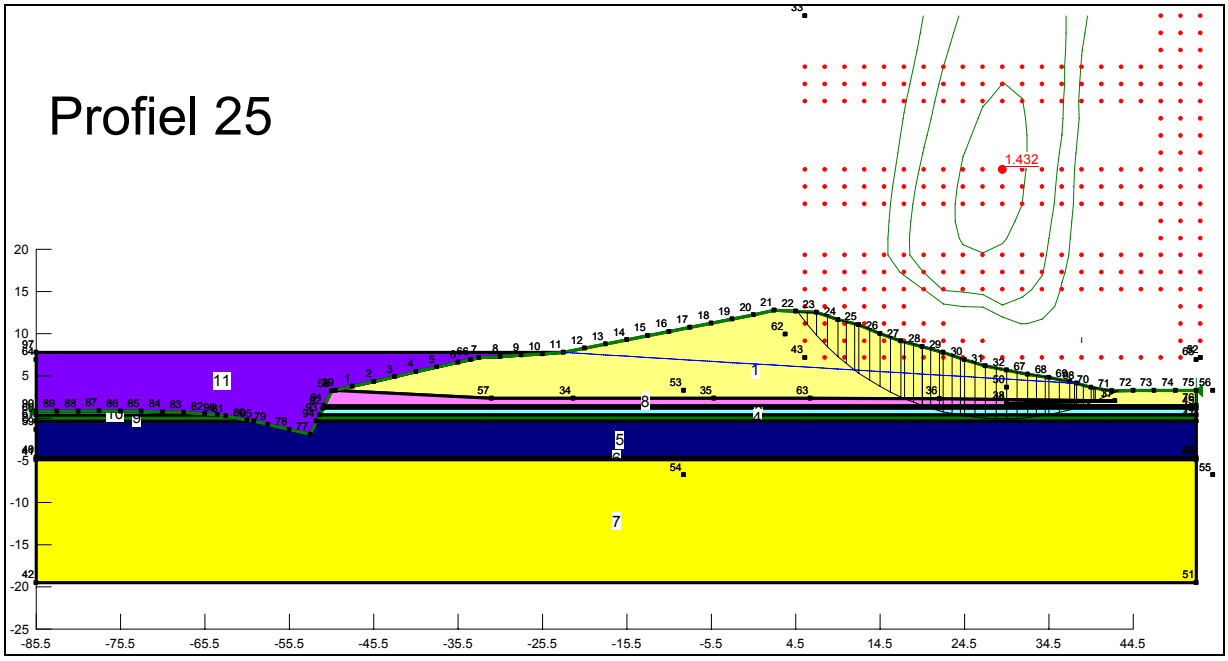

Figure 160 Inward macrostability d_25 (308) ***FS=1.43***

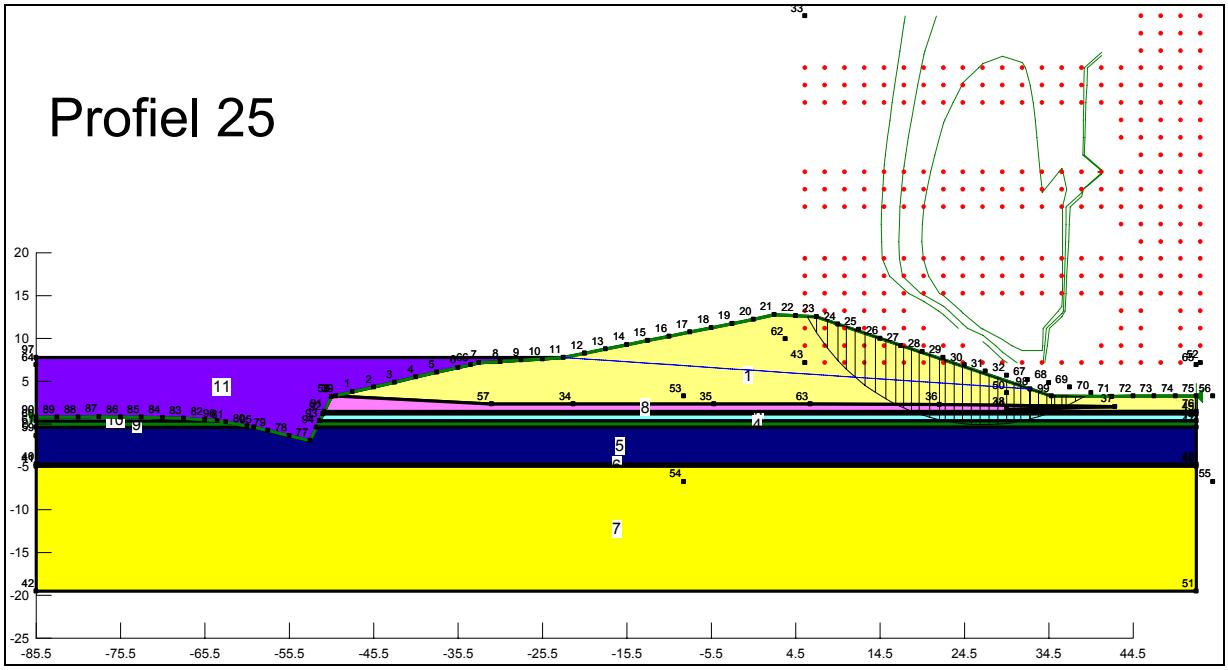

Figure 161 Inward macrostability d_25 (308) fictitious slope 1:3 ***FS=1.28***

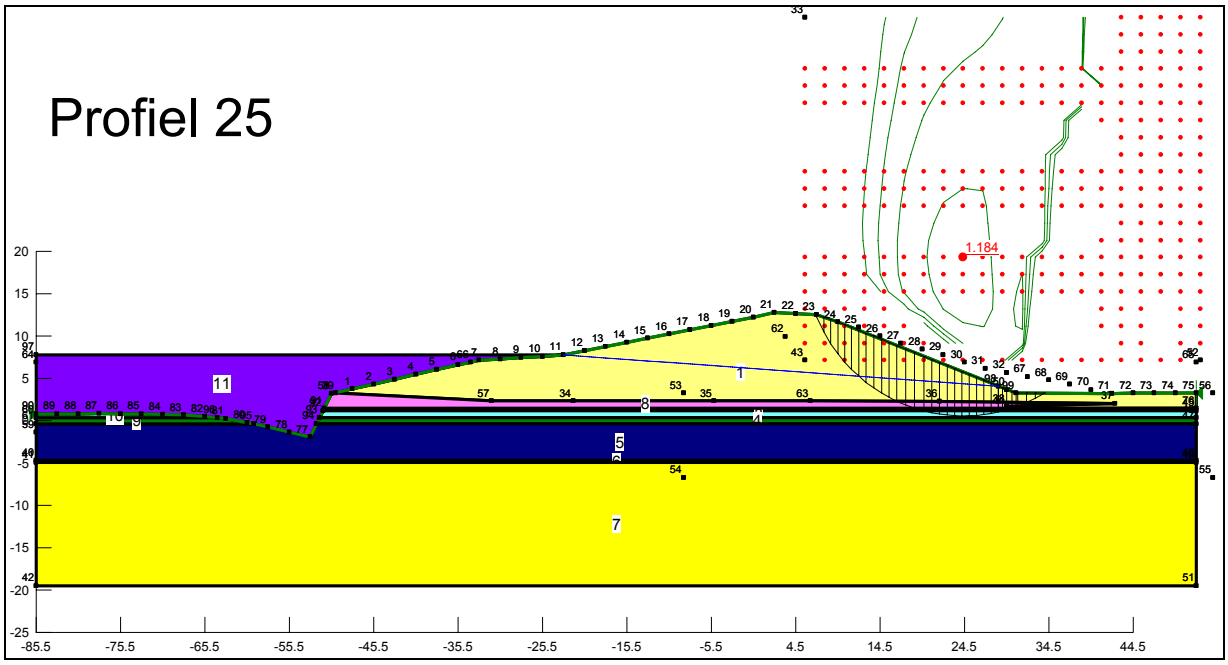

Figure 162 Inward macrostability d_25 (308) fictitious slope 1:2.5 ***FS=1.18***

11.3.3. Erosion of dike body – residual strength

According to the 'erosion model without mixing' used, the intrinsic erosion resistance of the dike core material is expressed as the parameter c_{RB}. The residual strength (residual time) is linearly proportional to this parameter. The calculations assumed somewhat arbitrarily a value c_{RB} of 30000ms (mediocre clay). Table 58 shows the residual strengths for the relevant profiles for the 40000 year return period:

profile no.	H_s (m)	$t_{res, 0}$ (h)	$t_{res, 7000}$ (h)	$t_{res, 30000}$ (h)	$t_{res, 54000}$ (h)
308	1.60	0	14	59	106
324	1.60	0	14	59	106
373	3.01	0	3	15	27
396	1.95	0	9	39	70
413	3.41	0	3	11	20
512	2.61	0	5	20	36
530	2.58	0	4	19	34
558	2.58	0	5	21	38
584	2.44	0	6	25	45
619	2.25	0	9	40	72
638	2.07	0	10	42	76
663	2.66	0	5	21	38
684	2.64	0	4	19	34
705	2.42	0	5	23	41
1032	1.79	0	11	48	86
1300	1.67	0	17	75	135
1318	1.58	0	21	92	166
1335	2.45	0	7	32	58

Table 58 Residual strength of the dike core for different erosion resistances (40000-year return period).

whereby

$t_{res, 0}$: residual strength of the dike core with c_{RB} = 0 (sand) [h];
$t_{res, 7000}$: residual strength of the dike core with c_{RB} = 7000 ms (poor clay) and 40000 y. [h];
$t_{res, 30000}$: residual strength of the dike core with c_{RB} = 30000 ms (mediocre clay) and 40000 y. [h];
$t_{res, 54000}$: residual strength of the dike core with c_{RB} = 54000 ms (good clay) and 40000 y. [h];

The remaining residual strength of the dike core for different erosion resistances considered with a 40000-year return period is given in Table 59:

prof.no.	$t_{res, 7000, net}$ (h)	$t_{res, 30000, net}$ (h)	$t_{res, 54000, net}$ (u)
308	**-16**	29	76
324	**-16**	29	76
373	**-27**	**-15**	**-3**
396	**-21**	9	40
413	**-27**	**-19**	**-10**
512	**-25**	**-10**	6
530	**-26**	**-11**	4
558	**-25**	**-9**	8
584	**-24**	**-5**	15
619	**-21**	10	42
638	**-10**	22	56
663	**-25**	**-9**	8
684	**-16**	**-1**	14
705	**-15**	3	21
1032	**-19**	18	56
1300	**-13**	45	105
1318	**-9**	62	136
1335	**-23**	2	28

Table 59 Remaining residual strength of the dike core for various erosion resistances (40000-year return period)

whereby

$t_{res,7000,net}$: difference between the residual strength of the dike core and the necessary residual strength, with 40000-year return period and c_{RB}=7000 ms [u];

$t_{res,30000,net}$: difference between the residual strength of the dike core and the necessary residual strength, with 40000-year return period and c_{RB}=30000 ms [u];

$t_{res,54000,net}$: difference between the residual strength of the dike core and the necessary residual strength, with 40000-year return period and c_{RB}=54000 ms [u].

Negative values indicate that the residual strength of the dike core is smaller than the roughly determined residual strength. If c_{RB} is equal to 0, the erosion model gives a residual strength equal to 0, ensuring that a failing revetment automatically results in failure of the dike. The profiles in question also fail with a limited erosion resistance (in accordance with 'poor' clay). However, it must be pointed out that the erosion model is rudimentary. In addition, the dike composition is uncertain.

11.4. Sensitivity analysis of the flood model and associated damage

This paragraph discusses the results of the simulations which are a part of the sensitivity analysis of the hydrodynamic flood model. The flood model was developed in Mike21 Flow Model (2D-model) for overland flow and Mike11 (1D-model) for dike breach. The development of the model is extensively discussed in chapter 9

The sensitivity analysis comprises the following items:

1. Influence of the roughness
2. Influence of the breach width on the flood results
3. Influence of the moment of dike breach
4. Influence of additional dike breaches.

11.4.1. Influence of the roughness

With regard to flood modelling, the Strickler coefficient (1/mannings n) is in the order of 20-40.

To evaluate the influence of roughness on the flood behaviour a sensitivity analysis was made for a limited submodel. To do so, a breach was integrated in the Zwin dike (International dike). The size of the breach took into account the dimensions of the Zwin mouth, as it determines the maximum velocity through the breach in the Zwin dike. At a second location, a breach was provided in the dune profiles near Het Zoute.

The greater the Strickler coefficient, the lower the resistance. In city centres it is recommended to use a lower Strickler coefficient. A small sensitivity analysis was made, whereby the model is attributed a homogeneous roughness with a Strickler coefficient of 20, 32 (recommended value in Manual mike21) and 40.

Figure 163 shows the location where the influence of the roughness on the flood depth was analysed. Figure 164to Figure 167show the water depth calculated for the various locations.

The results of the sensitivity analysis show that a shift of the water rise is limited to 5 to 25 minutes for a Strickler coefficient of 32 to a Strickler coefficient of 40. A Strickler coefficient of 20 easily results in a delay of 20 to 60 minutes further inland.

The maximum water level reached is influenced to a limited extent by the roughness.

For the flood model, used for the various scenarios, a homogeneous roughness (Strickler coefficient 32) is imposed on the entire model.

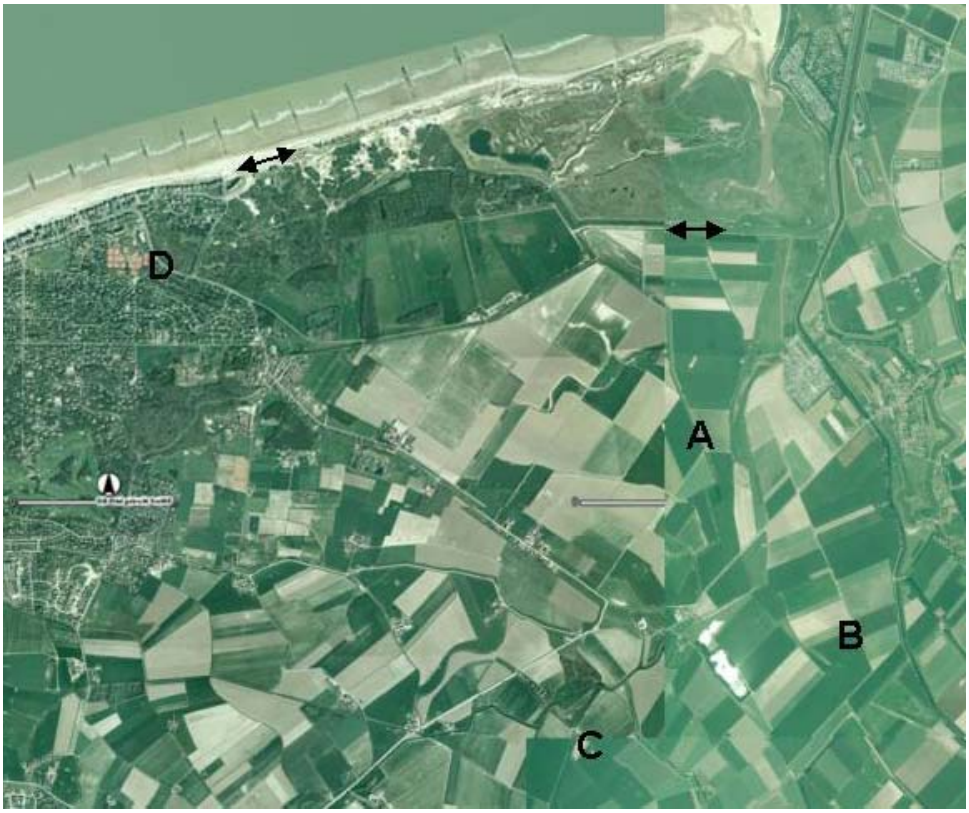

Figure 163: Locations for analysis of the influence of flood depth resistance.

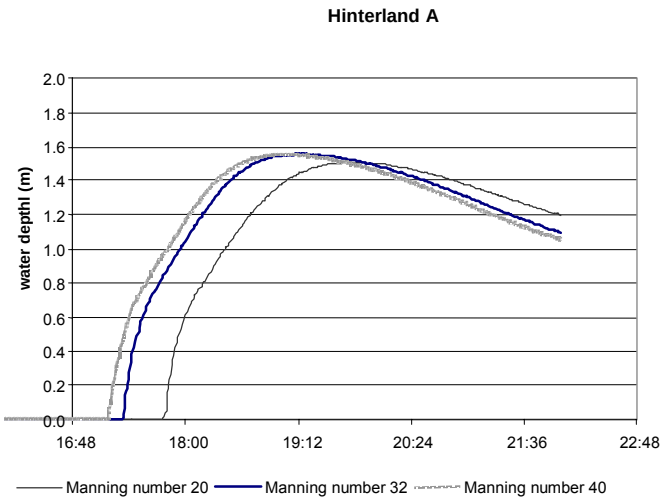

Figure 164: Flood depth at location A.

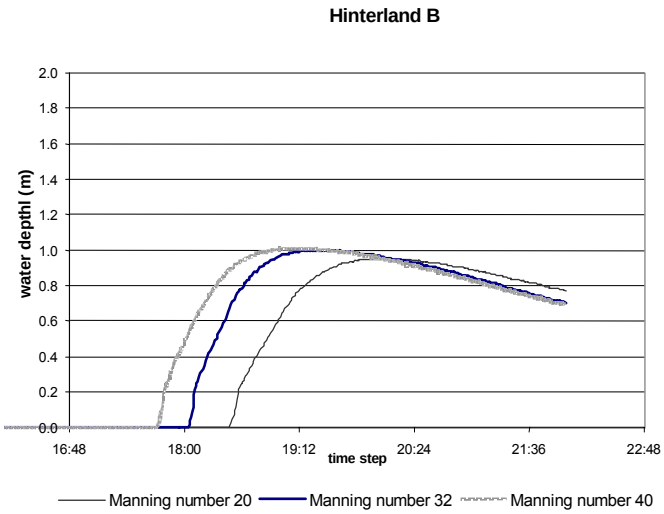

Figure 165: Flood depth at location B.

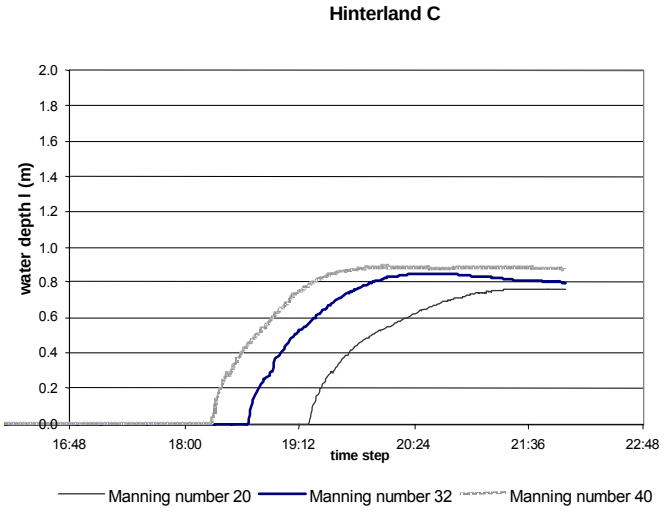

Figure 166: Flood depth at location C.

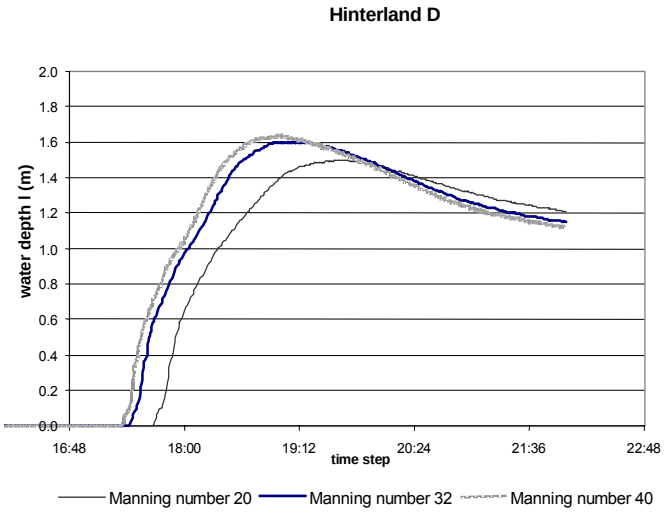

Figure 167: Flood depth at location D.

11.4.2. Influence of breach width

The width-wise breach development is connected with the erosion of the water-retaining structure located on both sides of the breach. The width development depends on a large number of parameters, including momentary hydraulic boundary conditions, geometry of the retaining structure and the material the water-retaining structure is made of. The final width of a breach is difficult to assess.

To assess the influence of the breach width on the flood results, two scenarios were taken into account in the flood model.

The first scenario takes into account two dike breaches with a maximum breach width limited to 100m. The first breach is located in Flanders at Het Zoute, the second breach is located at Walen dike near Nieuwe Sluis (Zeeland Flanders).

The second scenario calculates a dike breach for the same locations, with a maximum breach width of up to 200m.

An overview of the parameters used for the dike breaches for the 2 scenarios is included in the table below.

Table 60: Parameters for breach development with seawall failure: sensitivity analysis of breach width

Parameter	***Unit***	***Profiles for seawall failure***			
		Flanders	***Zeeland Flanders***	***Flanders***	***Zeeland Flanders***
		100m breach width		**200m breach width**	
Breach location		Het Zoute	Walen dike	Het Zoute	Walen dike
Moment of seawall failure	m T.A.W.	HW tide 2	HW tide 2	HW tide 2	HW tide 2
Initial width of the breach	m	20	20	20	20
Speed of width-wise breach development	m/hour	30	30	30	30
Maximum width of the underside of the breach	m	100	100	200	200
Duration of the maximum width of the breach	Hour	3	3	9	9
End height of the underside of the breach	m T.A.W.	6	3.5	6	3.5
Duration of the maximum depth of the breach	Hour	2	2	2	2

The results of the maximum water depth and maximum velocities are given in Figure 168 to Figure 171.

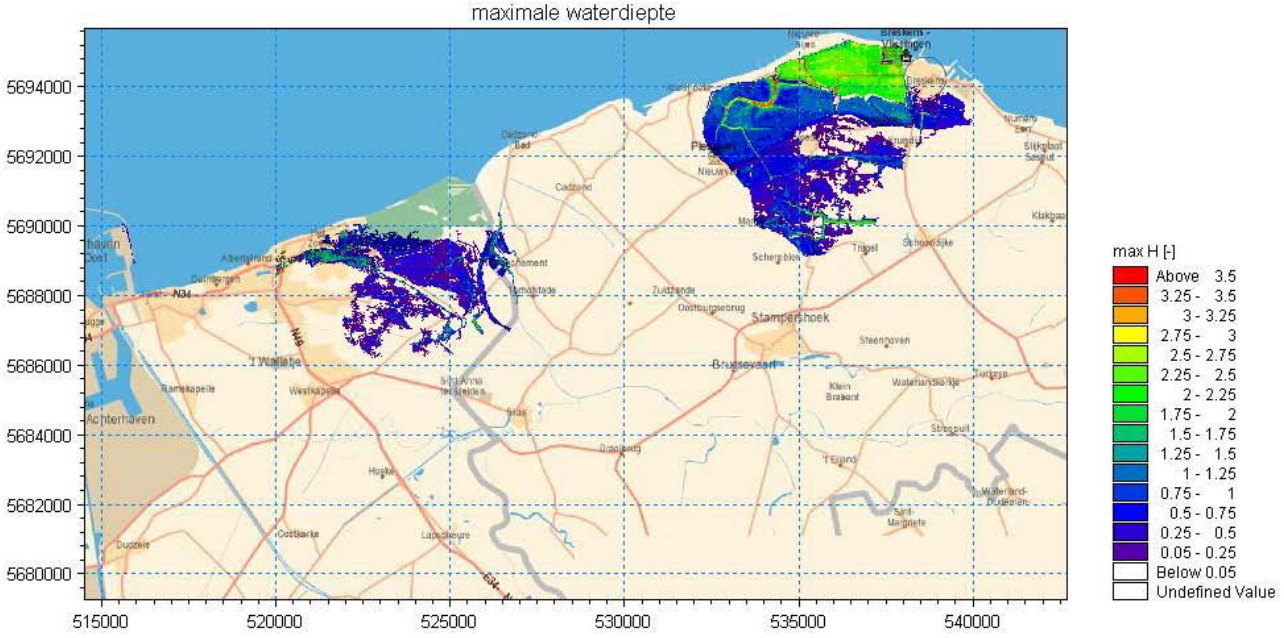

Figure 168: Maximum water depth (m) for a dike breach with a maximum breach width of 100m

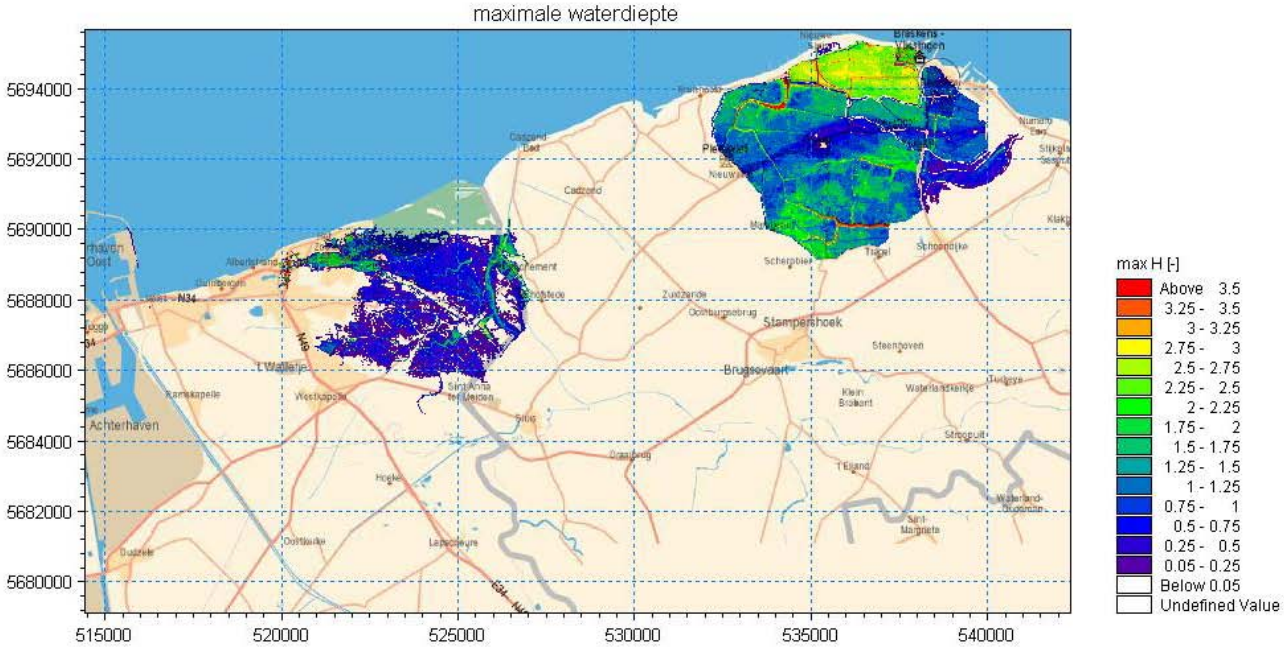

Figure 169: Maximum water depth (m) for a dike breach with a maximum breach width of 200m

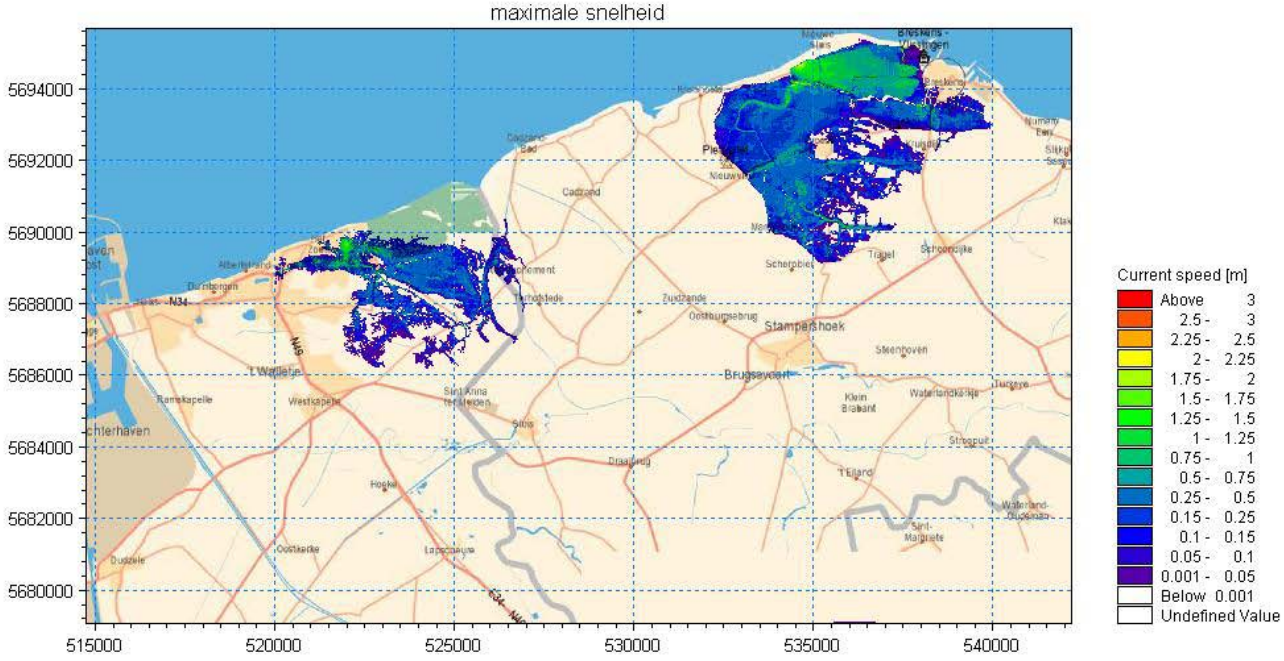

Figure 170: Maximum velocity (m/s) for a dike breach with a maximum breach width of 100m

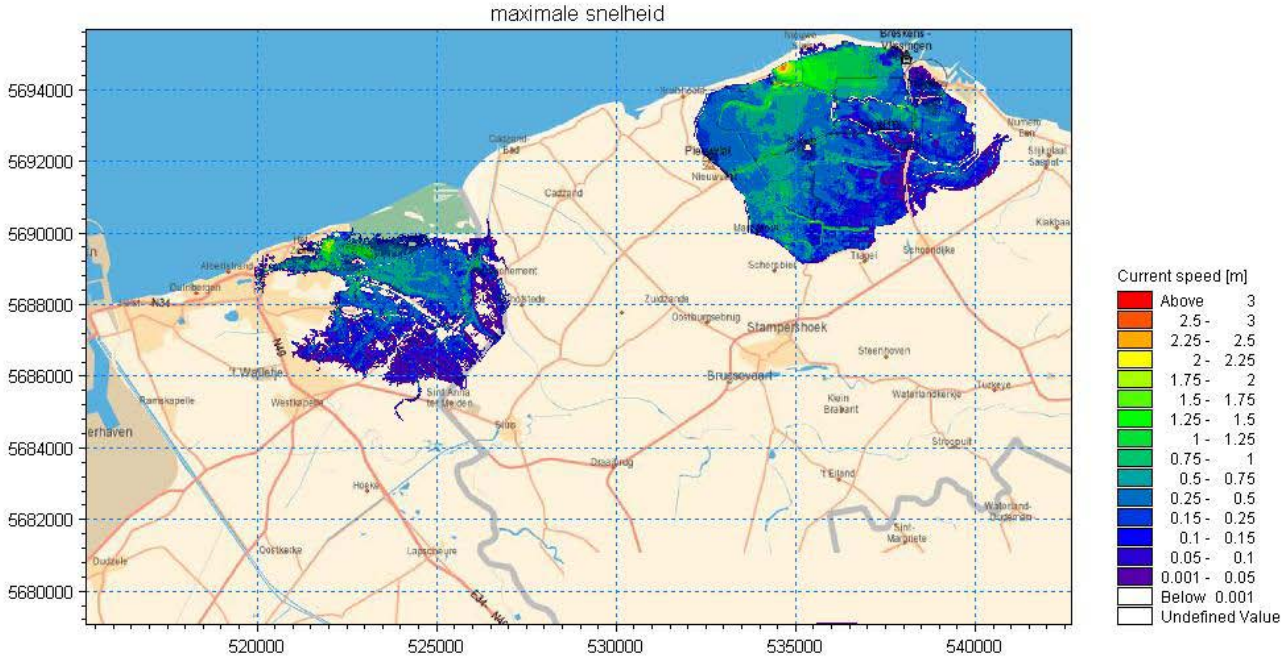

Figure 171: Maximum velocity (m/s) for a dike breach with a maximum breach width of 200m

This results in tabelled damage:

Table 61Damage depending on breach width (x1000 euro)

	Flanders	Zeeuws-Vlaanderen	Total
Breach of 100 m	129334	70793	200127
Breach of 200 m	227270	212931	440201

In Zeeuws-Vlaanderen is the difference associated with the flooding or non flooding of the city Breskens. In Flanders more of the city Knokke is flooded.

The number of casualties for a breach with of resp. 100 and 200 is for Zeeuws-Vlaanderen resp. 11 en 24 for Flanders resp resp. 0.3 en 0.7

Zeeuws Vlaanderen

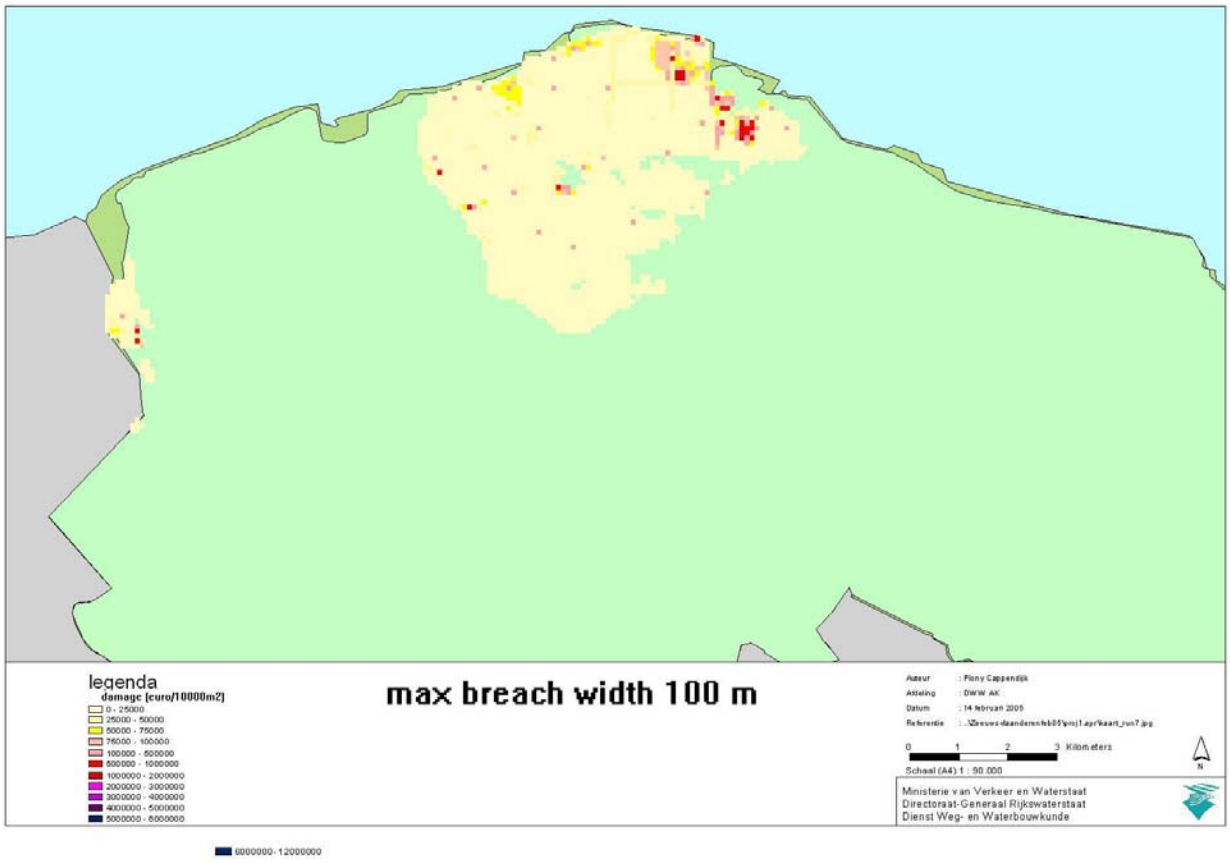

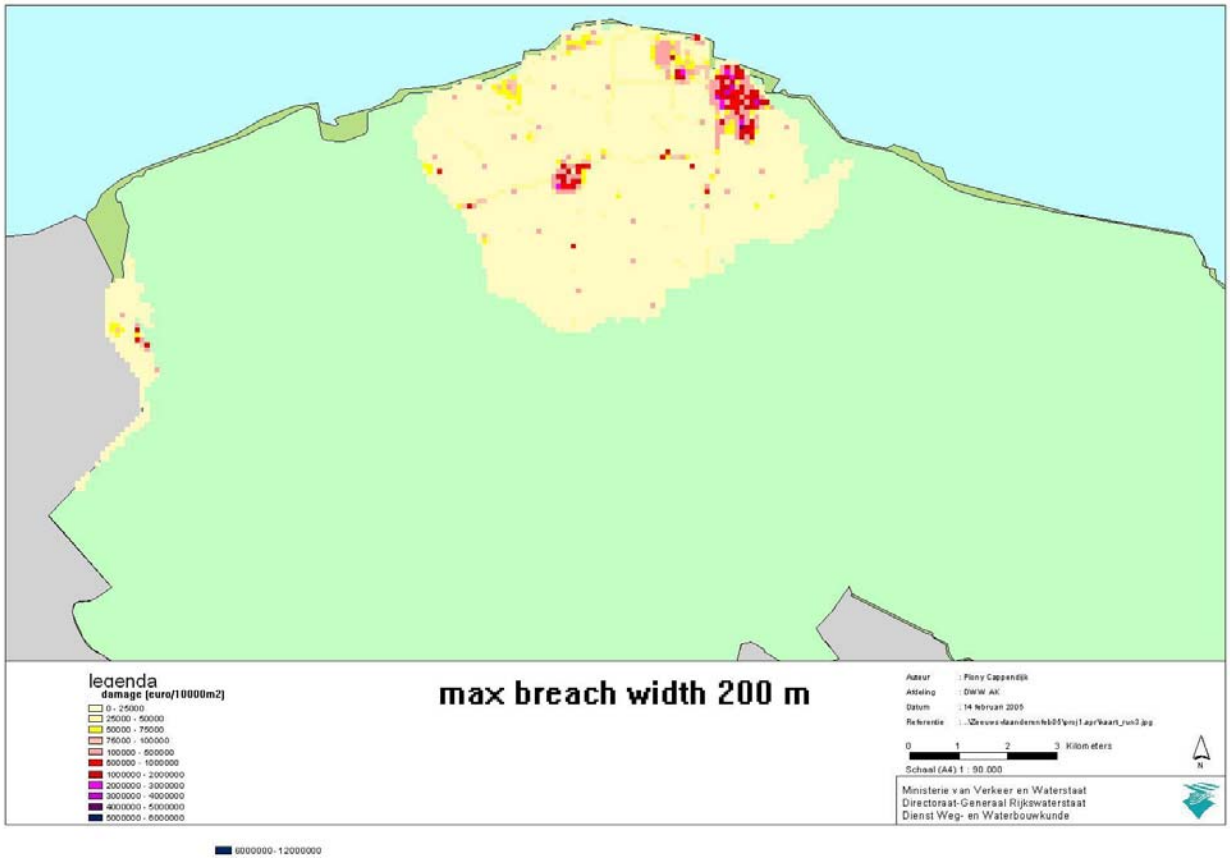

Figure 172Damage due to a breach of resp 100 and 200 m in Zeeuws Vlaanderen

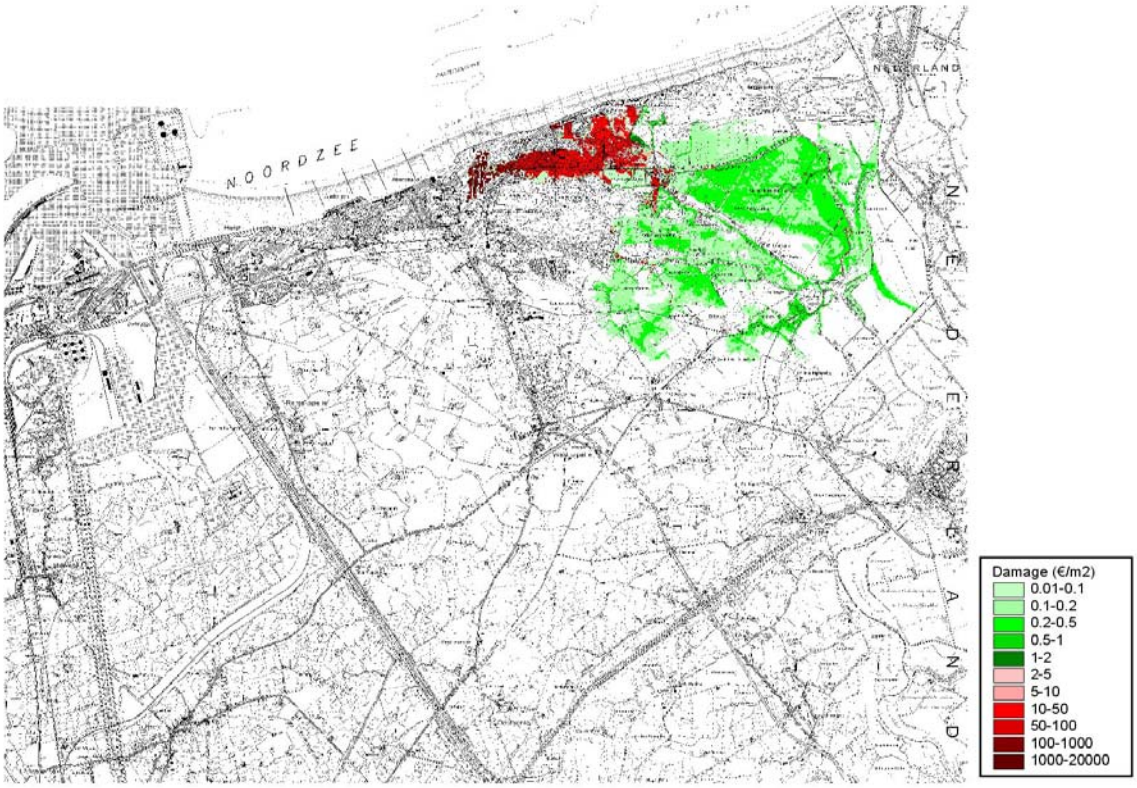

a)

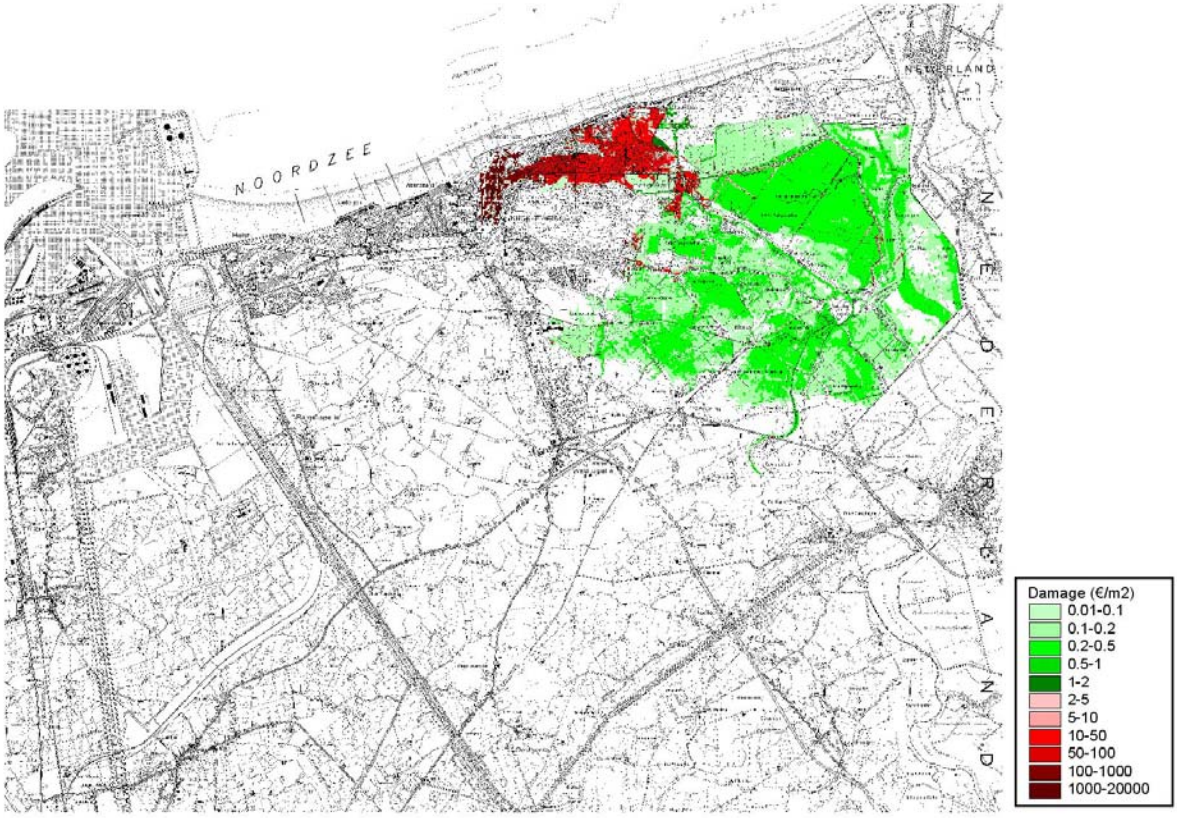

Figure 173Damage due to a breach of a) 100 and b) 200 m in Flanders

However, at some locations different dike failures occur over a length of a few kilometer. In case an innerdike is present, the whole area between sea dike and inner dike will fill up rapidely. The breach width will only influence the rate of filling.

11.4.3. Influence of the moment of dike breach

The influence of the moment of dike breach on the flood results was assessed by means of a simulation with a storm tide with a 40000-year return period. An overview of the 18 dike breaches for a storm tide with a 40000-year return period is given in chapter 9. For the sensitivity analysis, the starting times of the dike breaches were moved up 1 hour for Flanders (earlier is not realistic, as the failure mechanism consists of excessively high overtopping discharges, closely related with HW), and moved up 3 hours for the dike breaches in Zeeland Flanders. So, an important breach exists already at HW, which is not the case in the basic run. An overview of the starting moments of the various dike breaches for the 2 scenarios is included in the table below.

Figure 174: Parameters for seawall failure: sensitivity analysis of starting moment of dike breach

Breach number	***Breach location***	***Scenario 4: T40000 years***	***Sensitivity analysis: T40000 years: 1 to 3 hours earlier***
		Starting moment of dike breach	
373	Nieuwe Sluis	HW tide 2	HW-3 hours tide 2
396	Nieuwe Sluis	HW tide 2	HW-3 hours tide 2
413	Nieuwe Sluis	HW tide 2	HW-3 hours tide 2
512	Left of new locks (Walen dike)	HW tide 2	HW-3 hours tide 2
530	Left of new locks (Walen dike)	HW tide 2	HW-3 hours tide 2
496	Left of new locks (Walen dike)	HW tide 2	HW-3 hours tide 2
558	Zeeweg (Zwarte Gat)	HW tide 3	HW-3 hours tide 3
584	Zeeweg (Zwarte Gat)	HW tide 3	HW-3 hours tide 3
663	Zeeweg	HW tide 3	HW-3 hours tide 3
684	Zeeweg	HW tide 3	HW-3 hours tide 3
233	Knokke	HW+1 hour tide 1	HW tide 1
234	Knokke	HW tide 2	HW –1 hour tide 2
235	Knokke	HW+1 hour tide 2	HW tide 2
236	Knokke	HW+1 hour tide 2	HW tide 2
241	Het Zoute (Zwinlaan)	HW tide 2	HW- 1 hour tide 2
242	Het Zoute (Zwinlaan)	HW tide 1	HW-1 hour tide 1

243	Het Zoute (Zwinlaan)	HW tide 1	HW-1 hour tide 1
Zwin dike	Zwin dike inner dike	HW tide 2	HW-3 hours tide 2

The moment of dike breach is an important parameter for flood calculations. The figures below show that the flooded areas on Dutch soil are doubling. The Krabben dike and Sint Bavo dike cannot hold the water. The floods now also occur in the urbanised areas of Schoondijke, Oosburg and Ijzendijke. The floods extend to the model border to the east and south of the flood model. To the west, the water now flows past Slikkenburg; near Terhofstede the floods from the dike breaches in the Netherlands, Flanders and the Zwin dike flow together.

The maximum water depth in the Oud Bresken polder rises to 3.5m, in the polders located within the Krabben dike and the Sint Bavo dike the water depth rises to 2.5 to 3.5m.

The velocities in the vicinity of the dike breaches at Walen dike increase to more than 3m/s in the polder located between Walen dike, Puijen dike and Zoete Kreek.

The influence of the moved-up dike breach in Flanders is less outspoken.

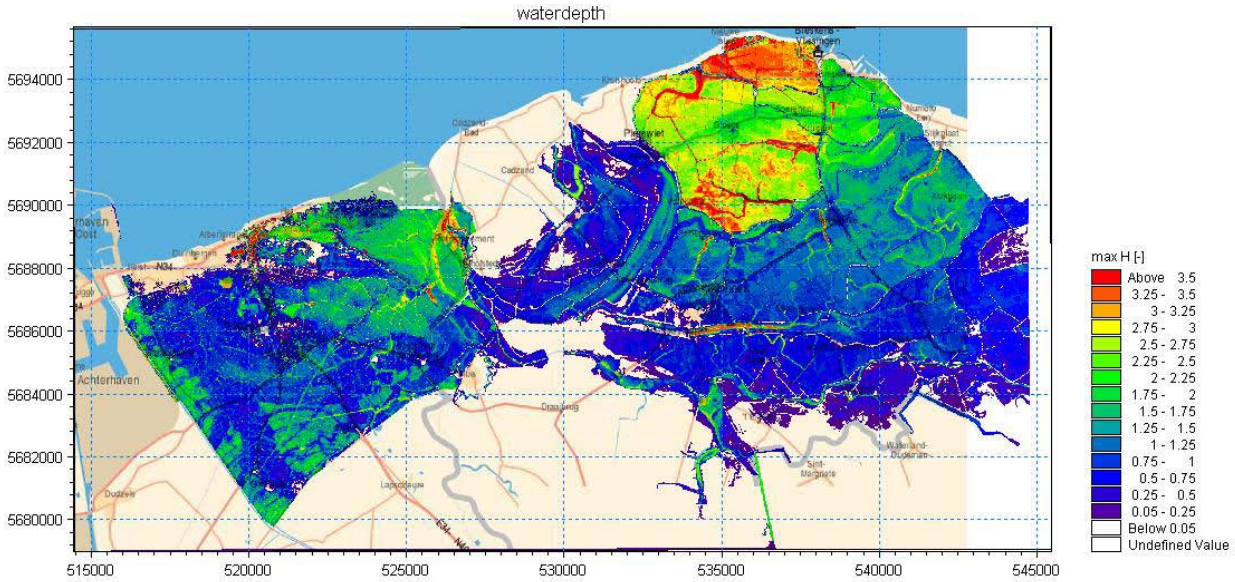

Figure 175: Maximum water depth during a storm tide with a 40000-year return period whereby a dike breach occurs befor HW.(to be compared with Figure 138)

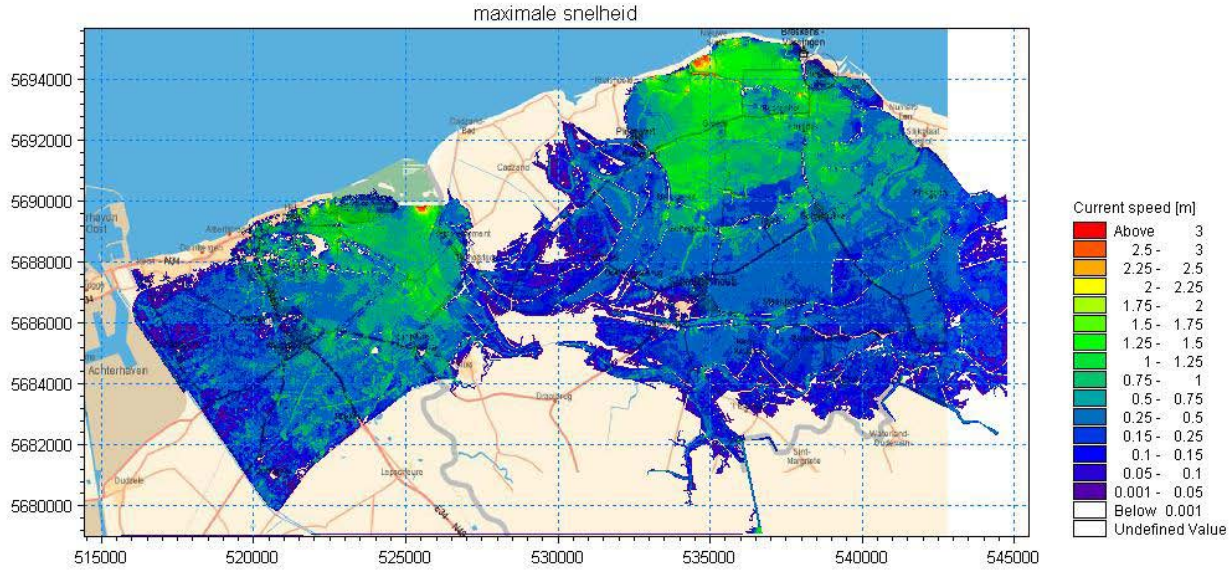

Figure 176: Maximum velocity during a storm tide with a 40000-year return period whereby a dike breach occurs befor HW (figure is to compare with.Figure 139)

The earlier failure of the dikes have important consequences for the number of casualties and the total damage as illustrated in

Table 62Damage depending on timing of breaching

	FLanders	Zeeuws-Vlaanderen	Total
T=40000	702108	280807	982915
T=40000 with earlier failure	865763	741096	1606859

Table 63Damage (x1000 euro)

The number of casualties rises in Zeeuws-Vlaanderen with a factor of 10 to 220 casualties. In Flanders the number of casualties rises from 4 to 5

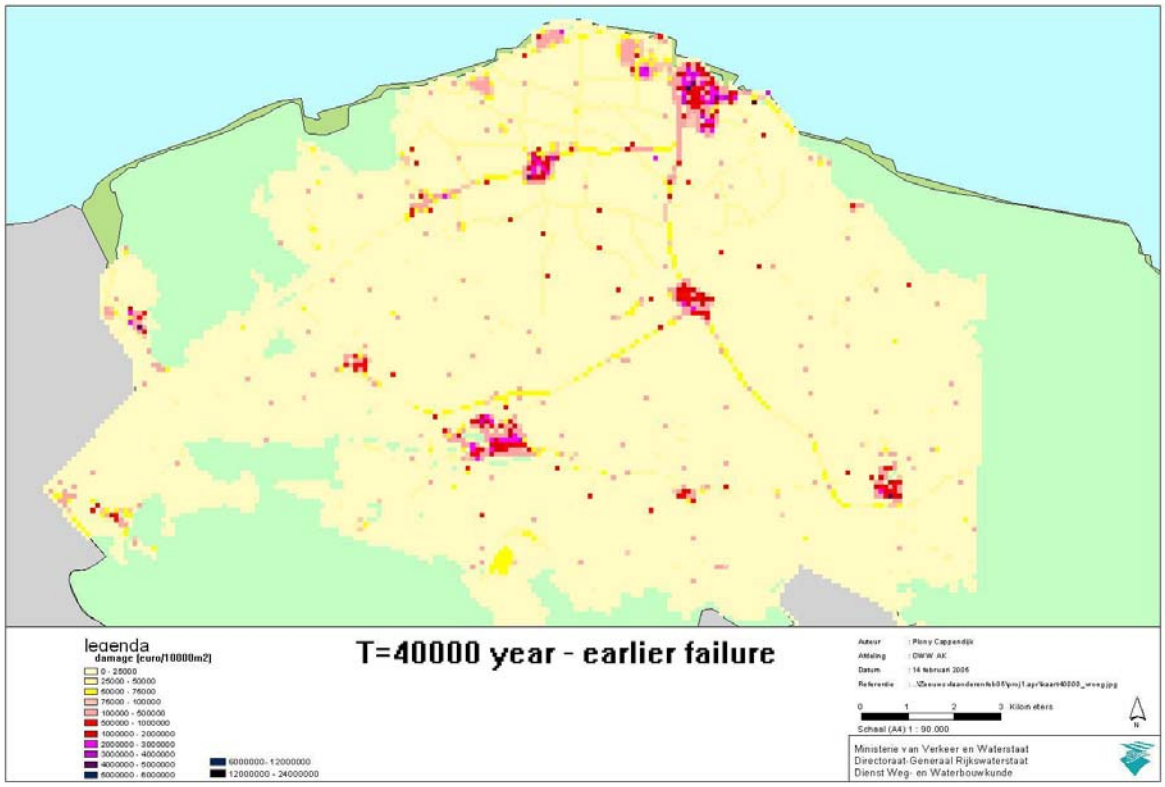

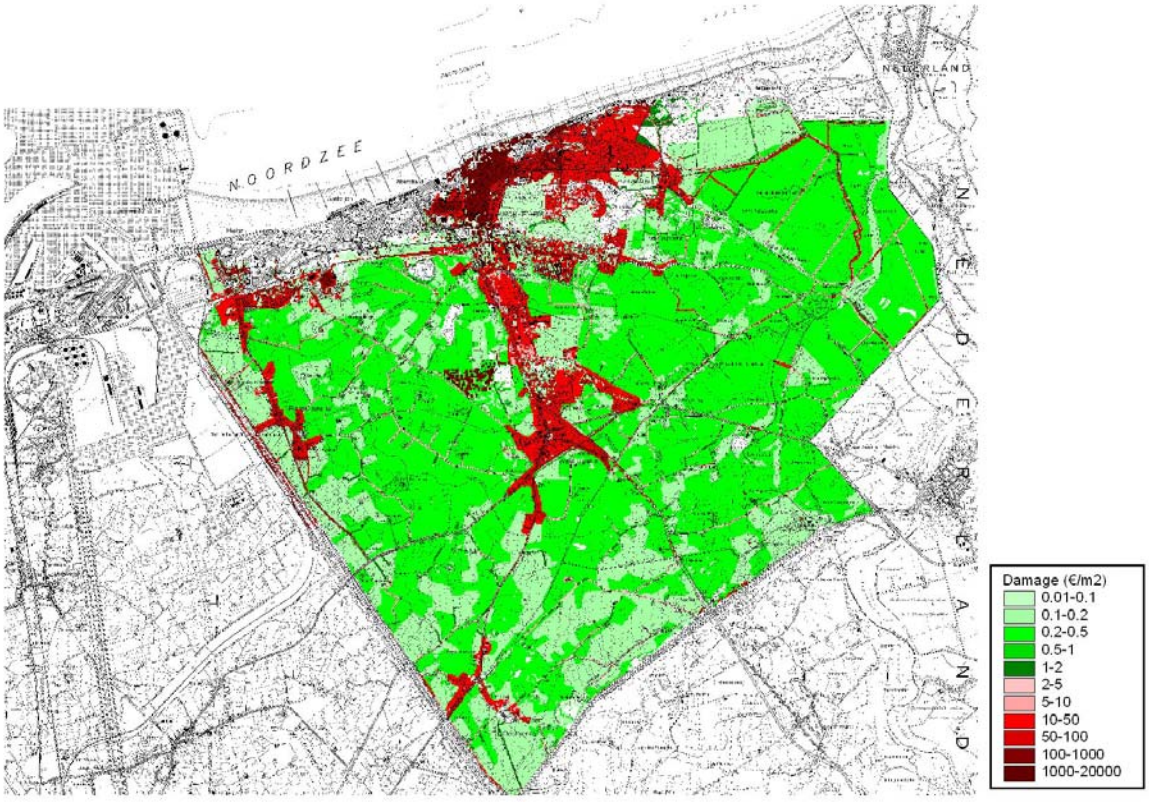

Figure 177Damage maps for Zeeuws-Vlaanderen en Flanders –earlier failure

11.4.4. Influence of additional dike breaches

The 18 dike profiles which fail during a storm tide with a 40000-year return period were taken into account in scenario 4. The analysis of the seawall failure of the dikes located in Zeeland Flanders showed that a series of dikes will hold out in a storm tide with a 40000-year return period, a number of which could fail in a bigger storm. In this scenario three-odd locations where a dike breach occurred are added to the 18 dike breaches in order to estimate the effect of additional dike breaches on the flood results. The three additional dike breaches are mainly located in the vicinity of Cadzand Bad.

An overview of the parameters used for the dike breaches at the 3 locations is included in the table below. The locations of the additional dike breaches are given in Figure 179.

Figure 178: Parameters for breach development following seawall failure during a storm tide with a 40000-year return period: additional dike breach near Cadzand

Parameter	***Unit***	***Profiles for seawall failure in Zeeland Flanders***		
		1032	**1335**	**1363**
Breach location		Cadzand (Zwarte Polderweg)	Cadzand-Bad	Cadzand-Bad to the west of the discharge canal
Moment of seawall failure		HW tide 3	HW tide 3	HW tide 2
Initial width of the breach	m	20	180	20
Speed of width-wise breach development	m/hour	30	-	30
Maximum width of the underside of the breach	m	121	180	92
End height of the underside of the breach	m T.A.W.	4	5.7	5.5
Duration of the maximum depth of the breach	hour	2	0	1

Figure 179: Locations of additional dike breaches at Cadzand

The dike breach at Zwarte Polderweg (dike profile 1032) causes additional flooding in the Tienhonderd polder reaching to the Strijder dike.
The dike breaches in Cadzand Bad cause flooding in the Kievit polder; the discharge canal (Cadzand) alongside it experiences flooding to a limited extent.
The water depth remains limited, with the exception of the area to the west of the discharge canal between Noor dike and Duinweg, where the water depth rises to 3 to 4m.

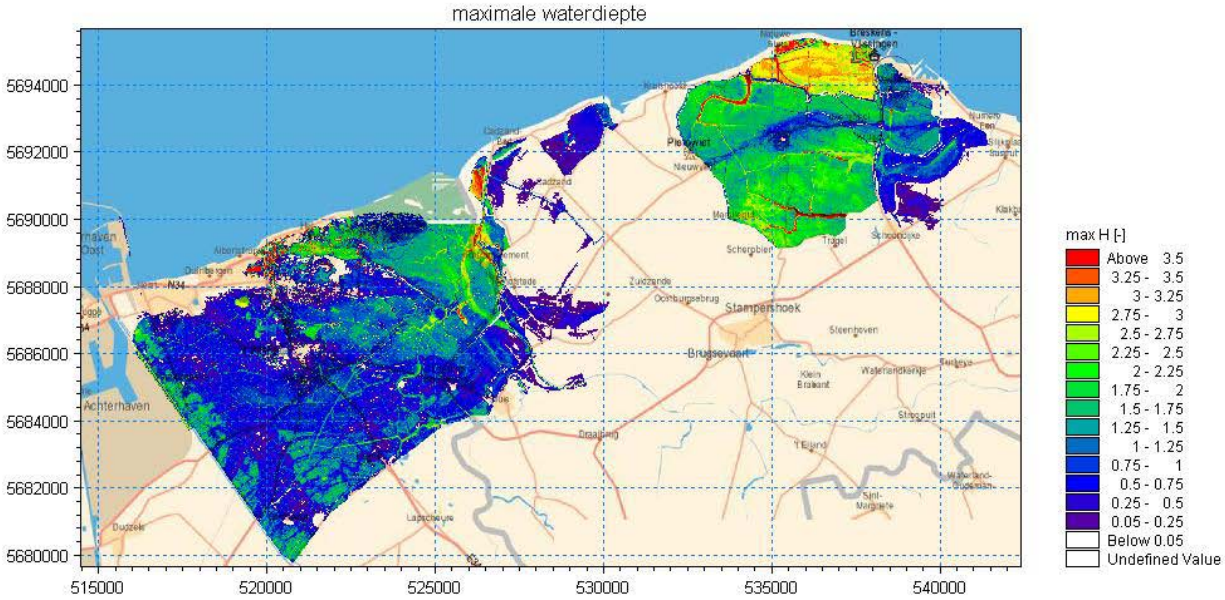

Figure 180: Maximum water depth during a storm tide with a 40000-year return period whereby 3 additional dike breaches occur in the vicinity of Cadzand.

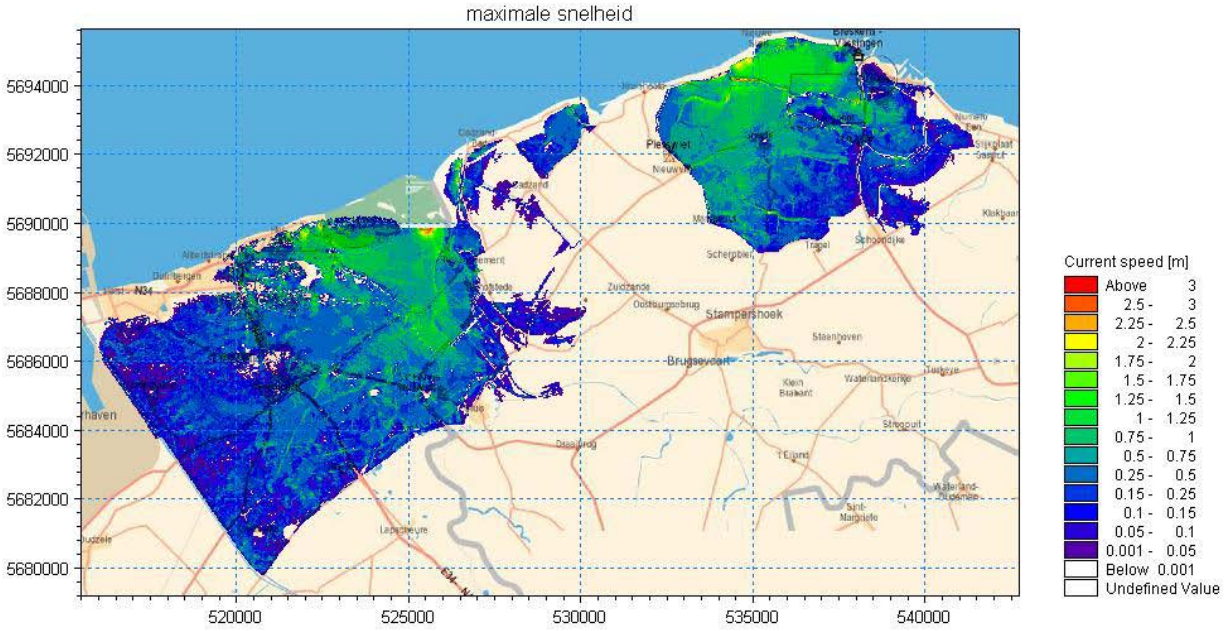

Figure 181: Maximum speeds during a storm tide with a 40000-year return period whereby 3 additional dike breaches occur in the vicinity of Cadzand.

These additional floodings causes an increase in damage of about 6% in Zeeuws-Vlaanderen

	Vlaanderen	Nederland	Totaal
T=40000	702108	280807	982915
T=40000 met extra doorbraak	704530	297647	1002177

Table 64 damage for extra failures (x1000 euro)

The number of casualties doubles in Zeeuws-Vlaanderen and doesn't change in Flanders.

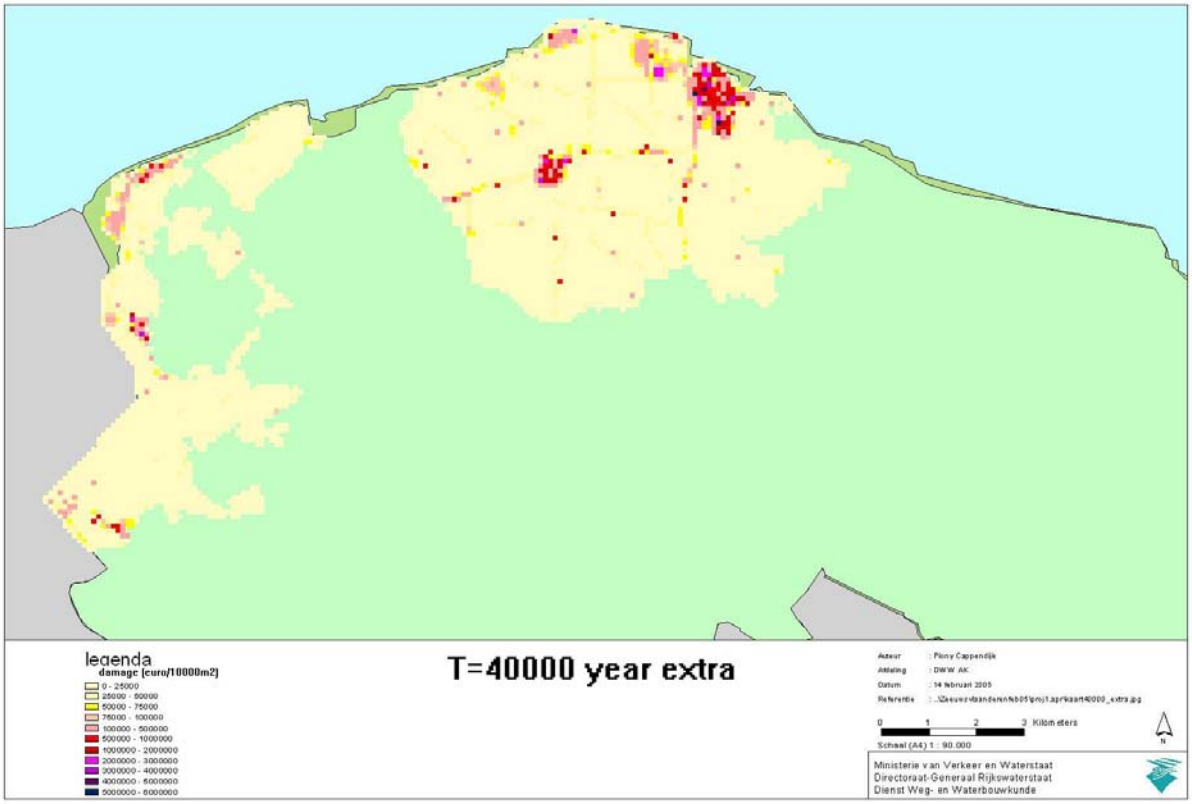

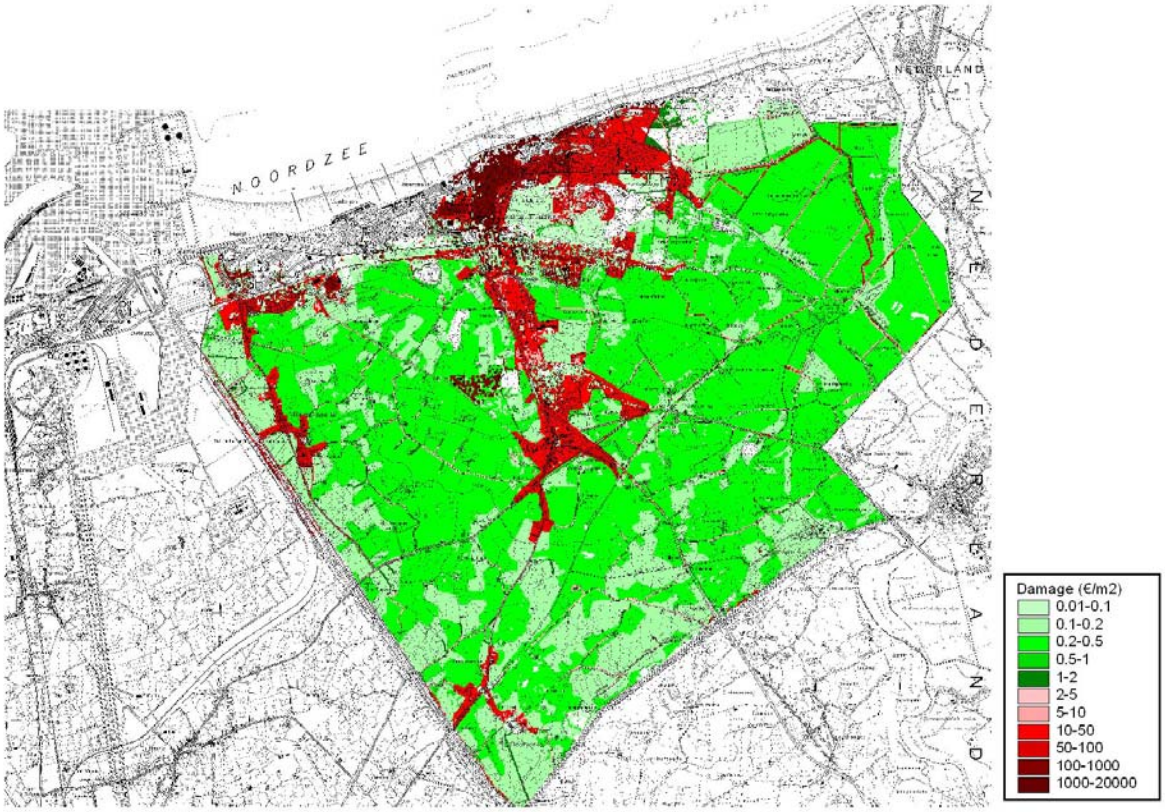

Figure 182 Damage maps for Zeeuws-Vlaanderen en Flanders – extra failure

11.4.5. Other uncertainties for damage calculations

The damage/casualties of course strongly depend on the maximum damage and the total number of people in the flood area. The value of a house is open to discussion: does it concern the replacement value, the cost price (considering the highly fluctuating value of houses, this may strongly vary), the value to build a new house in a safer place, etc.). The number of people in the area strongly depends on the season and the inclusion or non-inclusion of people residing in their second home (these are not included, however; in Knokke there are many houses registered as second homes). An extraordinary storm will not occur in the summer, so that the assumptions made are realistic.

Furthermore it is very difficult to estimate the exact damage functions for such exceptional (high water level) circumstances. For instance, if these damage functions are 10% steeper, the damage will also increase with 10%.

An analysis has shown that the share of vehicles is rather limited and that, with regard to the total damage, the evacuation factor does not have that big an influence on the whole. Also, it appears that the conservative 25 cm categorisation has a rather limited influence on the end result as long as thresholds are introduced for houses, industry and roads. If this categorisation is not made, a few cm difference in thresholds are responsible for fairly large differences in the end result (i.e. after categorisation we get a kind of average result of all cases without categorisation with varying thresholds)

Furthermore, the accuracy of the land use map is of course of paramount importance, more so than exactly knowing the probability of occurrence of a certain flood map. Also, the different conditions given by different data (e.g. census of 1991 and KBG 2001 is already 10 years old) influences the result to a non-negligible extent. This is a data problem, but with the currently available data there is an underestimation compared to control calculations in limited areas with data that do come from about the same moment. However, this problem cannot be solved as only a limited number of datasets is available.

Another aspect of possible errors is the statistical information that is used, which is not always up to date.

To calculate the number of casualties in Flanders, it is assumed that 50% can be evacuated. This is certainly realistic for people who can escape to higher floors. However, considering the high winds at that time, it may be assumed that traffic will soon come to a standstill (many people on the road at the same time + roads blocked by objects blown down).

12. CONCLUSIONS

12.1. Goal

The goal of the study is to develop a methodology to analyse the safety level/risk. The study aims to determine the macro damage. The study of the micro damage is part of the project “Flooding risks coast and Scheldt, case study Blankenberge”: for example damage to buildings positioned in the dunes, damage to houses due to overtopping water without breach formation…

The calculations are based on data measured on different moments. Most of the bathymetric data date from the year 2000. So these results only represent the conditions at this time. For example, in 2004 Knokke was suppleted by 300.000m^3, by which the actual failure chances will be much lower.

12.2. Hydrodynamic boundary conditions

At deep water, the registered wave and wind conditions were analysed and extreme value distribution for the different directions were determined. A similar analysis took place for the water level measurements in Ostend. The extreme analysis was performed on the storm surge, which was afterwards added to the astronomic tide.

The progress of the storm was determined by putting together the progress of the storm surge (theoretical progress, dependent on the storm duration) and an astronomic tide (spring tide). The duration of the storm was determined from analysis of historical data. In reality, the storms seem to be somewhat asymmetric.

The uncertainty (standard deviation) of the maximal water level is estimated on 30 to 40 cm, the uncertainty of the wave height (near shore) on 10% of the value.

It is important to know the wave height and wave period at the toe of the dike. Because of this, the erosion of the beach during storm conditions has to be taken into account. Therefore calculations with a morphological model were executed, with the theoretical storm progress and grain diameter as input.

Due to uncertainty of the storm progress and due to the asymmetry of the storm, first of all the erosion of the beach was calculated during the full storm and afterwards wave transformation was calculated to the toe of the dike, with the new bathymetry as input. Sensitivity analysis proves that this has a huge influence on the results, in case a bank in front of the dike is present

Determination of the wave height at the toe of the dike implies that wave transformation on the beach is known. Due to very small water depths, the wave model is subject to large impreciseness. Long waves will be developed, which cause temporary water level elevations and bigger overtopping discharges. To avoid this, the wave height at 70m out of the toe of the dike was conservatively used as value at the toe of the dike (with a maximum of 0.9 times the water depth at the toe).

12.3. Failure of dunes and dikes

For the dikes in Flanders, the Zwin and Zeeuws-Flanders, 3 return periods were considered: 1000, 4000 and 40000 years. The following failure mechanisms were considered:

- Piping/heave
- Outward macro stability
- Inward macro stability

- Micro stability
- State of dike covering
- Crest height of the dike

The Flemish dikes only fail by crest height. After abrasion of the beach profile, high overtopping discharges occur at some places, accompanied by high flow velocities over the crest. After damage of the crest level, erosion of the sand core of the dike will occur. For a return period of 1000 year, no problems are expected. For storm conditions with a return period of 4000 years, there are 4 locations with expected breach formations: profiles 233, 234, 242 and 243. All of these profiles will fail during the second peak of the storm. For storm conditions with a return period of 40000 years, also the profiles 235, 236 and 241 will fail during the second peak of the storm. Those profiles that failed due to a storm with return period of 4000 year, will fail now during the first peak of the storm.

For the return periods of 1000 and 4000 years, there is no risk for instability and breach formation of the Zwin dikes. For a return period of 40000 years, the southeastern part of the basin will be attacked by waves with a significant height of 1.3m. The grass cover and the covering clay layer at the outer side will resist the wave attack. However, for this part of the basin, the overtopping discharges are quite large, almost 10l/m/s. In combination with the steep inner slope of the Zwin dike (1:2.5), these volumes can cause softening of the soil and slip failure. Also the stability of the grass cover and the clay layer are no longer guaranteed due to the high overtopping velocities. Although failure of this part of the Zwin dike is uncertain, due to uncertainty of the different input parameters, failure can be supposed for such extreme conditions (40000 year return period).

For Zeeuws-Flanders, the mechanisms of failure of the cover layer and the failure of the outward macro stability (both in combination with the following erosion of the core material) cause the failure of some profiles. For a return period of 1000 years, 3 profiles will fail, for a return period of 4000 years 5 profiles will fail and for a return period of 40000 years, 10 profiles will fail.

After sensitivity analysis, the following conclusions can be made:

- The overtopping volume is highly dependent on wave height, wave period, water level and particle diameter of the beach sand
- The effect of crest level on the overtopping discharge is important
- The water table inside the dike and the composition of the dike material have a huge impact on the macro stability of the outward slope
- The erosion of the core (residual strength) is largely dependent on the composition of the core material.

An important factor seemed to be the residual strength. For dikes for example, failure of the cover layer or high overtopping discharges not necessarily provoke a dike breach. Including the necessary time to reach certain damage level of the dike seemed to be very important.

For the dunes, calculations were made by a time independent model. This model supposed the reach of an equilibrium state during the storm. The volume that is eroded is equal to the volume moved to the foreshore. If after the storm a volume smaller than the critical volume is left, a breach formation is supposed (supposed the overtopping volume will erode this critical volume). Important parameters are the particle diameter and the water level. However, nowhere problems due to dune erosion were calculated.

12.4. Flood modelling

A 2D model with Mike 21 was set-up. At the locations of breach formation, the water level was entered as input. The breach formation was derived from historical data of breach formation. The breach grows quite fast in depth (1 to 2 hours). Widthways, the breach grows between 0.5 and 82m/hour. Due to the extreme hydrodynamical conditions, a quite large value of 30m/hour was chosen. The effect of the breach dimensions seems to be large, meaning that more information on breach formation is necessary.

Calculations (see storm with return period of 40000 years) show that the hinterland is gradually flooded and that water level has a huge gradient. This means that for this area a 2D modelling is necessary. Because of high velocities a small time step is necessary, causing large calculation times.

An important assumption in the modelling is the secondary dike won't fail.

12.5. Damage calculations

For Flanders and the Netherlands, the Flemish and the Dutch methods are used respectively. The base of both methods are however similar: on the one hand, the maximum damage is determined from statistical data and land use charts, on the other hand functions are set up determining the damage relatively to the maximum damage in function of water level.

Remarkable, there is more damage in Flanders (during storms with large return periods), but there are more casualties in the Netherlands. This can be explained by the high rise velocities due to the secondary dikes, holding up the volume for a while. Because of these dikes, the flooded surface stays constant, but water depth is rising quickly. On the other hand, Knokke is the most expensive municipality of Flanders.

The positions of breach formation in the Netherlands for storm conditions with return period of 4000 and 10000 years are quite similar, but there is a large difference in damage. This illustrates clearly the importance of the water level at sea for the damage.

It is also important to mention that a lot of damage is not taken into account (for example damage to the economy outside of the flooded area, damage to nature, psychological damage…).

12.6. Risk

For a risk calculation, the damage should be integrated over the different return periods. The product of damage and probability of occurrence doesn't decrease with the return period. Therefore it is not possible to calculate the total risk without considering much higher return periods (100.000, 400.000, 1.000.000 years…). However, these calculations should be accompanied by much larger uncertainties of the input parameters and above all, the flooding will for certain not only be caused by a failure between Zeebruges and Breskens, but for example also from the Scheldt. So these calculations are less significant for a cost-benefit analysis.

A complete probabilistic approach is not significant in this case. In this approach, for each breach the most probable water level is considered. However, the damage calculations indicate that the damage

is largely dependent on water level, by which integration over all water levels is necessary. In fact, for every combination of failure, flooding calculations are necessary, which is not realistic in term of computation time.

The total uncertainty on the risk is determined by all uncertainties together. Expectations are that this uncertainty is at least a factor 10. However the calculations performed in this report are useful:

- Inform the public
- Work out of contingency plans
- Comparing the relative importance of coastal protection measures

13. REFERENTIES

Stroo M.C., Coremans C., Provoost A., Vereeke S.J.P., 2003. Toetsing op veiligheid, eindrapportage, Dijkring 32, Zeeuws-Vlaanderen, Waterschap Zeeuws-Vlaanderen.

Technische Adviescommissie voor de Waterkeringen, 2002. Technical report wave run-up and overtopping at dikes.

Schüttrumpf H., 2001. WellenOberlaufstromung bei Seedeichen -Experimentelle und Theoretische Untersuchungen, PhD thesis, Technische Universitat Braunschweig.

http:llwww. biblio. tu-bs.de/ediss/data/20010703a/20010703a.html.

Schüttrumpf H., 2003. Wave overtopping Flow on Seadikes -Experimental and Theoretical

Investigations. PIANC bulletin N°114.

SLOPE/W for slope stability analysis (version 5), User's guide.

Seijffert J.W., Verheij Ho, 1998. Grass mats and reinforcement measures, Dikes and Revetments, Editor: K. W. Pilarczyk, A.A. Balkerna.

http://www .minvenw.nl/lrws/dww/uitgaven/dwwwijzers/wijzer77/wijzer77.html

http://www.vhm.be/B2001/DeeI2/hfd21htm#_Toc504470991

Van de Walle B., 2003. Wave run-up on rubble mound breakwaters, PhD thesis, Ghent University.

De Rouck J., Van Damme L., 1996. Overall slope stability analysis of rubble mound breakwaters. Proceedings 25th I.C.CoEo, Orlando, Florida, pp. 1603-1616, Ed. B.L. Edge, ASCE, New Vork, Sept. 2-6, 1996.

Geuze E.C.W.A., Abbott MoB., 1961. Ground water movement in a sand dyke subject to tidal influence, Proceedings of the 5th I.C.S.M.F.E., 1961, pp 117-122.

Civieltechnisch Centrum Uitvoering Research en Regelgeving, 1992. Cementbetonnen plaatbekledingen op dijken en oevers, CUR rapport 156.

Civieltechnisch Centrum Uitvoering Research en Regelgeving, 1984. Leidraad cementbetonnen dijkbekledingen, CUR rapport 119.

De veiligheid van de primaire waterkeringen in Nederland, Voorschrift Toetsen op Veiligheid voor de tweede toetsronde 2001 -2006 (VTV), januari 2004

Civieltechnisch Centrum Uitvoering Research en Regelgeving, Technische Adviescommissie voor de Waterkeringen, 1992. Handboek voor dimensionering van gezette taludbekledingen, CUR/TAW handboek.

TNO-rapport 2003-CI-R0020, 2003. Theoriehandleiding PC-ring Versie 4.0 Technische Adviescommissie voor de Waterkeringen, 1999. Leidraad Toetsen op Veiligheid.

Goda (1970, estimation of the rate of irregular overtopping of seawalls, report of port and Jr institute, Vol 9, No 4)

Rijkswaterstaat, Dienst Weg- en Waterbouwkunde, 1993, Het ontwerpen van een bekleding voor een zeedijk.

WHL, november 2002, Risicobenadering bij waterbeheersingsplannen; methodolgy en case study Denderbekken , Wouter Vanneuville i.o. v. W HL, november 2002.

WHL, februari 2002, Risicobepaling overstromingen, Discussienota eerste versie, Wouter Vanneuville, februari 2002.

Addendum A:
Method of Schüttrumpf (2001) en Schüttrumpf (2003)

Below, the method of Schüttrumpf (Schüttrumpf, 2001 and Schüttrumpf, 2003) for the determination of layer thicknesses and overtopping velocities is expounded.

Wave run-up is calculated by means of the Schüttrumpf (2003) formula or the formula mentioned in TAW (2002). The Schüttrumpf (2003) formula is:

$$\frac{Ru_{2\%}}{H_s} = 1.5\xi_d \qquad \text{for } \xi_d < 2.0 \qquad \text{(A.1)}$$

$$\frac{Ru_{2\%}}{H_s} = 3.0 \qquad \text{for } \xi_d \geq 2.0 \qquad \text{(A.2)}$$

with $\xi_d = \dfrac{\tan\alpha}{\sqrt{\dfrac{H_s}{L_0}}}$ (with H_s = significant wave height (in time domain)) (A.3)

$$L_0 = \frac{gT_m^2}{2\pi} \quad \text{(with } T_m \text{ = average wave period (in time domain))} \qquad \text{(A.4)}$$

$$\tan\alpha = 1/n \qquad \text{(A.5)}$$

The TAW (2002) formula is:

$$\frac{Ru_{2\%}}{H_{m0}} = 1.75\gamma_b\gamma_f\gamma_\beta\xi_0 \leq \gamma_f\gamma_\beta\left(4.3 - \frac{1.6}{\sqrt{\xi_0}}\right) \qquad \text{(A.6)}$$

whereby $\xi_0 = \dfrac{\tan\alpha}{\sqrt{\dfrac{2\pi H_{m0}}{gT_{m-1,0}}}}$ (A.7)

with $H_{m0} = 4\sqrt{m_0}$ (A.8)

and $T_{m-1,0} = \dfrac{m_{-1}}{m_0}$ (A.9)

and γ_b = reduction factor for berm
γ_f = reduction factor for roughness
γ_β = reduction factor for slanting wave impact

The equation above applies to the average value of wave run-up (not the design value!). The reduction factors γ_b and γ_β are considered equal to 1. The roughness of the slope is taken into account with a reduction factor γ_f (table 6, cfr. TAW (2002)).

Table 6: Reduction factors γ_f for various revetments (TAW, 2002).

Material	γ_f [-]
concrete	1.00
asphalt	1.00
closed concrete blocks	1.00
grass	1.00
Vilvoorde stone	0.85
basalt	0.90
Haringman	0.90
fixtone, open stone asphalt	0.90
Armorflex	0.90
small blocks over 1/25 of the surface	0.85
small blocks over 1/9 of the surface	0.80
¼ of stone pitching, 10 cm up	0.90
ridges (optimum dimensions)	0.75
quarry stone, two courses thick	0.55
quarry stone, a single course	0.70

The van der Meer (1998) formula is:

$$\frac{Ru_{2\%}}{H_s} = 1.6\gamma_b\gamma_f\gamma_\beta\xi_{op} \leq 3.2\ \gamma_f\gamma_\beta \qquad \text{(A.10)}$$

Schüttrumpf states (via personal correspondence) that the van der Meer formulas can also be used, but that T_m must be used instead of T_p ! The relation between the various time parameters are given in TAW (2002):

- $T_p \cong T_{1/3}$

- $T_m / T_{1/3} = 1.15$, so that $T_m / T_p = 1.15$

- $T_p = 1.1\ T_{m-1,0}$

so that

$$\frac{Ru_{2\%}}{H_{m0}} = 1.84\gamma_b\gamma_f\gamma_\beta\xi_{op} \le \gamma_f\gamma_\beta\left(4.3 - \frac{1.6}{\sqrt{1.15\xi_{0p}}}\right) \qquad \text{(A.11)}$$

because ξ_{om} = 1.15 ξ_{op}.

The layer thickness on the seaward slope of the dike is calculated with:

$$h_A(x_*) = c_2^* x_* \tan\alpha \qquad \text{(A.12)}$$

whereby x_* = $x_Z - x_A$ en x_Z = $n\,Ru_{2\%}$ so that

$$h_A(x_A) = c_2^*(nRu_{2\%} - x_A)\tan\alpha = c_2^*\left(Ru_{2\%} - \frac{x_A}{n}\right) \qquad \text{(A.13)}$$

with c_2^* = 0.216 (for $h_{A,2\%}$) and c_2^* = 0.048 (for $\overline{h_A}$ ('time averaged' value for h_A)).

The layer thickness on the seaward end of the crest is calculated with:

$$h = c_2^*(Ru_{2\%} - R_C) \qquad \text{(A.14)}$$

with c_2^* = 0.168 (Schüttrumpf (2003): $h_C(0) = h_{A,50}(R_c)$). The velocity in the same place is given by:

$$\frac{v_A}{\sqrt{gH_s}} = 1.32\sqrt{\frac{Ru_{2\%} - R_C}{H_s}} \qquad \text{(A.15)}$$

When the wave run-up is larger than the freeboard, waves will top over and cause an overtopping discharge. On the crest the course of the layer thickness is given by

$$\frac{h_C(x_C)}{h_C(0)} = \exp\left(-0.75\frac{x_C}{B}\right) \qquad \text{(A.16)}$$

and the wave run-up velocity is given by

$$\frac{v_C(x_C)}{v_C(0)} = \exp\left(-\frac{x_C f}{2h_C}\right) \qquad \text{(A.17)}$$

with f = friction coefficient (f = 0.02 for a concrete slope and is 0.10 to 0.60 for rubble)

On the landward part of the dike the velocity is given by

$$v_B = \sqrt[3]{\frac{2gh_B(0)v_B(0)\sin\beta}{f}} \qquad \text{(A.18)}$$

whereby β = arctan(1/m), $h_B(0) = h_C(B)$ en $v_B(0) = v_C(B)$.

The layer thickness on the landward side of the slope is given by

$$h_B = \frac{v_B(0)h_B(0)}{v_B} \qquad \text{(A.19)}$$

The *average* layer thickness is used in the calculations because the *average* overtopping discharge is also used in the calculations. If the layer thickness $h_{98\%}$ (i.e. the layer thickness exceeded by 2% of the waves running up) were calculated, individual wave overtopping volumes must be used instead of q. Consequently, the c_2^* value corresponding with 98% must also be used in the calculations.